

# **Lawrence Berkeley National Laboratory**

## **Recent Work**

### **Title**

I. THE INDICATRIX OF COMPOSITE CRYSTALS. II. CALCULATION OF THE INDICATRIX OF SILICATE MINERALS WITH THE CLASSICAL POINT-DIPOLE MODEL. III. THE STRUCTURE OF TWO SODIUM-URANYL FLUORIDES

### **Permalink**

<https://escholarship.org/uc/item/4r97r5r4>

### **Author**

Hauser, James Robert.

### **Publication Date**

1977-04-01

0 0 0 0 / 1 0 8 0 2

110 11  
LBL-6233

c.1

- I. THE INDICATRIX OF COMPOSITE CRYSTALS
- II. CALCULATION OF THE INDICATRIX OF SILICATE MINERALS WITH THE CLASSICAL POINT-DIPOLE MODEL
- III. THE STRUCTURE OF TWO SODIUM-URANYL FLUORIDES

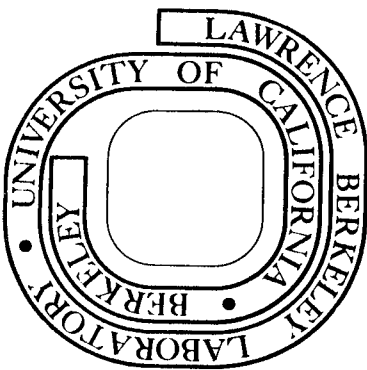
James Robert Hauser  
Ph. D. thesis

April 1977

Prepared for the U. S. Energy Research and Development Administration under Contract W-7405-ENG-48

**For Reference**

**Not to be taken from this room**



LBL-6233  
c.1

## **DISCLAIMER**

This document was prepared as an account of work sponsored by the United States Government. While this document is believed to contain correct information, neither the United States Government nor any agency thereof, nor the Regents of the University of California, nor any of their employees, makes any warranty, express or implied, or assumes any legal responsibility for the accuracy, completeness, or usefulness of any information, apparatus, product, or process disclosed, or represents that its use would not infringe privately owned rights. Reference herein to any specific commercial product, process, or service by its trade name, trademark, manufacturer, or otherwise, does not necessarily constitute or imply its endorsement, recommendation, or favoring by the United States Government or any agency thereof, or the Regents of the University of California. The views and opinions of authors expressed herein do not necessarily state or reflect those of the United States Government or any agency thereof or the Regents of the University of California.

**I. THE INDICATRIX OF COMPOSITE CRYSTALS****II. CALCULATION OF THE INDICATRIX OF SILICATE MINERALS  
WITH THE CLASSICAL POINT-DIPOLE MODEL****III. THE STRUCTURE OF TWO SODIUM-URANYL FLUORIDES**

James Robert Hauser

Materials and Molecular Research Division  
Lawrence Berkeley Laboratory

and

Department of Physics  
University of California  
Berkeley, California 94720

April 1977

**ABSTRACT**

The results of three distinct studies are discussed. The first two chapters describe calculations of the geometric optical properties of crystals; the third chapter is concerned with the crystal structure analysis of two new double salts.

In the first chapter a model based on the volume average of the dielectric tensor is derived and applied to several composite systems. A composite system is defined as an optically homogeneous material composed of domains with differing chemical composition, orientation, or structure. If the domains are larger than the scale of the unit cell but smaller than the wavelength of light, the volume averaged dielectric tensor should accurately describe the geometric optical properties of these composites.

Calculations with this model for several composite systems compare favorably to experimental measurements. For calcite the good agreement supports the hypothesis that submicroscopic twinning is the cause of biaxiality in this system. Application of the model to alkali feldspars indicates that some orthoclase consists of submicroscopically twinned microcline. When applied to plagioclase feldspars, the model explains the optical migration curves of this system.

In the second chapter a version of the point-dipole model of the electric polarization is developed and applied to calculate the geometric optical properties of several silicate minerals. This version of the point-dipole model assigns a scalar polarizability to each chemical species in the crystal. The first part of the chapter is concerned with the mathematics needed to implement the theory. A method of doing the lattice sums in reciprocal space is discussed. Calculations for several systems show the model is not able to adequately describe the optical properties of complex silicate minerals. This is attributed to the approximation of assigning the same polarizability to crystallographically distinct atoms.

The third chapter describes the crystal structure analysis of two new sodium-uranyl double fluorides,  $\text{Na}_3(\text{UO}_2)_2\text{F}_7 \cdot n\text{H}_2\text{O}$  with  $n = 2$  and  $n = 6$ . The uranium ion in both structures has seven-fold coordination with the two uranyl oxygen atoms forming the axis and five fluorine atoms forming the equator of a pentagonal bipyramid. The new salts are shown to be members of a series of uranyl salts which share this structural feature.

David H. Rempleton

## TABLE OF CONTENTS

CHAPTER 1: THE VOLUME AVERAGED DIELECTRIC TENSOR . . . . .	1
I. Introduction . . . . .	1
II. The Indicatrix . . . . .	5
III. The Dielectric Tensor of Composites . . . . .	12
IV. Mathematics to Implement $\epsilon$ . . . . .	22
V. Biaxial Calcite . . . . .	31
VI. Alkali Feldspars (Na, K)AlSi <sub>3</sub> O <sub>8</sub> . . . . .	43
VII. Plagioclase (Ca, Na) (Al, Si)AlSi <sub>2</sub> O <sub>8</sub> . . . . .	50
VIII. Conclusions . . . . .	62
IX. References . . . . .	63
CHAPTER 2: CALCULATIONS WITH THE POINT-DIPOLE MODEL . . . . .	66
I. Motivations . . . . .	66
II. Physical Principles and Objectives of the Point-Dipole Model . . . . .	73
III. Derivation of the Dielectric Tensor in the Point-Dipole Model . . . . .	77
IV. Transformation of the Lattice Sums to Fourier Space . . . . .	87
V. The Matrix Elements of the Lattice Sums . . . . .	92
VI. Discussion of Calculation Procedure . . . . .	98
VII. Enstatite Revisited with the Point-Dipole Model . . . . .	102
VIII. Solid Solutions and the Point-Dipole Model . . . . .	109
IX. Quartz and Corundum . . . . .	120
X. Conclusions . . . . .	125

XI. Appendix on the FORTRAN Lattice Sum Program . . . . .	129
XII. References . . . . .	134
CHAPTER 3: THE CRYSTAL STRUCTURES OF $\text{Na}_3(\text{UO}_2)_2\text{F}_7 \cdot n\text{H}_2\text{O}$ FOR	
N = 2, 6 . . . . .	136
I. Introduction . . . . .	136
II. Experimental Section . . . . .	137
III. Unit Cells and Space Groups . . . . .	140
IV. Determination of the Structures . . . . .	142
V. Description of the Structures . . . . .	146
VI. Other Alkali Metal-Uranyl Fluorides . . . . .	157
VII. Appendix on Observed and Calculated Structure Factors .	160
VIII. References . . . . .	188

## CHAPTER 1: THE VOLUME AVERAGED DIELECTRIC TENSOR

## I. Introduction

The refractive index in optically homogeneous material is generally not constant but varies with direction. This variation can be described with six optical parameters. By measuring the refractive indices (three parameters) and how they vary with direction (three parameters) pure single crystals can be simply and routinely identified. However, optical homogeneity is not restricted to single crystals. Glasses are a well known example of noncrystalline material which is optically homogeneous.

A material will be optically homogeneous if all structural and chemical inhomogeneities vanish when averaged over a region smaller than the wavelength of light (~5000 Å). Single crystals and glasses obviously satisfy this criterion. This chapter is concerned with optically homogeneous material whose scale of chemical or structural inhomogeneity is larger than that encountered in single crystals and glasses. In particular it is concerned with materials composed of submicroscopic\* domains with differing chemical compositions and orientations.

Mainly as a result of electron microscopic studies it has become clear that many optically homogeneous mineral crystals are composed of submicroscopic domains (see Figure I.1). Submicroscopically twinned

---

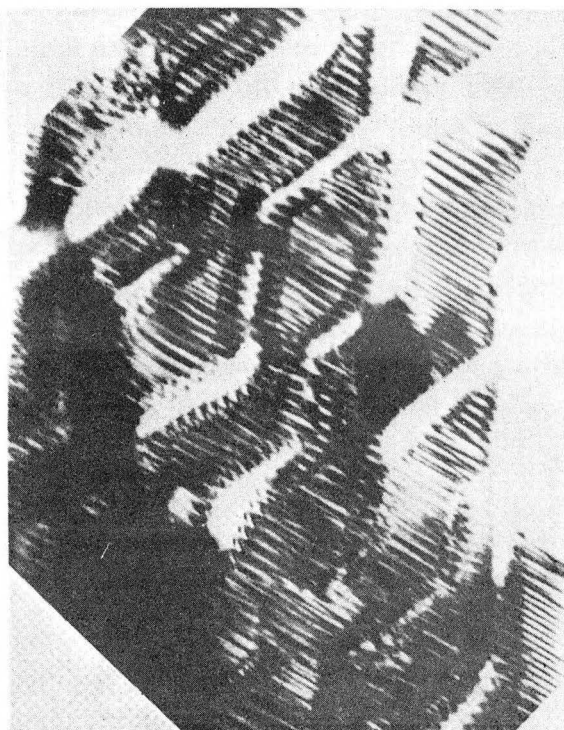
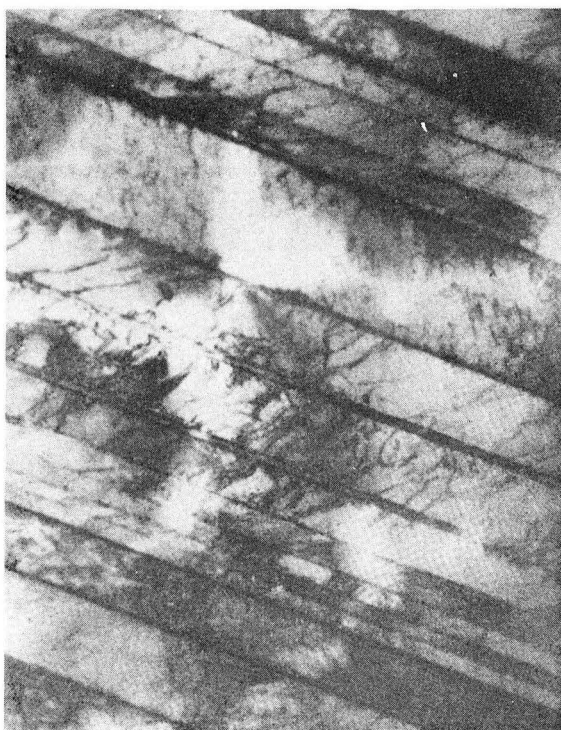
\*In this work microscopic (submicroscopic) will refer to objects that are large enough (too small) to be visible in an optical microscope.

calcite is an example of a material whose domains differ only in orientation. Cryptoperthites have been found to consist of a sub-microscopic intergrowth of albite and microcline feldspars often twinned and forming complicated textures.

In the first part of this chapter a theory is developed based on the volume average of the dielectric tensor which can be used to predict the geometric optical properties of these composites. The theory is applied subsequently to several mineral systems.

0 0 0 0 4 7 1 0 8 6 6

3



5  $\mu m$

a)

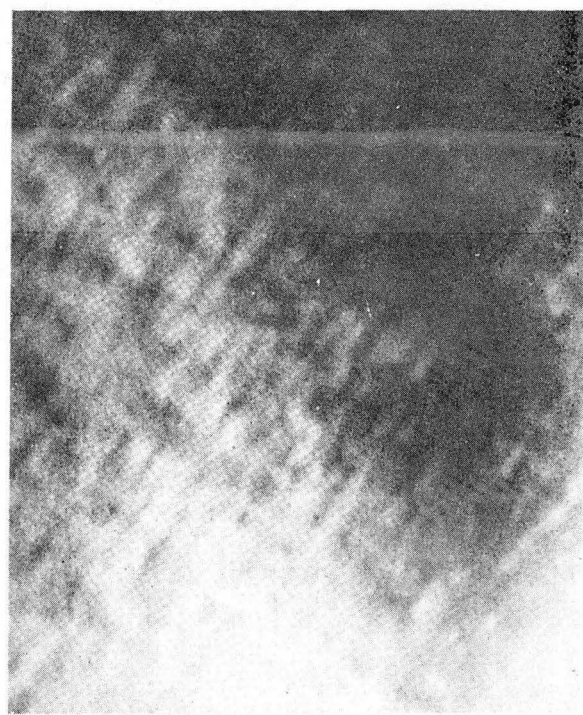
0.5  $\mu m$

b)



1  $\mu m$

c)



1  $\mu m$

d)

Figure (I.1)

Figure I.1. Photomicrographs of some submicroscopic domain textures.

These photographs will be discussed later in this work; the following notation will be defined at that time.

a) Calcite. Experimentally deformed single crystal VW163. Notice narrow microtwins and dislocations.

Brightfield transmission electron microscopy photograph (courtesy of D. Barber). b) Cryptoperthite.

Narrow zigzag bands corresponds to microcline in two twin orientations, the striated part is twinned albite (cf. Brown et al.<sup>1</sup>). Brightfield transmission electron microscopy photograph (courtesy of W. L. Brown and M. Gandais).

c) Labradorite with blue-green schiller, An53 from Labrador, Canada. The lamellar structure is due to exsolution into an An-rich and an An-poor phase. Brightfield transmission electron microscopy photograph (courtesy of H. -U. Nissen). d) Bytownite from lunar basalt 14310 (cf. Wenk et al.<sup>2</sup>). Notice the fine tweed texture which is typical of rapidly cooled, volcanic crystals. Darkfield transmission electron microscopy photograph (courtesy of W. Müller).

## II. The Indicatrix

It is convenient when discussing the geometric optical properties of crystals to use the construction known as the index ellipsoid or indicatrix. Although Maxwell's equations give a complete algebraic description of crystal optics, it is useful to have a geometric description of this geometric phenomenon. This section begins with a definition of the indicatrix and a description of some of its properties. Next, the effect of the crystal's point group symmetry on the indicatrix is summarized. Finally, the relationship between the indicatrix and the dielectric tensor is demonstrated with Maxwell's equations. An assumption throughout this study is that the crystals are nonmagnetic, that is,  $\underline{B} = \underline{H}$  ( $\underline{\mu} = 1$ ).

Consider a ray of light (plane wave) propagating in a crystal. Associated with this ray is an electric displacement  $\underline{D}$  (conventionally called the vibration direction) and a phase velocity or refractive index  $n$  which depends only upon the direction of  $\underline{D}$ . From a point fixed in the crystal construct a vector of length  $n$  in the vibration direction. The indicatrix is the locus of the end points of this vector when one considers all possible ray directions. For a cubic crystal or a glass, the indicatrix is spherical; in general, it is a triaxial ellipsoid. The three semi-axes form an orthogonal triad called the principal directions of the indicatrix. The lengths of the semi-axes are the principal refractive indices and are denoted by  $n_\alpha$ ,  $n_\beta$ , and  $n_\gamma$  with  $n_\alpha < n_\beta < n_\gamma$  by convention. Six parameters suffice to describe the indicatrix: the shape is determined by the three principal indices,

the orientation is determined by three angles which relate the principal directions to the crystal coordinate system. The indicatrix is analogous to the thermal ellipsoid of x-ray crystallography and the inertia ellipsoid of classical mechanics.

Although there exist elegant constructions for determining from the indicatrix the two ray and vibration directions associated with each wave vector,<sup>3</sup> this section will be concerned only with the effect of the crystal's point group symmetry on the shape and orientation of the ellipsoid. When the crystal is rotated or reflected so is the indicatrix, for when the material in the crystal is displaced, the geometric description of the material's effect on light also must be displaced. In other words the point group of the crystal must be a subgroup of the point group of the indicatrix ( $2/m\ 2/m\ 2/m$  with the principal directions coinciding with the two-fold axes). This places constraints on the shape and orientation of the indicatrix, and, therefore, can reduce the number of parameters needed for a complete description.

For example, consider a monoclinic phase. Because the crystal is invariant with respect to either a two-fold rotation about the b axis or a reflection in a plane normal to this axis, so must the indicatrix. Therefore, one of the principal directions must be along the b axis. Although this places no constraints on the shape, the number of orientation parameters is reduced from three to one.

Next consider a crystal with a three-fold axis. The indicatrix also must have this symmetry. This is true only if the indicatrix is

an ellipsoid of revolution with the circular cross-section normal to the crystal three-fold axis. This fixes the orientation and reduces the shape parameters from three to two (length of indicatrix along the three-fold axis and radius of the circular section).

Similar considerations<sup>4</sup> can be applied to the seven symmetry classes; Table II.1 is a summary of the results. Notice that the crystal systems can be placed in one of three classes depending on the number of circular sections that are obtained when the indicatrix is sliced with a plane passing through its center. The spherical indicatrix of the cubic system has an infinite number of circular sections and is in a class by itself. The indicatrix of the trigonal, hexagonal, and tetragonal systems is an ellipsoid of revolution and has only one circular section which is normal to the unique axis. Less obvious is that the triaxial ellipsoid of the triclinic, monoclinic, and orthorhombic systems has two circular sections both of which contain the principal axis corresponding to the intermediate principal index  $n_\beta$ . The directions normal to a circular section are called the optic axes. Crystals with one optic axis are uniaxial; those with two are biaxial. Light which propagates along an optic axis is not doubly refracted, for the circular section implies that all vibration directions have the same index of refraction. The angle between the optic axes in a biaxial crystal is the axial angle which is denoted by  $2V$ . The plane containing these axes is the optic plane. A uniaxial crystal can be described as a biaxial crystal with  $2V = 0$  or  $2V = 180^\circ$ .

Table II.1

System	Number of shape parameters	Number of orientation parameters	Total number of parameters	Number of circular sections
Triclinic	3	3	6	2
Monoclinic	3	1	4	2
Orthorhombic	3	0	3	2
Trigonal	2	0	2	1
Hexagonal	2	0	2	1
Tetragonal	2	0	2	1
Cubic	1	0	1	$\infty$

Symmetry and the Indicatrix

To end this section the relationship between the indicatrix and the dielectric tensor will be demonstrated. Maxwell's equations for nonmagnetic material ( $\mu = 1$ ) are

$$\underline{\nabla} \cdot \underline{D} = 0$$

$$\underline{\nabla} \cdot \underline{B} = 0$$

$$\underline{\nabla} \times \underline{E} = -\frac{1}{C} \frac{\partial \underline{B}}{\partial t}$$

$$\underline{\nabla} \times \underline{B} = \frac{1}{C} \frac{\partial \underline{D}}{\partial t}.$$

For a plane wave with an  $\exp(k \cdot \underline{x} - \omega t)$  dependence these become

$$\hat{\underline{k}} \cdot \underline{D} = 0$$

$$\hat{\underline{k}} \cdot \underline{B} = 0$$

$$\hat{\underline{k}} \times \underline{E} = \underline{B}/n$$

$$\hat{\underline{k}} \times \underline{B} = -\underline{D}/n$$

where  $\hat{\underline{k}}$  is a unit wave vector, and  $n = kc/\omega$  is the index of refraction.

The constitutive relation  $\underline{D} = \underline{\epsilon} \underline{E}$  where  $\underline{\epsilon}$  is the dielectric tensor can be used to eliminate the electric field from the equations:

$$\hat{\underline{k}} \cdot \underline{D} = 0 \quad (\text{II.1})$$

$$\hat{\underline{k}} \cdot \underline{B} = 0 \quad (\text{II.2})$$

$$\hat{\underline{k}} \times \underline{\epsilon}^{-1} \underline{D} = \underline{B}/n \quad (\text{II.3})$$

$$\hat{\underline{k}} \times \underline{B} = -\underline{D}/n. \quad (\text{II.4})$$

Crossing (II.3) with  $\hat{\underline{k}}$  and using (II.4)  $\underline{B}$  can be eliminated:

$$\hat{\underline{k}} \times [\hat{\underline{k}} \times \underline{\epsilon}^{-1} \underline{D}] = \hat{\underline{k}} \times \underline{B}/n = -\underline{D}/n^2$$

or

$$\underline{\epsilon}^{-1} \underline{D} - \hat{\underline{k}}(\hat{\underline{k}} \cdot \underline{\epsilon}^{-1} \underline{D}) = \underline{D}/n^2.$$

Dotting both sides with  $\underline{D}$  and using (II.1) yields

$$\underline{D} \cdot \underline{\varepsilon}^{-1} \underline{D} = D^2/n^2$$

or

$$\underline{X} \cdot \underline{\varepsilon}^{-1} \underline{X} = 1 \quad (\text{II.5})$$

where

$$\underline{X} = n \hat{\underline{D}}.$$

$\underline{X}$  is a vector of length  $n$  in the vibration direction, and by definition terminates on the surface of the indicatrix. Therefore, equation (II.5) defines the indicatrix by the constraint it places on  $\underline{X}$ . That (II.5) is the equation of a triaxial ellipsoid can be shown by noting that  $\underline{\varepsilon}$  is a symmetric tensor. Therefore, by choosing a coordinate system in which the axes are the eigenvectors of  $\underline{\varepsilon}$ , this tensor can be represented by a diagonal matrix:

$$\underline{\varepsilon} = \begin{pmatrix} \varepsilon_1 & 0 & 0 \\ 0 & \varepsilon_2 & 0 \\ 0 & 0 & \varepsilon_3 \end{pmatrix}$$

where the  $\varepsilon_i$  are the eigenvalues of  $\underline{\varepsilon}$ . The same coordinate system will diagonalize  $\underline{\varepsilon}^{-1}$ :

$$\underline{\varepsilon}^{-1} = \begin{pmatrix} 1/\varepsilon_1 & 0 & 0 \\ 0 & 1/\varepsilon_2 & 0 \\ 0 & 0 & 1/\varepsilon_3 \end{pmatrix}.$$

By representing  $\underline{X}$  in this system by

$$\underline{X} = \begin{pmatrix} x \\ y \\ z \end{pmatrix}$$

equation (II.5) becomes

$$x^2/\epsilon_1 + y^2/\epsilon_2 + z^2/\epsilon_3 = 1$$

which is the equation of a triaxial ellipsoid with semi-axes of length  $\sqrt{\epsilon_i}$  parallel to the coordinate axes. Therefore, the principal axes and principal indices of the indicatrix are the eigenvectors and square roots of the eigenvalues of the dielectric tensor.

### III. The Dielectric Tensor of Composites

In this section an exact expression will be found for the dielectric tensor of composites which consist of two types of plane parallel layers. The width of these lamellae is assumed to be less than the wavelength of light. By ignoring the effect of surface charge induced at the lamella interfaces, this exact formula reduces to an approximate result which can be generalized to apply to composite material with any number of arbitrarily shaped submicroscopic domain types. The validity of this approximate formula is discussed.

If the size of the domains is larger than the wavelength of light, the path of a ray propagating in the material can be predicted with geometric optics. Each domain has its own indicatrix; Snell's law must be applied at each domain interface. By following a light ray in this manner through a lamellar composite of two isotropic materials an effective refractive index can be defined and calculated. The calculation shows, however, that this effective index is a complicated function of the ray direction and lamella thickness and does not describe the behavior of optically homogeneous material.

On the other hand, it is clear that the optical behavior of real composite material is a continuous function of the domain size, and it is possible that geometric optics describes some aspects of material with submicroscopic domains. Similarly, the theory developed in this section could describe some aspects of the optical behavior of composites with small but not necessarily submicroscopic domains. This point will be discussed in the next section.

If the domains are smaller than the wavelength of light, a more fundamental theory is necessary; the susceptibility  $\underline{\underline{\chi}}$  must be introduced:

$$\underline{\underline{\epsilon}} = \underline{\underline{I}} + 4\pi\underline{\underline{\chi}} \quad (\text{III.1})$$

where  $\underline{\underline{I}}$  is the identity tensor, and CGS units have been used. The susceptibility is defined as the tensor coefficient which relates the electric field  $\underline{\underline{E}}$  to the induced dipole moment per unit volume  $\underline{\underline{P}}$ :

$$\underline{\underline{P}} = \underline{\underline{\chi}} \underline{\underline{E}}. \quad (\text{III.2})$$

Equation (III.2) is an example of Hooke's law: the strain  $\underline{\underline{P}}$  is directly proportional to the stress  $\underline{\underline{E}}$ . The  $\underline{\underline{E}}$  field is the macroscopic electric field, i.e., the field which appears in Maxwell's equations for material media. This field is defined as the spatial average of the microscopic electric field  $\underline{\underline{e}}$  over a volume large enough to be representative of the medium, e.g., a unit cell for single crystals. The microscopic field  $\underline{\underline{e}}$  exhibits extreme variations on the atomic scale. The local field  $\underline{\underline{e}}_{\text{loc}}$  which directly induces polarization at an atomic site is that part of  $\underline{\underline{e}}$  not due to the atom itself. For a more complete discussion see Chapter 2 of this work and Kittel.<sup>5</sup>

Composites with submicroscopic domains for which the volume fraction of each domain type is constant throughout are characterized by a single dielectric tensor; there is one indicatrix which describes the optics of the material as a whole. To find this tensor for material composed of two types of layers consider a volume element  $\Delta V$  which contains two lamellae  $\Delta V_1$  and  $\Delta V_2$ . The lamellae are assumed to extend indefinitely perpendicular to the stacking direction;  $\Delta V$

contains only a small part of each layer. When  $\Delta V$  is placed in an electric field,  $\underline{E}_1$  and  $\underline{E}_2$  are produced in the lamellae. These fields are spatial averages of the microscopic field over a region representative of each layer. If  $\underline{E}_1$  differs from  $\underline{E}_2$  a charge density  $\sigma$  is induced at the domain interface:

$$\underline{E}_2 = \underline{E}_1 + 4\pi\sigma\underline{\hat{N}} \quad (\text{III.3})$$

where  $\hat{N}$  is a unit vector normal to the interface. The width of the lamellae is assumed to be larger than the scale of the unit cell so any discussion of the microscopic field can be avoided, but smaller than the wavelength of light so that the material is optically homogeneous. It is also assumed that strain effects at the domain interface are negligible. Under these conditions each domain can be characterized by its macroscopic susceptibility, that is

$$\underline{\chi}_1 = \underline{x}_1 \underline{E}_1, \quad \underline{\chi}_2 = \underline{x}_2 \underline{E}_2 \quad (\text{III.4})$$

from equation (III.2). To obtain fields representative of the composite compute a spatial average:

$$\underline{E} = f_1 \underline{E}_1 + f_2 \underline{E}_2 \quad (\text{III.5a})$$

$$\begin{aligned} \underline{P} &= f_1 \underline{P}_1 + f_2 \underline{P}_2 \\ &= f_1 \underline{x}_1 \underline{E}_1 + f_2 \underline{x}_2 \underline{E}_2 \end{aligned} \quad (\text{III.5b})$$

where  $f_i = \Delta V_i / \Delta V$ .

Ignore temporarily the surface charge. Noting that  $\sigma = 0$  implies  $\underline{E}_1 = \underline{E}_2 = \underline{E}$  gives

$$\underline{P} = \langle \underline{x} \rangle \underline{E} \quad (\text{III.6})$$

where

$$\langle \underline{\underline{\chi}} \rangle \equiv f_1 \underline{\underline{\chi}}_1 + f_2 \underline{\underline{\chi}}_2 \quad (\text{III.7})$$

which by (III.1) and (III.2) gives

$$\underline{\underline{\epsilon}} = f_1 \underline{\underline{\epsilon}}_1 + f_2 \underline{\underline{\epsilon}}_2 \equiv \langle \underline{\underline{\epsilon}} \rangle. \quad (\text{III.8})$$

The surface charge in (III.3) is related to the polarization density in each domain:

$$\sigma = \hat{\underline{\underline{N}}} \cdot (\underline{\underline{P}}_1 - \underline{\underline{P}}_2).$$

Later in this section it is shown that when this charge density is included in the calculation the exact dielectric tensor is

$$\underline{\underline{\epsilon}} = \langle \underline{\underline{\epsilon}} \rangle - F \underline{\underline{V}} \underline{\underline{V}} \quad (\text{III.9})$$

where

$$F = \frac{f_1 f_2}{\hat{\underline{\underline{N}}} \cdot (f_1 \underline{\underline{\epsilon}}_2 + f_2 \underline{\underline{\epsilon}}_1) \hat{\underline{\underline{N}}}}$$

and  $\underline{\underline{V}} \underline{\underline{V}}$  is a matrix whose components in any cartesian coordinate system are

$$(\underline{\underline{V}} \underline{\underline{V}})_{ij} = V_i V_j$$

where  $V_i$  are the cartesian components of the vector

$$\underline{\underline{V}} = (\underline{\underline{\epsilon}}_1 - \underline{\underline{\epsilon}}_2) \hat{\underline{\underline{N}}}.$$

Notice that the exact dielectric tensor differs from  $\langle \underline{\underline{\epsilon}} \rangle$  by a term that is second order in the difference  $\underline{\underline{\epsilon}}_1 - \underline{\underline{\epsilon}}_2$ . To estimate the size of this term (III.9) can be written

$$\underline{\underline{\epsilon}} = \langle \underline{\underline{\epsilon}} \rangle (I + \underline{\delta})$$

with  $\underline{\delta} = \langle \underline{\underline{\epsilon}} \rangle^{-1} F \underline{\underline{V}} \underline{\underline{V}}$ . The maximum value of  $\underline{\delta}$  can be estimated by letting

$$f_1 = f_2 = 1/2$$

$$\underline{\epsilon}_1 = \epsilon_{\max}$$

$$\underline{\epsilon}_2 = \epsilon_{\min}$$

where  $\sqrt{\epsilon_{\max}} \left( \sqrt{\epsilon_{\min}} \right)$  is the maximum (minimum) of the six refractive indices of the two domain types. With these assignments

$$\underline{\delta} \lesssim \left( \frac{\epsilon_{\max} - \epsilon_{\min}}{\epsilon_{\max} + \epsilon_{\min}} \right)^2 \quad (\text{III.10})$$

For plagioclase exsolutions with  $\epsilon_{\max} = (1.58)^2$  and  $\epsilon_{\min} = (1.52)^2$  equation (III.10) gives  $\underline{\delta} \lesssim 0.0015$ . For twinned calcite with  $\epsilon_{\max} = (1.658)^2$  and  $\epsilon_{\min} = (1.486)^2$  equation (III.10) gives  $\underline{\delta} \lesssim 0.012$ .

These estimates of  $\underline{\delta}$  are in fact much too large. Calculations using both (III.8) and (III.9) indicate the actual errors are at least ten times smaller than implied by (III.10).

For material composed of  $N$  domain types which are not parallel layers, e.g., multiply twinned calcite, the exact dielectric tensor can not be derived. However, the generalization of (III.8)

$$\langle \underline{\epsilon} \rangle = \sum_{i=1}^N f_i \underline{\epsilon}_i \quad (\text{III.11})$$

may be a good approximation. The difference between (III.11) and the exact result is due to surface charge at the domain boundaries.

That the effect of the surface charge is always second order in the differences  $\underline{\epsilon}_i - \underline{\epsilon}_j$  can be seen with the following argument. Consider two adjacent domains ( $i$  and  $j$ ) separated by a boundary. The surface charge is proportional to the difference in polarization density across the boundary:

$$\sigma \sim (\underline{P}_i - \underline{P}_j)$$

which by (III.1) and (III.2) becomes

$$\sigma \sim (\underline{\epsilon}_i - \underline{\epsilon}_j).$$

It has been assumed that  $\underline{E}_i = \underline{E}_j$ . Changes in these fields due to  $\sigma$  are directly proportional to  $\sigma$ . Therefore,

$$\Delta \underline{E}_i \sim (\underline{\epsilon}_i - \underline{\epsilon}_j) \quad (\text{III.12})$$

$$\Delta \underline{E}_j = -\Delta \underline{E}_i. \quad (\text{III.13})$$

The sign difference is due to the well known result from electrostatics that the field produced by a surface charge points in opposite directions on different sides of the surface.

By (III.2) changes in the electric field produce changes in the polarization density:

$$\Delta \underline{P}_i = \underline{x}_i \Delta \underline{E}_i \sim \underline{x}_i (\underline{\epsilon}_i - \underline{\epsilon}_j)$$

$$\Delta \underline{P}_j = \underline{x}_j \Delta \underline{E}_j \sim -\underline{x}_j (\underline{\epsilon}_i - \underline{\epsilon}_j).$$

Thus the net changes in the polarization density and electric field are

$$\Delta \underline{P} = \Delta \underline{P}_i + \Delta \underline{P}_j \sim (\underline{x}_i - \underline{x}_j)(\underline{\epsilon}_i - \underline{\epsilon}_j) = (\underline{\epsilon}_i - \underline{\epsilon}_j)^2 \quad (\text{III.14})$$

$$\Delta \underline{E} = \Delta \underline{E}_i + \Delta \underline{E}_j \sim 0. \quad (\text{III.15})$$

Because by (III.2)

$$\Delta \underline{P} = \Delta \underline{x} \underline{E} + \underline{x} \Delta \underline{E}$$

and by (III.15)  $\Delta \underline{E} \sim 0$ , the change in polarization density is proportional to the change in susceptibility:

$$\Delta \underline{P} \sim \Delta \underline{x}$$

or by (III.14)

$$\Delta \underline{x} \sim (\underline{\epsilon}_i - \underline{\epsilon}_j)^2$$

or by (III.1)

$$\Delta\epsilon \sim (\epsilon_i - \epsilon_j)^2.$$

Because the effects of the surface charge are additive, the preceding argument can be extended to N domain types by summing over adjacent pairs of domains.

A solid solution can be considered a composite material if the individual unit cells are considered as domains.\* However, the above theory does not apply, for the local field can not be ignored on this scale. Because the local field depends critically on the structure and crystal symmetry, one can not hope to derive an approximate dielectric tensor that would work equally well for all crystals. However, it is possible to show that  $\langle\epsilon\rangle$  may be a good approximation for a restricted class of solid solutions: lattice strain caused by atomic substitution must be negligible, and all atoms must have cubic site symmetry. Under these circumstances, the Clausius-Mosotti equation for mixtures can be derived:<sup>6</sup>

$$\frac{\epsilon - 1}{\epsilon - 2} = \sum_i f_i \left( \frac{\epsilon_i - 1}{\epsilon_i + 2} \right).$$

When the  $\epsilon_i$  are slightly different so that  $\epsilon_i + 2 \approx \epsilon + 2$ , the above becomes

$$\epsilon \approx \sum_i f_i \epsilon_i = \langle\epsilon\rangle$$

---

\*Strictly speaking a solid solution has no unit cell. A unit cell in this context will be defined as a structural unit in the solid solution that would be a unit cell in the pure end member.

using  $\sum_i f_i = 1$ . Because the Clausius-Mosotti equation is approximately valid for liquid solutions,  $\langle \epsilon \rangle$  has been used successfully to predict the dielectric constant of mixtures of two or more liquids.<sup>6</sup>

This discussion was not meant to imply that  $\langle \epsilon \rangle$  is a poor approximation for other types of solid solutions. Each crystal is a different system; and under special circumstances which are difficult to evaluate,  $\langle \epsilon \rangle$  might be a good approximation.

To end this section exact result (III.9) will be derived. Combining (III.3) and (III.4) with  $\sigma = \hat{N} \cdot (\underline{P}_1 - \underline{P}_2)$  gives

$$\underline{E}_2 + 4\pi\hat{N}(\hat{N} \cdot \underline{x}_2 \underline{E}_2) = \underline{E}_1 + 4\pi\hat{N}(\hat{N} \cdot \underline{x}_1 \underline{E}_1). \quad (\text{III.16})$$

To continue dyadics must be introduced. A dyadic is a tensor generated by two vectors. The dyadic  $\underline{A} \underline{B}$  operating on a general vector  $\underline{V}$  gives

$$(\underline{A} \underline{B}) \underline{V} = \underline{A} (\underline{B} \cdot \underline{V}).$$

With this definition (III.16) can be rewritten

$$\underline{E}_2 = \underline{R} \underline{E}_1$$

with

$$\underline{R} = (\underline{I} + 4\pi\hat{N}\hat{N} \underline{x}_2)^{-1} (\underline{I} + 4\pi\hat{N}\hat{N} \underline{x}_1).$$

Carrying out the averaging in (III.5) gives

$$\underline{E} = (f_1 + f_2 \underline{R}) \underline{E}_1 \quad (\text{III.17a})$$

$$\underline{P} = (f_1 \underline{x}_1 + f_2 \underline{x}_2 \underline{R}) \underline{E}_1 \quad (\text{III.17b})$$

Combining (III.17) with (III.1) and (III.2) gives

$$\underline{\epsilon} = (f_1 \underline{\epsilon}_1 + f_2 \underline{\epsilon}_2 \underline{R}) (f_1 + f_2 \underline{R})^{-1}.$$

With  $\underline{S} = \underline{R} - \underline{I}$  this becomes

$$\underline{\epsilon} = \langle \epsilon \rangle - \underline{Q}$$

where

$$\underline{Q} = f_1 f_2 (\underline{\varepsilon}_1 - \underline{\varepsilon}_2) (\underline{I} + f_2 \underline{S})^{-1} \underline{S}. \quad (\text{III.18})$$

After a little algebra one can show

$$\underline{S} = (\underline{I} + 4 \underline{N} \hat{\underline{N}} \underline{\chi}_2)^{-1} \hat{\underline{N}} (\underline{\varepsilon}_1 - \underline{\varepsilon}_2). \quad (\text{III.19})$$

To continue the following identity is required:

$$(\hat{\underline{N}} \hat{\underline{A}}) \hat{\underline{N}} = (\underline{N} \cdot \underline{A} \underline{N}) \hat{\underline{N}} \hat{\underline{N}} \quad (\text{III.20})$$

This can be proven by operating on an arbitrary vector.  $\underline{A}$  is any tensor. Using this identity one can show that

$$(\underline{I} + \hat{\underline{N}} \hat{\underline{A}})^{-1} \hat{\underline{N}} \hat{\underline{N}} = \frac{1}{1 + \underline{N} \cdot \underline{A} \underline{N}} \hat{\underline{N}} \hat{\underline{N}}. \quad (\text{III.21})$$

Combining this result with (III.19) gives

$$\underline{S} = \frac{1}{\underline{N} \cdot \underline{\varepsilon}_2 \underline{N}} \hat{\underline{N}} \hat{\underline{N}} (\underline{\varepsilon}_1 - \underline{\varepsilon}_2).$$

Combining this result with (III.18) gives

$$\begin{aligned} \underline{Q} &= f_1 f_2 (\underline{\varepsilon}_1 - \underline{\varepsilon}_2) [\underline{N} \cdot \underline{\varepsilon}_2 \underline{N} + f_2 \hat{\underline{N}} \hat{\underline{N}} (\underline{\varepsilon}_1 - \underline{\varepsilon}_2)]^{-1} \\ &\times \hat{\underline{N}} \hat{\underline{N}} (\underline{\varepsilon}_1 - \underline{\varepsilon}_2). \end{aligned}$$

Applying a slightly modified version of (III.21) to this result gives

$$\underline{Q} = F (\underline{\varepsilon}_1 - \underline{\varepsilon}_2) \hat{\underline{N}} \hat{\underline{N}} (\underline{\varepsilon}_1 - \underline{\varepsilon}_2) \quad (\text{III.22})$$

where

$$F = f_1 f_2 / [\underline{N} \cdot (f_1 \underline{\varepsilon}_2 + f_2 \underline{\varepsilon}_1) \underline{N}].$$

Because  $\underline{\varepsilon}_1$  and  $\underline{\varepsilon}_2$  are symmetric so is their difference. Therefore,

$$\underline{Q} = F \underline{V} \underline{V}$$

where

$$\underline{V} = (\underline{\varepsilon}_1 - \underline{\varepsilon}_2) \hat{\underline{N}}.$$

In a cartesian coordinate system the matrix elements of  $\underline{V} \underline{V}$  are defined as

$$(\underline{V} \underline{V})_{\ell m} = \hat{\underline{x}}_\ell \cdot \underline{V} \underline{V} \hat{\underline{x}}_m$$

where  $\hat{\underline{x}}$  are unit basis vectors. From the definition of a dyadic this becomes

$$(\underline{V} \underline{V})_{\ell m} = V_\ell V_m$$

where

$$V_\ell = \hat{\underline{x}}_\ell \cdot \underline{V}.$$

#### IV. Mathematics to Implement $\langle \underline{\epsilon} \rangle$

This section concerns the mathematical machinery needed to implement the formula  $\langle \underline{\epsilon} \rangle = \sum_i f_i \underline{\epsilon}_i$ . A coordinate system will be defined, and a method described whereby measured optical parameters can be related to the dielectric tensor for each domain type. As an illustration, the machinery will be applied to a composite of two uniaxial phases.

For each composite one domain type will be designated the host. Given the crystal axes of the host  $\underline{a}$ ,  $\underline{b}$ , and  $\underline{c}$  define a cartesian system as follows:

$$\begin{aligned}\hat{\underline{z}} &= \hat{\underline{c}} = \underline{c}/c \\ \hat{\underline{y}} &= \hat{\underline{b}}^* = \underline{b}^*/b^* \\ \hat{\underline{x}} &= \hat{\underline{y}} \times \hat{\underline{z}}\end{aligned}\tag{IV.1}$$

where  $\underline{a}^*$ ,  $\underline{b}^*$ , and  $\underline{c}^*$  are the reciprocal lattice vectors:

$$\underline{a}^* = (\underline{b} \times \underline{c})/\underline{a} \cdot (\underline{b} \times \underline{c})$$

and so forth. Vectors and tensors associated with all domain types in the composite will be referred to this system. In particular the direction associated with a principal axis will be represented by a unit vector which depends on two Goldschmidt angles:

$$\begin{aligned}\hat{\underline{v}} &= \sin\rho \sin\phi \hat{\underline{x}} + \sin\rho \cos\phi \hat{\underline{y}} + \cos\rho \hat{\underline{z}} \\ &= \begin{pmatrix} \sin\rho \sin\phi \\ \sin\rho \cos\phi \\ \cos\rho \end{pmatrix}\end{aligned}$$

where  $\rho$  is the angle between  $\hat{\underline{v}}$  and  $\hat{\underline{z}}$  ( $0 \leq \rho \leq 180^\circ$ ), and  $\phi$  is the angle between the projection of  $\hat{\underline{v}}$  in the xy plane and  $\hat{\underline{y}}$  ( $0 \leq \phi \leq 360^\circ$ ). The positive sense of  $\phi$  is such that  $\hat{\underline{y}}$  can be rotated by  $\Delta\phi = +90^\circ$  to coincide with  $\hat{\underline{x}}$ .

The dielectric tensor for each domain type is represented by

$$\underline{\epsilon} = \underline{R} \underline{\epsilon}_D \underline{R}^{-1} \quad (\text{IV.2})$$

where

$$\underline{\epsilon}_D = \begin{pmatrix} n_1^2 & 0 & 0 \\ 0 & n_2^2 & 0 \\ 0 & 0 & n_3^2 \end{pmatrix} \quad (\text{IV.3})$$

and

$$R_{ij} = v_i^j \quad (\text{IV.4})$$

where  $v_i^j$  is the  $i^{\text{th}}$  component of the unit vector in the direction of the principal axis with index  $n_j$  [ $v_i^j = (\hat{v}_i^j)_i$ ]. These specifications insure that

$$\underline{\epsilon} \hat{v}_j^j = n_j^2 \hat{v}_j^j$$

that is,  $\hat{v}_j^j$  is an eigenvector of  $\underline{\epsilon}$  with eigenvalue  $n_j^2$ . To show this start with the following which can be verified by direct substitution:

$$\underline{\epsilon}_D \hat{x}_j^j = n_j^2 \hat{x}_j^j \quad (\text{IV.5})$$

where

$$\hat{x}_1^1 = \hat{x} = \begin{pmatrix} 1 \\ 0 \\ 0 \end{pmatrix}$$

$$\hat{x}_2^2 = \hat{y} = \begin{pmatrix} 0 \\ 1 \\ 0 \end{pmatrix}$$

$$\hat{x}_3^3 = \hat{z} = \begin{pmatrix} 0 \\ 0 \\ 1 \end{pmatrix}$$

Note that

$$\underline{x}_i^j \equiv \left( \hat{\underline{x}}^j \right)_i = \delta_{ij} \quad (\text{IV.6})$$

where  $\delta_{ij}$  equal 1 when  $i = j$  and 0 otherwise.

Now multiply (IV.5) by  $\underline{R}$ :

$$\underline{R} \underline{\varepsilon}_D \hat{\underline{x}}^j = n_j^2 \underline{R} \hat{\underline{x}}^j.$$

Because  $\underline{R} \underline{R}^{-1} = \underline{I}$ , this can be written

$$(\underline{R} \underline{\varepsilon}_D \underline{R}^{-1}) \underline{R} \hat{\underline{x}}^j = n_j^2 \underline{R} \hat{\underline{x}}^j$$

or by (IV.2)

$$\underline{\varepsilon}(\underline{R} \hat{\underline{x}}^j) = n_j^2 (\underline{R} \hat{\underline{x}}^j).$$

The proof is complete if the vector  $\underline{R} \hat{\underline{x}}^j$  is along the principal direction corresponding to  $n_j$ . That is, one has to show

$$\underline{R} \hat{\underline{x}}^j = \hat{\underline{v}}^j \quad (\text{IV.7})$$

or in component form

$$\sum_k R_{ik} x_k^j = v_i^j.$$

But this last result is an identity by definitions (IV.4) and (IV.6), so the proof is complete.

There is a simple geometrical interpretation of this algebra: when the indicatrix rotates [equation (IV.2)], the principal directions rotate [equation (IV.7)].

To illustrate this procedure, consider a composite of two trigonal phases. Because this example will be used in the next section to describe submicroscopically twinned calcite, the two domain types will differ only in orientation. The hexagonal axes of the host are  $\underline{a}_1$ ,  $\underline{b}_1$ , and  $\underline{c}_1$ ; those of the other twin are  $\underline{a}_2$ ,  $\underline{b}_2$ , and  $\underline{c}_2$ . From (IV.1)

$$\hat{\underline{z}} = \hat{\underline{c}}_1$$

$$\hat{\underline{y}} = \hat{\underline{b}}_1^*$$

$$\hat{\underline{x}} = \hat{\underline{y}} \times \hat{\underline{z}} = \hat{\underline{a}}_1.$$

With the calcite application in mind, the relationship between the domain types will be as follows:  $\underline{c}_2$  is obtained from  $\underline{c}_1$  by a rotation of R degrees about  $\underline{a}_1$  (see Figure IV.1).

The dielectric tensor of the host can be written immediately, for the principal axes coincide with the cartesian system:

$$\underline{\epsilon}_1 = \begin{pmatrix} \epsilon_\gamma & 0 & 0 \\ 0 & \epsilon_\gamma & 0 \\ 0 & 0 & \epsilon_\alpha \end{pmatrix}.$$

$\epsilon_\gamma$  ( $\epsilon_\alpha$ ) is the square of the ordinary (extraordinary) index. From Figure (IV.1) the principal directions of the other twin are

$$\hat{\underline{v}}^1 = \begin{pmatrix} 1 \\ 0 \\ 0 \end{pmatrix}, \quad \hat{\underline{v}}^2 = \begin{pmatrix} 0 \\ \cos R \\ -\sin R \end{pmatrix}, \quad \hat{\underline{v}}^3 = \begin{pmatrix} 0 \\ \sin R \\ \cos R \end{pmatrix}$$

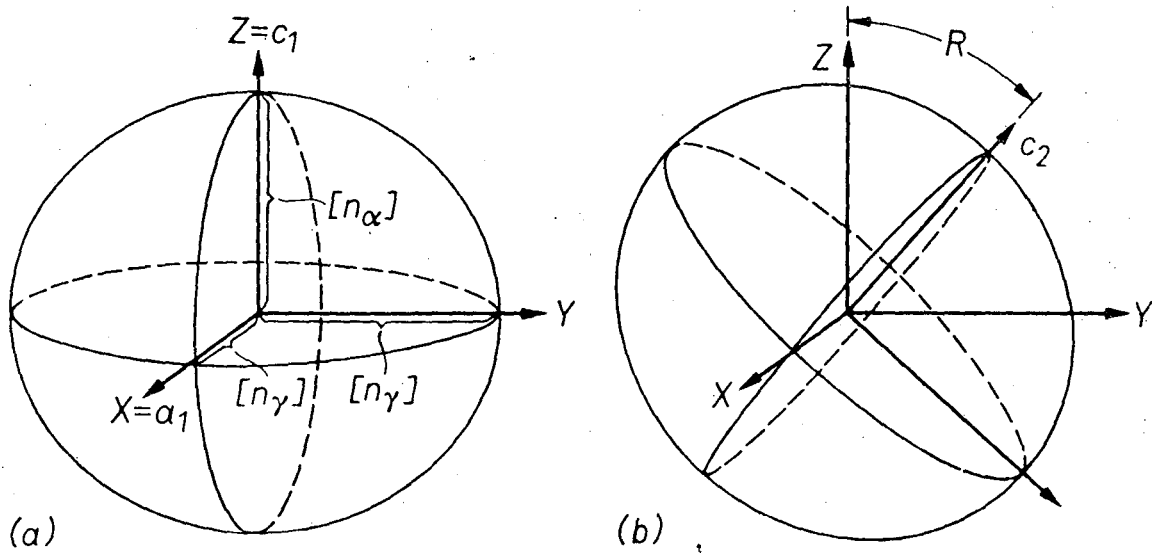
with

$$n_1^2 = \epsilon_\gamma, \quad n_2^2 = \epsilon_\gamma, \quad n_3^2 = \epsilon_\alpha.$$

Definitions (IV.3) and (IV.4) give

$$\underline{\epsilon}_D = \begin{pmatrix} \epsilon_\gamma & 0 & 0 \\ 0 & \epsilon_\gamma & 0 \\ 0 & 0 & \epsilon_\alpha \end{pmatrix}$$

and



XBL 773-8150

Figure (IV.1). The indicatrix of calcite. a) Host. b) Twin indicatrix rotated by  $R$  degrees about  $a_1$ .

$$\underline{R} = \begin{pmatrix} 1 & 0 & 0 \\ 0 & \cos R & \sin R \\ 0 & -\sin R & \cos R \end{pmatrix}.$$

Because  $\underline{R}$  is unitary ( $\underline{R}^t = \underline{R}^{-1}$ ) equation (IV.2) gives

$$\underline{\epsilon}_2 = \underline{R} \underline{\epsilon}_D \underline{R}^t = \begin{pmatrix} \epsilon_\gamma & 0 & 0 \\ 0 & \epsilon_\gamma \cos^2 R + \epsilon_\alpha \sin^2 R & (\epsilon_\alpha - \epsilon_\gamma) \cos R \sin R \\ 0 & (\epsilon_\alpha - \epsilon_\gamma) \cos R \sin R & \epsilon_\gamma \sin^2 R + \epsilon_\alpha \cos^2 R \end{pmatrix}. \quad (\text{IV.8})$$

The volume averaged dielectric tensor  $\underline{\epsilon}' = f_1 \underline{\epsilon}_1 + f_2 \underline{\epsilon}_2$  has the eigenvalues

$$\epsilon'_\gamma = \epsilon_\gamma$$

$$\epsilon'_\beta = \frac{1}{2} [(\epsilon_\gamma + \epsilon_\alpha) + Q(\epsilon_\gamma - \epsilon_\alpha)]$$

$$\epsilon'_\alpha = \frac{1}{2} [(\epsilon_\gamma + \epsilon_\alpha) - Q(\epsilon_\gamma - \epsilon_\alpha)]$$

where

$$Q = (1 - 4f_1 f_2 \sin^2 R)^{1/2}.$$

These three distinct eigenvalues give three distinct indices of refraction and, therefore, a biaxial indicatrix:

$$n_\gamma = \sqrt{\epsilon'_\gamma}, \quad n_\beta = \sqrt{\epsilon'_\beta}, \quad n_\alpha = \sqrt{\epsilon'_\alpha}$$

with  $n_\gamma > n_\beta > n_\alpha$ . The eigenvector corresponding to  $\epsilon'$  is  $\hat{x}$ , so the  $n_\gamma$  axis of the indicatrix is in the  $a_1$  (=x) direction. This means that the  $n_\alpha$  and  $n_\beta$  axes must lie in the plane containing  $c_1$  and  $c_2$  (=yz plane). By computing the other eigenvectors, the  $n_\alpha$  axis and, therefore, the axial plane is  $\theta$  degrees from  $c_1$  in the direction of  $c_2$  where

$$\tan\theta = \tan R - (1 - Q)/[f_2 \sin(2R)]$$

(see Figure IV.2).

Now that the parameters defining the composite indicatrix have been established, the axial angle can be computed from the formula<sup>7</sup>

$$\tan^2 V_\gamma = \frac{1/\epsilon_\alpha - 1/\epsilon_\beta}{1/\epsilon_\beta - 1/\epsilon_\gamma}.$$

Because  $2V_\gamma$  computed with this equation is greater than  $90^\circ$ , the  $n_\alpha$  axis bisects  $2V_\alpha$  which is defined as

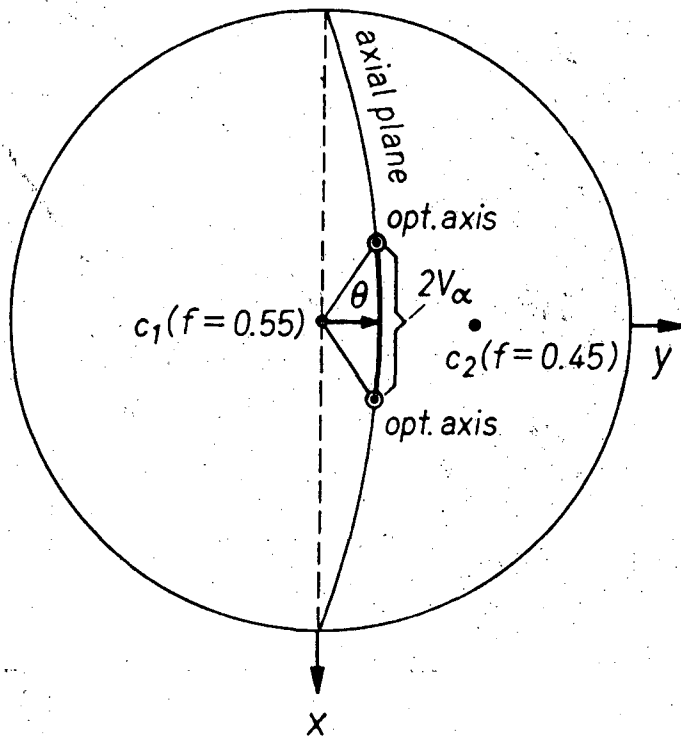
$$2V_\alpha = 180^\circ - 2V_\gamma.$$

Figure (IV.3) is a graph of  $\theta$  and  $2V_\alpha$  as functions of the volume fraction of twin<sub>2</sub> for  $R = 52.5^\circ$ .

This example has shown that a composite of uniaxial phases can have a biaxial indicatrix. This also follows from symmetry considerations. Although each domain has three-fold symmetry, the composite does not. However, for calcite with point group  $\bar{3}$  2/m each domain has a common mirror plane normal to  $a_1$ . Therefore, the composite retains this mirror and has a biaxial monoclinic indicatrix.

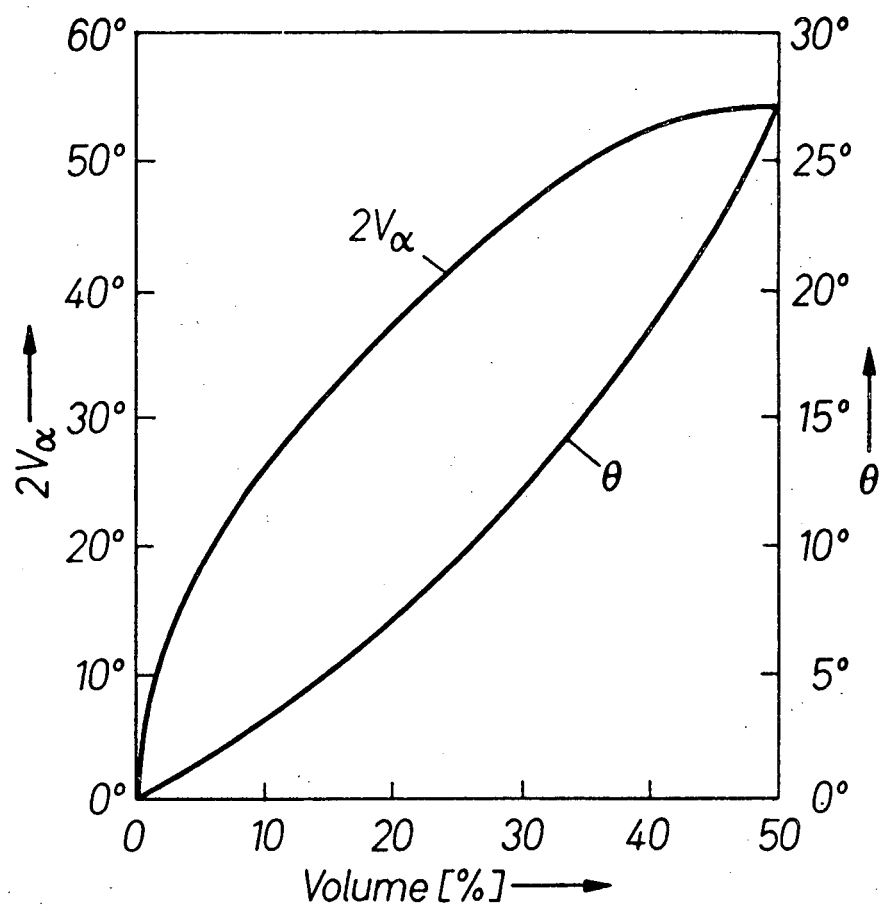
0 0 0 0 4 7 1 0 8 7 9

29



XBL 773-8148

Figure (IV.2). Stereogram illustrating axial plane and axial angle for  $f_1 = .55$  and  $f_2 = .45$ .



XBL 773-8152

Figure (IV.3). Graph of axial angle  $2V_\alpha$  and tilt angle  $\theta$  as a function of the volume fraction of twin<sub>2</sub>.

#### V. Biaxial Calcite

Although ideal single crystal calcite ( $\text{CaCO}_3$ , point group  $\bar{3}$  2/m) is uniaxial, experimental studies<sup>8-12</sup> have shown that biaxiality is common in natural and experimentally deformed calcite, particularly if deformation took place at low temperature. A brief survey of the University of California collection of metamorphic carbonate rocks from the Alps, California, and Central Australia has shown that  $2V_\alpha$  of  $2\text{--}5^\circ$  is ubiquitous except in well annealed amphibolite-facies marbles; it reaches  $35\text{--}45^\circ$  in some heavily sheared rocks (e.g. from Santa Lucia range, California and Mount Davies, S. Australia).

Before discussing biaxial calcite in the context of the volume averaged dielectric tensor, it is of interest to estimate the amount of elastic strain required to produce an axial angle of say  $20^\circ$  in calcite. A well known example of such elastic strain induced optical behavior is the birefringence caused by stress in otherwise isotropic plastic scale models used by structural engineers. Stress induced change in the refractive indices is called the photoelastic effect. If, for example, a single uniaxial crystal of calcite is subjected to a tensile stress normal to one of the mirror planes, the strained crystal retains only this mirror resulting in a biaxial monoclinic indicatrix.

However, no elastic strain that can be induced in calcite is large enough to be responsible for an axial angle of  $20^\circ$ . Long before the strain reaches such levels it would be relieved by twinning on e. To see this write the equation for the indicatrix in a general cartesian system [see equation (II.5)]:

$$\sum_{ij} \epsilon_{ij}^{-1} X_i X_j = 1.$$

The distortion of the indicatrix due to a strain  $\epsilon_{rs}$  is<sup>13</sup>

$$\Delta\epsilon_{ij}^{-1} = \sum_{rs} P_{ijrs} \epsilon_{rs} \quad (V.1)$$

where the  $P_{ijrs}$  are the elasto-optical coefficients. Since  $\epsilon_{ij}^{-1}$  are of the order of magnitude unity, the  $\Delta\epsilon_{ij}^{-1}$  are a measure of the relative distortion of the indicatrix. To produce an axial angle of  $20^\circ$  the uniaxial indicatrix of calcite must be distorted by about one percent. Since for many similar ionic crystals  $P_{ijrs} \sim .1$ ,<sup>13</sup> equation (V.1) implies that a strain of ten percent is required to produce such a large axial angle. The strain would be relieved by e-twinning; Hooke's law would fail.

It was shown in the preceeding section that this twinning on a submicroscopic scale will produce a biaxial indicatrix. In a transmission electron microscope study of Alpine carbonate rocks, Barber and Wenk<sup>14</sup> have observed a high density of such microtwins [see Figure (I.1a)]. Figure (IV.3) shows that an axial angle of  $20^\circ$  will occur with only ten percent twinned material when twinning is on a single system.

Calcite is trigonal and has, therefore, three e planes on which it can twin, giving a total of four orientations which can be present with variable volume fractions. With the conventions from the preceeding section ( $twin_1$  = host), the volume averaged dielectric tensor is

$$\epsilon' = \sum_{i=1}^4 f_i R_i \epsilon_1 R_i^{-1} \quad (V.2)$$

where

$$\underline{\epsilon}_1 = \begin{pmatrix} \epsilon_\gamma & 0 & 0 \\ 0 & \epsilon_\gamma & 0 \\ 0 & 0 & \epsilon_\alpha \end{pmatrix}$$

and  $\underline{R}_1 = \underline{I}$ . For  $i > 1$

$$\underline{R}_i = \begin{pmatrix} \cos\phi_i & -\sin\phi_i \cos R & -\sin\phi_i \sin R \\ \sin\phi_i & \cos\phi_i \cos R & \cos\phi_i \sin R \\ 0 & -\sin R & \cos R \end{pmatrix}$$

with  $\phi_2 = 0$ ,  $\phi_3 = 120^\circ$ , and  $\phi_4 = 240^\circ$ . The angle  $R (= 52.5^\circ)$  is twice the angle between the normal to the e plane and the c axis in untwinned calcite. When  $f_3 = f_4 = 0$ , the results for twinning on a single system are recovered.

The computer solution for the eigenvectors and eigenvalues of (V.2) was used to find the orientation of the axial plane and the value of the axial angle for selected values of the volume fractions. The results are in Table (V.1). The orientation angles are defined in Figure (V.1).  $\theta_1$  is the angle between  $\underline{a}_1$  and the trace of the axial plane in the plane normal to  $\underline{c}_1$ .  $\theta_2$  is the angle between  $\underline{c}_1$  and the axial plane.  $\theta_2$  was called simply  $\theta$  in the last section.  $\theta_3$  is the angle between the trace of the axial plane in the plane normal to  $\underline{c}_1$  and the  $n_\alpha$  axis.

In order to test this theory two experimentally deformed calcite crystals were analyzed in some detail. Optically biaxial grains were selected with no visible microscopic twins in a thin section. First the optical properties were measured on the universal-stage

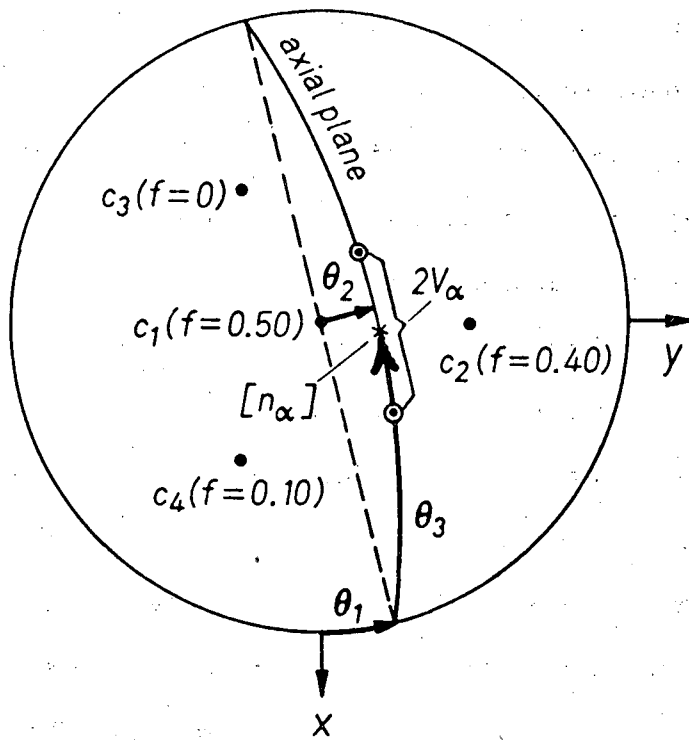
Table (V.1). Angles defining the indicatrix of multiply twinned calcite for selected volume fractions.

Volume fractions				Refractive indices axes of indicatrix			$2V_\alpha$	Orientation angles		
$f_1$	$f_2$	$f_3$	$f_4$	$n_\alpha$	$n_\beta$	$n_\gamma$		$\theta_1$	$\theta_2$	$\theta_3$
1.0	0	0	0	1.486	1.658	1.658	0°	0°	0°	90°
0.95	0.05	0	0	1.492	1.653	1.658	19	0	1.5	90
0.90	0.10	0	0	1.497	1.648	1.658	27	0	3.2	90
0.90	0.05	0.05	0	1.497	1.650	1.656	19	-30	0	91.5
0.85	0.15	0	0	1.502	1.644	1.658	33	0	5.1	90
0.85	0.10	0.05	0	1.503	1.646	1.655	26	-16	2.0	92.0
0.85	0.05	0.05	0.05	1.503	1.650	1.650	0	0	0	90
0.80	0.20	0	0	1.507	1.639	1.658	38	0	7.2	90
0.80	0.15	0.05	0	1.508	1.642	1.655	33	-11	4.1	92.2
0.80	0.10	0.05	0.05	1.509	1.645	1.650	20	0	1.7	90
0.80	0.10	0.10	0	1.508	1.643	1.653	30	-30	0	93.3
0.75	0.20	0.05	0	1.513	1.637	1.655	38	-9	6.4	92.3
0.75	0.15	0.10	0	1.513	1.638	1.653	35	-22	2.3	94.0
0.75	0.15	0.05	0.05	1.514	1.640	1.650	29	0	3.8	90
0.75	0.05	0.10	0.10	1.514	1.643	1.648	22	-90	0	88.2
0.70	0.20	0.10	0	1.518	1.634	1.652	40	-18	4.8	94.6
0.70	0.20	0.05	0.05	1.519	1.636	1.650	36	0	6.1	90
0.70	0.10	0.10	0.10	1.520	1.642	1.642	0	0	0	90
0.70	0	0.15	0.15	1.519	1.635	1.651	39	-90	0	84.6

XBL 773-8171

0 0 0 0 4 7 1 0 8 8 2

35



XBL 773-8147

Figure (V.1). Stereogram defining the orientation angles  $\theta_1$ ,  $\theta_2$ , and  $\theta_3$ .

microscope, both  $2V_a$  and the orientation of the axial plane relative to the thin section in conoscopic mode. Then the crystals were removed from the thin section and analyzed in the same orientation on an x-ray precession camera to check for submicroscopic twinning. In precession  $0kl$  photographs there are weak additional reflections which can be attributed to twinning on  $(018) = e^*$  [see Figure (V.2)]. The twin of the strong reflection  $0\bar{1}\bar{4}$  is marked on the photographs. A higher layer precession c photograph through the additional  $\{01\bar{4}\}$  spots shows that in both samples twinning occurred on all three systems. Examination of specimen VW163 with the electron microscope confirmed the existence of microtwins [Figure (I.1a)]. The intensities of the x-ray reflections were then measured on a densitometer thereby determining the volume fraction of each twin orientation. The properties of the composite indicatrix were then calculated from the volume fractions and (V.2). The calculations are summarized in Table (V.2) which also includes information on the calcite samples and their measured optical parameters and volume fractions. The uncertainty in the calculated axial angle is estimated to be  $1-2^\circ$  due to the uncertainties of the measured volume fractions.

There is qualitative agreement between theory and experiment. Unfortunately the difficulty in making accurate measurements with the polarizing microscope precludes the possibility of establishing this relationship more precisely.

\* Laue indices (notice the four times larger c/a ratio in the x-ray unit cell as compared with the morphological unit cell).

0 0 0 0 4 7 1 0 8 8 3

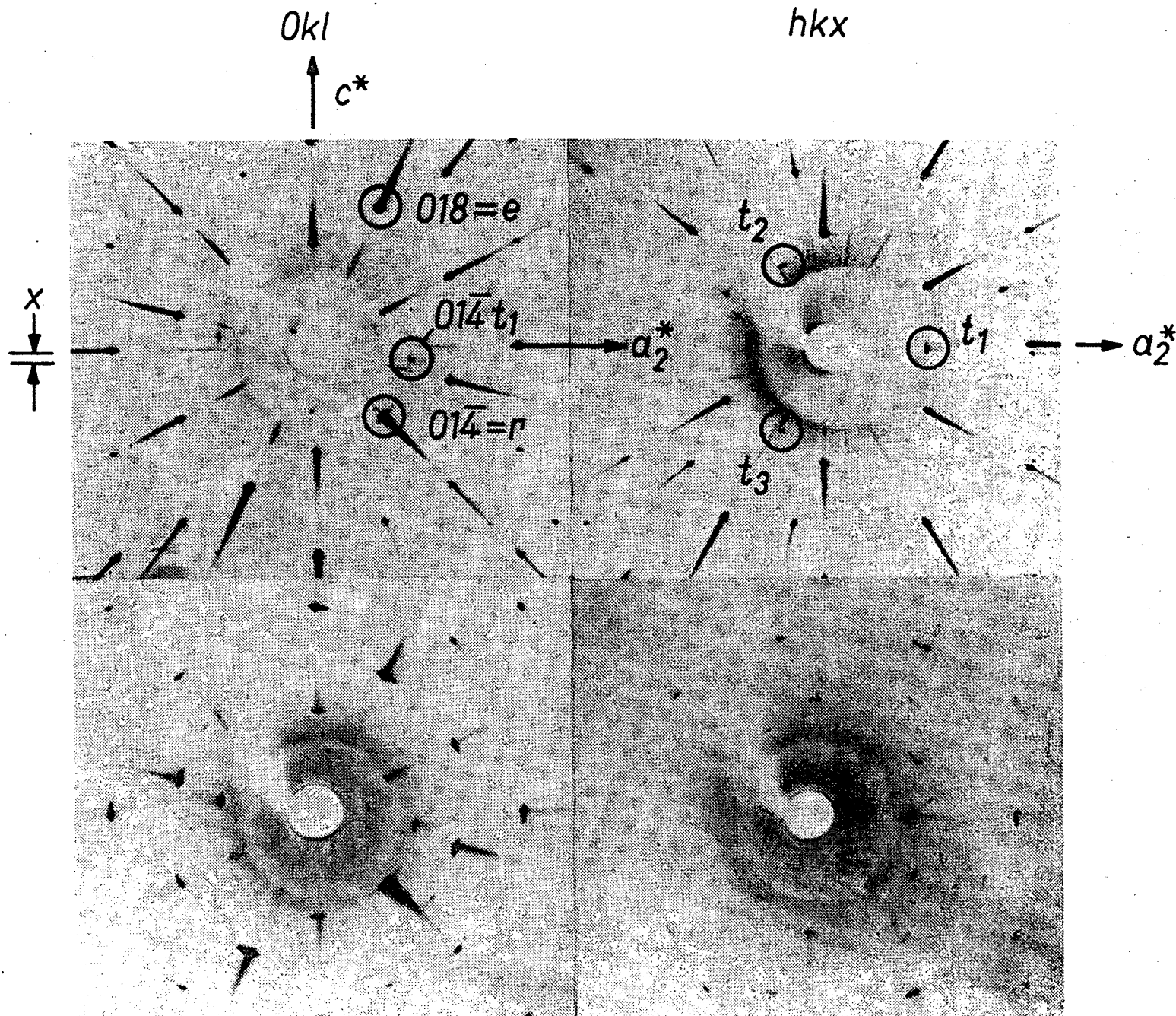


Figure (V.2). Precession photographs showing twinning on  $\{018\} = e$ . Mo radiation, Zr filter.

XBB 773-2689

Table (V.2). Specifications of calcite samples used in this study; observed and calculated optical parameters.

Sample number	VW 163	212-231
Locality	Iceland spar Chihuahua	Yule marble
Conditions of deformation	25°C, 1 kbar compression $\perp c$	25°C, 9 kbar extension
Amounts of twinned material		
$f_1$ (host)	81.3%	89.8%
$f_2$	6.7%	7.4%
$f_3$	5.8%	1.6%
$f_4$	6.3%	1.3%
$2V_\alpha$ measured on universal stage	5-10°	25°
$2V_\alpha$ calculated	8°	21°
Orientation angles, calculated	$\theta_1$ $\theta_2 = 0$ $\theta_3$	17° 0.16° 89.8°
Orientation of axial plane measured on universal stage	$\theta_1$ $\theta_2, \theta_3$	5-25° $\theta_2 \sim 0^\circ, \theta_3 \sim 90^\circ$
(not measured with significant accuracy)		

XBL 773-8157

There is a qualitative feature of the data in Table (V.2) that provides additional support for the theory. Notice that the larger observed axial angle  $2V_\alpha$  is associated with the sample with the smaller amount of twinned material relative to the host. In spite of the larger amount of twinning, sample VW163 is more nearly uniaxial.

The measured volume fractions provide an explanation: the larger amount of twinned material in sample VW163 is distributed more uniformly among the three equivalent systems thereby causing a smaller deviation from three-fold symmetry. Therefore, the experimental correlation between the deviation from uniaxial behavior of light and the deviation from three-fold symmetry in the distribution of twinned material provides strong evidence that e-twinning is the cause of biaxiality in calcite.

Other qualitative predictions of the theory have been confirmed. In the last section it was shown that for twinning on a single system the axial plane can be obtained from the plane containing  $\underline{c}_1$  and  $\underline{a}_1$  by a rotation of  $\theta$  degrees about  $\underline{a}_1$  toward  $\underline{b}_1^*$ . The  $n_\alpha$  axis can be obtained from  $\underline{c}_1$  by the same operation. By examining Table (V.2) it is clear that the same qualitative predictions are obtained when one system predominates. In his comprehensive universal-stage study Turner<sup>15,16</sup> found that the axial plane is in most cases inclined slightly towards and roughly normal to  $\underline{b}_1^*$  indicating according to the theory that one system predominates. Only when  $2V_\alpha$  is large does the model predict that this inclination is large enough to be measured. In crystals with small  $2V_\alpha$  Turner found no significant deviation of

$n_\alpha$  from  $c_1$ . But among a few cases of high  $2V_\alpha$  ( $35-45^\circ$ ), he finds that whenever the orientation of the crystal and indicatrix can be established unequivocally  $n_\alpha$  is indeed inclined towards  $b_1^*$  by  $5-10^\circ$ .

Thus experimental evidence concerning both the magnitude of the axial angle and orientation of the axial plane is consistent with the hypothesis that biaxial calcite consists of material which is submicroscopically twinned on  $e$ , and that the volume averaged dielectric tensor can predict the qualitative and some quantitative features of the optical behavior of this material.

This section will end with a discussion of the transition from submicroscopic to macroscopic lamella thickness. In calcite  $e$ -twinning can occur on all scales; the lamella thickness  $L$  ranges from submicroscopic ( $L < \lambda$ ) thru microscopic ( $\lambda < L < 5\lambda$ ) to macroscopic ( $5\lambda < L$ ) where  $\lambda \approx .0005$  mm is the wavelength of light. The question arises: as the domain size increases how do the experimental optical properties of the composite vary? In particular, how does the true biaxial behavior in the submicroscopic region evolve to the complex behavior of the macroscopic region? Also, can the volume averaged dielectric tensor be used to predict accurately the optical properties of crystals with domains larger than the wavelength of light?

The work of Turner<sup>16</sup> can help answer these questions. His study was concerned with the optical properties of calcite with  $e$ -twins which were visible with an optical microscope ( $\lambda < L < 5\lambda$ ). He examined specimens in which only one of the three equivalent  $e$ -twin systems were present in addition to the host. He found that when the

thickness of the twin lamella was less than .0015 mm ( $\sim 3\lambda$ ), the specimens produce a conoscopic figure which appears essentially biaxial. Although the figure is distorted somewhat, the axial angle and orientation of the axial plane can be defined and measured. For wider lamellae the distortion becomes increasingly pronounced and completely disrupts the biaxial configuration of the conoscopic figure if the lamellae exceed .0025 ( $\sim 5\lambda$ ) in thickness.

In the same work Turner describes a simple theory based on geometric optics which he uses to predict the optical properties of those specimens that have mildly distorted biaxial figures. His theory consists of two conditions which determine the direction of the optic axes. The optic axes are defined in his theory as those directions in which the birefringence of one lamella type cancels the birefringence of the other type. The first condition requires that the vibration directions in each lamella are parallel for a ray propagating along an optic axis. The second condition requires that the difference in the two refractive indices associated with this ray times the lamella thickness is equal and opposite in sign when calculated for each layer.

The first condition yields a relationship between the axial angle and the orientation of the axial plane which is identical with the predictions of the volume averaged dielectric tensor in the limit of small lamella thickness. Even for the case of maximal twinning (1/2 host, 1/2 twin) the models differ on this point by amounts too small to measure. The second condition yields a relationship between

the fraction of twinned material and the optic angle. Because the second condition uses a concept from geometric optics (the refractive index) one would expect discrepancies between Turner's model and the volume averaged dielectric tensor on this point. This is the case, for Turner's model consistently predicts an axial angle about three degrees larger. Both models reproduce the qualitative features of Turner's experimental data, although his model predicts values for the axial angle within experimental error ( $\pm 2^\circ$ ), and the volume averaged model does not.

This discussion indicates that the volume averaged dielectric tensor can be used to predict successfully the qualitative and some quantitative features of the indicatrix whenever the domain size is small enough to produce a regular conoscopic figure, whether or not the domains are negligible compared to the wavelength of light.

## VI. Alkali Feldspars ( $\text{Na, K}\text{AlSi}_3\text{O}_8$ )

It has long been known, particularly through fundamental studies of Laves,<sup>17,18</sup> that submicroscopic intergrowths play an important role in the structure of feldspars. These submicroscopic features have been recently imaged with the electron microscope. Composite feldspar structures with lamella widths on the order of 50-5000 Å should provide additional test cases for the theory of the volume averaged dielectric tensor.

Laves proposed that monoclinic orthoclase ( $\text{Na, K}\text{AlSi}_3\text{O}_8$ ) consists of triclinic microcline ( $\text{Na, K}\text{AlSi}_3\text{O}_8$ ) which is submicroscopically twinned after the albite and pericline laws as a result of a symmetry change during transition from a disordered to an ordered state. Recently some orthoclase has been found to be cryptoperthite in which twinning is combined with a lamellar exsolution of K and Na-rich phases resulting in a complicated submicroscopic intergrowth of K feldspar and albite  $\text{NaAlSi}_3\text{O}_8$  [see Figure (I.1b)]. The various textures which develop are a function of the geological history; they have been reviewed by Willaime *et al.*<sup>19</sup>

In this section the optical properties of several of these composites are calculated with the volume averaged dielectric tensor and compared with those of natural orthoclase. For each of three types of microcline ( $M_1$ ,  $M_2$ ,  $M_3$ ) the following models were calculated:

### I. $\text{Or}_{\text{ai}}$

50% Microcline ( $M_i$ )

50% Microcline twinned after the albite law ( $M_{\text{ai}}^1$ )

II.  $Or_{api}$

25% Microcline ( $M_i$ )

25% Microcline twinned after the albite law ( $M_{ai}$ )

25% Microcline twinned after the pericline law ( $M_{pi}$ )

25% Microcline twinned after the pericline  
and albite laws ( $M_{api}$ )

III.  $P_i$  (cryptoperthite)

25% Microcline ( $M_i$ )

25% Microcline twinned after albite law ( $M_{ai}$ )

25% Albite (Ab)

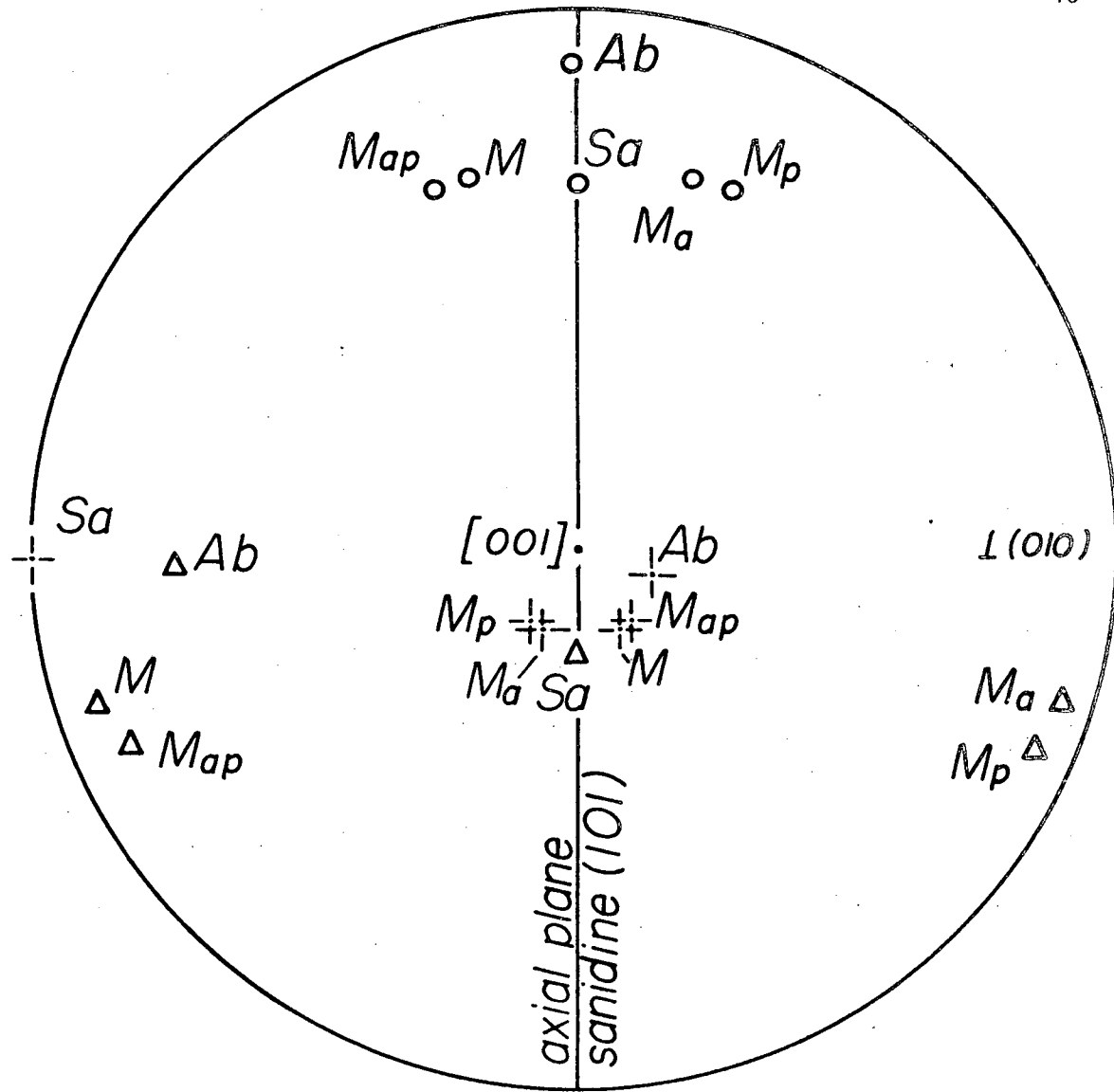
25% Albite twinned after albite law ( $Ab_a$ )

For each calculation the untwinned microcline ( $M_i$ ) was designated the host. The experimental optical parameters for albite and the three types of microcline are listed in Table (VI.1). The optical data for the albite and percline twins were calculated with the data in Table (VI.1) and the twinning geometry.  $M_3$  is maximum microcline which is characterized by a high degree of Al/Si order;  $M_1$  and  $M_2$  are intermediate microclines characterized by partial Al/Si disorder. Figure (VI.1) is a stereogram illustrating the principal axes for twinned and untwinned maximum microcline ( $M_3$ ), albite, and for comparison purposes monoclinic sanidine (Sa),  $KAlSi_3O_8$ .

Unfortunately, good optical data on alkali feldspar are scarce. Accurate measurement of all optical parameters coupled with a good chemical and structural description have rarely been done with the same specimen. This limits the comparisons that can be made between

Table (VI.1). Optical data of alkali feldspar. Microcline data is from Marfunin.<sup>20</sup> Low albite data is from Burri, Parker and Wenk.<sup>22</sup>  $\rho_\alpha$  and  $\phi_\alpha$  are the Goldschmidt angles of  $n_\alpha$ , etc. [see Section IV].

	M <sub>1</sub>	M <sub>2</sub>	M <sub>3</sub>	Ab
$\rho_\alpha$	70.80°	71.00°	71.18°	84.00°
$\phi_\alpha$	259.0°	256.0°	252.91°	270.80°
$\rho_\beta$	19.22°	19.10°	19.04°	17.50°
$\phi_\beta$	76.0°	69.86°	63.74°	161.40°
$\rho_\alpha$	89.07°	88.10°	87.18°	73.60°
$\phi_\gamma$	168.68°	165.35°	161.95°	2.60°
$n_\alpha$	1.5203	1.5195	1.5200	1.5287
$n_\beta$	1.5240	1.5233	1.5233	1.5327
2V <sub>y</sub>	114.0°	106.0°	95.77°	78.0°



XBL 774-8385

Figure (VI.1). Stereogram showing the measured principal axes of maximum microcline (M), albite (Ab), and sanidine (Sa). Circles:  $n_\alpha$ , crosses:  $n_\beta$ , triangles:  $n_\gamma$ . Data from Table (VI.1).

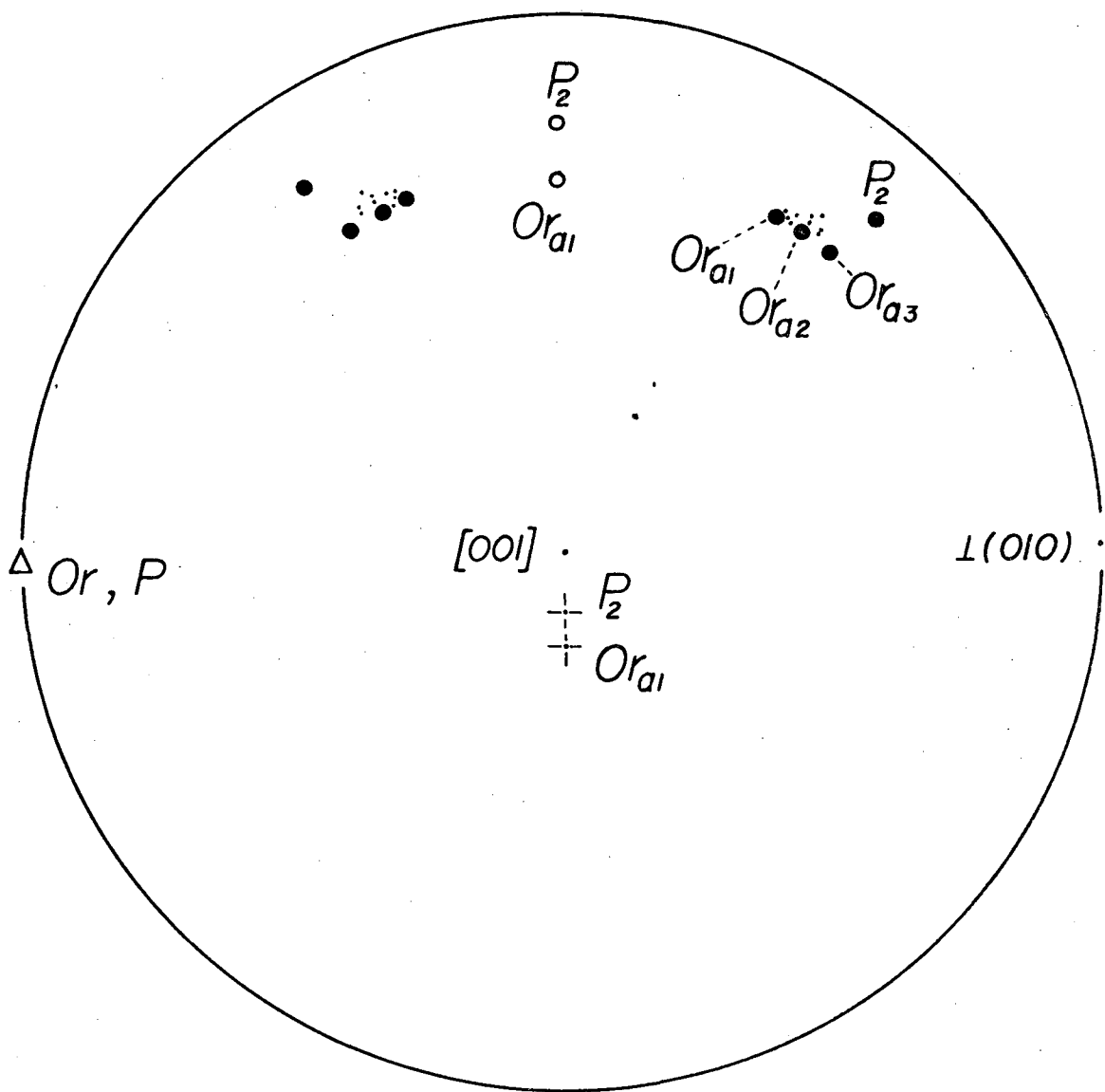
measured and calculated optical parameters. However, it was possible to find good data on the directions of the optic axes for natural orthoclase.<sup>20</sup>

Figure (VI.2) is a stereogram illustrating the calculated (large solid dots) and measured (small dots) optic axes. Because the three models for cryptoperthite ( $P_i$ ) gave nearly the same results, only  $P_2$  has been plotted. Also, the results for  $Or_{api}$  were almost identical to  $Or_{ai}$  so only the latter are shown.

That the differences between observation and  $Or_{ai}$  are less than the differences between observation and  $P_i$  can be understood by noting that the geological origin (non-volcanic) of these natural orthoclase specimens make it unlikely that they are cryptoperthites.

Notice also that the measured axial planes are on the average slightly more inclined from [001] than the models  $Or_{ai}$ . This can be attributed to the higher sodium (albite:  $NaAlSi_3O_8$ ) content of the natural orthoclase (~25%) compared to that of the microclines used in the calculations (~10%).

The models with intermediate microcline ( $Or_{a1}$ ,  $Or_{a2}$ ) are slightly better than that with maximum microcline ( $Or_{a3}$ ). Intermediate microcline has an Al/Si disorder; ideal maximum microcline does not. From this it appears that perhaps some natural orthoclase consists of a mixture of microcline twins with a partially disordered Al/Si distribution. Such a structure is a compromise between the view of Laves that orthoclase has a submicroscopic twin texture produced during ordering of sanidine and the model of Barth<sup>21</sup> which interprets orthoclase as a monoclinic feldspar structure with partial Al/Si order.



XBL 773-8160

Figure (VI.2). Calculated (large solid dots) and measured (small dots) optic axes for orthoclase. Other symbols defined in Figure (VI.1). Measured optic axes are from Marfunin.<sup>20</sup>

Unfortunately these conclusions are based on few data. As with submicroscopically twinned calcite more experimental work is needed. Specifically, universal-stage, TEM, x-ray, and microprobe measurements must be made on the same specimen. This data would support or disprove the above conclusions and provide a more rigorous test of the volume averaged dielectric tensor.

## VII. Plagioclase (Ca, Na) (Al, Si)AlSi<sub>2</sub>O<sub>8</sub>

In this section the volume averaged dielectric tensor will be applied to the plagioclase feldspars. This series includes anorthite ( $An = CaAl_2Si_2O_8$ ), albite ( $Ab = NaAlSi_3O_8$ ), and all intermediate phases.  $Ca^{+2}Al^{+3}$  substitutes for  $Na^{+1}Si^{+4}$ . The standard notation for a member of this series is  $Ab_xAn_y$  with  $x + y = 100$ , or more simply  $Abx$  or  $Any$ .

There are actually two complete series, a high and low temperature form.

It has become increasingly clear in recent years, mainly from electron microscopic studies and particularly the pioneering work of Nissen,<sup>23-25</sup> that low (temperature) plagioclase is not a simple solid solution. Apart from crystals with compositions near An0-2.5, An35, An65, and An92-100, most low plagioclase consists of an intergrowth of two chemically different phases (for a review see Champness and Lorimer<sup>26</sup>). In slowly cooled igneous rocks, the two phases form coherent exsolution lamellae spaced 500 - 10000 Å and rarely larger [see Figure (I.1c)], in volcanic rocks a fine tweed structure is often present [see Figure (I.1d)], and in metamorphic rocks an intergrowth often on a very fine scale is formed during growth.<sup>27</sup>

An0-2.5, An35, An65, and An92-100 appear homogeneous with an electron microscope, and are usually assumed to be phases in which albite and anorthite are completely miscible. On a phase diagram the regions between An2.5 and An35, An 35 and An65, An65 and An92 are known respectively as the peristerite, labradorite and bytownite miscibility gaps. In contrast, albite and anorthite are completely miscible throughout the entire high plagioclase series.

The orientation of the indicatrix in low plagioclase changes by rotations of over 90° between albite and anorthite, and thus has been used extensively in the determination of chemical composition and structural state, but the nature of this movement has not been explained quantitatively. In an attempt at such an explanation a model based on the volume averaged dielectric tensor was calculated for low plagioclase.

First a comment about coordinate systems should be made. The theory requires that orientation angles of each phase be measured relative to the same cartesian system. However, the data in Table (VII.1) and the experimental data points in Figures (VII.1) and (VII.2) were measured relative to a series of different cartesian systems. For example the An2.5 data in Table (VII.1) were measured relative to a system derived from the An2.5 crystal axes:

$$\begin{aligned}\hat{\underline{z}} &= \hat{\underline{c}} \\ \hat{\underline{y}} &= \hat{\underline{b}}^* \\ \hat{\underline{x}} &= \hat{\underline{y}} \times \hat{\underline{z}}\end{aligned}$$

whereas the An35 data were measured relative to an analogous system defined from the An35 crystal axes. However, the difference between the various systems is negligible. If a phase in one of the miscibility gaps is subjected to an x-ray analysis, there is no doubling of reflections due to the overlap of dissimilar reciprocal lattices. Therefore, all cartesian systems were assumed to be identical, and all data were assumed to have been measured relative to one system.

For the calculation of the optical properties of low plagioclase, the following model was adopted: the lamellae of the peristerite gap were assumed to be pure An2.5 and An35. That is for  $2.5 \leq X \leq 35$

$$\epsilon_{AnX} = f_1 \epsilon_{An2.5} + f_2 \epsilon_{An35}$$

with

$$f_1 = \frac{35-X}{32.5}$$

$$f_2 = 1 - f_1.$$

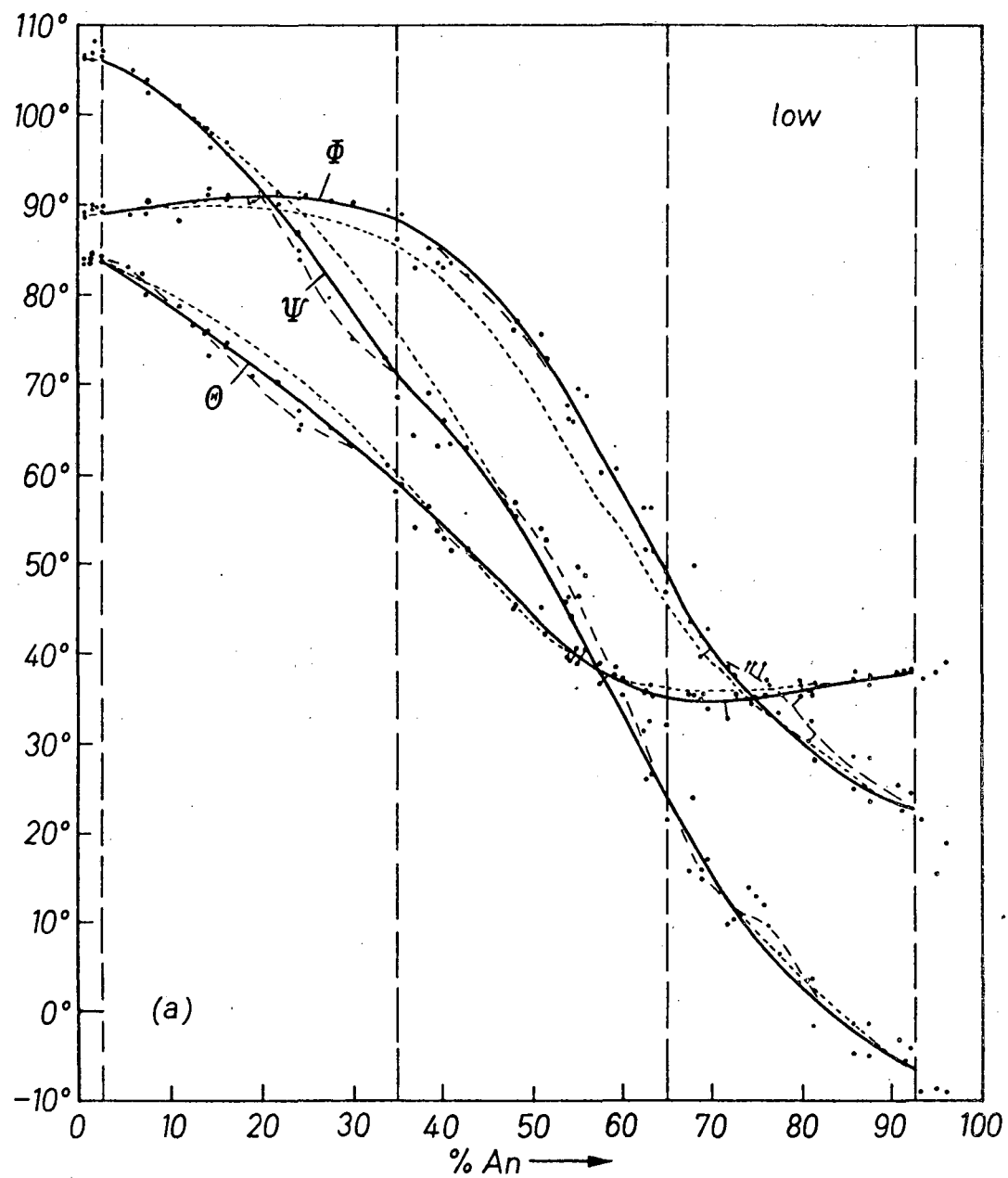
Similarly, the lamellae of the labradorite gap were assumed to be pure An35 and An65, and those of the bytownite gap were assumed to be An65 and An92.5. This specification of the dielectric tensor will be referred to as the lamella model.

The dielectric tensors for the pure phases were calculated by the methods of Section IV from the data in Table (VII.1) (from Burri, Parker and Wenk<sup>22</sup>). This work will be referred to as BPW). The predictions of the lamella model for low plagioclase are displayed in Figures (VII.1) and (VII.2). Figure (VII.1) illustrates the change in orientation of the indicatrix measured by Euler angles defined in BPW. Figure (VII.2) is a similar diagram showing the change in the axial angle throughout the low plagioclase series. In both diagrams the solid curve is the result of the calculation. The long-dashed curve is an empirical determination curve which was drawn as a best fit to the measured data points. Both the empirical curve and the experimental points are from BPW. The short-dashed curve will be discussed later in this section.

Table (VII.1). Optical parameters of end members of miscibility gaps in the plagioclase series.  $\rho$  and  $\phi$  are Goldschmidt angles. From BPW.

	albite, An 2.5		andesine, An 35		labradorite, An 65		anorthite, An 92.5	
	$\phi$	$\rho$	$\phi$	$\rho$	$\phi$	$\rho$	$\phi$	$\rho$
low	$n_x$	269.2	83.9	268.3	58.9	228.7	34.7	202.4
	$n_\beta$	19.2	17.4	122.1	36.0	118.7	76.7	297.6
	$n_\gamma$	177.4	73.8	8.4	73.7	20.4	58.6	30.6
	$2V_\gamma$	78.1		87.0		86.0		101.8
	$n_x$	1.5290		1.5464		1.5614		1.5730
	$n_\beta$	1.5391		1.5539		1.5693		1.5853
high	$n_x$	274.7	72.8	271.2	62.0	233.2	35.5	200.6
	$n_\beta$	59.9	22.2	133.6	35.8	120.5	74.6	296.5
	$n_\gamma$	180.4	76.4	12.6	69.6	20.9	58.9	29.8
	$2V_\gamma$	129.8		93.6		80.0		101.0
	$n_x$	1.5284		1.5464		1.5612		1.5735
	$n_\gamma$	1.5363		1.5539		1.5694		1.5864

XBL 773-8155

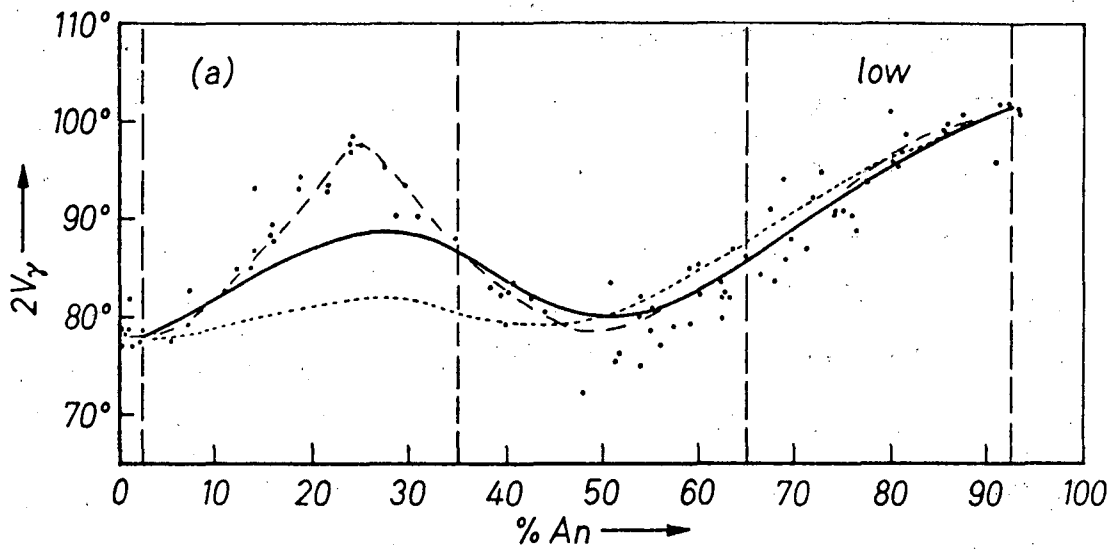


XBL 773-8153

Figure (VII.1). Experimental and calculated Euler angles for the indicatrix of low plagioclase.

0 0 0 0 4 7 1 0 8 9 2

55



XBL 773-8149

Figure (VII.2). Experimental and calculated axial angle for low plagioclase.

The agreement between the calculated curve and the data points is good. However, it is important to note that the lamella model forced agreement with the empirical curve at An35 and An65 in addition to the end points. The largest discrepancy is the axial angle in the peristerite gap.

In an attempt to remove this discrepancy, the refractive indices of the end members An35 and An2.5 were varied by the probable uncertainty ( $\pm .001$ ) but the calculated parameters did not change on the scale of the figures. Taking into account the surface charge induced at the lamella boundaries (normal vector near  $(0\bar{4}1)$ ,  $\rho_N = 79^\circ$ ,  $\phi_N = 175^\circ$  for peristerite gap) by using the exact dielectric tensor (III.9) did lessen the discrepancy by  $1-2^\circ$  leaving the Euler angles unchanged on the scale of the figure. Although the discrepancy remains it is not that significant, for the axial angle is extremely sensitive to changes in the refractive indices of the composite indicatrix.

As discussed in Section III, the volume averaged dielectric constant has been used to predict the optical properties of liquid solutions. In that section it was shown that this theory may work well for a solid solution of cubic phases. It would be interesting to see how well the theory works for the solid solution series of triclinic high plagioclase. A calculation was done in which the dielectric tensor of high plagioclase was

$$\underline{\epsilon}_{AnX} = f_1 \underline{\epsilon}_{An2.5} + f_2 \underline{\epsilon}_{An92.5}$$

for  $2.5 \leq X \leq 92.5$  with

$$f_1 = \frac{92.5-x}{90.}$$

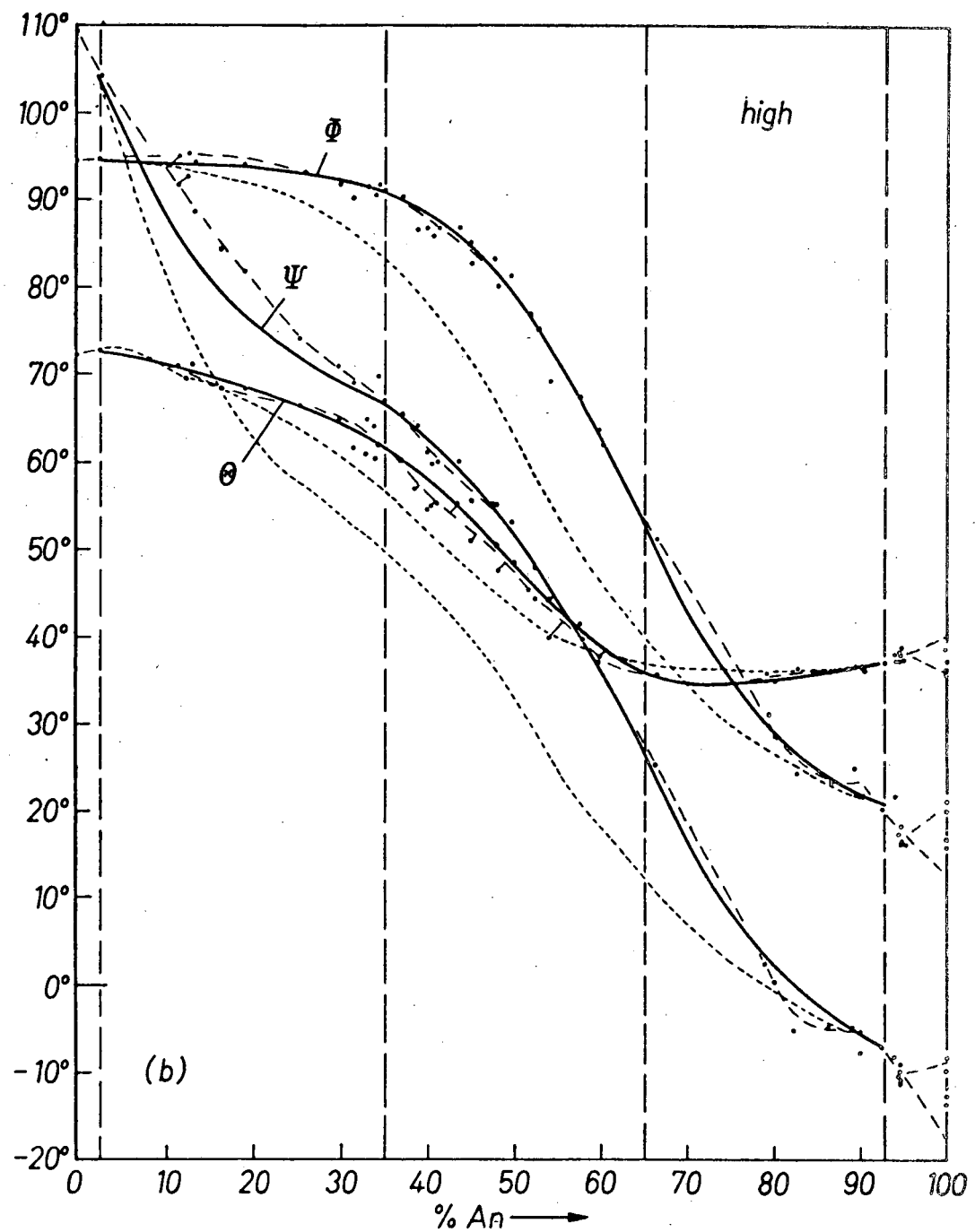
$$f_2 = 1 - f_1.$$

This specification of the dielectric tensor will be referred to as the solution model.

The results of the calculation are displayed in Figures (VII.3) and (VII.4) as short-dashed lines. The empirical curve (long-dashed) and data points are from BPW. The calculated orientation angles differ from the data points by at most 15-20°. The agreement for the axial angle is good.

The agreement was better than expected. A possible reason is that the volume averaged dielectric tensor provides an interpolation scheme that has the advantage of including the geometry of the system. This scheme is better than simply connecting the end members with straight lines because the latter method is algebraic and ignores the geometry of the system. This geometry is built into the tensor nature of the interpolation scheme of the solution model. The agreement is more impressive when one notes the complexity of the optical migration from albite to anorthite. To a first approximation the migration can be described as rotations of the indicatrix about three different fixed axes.

For the purposes of comparison the models described for low and high plagioclase were applied to high and low plagioclase respectively. That is, the optical parameters of low plagioclase were calculated with the solution model, and those of high plagioclase with the lamella model.

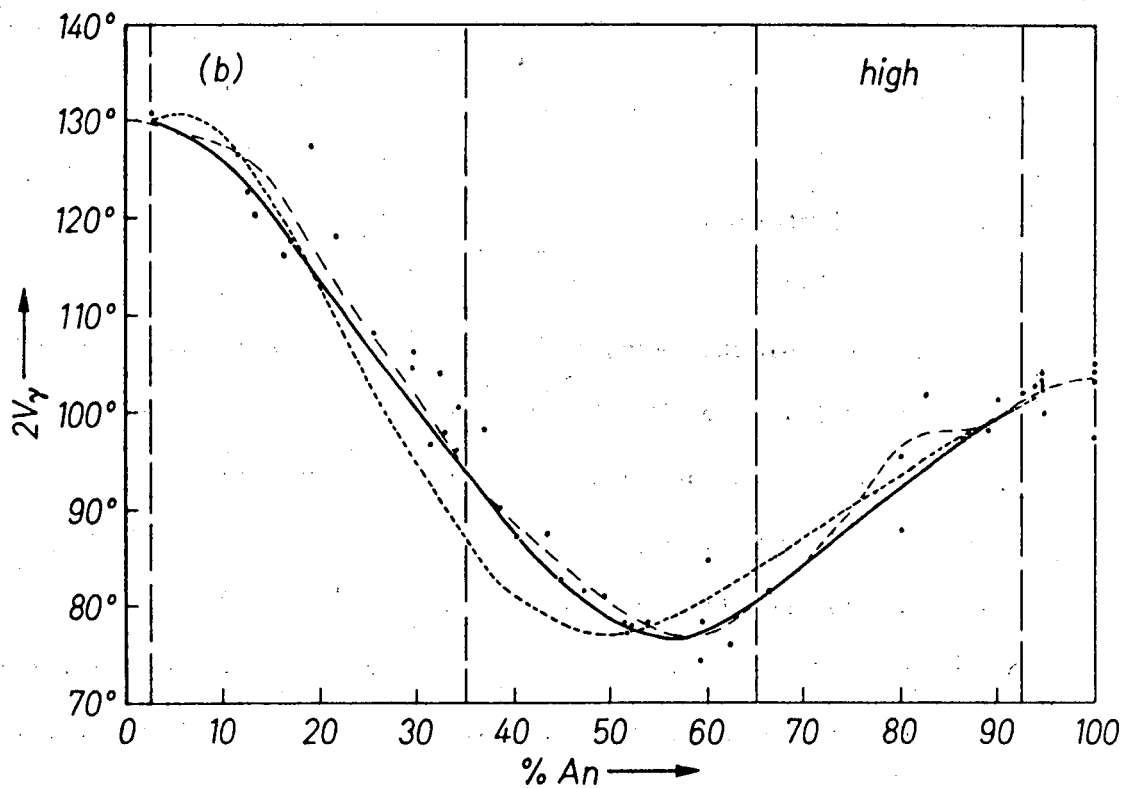


XBL 773-8154

Figure (VII.3). Experimental and calculated Euler angles for the indicatrix of high plagioclase.

0 0 0 0 4 7 1 0 8 9 4

59



XBL 773-8151

Figure (VII.4). Experimental and calculated axial angle for high plagioclase.

For high plagioclase the lamella model [solid curve in Figures (VII.3) and (VII.4)] improved the agreement, but this was expected.

The lamella model forces the theoretical curve to agree with the empirical curve at two additional points, An35 and An65. However, even with the additional constraints the lamella model does not fit the orientation data as well as the same model when applied to low plagioclase.

For low plagioclase, the solution model [short-dashed curve in Figures (VII.1) and (VII.2)] gives results that are remarkably close to that of the lamella model considering the constraints at An35 and An65 have been removed. A possible explanation can be found by considering the phases An35 and An65. Because the composite dielectric tensor is linear in the volume fractions, it can easily be shown that if the predictions of the solution model matched the empirical curves at An35 and An65, then the solution model would be identical to the lamella model. Therefore, the reason the solution model and lamella model are nearly the same for low plagioclase can be traced to the fact that the solution model accurately predicts the optical properties of An35 and An65. The question remains - why does the solution model work well for the homogeneous phases An35 and An65 while giving poorer results when applied to the same homogeneous phases in the high series? In both cases poor results are expected because the volume averaged dielectric tensor was derived for composites with small domains, not solid solutions.

A possible explanation for the better than expected results for low plagioclase can be found when one notes that although low An35 and low An65 appear homogeneous with the electron microscope, they do not have the complete thermal disorder which characterizes the high series. Recent work<sup>28,29</sup> has shown low An35 and An65 have a superstructure in which layers of albite unit cells alternate with layers of anorthite unit cells. These lamellae are a few unit cells wide. Therefore, the solution model works for low An35 and low An65 because they are lamellar composites of albite and anorthite.

### VIII. Conclusions

It has been demonstrated that the volume averaged dielectric tensor can predict the qualitative and many quantitative features of the geometric optical properties of material composed of small domains with differing orientation and chemical composition. However, it is difficult to say more because complete optical, structural, and chemical measurements have rarely been done on the same specimen in the studied mineral systems. Perhaps a carefully prepared synthetic lamellar composite could provide a rigorous test of the theory. It might be possible with such a system to see the effect of the surface charge, that is, obtain accurate predictions only by using the exact result (III.9) for the dielectric tensor. This system could answer the question of the upper and lower limits on the domain size for the applicability of the theory. The calcite system has indicated that the theory can describe many features of the optical behavior when the lamella thickness is larger than the wavelength of light as long as the optical properties are those of an optically homogeneous material. The study of the phases low An35 and An65 indicates that the theory can work well for lamella only a few unit cells wide.

The high plagioclase series has shown that the theory can be used as a first approximation to describe the optical properties of some solid solutions. Its validity is that of an interpolation scheme which considers the geometry of the system.

## IX. References

1. W. L. Brown, C. Willaime et C. Guillemin (1972). Bull. Soc. Franc. Mineral. Crystallogr., 95, 429-436.
2. H. -R. Wenk, M. Ulbrich and W. F. Müller (1972). "Proc. Third Lunar Sci. Conf.", Suppl. 3. Geochim. Cosmochim. Acta. Vol. 1, 569-579.
3. F. Donald Bloss (1961). "An Introduction to the Methods of Optical Crystallography", p. 160-162. Holt, Rinehart and Winston, New York.
4. J. F. Nye (1969). "Physical Properties of Crystals, their Representation by Tensors and Matrices", p. 237-238. Oxford University Press, London.
5. C. Kittel (1970). "Introduction to Solid State Physics", p. 449. Wiley and Sons, New York.
6. C. J. F. Böttcher (1952). "Theory of Electric Polarization", Elsevier, Amsterdam.
7. Reference 3, p. 156.
8. J. L. A. Gillson (1927). Amer. Mineral., 12, 357-360.
9. D. J. Barber and H. -R. Wenk (1973). J. Mat. Sci., 8, 500-508.
10. D. J. Barber and H. -R. Wenk (1976). In "Electron Microscopy in Mineralogy", H. -R. Wenk edit., p. 428-442. Springer, Berlin, Heidelberg, New York.
11. F. J. Turner (1975). Contrib. Mineral. Petrol., 50, 247-252.
12. F. J. Turner (1975). Contrib. Mineral. Petrol., 53, 241-252.
13. Reference 4, p. 243-245.

14. Reference 10.
15. Reference 11.
16. Reference 12.
17. F. Laves (1950). J. Geol., 58, 548-571.
18. F. Laves (1952). J. Geol., 60, 436-450, 549-574.
19. C. Willaime, W. L. Brown and M. Gandais (1976). In "Electron Microscopy in Mineralogy", H. -R. Wenk edit., p. 248-257. Springer, Berlin, Heidelberg, New York.
20. A. S. Marfunin (1966). "The Feldspars: Phase Relations, Optical Properties and Geological Distribution", p. 140. (Tranl. from the Russian edition, 1962). Israel. Progr. Scient. Transl., Jerusalem.
21. T. F. W. Barth (1965). Tschermaks Mineral. petrog. Mitt., 10, 14-33.
22. C. Burri, R. C. Parker und E. Wenk (1967). "Die optische Orientierung der Plagioklase". Birkhäuser, Basel und Stuttgart.
23. H. -U. Nissen (1968). Schweiz. mineral. petrogr. Mitt., 48, 53-55.
24. H. -U. Nissen (1974). In "The Feldspars", MacKenzie and Zussman edits., p. 491-521. Manchester, University Press.
25. H. -U. Nissen, H. Eggmann and F. Laves (1967). Schweiz. mineral. petrogr. Mitt., 47, 289-302.
26. P. E. Champness and G. W. Lorimer (1976). In "Electron Microscopy in Mineralogy", H. -R. Wenk edit., p. 174-204. Springer, Berlin, Heidelberg, New York.

0 0 9 0 4 7 1 0 8 9 7

65

27. E. Wenk, H. -R. Wenk, A. Glauser and H. Schwander (1975).  
Contrib. Mineral. Petrol., 53, 311-325.
28. N. Korekawa and W. Horst (1974). Fortschr. Mineral., 52,  
Beiheftz, 37-40.
29. H. Hashimoto, H. -U. Nissen, A. Ono, A. Kumao, H. Endoh and  
C. F. Woensdregt (1976). In "Electron Microscopy in Mineralogy",  
H. -R. Wenk edit., p. 332-344. Springer, Berlin, Heidelberg,  
New York.

## CHAPTER 2: CALCULATIONS WITH THE POINT-DIPOLE MODEL

## I. Motivations

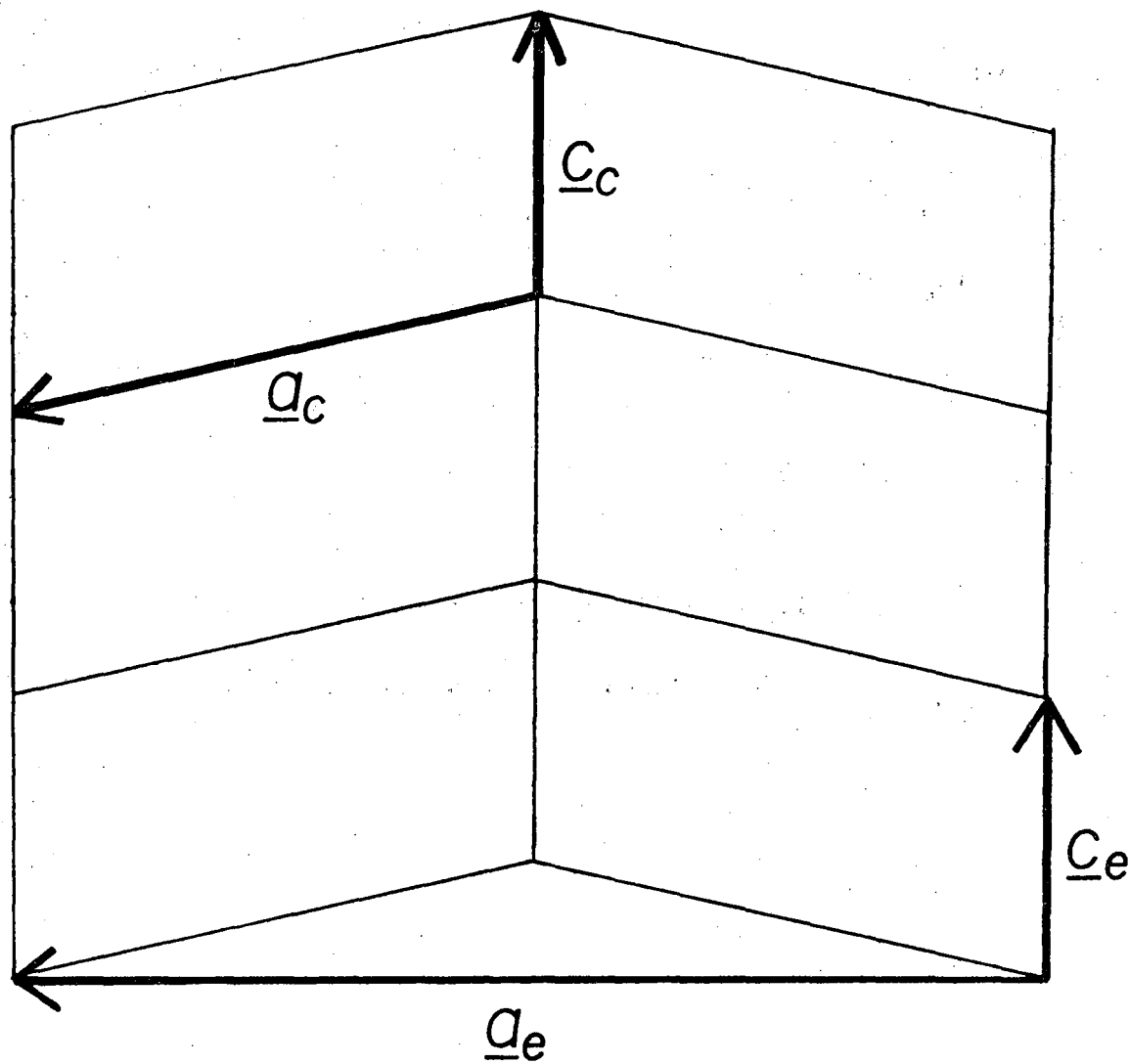
This section will describe the steps which led to the application of the point-dipole model to silicate minerals. It is demonstrated that the volume averaged dielectric tensor fails to describe the optical properties of a composite with lamellae one unit cell wide. This failure shows the need for a theory based on the structure at the atomic scale.

The  $\text{MgSiO}_3$  system provides an example of a lamellar composite in which the layers are one unit cell wide ( $\sim 10 \text{ \AA}$ ) with no strain at the layer interface. Enstatite, the orthorhombic polymorph, can be described as polysynthetically twinned monoclinic clinoenstatite. Figure (I.1a) illustrates the relationship between the unit cells. The two monoclinic units of the orthorhombic cell are related by a reflection in the enstatite c-b plane and a translation by  $b/2$ . The important point is that the monoclinic units can stack in this zig zag fashion with negligible distortion of the atomic positions: one could build a ball and stick model of enstatite by using additional sticks to connect two models of clinoenstatite. Later in this chapter the geometry will be considered in more detail.

The lack of distortion of the atomic positions gives an opportunity to test the volume averaged dielectric tensor on a system with extremely thin lamellae uncomplicated by the disturbing effects of strain. Table (I.1) lists the optical parameters for both polymorphs. The  $n_\gamma$  axis of clinoenstatite is  $\theta$  ( $= 22^\circ$ ) degrees from

0 0 0 0 4 7 1 0 8 9 8

67



XBL 773-8165

Figure (I.1a). The relationship between the unit cells of enstatite and clinoenstatite. The  $b$  axes are parallel,  $b_e = b_c$ .

Table I.1. Optical Parameters for  $\text{MgSiO}_3$ . From Smith.<sup>1</sup>

Enstatite

$n_{\alpha e}$  = 1.650 along  $\underline{b}_e$

$n_{\beta e}$  = 1.652 along  $\underline{a}_e$

$n_{\gamma e}$  = 1.658 along  $\underline{c}_e$

Clinoenstatite

$n_{\alpha c}$  = 1.651 along  $\underline{b}_c$

$n_{\beta c}$  = 1.654 22° from  $\underline{c}_c$  towards  $\underline{a}_c$

$n_{\gamma c}$  = 1.660 ⊥ to other two principal axes

$\underline{c}_c$  in the direction of  $\underline{a}_c$ . If clinoenstatite is designated the host for defining a cartesian system

$$\hat{\underline{z}} = \underline{c}_c$$

$$\hat{\underline{y}} = \underline{b}_c$$

$$\hat{\underline{x}} = \hat{\underline{y}} \times \hat{\underline{z}}$$

the dielectric tensor for this phase is represented by

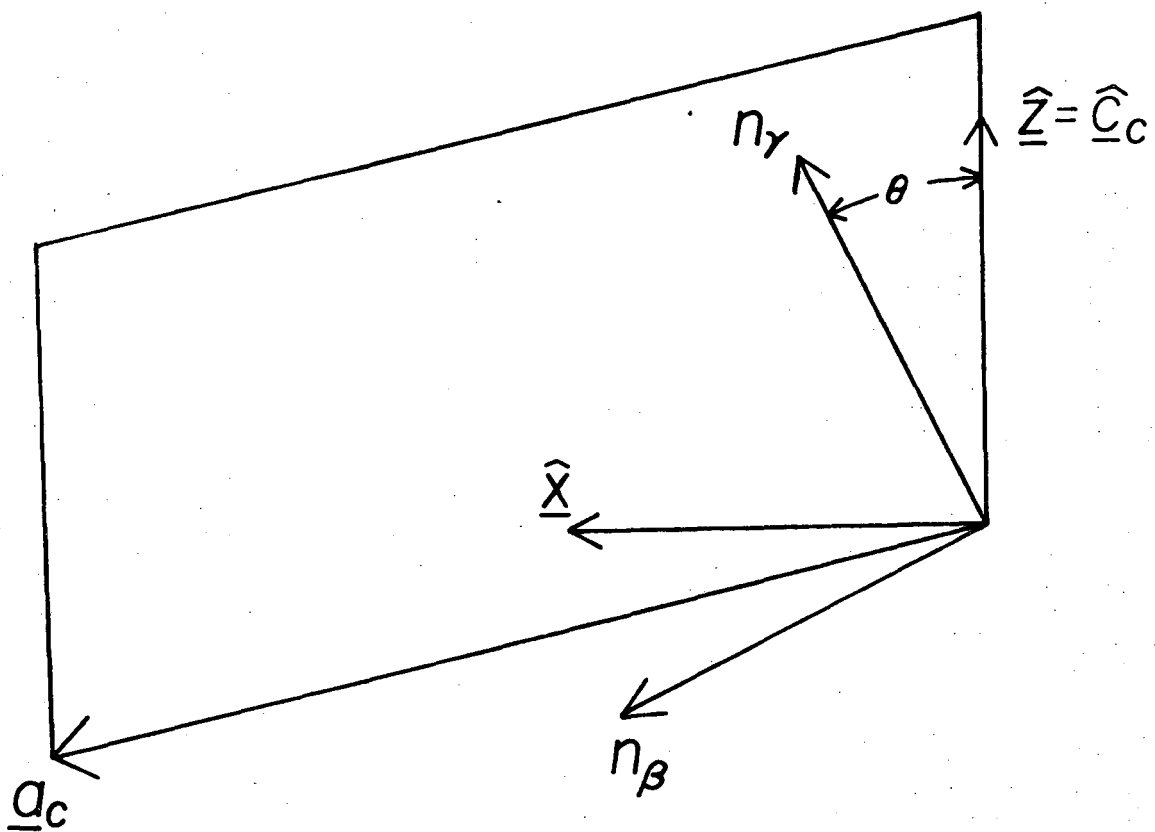
$$\underline{\epsilon}_1 = \begin{pmatrix} n_{\gamma c}^2 \sin^2 \theta + n_{\beta c}^2 \cos^2 \theta & 0 & \cos \theta \sin \theta (n_{\gamma c}^2 - n_{\beta c}^2) \\ 0 & n_{ac}^2 & 0 \\ \cos \theta \sin \theta (n_{\gamma c}^2 - n_{\beta c}^2) & 0 & n_{\gamma c}^2 \cos^2 \theta + n_{\beta c}^2 \sin^2 \theta \end{pmatrix}.$$

This can be verified by examining Figure (I.1b) and reviewing Section IV of Chapter I. See in particular equation (IV.8). Because the two monoclinic units are related by reflection in the b-c plane, the tensor for the other monoclinic domain type  $\underline{\epsilon}_2$  can be derived from  $\underline{\epsilon}_1$  by changing  $\theta$  to  $-\theta$ . The volume averaged dielectric tensor without the surface charge correction can be computed by noting that enstatite is an equal mixture of the monoclinic units:

$$\underline{\epsilon} = \frac{1}{2} \underline{\epsilon}_1 + \frac{1}{2} \underline{\epsilon}_2 =$$

$$\begin{pmatrix} n_{\gamma c}^2 \sin^2 \theta + n_{\beta c}^2 \cos^2 \theta & 0 & 0 \\ 0 & n_{ac}^2 & 0 \\ 0 & 0 & n_{\gamma c}^2 \cos^2 \theta + n_{\beta c}^2 \sin^2 \theta \end{pmatrix}.$$

By noting that the normal vector to the domain interface is  $\hat{\underline{x}}$  the exact dielectric tensor including the surface charge correction can be computed from equation (III.9), Chapter 1:



XBL 773-8158

Figure (1.1b). The orientation of the principal axes of clinoenstatite. The  $n_\alpha$  axis is along the  $y (= b_c)$  axis;  $\theta = 22^\circ$ .

$$\underline{\underline{\epsilon}} = \frac{1}{2} \underline{\underline{\epsilon}}_1 + \frac{1}{2} \underline{\underline{\epsilon}}_2 - F \underline{V} \underline{V} =$$

$$\left( \begin{array}{ccc} n_{\gamma c}^2 \sin^2 \theta + n_{\beta c}^2 \cos^2 \theta & 0 & 0 \\ 0 & n_{\alpha c}^2 & 0 \\ 0 & 0 & \frac{n_{\gamma c}^2 n_{\beta c}^2}{n_{\gamma c}^2 \sin^2 \theta + n_{\beta c}^2 \cos^2 \theta} \end{array} \right)$$

By noting Table (I.1) it is clear that the indicatrix for enstatite can be represented in this system by

$$\underline{\underline{\epsilon}}_e = \left( \begin{array}{ccc} n_{\beta e}^2 & 0 & 0 \\ 0 & n_{\alpha e}^2 & 0 \\ 0 & 0 & n_{\gamma e}^2 \end{array} \right)$$

when enstatite is oriented so that  $\underline{b}_e$  is parallel to  $\underline{b}_c$  and  $\underline{c}_e$  is parallel to  $\underline{c}_c$ .

If the volume averaged dielectric tensor with surface charge correction accurately describes the optical properties of enstatite, it is clear that

$$n_{\alpha e}^2 = n_{\alpha c}^2$$

$$n_{\beta e}^2 = n_{\beta c}^2 \cos^2 \theta + n_{\gamma c}^2 \sin^2 \theta$$

$$n_{\gamma e}^2 = \frac{n_{\gamma c}^2 n_{\beta c}^2}{n_{\beta c}^2 \cos^2 \theta + n_{\gamma c}^2 \sin^2 \theta}$$

by equating diagonal matrix elements. The result  $n_{\alpha e} = n_{\alpha c}$  is easy to understand. The  $n_{\alpha c}$  axes of both orientations of clinoenstatite are parallel, so the refractive index of the composite in this direction

should also be  $n_{\alpha c}$ . This prediction is supported by the data:

$n_{\alpha e}$  ( $= 1.650$ ) equals  $n_{\alpha c}$  ( $= 1.651$ ) to within the experimental error ( $= \pm .001$ ).

Without evaluating the remaining expressions it is clear that the theory has failed. The two expressions can be written

$$n_{\beta e}^2 = n_{\beta c}^2 + (n_{\gamma c}^2 - n_{\beta c}^2) \sin^2 \theta$$

$$n_{\gamma e}^2 n_{\beta e}^2 = n_{\gamma c}^2 n_{\beta c}^2.$$

Because experimentally  $n_{\gamma c} > n_{\beta c}$ , the first equation requires that the  $n_{\beta}$  index be larger in the orthorhombic phase. This requirement coupled with the second equation says that the  $n_{\gamma}$  index is smaller in the orthorhombic phase. In other words, there should be a trade-off: when the composite is formed  $n_{\beta}$  should grow at the expense of  $n_{\gamma}$ . This does not happen; both measured indices are smaller in enstatite.

Therefore, it is not possible to assign a macroscopic dielectric tensor to each layer, and a more fundamental theory based on the detailed atomic structure is needed to understand this system. The simplest theory which deals with the microscopic origin of the refractive index is based on the point-dipole model of atomic polarization. In the next section the physical principles of this model will be discussed.

## II. Physical Principles and Objectives of the Point-Dipole Model

In this section the physical principles of the point-dipole model will be discussed in the context of crystal systems with arbitrary symmetry. Three main objectives of the application of this theory to silicate minerals will be described.

In the derivation of the volume averaged dielectric tensor, it was assumed that each of the domains were large enough to be characterized by a macroscopic dielectric tensor. When the domains are too small to satisfy this condition, a more fundamental theory involving the microscopic electric field is needed to understand and predict the optical properties.

The simplest such theory is the classical point-dipole model in which each atom is represented by an infinitely small electron oscillator. The coordinates of these point-dipoles are supposed to be known from an x-ray structure analysis.

Ewald<sup>2,3</sup> used this model in his theory of birefringence in crystals. He introduced the concept that a plane electromagnetic wave should exist self-consistently in an infinite medium: all the spherical waves, emitted with a speed  $c$  from the individual dipole oscillators, should add up to a plane wave traveling with phase velocity  $V$ , and it is this plane wave which in turn excites the oscillators. The condition of self-consistency yields a ratio between  $c$  and  $V$  which is the refractive index. In optically anisotropic material, birefringence is accounted for by the fact that the dipole sums depend on the polarization of the wave, thus

giving rise to different refractive indices for light with different polarization.

This work is concerned only with the infinite wavelength (static field) approximation to this model. Although it is possible to carry out the program as outlined above and then take the limit  $\lambda \rightarrow \infty$ , it is easier to use the mathematically equivalent method of working with the static fields. This simpler calculation scheme will be used in this work. For a complete discussion of the former scheme in the context of crystal optics the reader is referred to the comprehensive treatment of Reijnhart.<sup>4</sup>

The most general point-dipole model would assign a tensor polarizability  $\underline{\alpha}$  to each crystallographically distinct atomic species. The dipole moment induced at each site would be

$$\underline{p}_i = \underline{\alpha}_i \underline{e}_{loc}(i)$$

where  $\underline{e}_{loc}(i)$  is the microscopic electric field at the  $i^{\text{th}}$  atomic site due to all other dipoles. Giving the polarizability a tensor character would allow one to model some aspects of the chemical and physical environment of each atom. For example, an oxygen ion in quartz could have a different polarizability along and normal to the approximate Si-O-Si axis.

Enstatite has ten crystallographically distinct atoms. If each is assigned a general, symmetric tensor polarizability, a total of sixty parameters would be needed to specify completely the polarization response. Because these parameters are defined only in the context

of the point-dipole model, they cannot be calculated independently. One must use the point-dipole model itself to yield empirical polarization parameters.

Except for the simplest systems, the problem of determining the most general polarizabilities is hopelessly underdetermined. For enstatite only three optical parameters (three indices) are available to determine the sixty polarization parameters. To avoid this difficulty another method of modeling the polarization response was used in all the calculations in this study: regardless of crystallographic environment each atomic species was assigned a scalar polarizability. With this model the three refractive indices of enstatite uniquely determine the three empirical scalar polarizabilities ( $\alpha_{\text{Mg}}$ ,  $\alpha_{\text{Si}}$ , and  $\alpha_0$ ).

The closer the point symmetry of a site is to cubic, the better this scalar approximation. The general tensor polarizability has an associated ellipsoid analogous to the indicatrix. The point group of a site must be a subgroup of the point group of the polarization ellipsoid. Just as a cubic point group of a crystal constrains the indicatrix to be spherical, a cubic point group of a site constrains the polarization ellipsoid of that site to be spherical. The radius of the polarization sphere is the scalar polarizability. The anisotropic polarization response of an ion is determined mainly by the distribution of nearest neighbors. If this distribution has nearly cubic symmetry, the scalar polarization approximation should be valid for this site. Therefore, the scalar approximation should apply to the tetrahedrally coordinated silicon ion in silicate minerals.

Before developing the theory further, the objectives of the application of the model to mineral systems should be stated. First, it was hoped the model would give insight into the optical behavior of the enstatite system. The program is to calculate the empirical polarizabilities of enstatite and clinoenstatite. The optical behavior of this system would be said to have been understood in the context of the point-dipole model if the analogous empirical parameters are nearly equal, that is  $(\alpha_{Mg})_{\text{enstatite}} \approx (\alpha_{Mg})_{\text{clino}}$  and so forth.

Secondly, it was hoped that the model would give more accurate predictions for the optical properties of solid solutions than the volume averaged dielectric tensor. It was assumed that the polarizability of a substituted site was  $\alpha_{\text{site}} = f_1 \alpha_1 + f_2 \alpha_2$  where  $f_1$  and  $f_2$  are the percentages of each end member in the solid solution.  $\alpha_1$  and  $\alpha_2$  are the polarizabilities of the site for each end member determined from the optical parameters of each end member.

Finally, it was hoped that the empirical polarizabilities derived from the optical parameters of a subset of silicate minerals could be used to predict successfully the optical parameters of other silicate minerals. That is, if the empirical polarizability of each atomic species was nearly constant from mineral to mineral, it would be possible to compile a list of these parameters analogous to a list of ionic radii.

Each of these objectives will be discussed in the context of specific mineral systems later in this work.

### III. Derivation of the Dielectric Tensor in the Point-Dipole Model

In this section the point-dipole model is developed quantitatively.

Although, in the numerical calculations each atomic species will have a scalar polarizability, the theory will be more general. Each atom in a unit cell will be assigned a tensor polarizability. Subscripts and superscripts  $i$  and  $j$  will range only over the atoms in one unit cell ( $i, j = 1, N$ ).

The key to the physics of the derivation is to understand the various electric fields which are

- 1)  $\underline{e}$  (The microscopic field)

This is the total electric field in the medium due to all the charges in the medium. The force on a test charge  $Q$  is  $Q\underline{e}$ .

This field exhibits extreme variation on the atomic scale.

- 2)  $\underline{e}_{loc}^i$  (i) (The local field at the  $i^{th}$  atomic site)

This is that part of  $\underline{e}$  at the  $i^{th}$  site not due to the  $i^{th}$  atom. This is the field which directly induces the  $i^{th}$  dipole:

$$\underline{P}_i = \alpha_i \underline{e}_{loc}^i (i). \quad (\text{III.1})$$

- 3)  $\underline{E}$  (The macroscopic field)

This is the field which appears in Maxwell's equations for material media. It is the average of the microscopic field  $\underline{e}$  over a volume representative of the material. It is the field contained in the definition of the electric susceptibility  $\chi$ :

$$\underline{P} = \chi \underline{E} \quad (\text{III.2})$$

where

$$\underline{P} = \frac{1}{V_c} \sum_{i=1}^N \underline{P}_i \quad (\text{III.3})$$

is the polarization density.  $V_c$  is the volume of a unit cell containing  $N$  atoms.

The susceptibility  $\underline{\chi}$  is the object of the calculation, for  $\underline{\epsilon} = \underline{I} + 4\pi\underline{\chi}$ . By appropriate manipulation of (III.1), (III.2), and (III.3),  $\underline{\chi}$  can be found if the relationship between  $\underline{E}$  and  $\underline{e}_{\text{loc}}(i)$  is known.

To find this relationship consider a sphere of radius  $R$  centered on the  $i^{\text{th}}$  site [see Figure (III.1)]. To calculate  $\underline{E}$ ,  $\underline{e}$  can be averaged over this sphere. Therefore, it should be macroscopically small but large enough to contain a volume representative of the material. The sphere divides the sources of  $\underline{e}$  into two types: those inside and those outside the sphere:

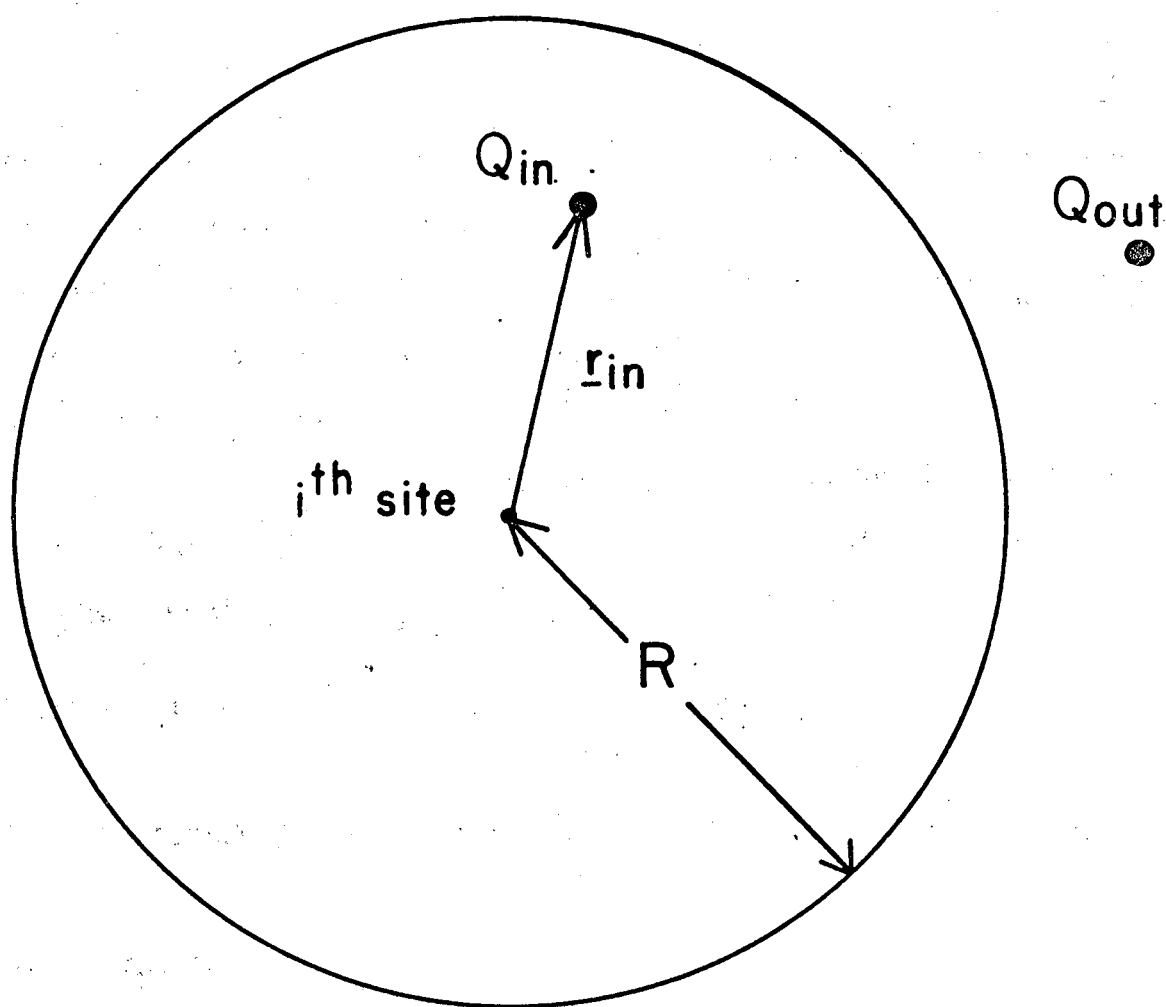
$$\underline{e} = \sum_{Q \text{ in}} \underline{e}_Q + \sum_{Q \text{ out}} \underline{e}_Q . \quad (\text{III.4})$$

To average  $\underline{e}$  over the sphere, average the field from one typical  $Q_{\text{out}}$  and one typical  $Q_{\text{in}}$  and add the results:

$$\begin{aligned} \underline{E} &= \langle \underline{e} \rangle_{\text{sphere}} \\ &= \sum_{Q \text{ in}} \langle \underline{e}_Q \rangle_{\text{sphere}} + \sum_{Q \text{ out}} \langle \underline{e}_Q \rangle_{\text{sphere}} \end{aligned} \quad (\text{III.5})$$

$Q_{\text{out}}$

From gravitation theory it is well known that a point mass attracts a spherical body as if the mass of the sphere were concentrated at the center. Therefore, the field of  $Q_{\text{out}}$  averaged over the sphere is the value of that field evaluated at the center:



XBL 773-8164

Figure (III.1). A sphere of radius  $R$  centered at the  $i^{\text{th}}$  site.  
 $\underline{r}_{\text{in}}$  is a vector from the  $i^{\text{th}}$  site to a typical  $Q_{\text{in}}$ .

$$\langle \underline{e}_Q \rangle_{\text{sphere}} = \underline{e}_Q(\text{center}) = \underline{e}_Q(i) \quad (\text{III.6})$$

$Q_{in}$

Gravitation theory also shows that a point mass inside a spherical mass shell experiences no net force from the shell. Therefore, the field of  $Q_{in}$  averaged over the spherical shell with inner radius  $r_{in}$  and outer radius  $R$  is zero. The discussion of  $Q_{out}$  shows that the field of  $Q_{in}$  averaged over the remaining sphere of radius  $r_{in}$  is the value of that field at the center. Therefore,

$$\begin{aligned} \langle \underline{e}_Q \rangle &= (\text{Fraction of the volume which is less than } r_{in} \text{ from} \\ &\quad \text{the center}) \times (\text{Field due to } Q_{in} \text{ evaluated at the center}) \\ &= \left( \frac{1}{V} \frac{4}{3} \pi r_{in}^3 \right) \times \left( -\frac{Qr_{in}}{r_{in}^3} \right) \end{aligned} \quad (\text{III.7})$$

where  $V$  is the volume of the sphere of radius  $R$ . Rewriting (III.7) gives

$$\langle \underline{e}_Q \rangle = -\frac{4\pi}{3} \frac{1}{V} \underline{P}_Q \quad (\text{III.8})$$

where  $\underline{P}_Q = Qr_{in}$  is the dipole moment of  $Q_{in}$  with respect to the center of the sphere.

Equation (III.5) now becomes

$$\underline{E} = -\frac{4\pi}{3} \underline{P} + \sum_{Q_{out}} \underline{e}_Q(i) \quad (\text{III.9})$$

where

$$\underline{P} = \frac{1}{V} \sum_{Q_{in}} \underline{P}_Q \quad (\text{III.10})$$

is the polarization density of equation (III.2). The second term in (III.9) is that part of  $\underline{e}_{loc}(i)$  due to charges outside the sphere.

Because  $\underline{e}_{loc}(i)$  can be written as

$$\underline{e}_{loc}(i) = \sum'_{Q_{in}} \underline{e}_Q(i) + \sum_{Q_{out}} \underline{e}_Q(i) \quad (III.11)$$

where the prime on the summation symbol means exclude the charge at the  $i^{th}$  site, equation (III.9) can be used to give

$$\underline{e}_{loc}(i) = \underline{E} + \frac{4\pi}{3} \underline{P} + \sum'_{Q_{in}} \underline{e}_Q(i). \quad (III.12)$$

$R$  is chosen large enough so that the sum in (III.12) converges.

When the charges are confined to dipoles, the sum in (III.12) is

$$\sum_{s \neq i} \frac{3(\hat{\underline{x}}_{is} \cdot \underline{p}_s) \hat{\underline{x}}_{is} - \underline{p}_s}{(\underline{x}_{is})^3} \quad (III.13)$$

where  $\underline{x}_{is}$  is a vector from site  $s$  to site  $i$ . The sum is over all sites in the sphere except the  $i^{th}$  site. To continue independently of a coordinate system, dyadic notation will be used. Equation (III.13) can be written

$$\sum_{s \neq i} \underline{\beta}^{is} \underline{p}_s \quad (III.14)$$

with

$$\underline{\beta}^{is} = \frac{3\hat{\underline{x}}_{is}\hat{\underline{x}}_{is} - \underline{I}}{(\underline{x}_{is})^3}. \quad (III.15)$$

For a crystal with  $N$  atoms in the unit cell, first sum the dipoles at site  $j$  over the entire lattice, then sum over all sites  $j$ :

$$\sum_{s \neq i} \underline{\beta}^{is} \underline{p}_s = \frac{1}{V_c} \sum_{j=1}^N \underline{A}^{ij} \underline{p}_j \quad (\text{III.16})$$

where

$$\underline{A}^{ij} = \begin{cases} V_c \sum_{\underline{\ell}} \underline{\beta}^{ij\underline{\ell}} & i \neq j \\ V_c \sum_{\underline{\ell}}' \underline{\beta}^{ii\underline{\ell}} & i=j \end{cases}$$

$$\underline{\beta}^{ij\underline{\ell}} = \frac{3\hat{x}_{ij\underline{\ell}} \hat{x}_{ij\underline{\ell}} - I}{(x_{ij\underline{\ell}})^3}$$

with

$$\begin{aligned} x_{ij\underline{\ell}} &= x_i - x_j - \underline{\ell} \\ \underline{\ell} &= \underline{\ell}_1 \underline{a} + \underline{\ell}_2 \underline{b} + \underline{\ell}_3 \underline{c} \\ &= \text{lattice vector } (\underline{\ell}_i = \text{integer}) \end{aligned}$$

and

$\underline{x}_i$  = position vector of the  $i^{\text{th}}$  site measured relative to the origin of the cell which contains the site.

With these results, equation (III.12) becomes

$$\underline{e}_{\text{loc}}(i) = \underline{E} + \frac{4\pi}{3} \underline{P} + \frac{1}{V_c} \sum_{j=1}^N \underline{A}^{ij} \underline{p}_j. \quad (\text{III.17})$$

Noting that  $\underline{P} = \frac{1}{V_c} \sum_{j=1}^N \underline{p}_j$ , this becomes

$$\underline{e}_{\text{loc}}(i) = \underline{E} + \frac{1}{V_c} \sum_{j=1}^N \left( \frac{4\pi}{3} I + \underline{A}^{ij} \right) \underline{p}_j. \quad (\text{III.18})$$

This is the sought after relationship between  $\underline{E}$  and  $\underline{e}_{\text{loc}}(i)$ . Combining this result with (III.1) gives

$$\begin{aligned} \underline{P}_i &= \underline{\alpha}_i \underline{e}_{\text{loc}}(i) \\ &= \underline{\alpha}_i [\underline{E} + \frac{1}{V_c} \sum_{j=1}^N (\frac{4\pi}{3} \underline{I} + \underline{A}^{ij}) \underline{P}_j]. \end{aligned} \quad (\text{III.19})$$

After a little algebra this becomes

$$\frac{1}{V_c} \sum_{j=1}^N \underline{G}^{ij} \underline{P}_j = \underline{E} \quad (\text{III.20})$$

with

$$\underline{G}^{ij} = \delta_{ij} (\underline{\alpha}_i / V_c)^{-1} - \frac{4\pi}{3} \underline{I} - \underline{A}^{ij}. \quad (\text{III.21})$$

$\delta_{ij}$  equals 1 when  $i=j$  and equals 0 otherwise. To make the calculation more transparent, the unit cell will contain only two atoms. Introducing a matrix notation (III.20) becomes

$$\frac{1}{V_c} \begin{pmatrix} \underline{G}^{11} & \underline{G}^{12} \\ \underline{G}^{21} & \underline{G}^{22} \end{pmatrix} \begin{pmatrix} \underline{P}_1 \\ \underline{P}_2 \end{pmatrix} = \begin{pmatrix} \underline{E} \\ \underline{E} \end{pmatrix} \quad (\text{III.22})$$

or

$$\frac{1}{V_c} \underline{M} \begin{pmatrix} \underline{P}_1 \\ \underline{P}_2 \end{pmatrix} = \begin{pmatrix} \underline{E} \\ \underline{E} \end{pmatrix} \quad (\text{III.23})$$

with

$$\underline{M} = \begin{pmatrix} \underline{G}^{11} & \underline{G}^{12} \\ \underline{G}^{21} & \underline{G}^{22} \end{pmatrix}.$$

In general  $\underline{M}$  is a  $3N$  by  $3N$  matrix. In a cartesian coordinate system

$$M_s + 3(i-1), t + 3(j-1) = G_{st}^{ij} \quad (\text{III.24})$$

with

$$s, t = 1, 2, 3$$

$$i, j = 1, \dots, N.$$

Next, invert  $\underline{M}$  to get  $\underline{M}^{-1}$ . Equation (III.23) becomes

$$\frac{1}{V_c} \begin{pmatrix} \underline{P}_1 \\ \underline{P}_2 \end{pmatrix} = \underline{M}^{-1} \begin{pmatrix} \underline{E} \\ \underline{E} \end{pmatrix}.$$

Let the following equation define the matrices  $\underline{\underline{H}}^{ij}$ :

$$\begin{pmatrix} \underline{\underline{H}}^{11} & \underline{\underline{H}}^{12} \\ \underline{\underline{H}}^{21} & \underline{\underline{H}}^{22} \end{pmatrix} = \underline{M}^{-1}. \quad (\text{III.25})$$

with this definition (III.24) becomes

$$\frac{1}{V_c} \begin{pmatrix} \underline{P}_1 \\ \underline{P}_2 \end{pmatrix} = \begin{pmatrix} \underline{\underline{H}}^{11} & \underline{\underline{H}}^{12} \\ \underline{\underline{H}}^{21} & \underline{\underline{H}}^{22} \end{pmatrix} \begin{pmatrix} \underline{E} \\ \underline{E} \end{pmatrix}. \quad (\text{III.26})$$

Dispersing with the matrix notation and reconsidering N atoms in the unit cell, (III.26) becomes

$$\frac{1}{V_c} \underline{P}_i = \sum_{j=1}^N \underline{\underline{H}}^{ij} \underline{E}. \quad (\text{III.27})$$

Now sum both sides over i

$$\frac{1}{V_c} \sum_{i=1}^N \underline{P}_i = \left( \sum_{i,j=1}^N \underline{\underline{H}}^{ij} \right) \underline{E}. \quad (\text{III.28})$$

Recalling the definition (III.3) for the polarization density  $\underline{P}$  this becomes

$$\underline{P} = \chi \underline{E}$$

with

$$\chi = \sum_{i,j=1}^N \underline{\underline{H}}^{ij}. \quad (\text{III.29})$$

In a cartesian system

$$\chi_{st} = \sum_{i,j=1}^N H_{st}^{ij} = \sum_{i,j=1}^N M_s^{-1} + 3(i-1), t + 3(j-1). \quad (\text{III.30})$$

The road to X is now clear.

- 1) Calculate the lattice sums  $\underline{A}^{ij}$  [see (III.16)].
- 2) Calculate the  $\underline{G}^{ij}$ 's from the lattice sums and the polarizabilities [see (III.21)].
- 3) Calculate  $\underline{M}$  and its inverse  $\underline{M}^{-1}$  [see (III.24)].
- 4)  $\chi_{st} = \sum_{i,j=1}^N M_s^{-1} + 3(i-1), t + 3(j-1).$

This derivation of X ignored all crystal symmetry except that of the lattice. Question: if other symmetry were considered would major simplifications in the calculation occur? A major simplification would be the reduction of the order of  $\underline{M}$  from  $3N$  to  $3N'$  where  $N'$  is the number of atoms in the asymmetric unit. Answer: although the additional symmetry reduces the number of independent lattice sums  $\underline{A}^{ij}$ , the order of  $\underline{M}$  cannot be reduced. The calculation of the lattice sums simplifies because they are geometric quantities; they depend only on the atomic coordinates. The coordinates are assumed to remain constant when the crystal is subjected to an electric field. Therefore, the lattice sums reflect the symmetry of the unperturbed crystal. However, the symmetry of the system is not that of the unperturbed crystal. The physical system is the crystal with an electric field. With a general constant vector field, the only symmetry that remains is that of the lattice. The physical asymmetric unit is the entire primitive unit cell. Therefore, the order of  $\underline{M}$  cannot be less than

$3N$ ,  $N$  being the number of atoms in the primitive unit cell.

#### IV. Transformation of the Lattice Sums to Fourier Space

The most difficult step in the calculation of the electric susceptibility is the evaluation of the lattice sums. It is well known that such sums converge only conditionally. In a test calculation of the lattice sums for a cubic structure with a 5 Å lattice constant, convergence to .5% occurred after the inclusion of about 300 terms out to 25 Å. However, the sums had converged to only .5% when the calculation was extended out to 75 Å and included over 15,000 terms!

The usual way to avoid the poor convergence is to do part of the sum in Fourier space. This method was introduced by Ewald<sup>5</sup> and has been considerably extended.<sup>6,7</sup>

The essential idea is the introduction of a cutoff function  $\phi(\underline{x})$  which falls off rapidly for large  $\underline{x}$ . With the convergence function, a general lattice sum

$$S(\underline{x}) = \sum_{\underline{\ell}} f(\underline{x} - \underline{\ell}) \quad (\text{IV.1})$$

can be written

$$S(\underline{x}) = S_1(\underline{x}) + S_2(\underline{x}) \quad (\text{IV.2})$$

where

$$S_1(\underline{x}) = \sum_{\underline{\ell}} f(\underline{x} - \underline{\ell}) \phi(|\underline{x} - \underline{\ell}|) \quad (\text{IV.3})$$

$$S_2(\underline{x}) = \sum_{\underline{\ell}} f(\underline{x} - \underline{\ell}) [1 - \phi(|\underline{x} - \underline{\ell}|)]. \quad (\text{IV.4})$$

$S_1$  converges rapidly in direct space because of  $\phi$ , while the Fourier transform of  $S_2$  converges rapidly in Fourier space. Although the

reason for the rapid convergence in Fourier space has been discussed in terms of fictitious charge distributions in direct space, the most physical explanation is as follows. The sum  $S$  is a field due to an infinite lattice of sources. Because of the nature of the cutoff function,  $S_1$  is the contribution from the nearby sources, while  $S_2$  is due to the distant ones. The field due to many distant sources is relatively smooth, so the Fourier representation of this field has few Fourier components. Therefore, the Fourier transform of  $S_2$  is a sum of few terms.

Notice that  $S_2(\underline{x})$  as a function of  $\underline{x}$  has the periodicity of the lattice. Therefore, its Fourier transform is non-zero only at the reciprocal lattice points:<sup>8</sup>

$$S_2(\underline{x}) = \frac{1}{V_c} \sum_{\underline{k}} T(\underline{k}) e^{-i \underline{k} \cdot \underline{x}} \quad (\text{IV.5})$$

$$T(\underline{k}) = \int f(\underline{x}) [1 - \phi(\underline{x})] e^{i \underline{k} \cdot \underline{x}} d^3x \quad (\text{IV.6})$$

where the integral is over all of direct space and

$$\underline{k} = 2\pi(h_1 \underline{a}^* + h_2 \underline{b}^* + h_3 \underline{c}^*) \quad (\text{IV.7})$$

with  $h_i$  = integer and  $\underline{a}^*$ ,  $\underline{b}^*$ ,  $\underline{c}^*$  are reciprocal lattice vectors defined by

$$\underline{a}^* = \frac{\underline{b} \times \underline{c}}{\underline{a} \cdot (\underline{b} \times \underline{c})}$$

and so forth. To apply this general formalism to dipole sums the following identifications are made

$$S(\underline{x}_{ij}) = A^{ij}/V_c \quad (\text{IV.8})$$

$$f(\underline{x}) = \frac{3 \hat{\underline{x}} \hat{\underline{x}} - \underline{I}}{3} \quad (\text{IV.9})$$

The cutoff function is chosen to allow an analytic evaluation of  $T(\underline{k})$  with  $f(\underline{x})$  given by (IV.9):<sup>7</sup>

$$\phi(\underline{x}) = \Gamma(5/2, \pi \underline{x}^2 / B^2) / \Gamma(5/2) \quad (\text{IV.10})$$

where

$$\Gamma(n, y) = \int_y^\infty e^{-t} t^{n-1} dt \quad (\text{IV.11})$$

is the incomplete gamma function, and  $\Gamma(n)$  is the gamma function.

$B$  is the Bertaut parameter which can be varied to optimize the rate of convergence of  $S_2$ . By integrating (IV.11) by parts it can be shown that

$$\phi(\underline{x}) = \text{ERFC}(\sqrt{\pi} \underline{x}) + \frac{4}{3} e^{-\pi \underline{x}^2} (\pi \underline{x}^3 + \frac{3}{2} \underline{x}) \quad (\text{IV.12})$$

with  $t = \underline{x}/B$  and

$$\text{ERFC}(y) = \frac{2}{\sqrt{\pi}} \int_y^\infty e^{-s^2} ds \quad (\text{IV.13})$$

is the complimentary error function. Therefore,  $\phi$  can be thought of as a generalized Gaussian function with a width  $\Delta \underline{x} \approx B$ . It is not surprising, then, that the Fourier transform of  $S_2$  is a generalized Gaussian with a width  $\Delta k \approx 1/B$ :<sup>7</sup>

$$T(\underline{k}) = \begin{cases} -\frac{4\pi}{3} (3 \hat{\underline{k}} \hat{\underline{k}} - \underline{I}) e^{-\frac{k^2 B^2}{4\pi}} & (\underline{k} \neq 0) \\ 0 & (\underline{k} = 0) \end{cases} \quad (\text{IV.14})$$

Summarizing the results of this section gives

$$\underline{A}^{ij}/v_c = s_1(x_{ij}) + s_2(x_{ij}) \quad (\text{IV.15})$$

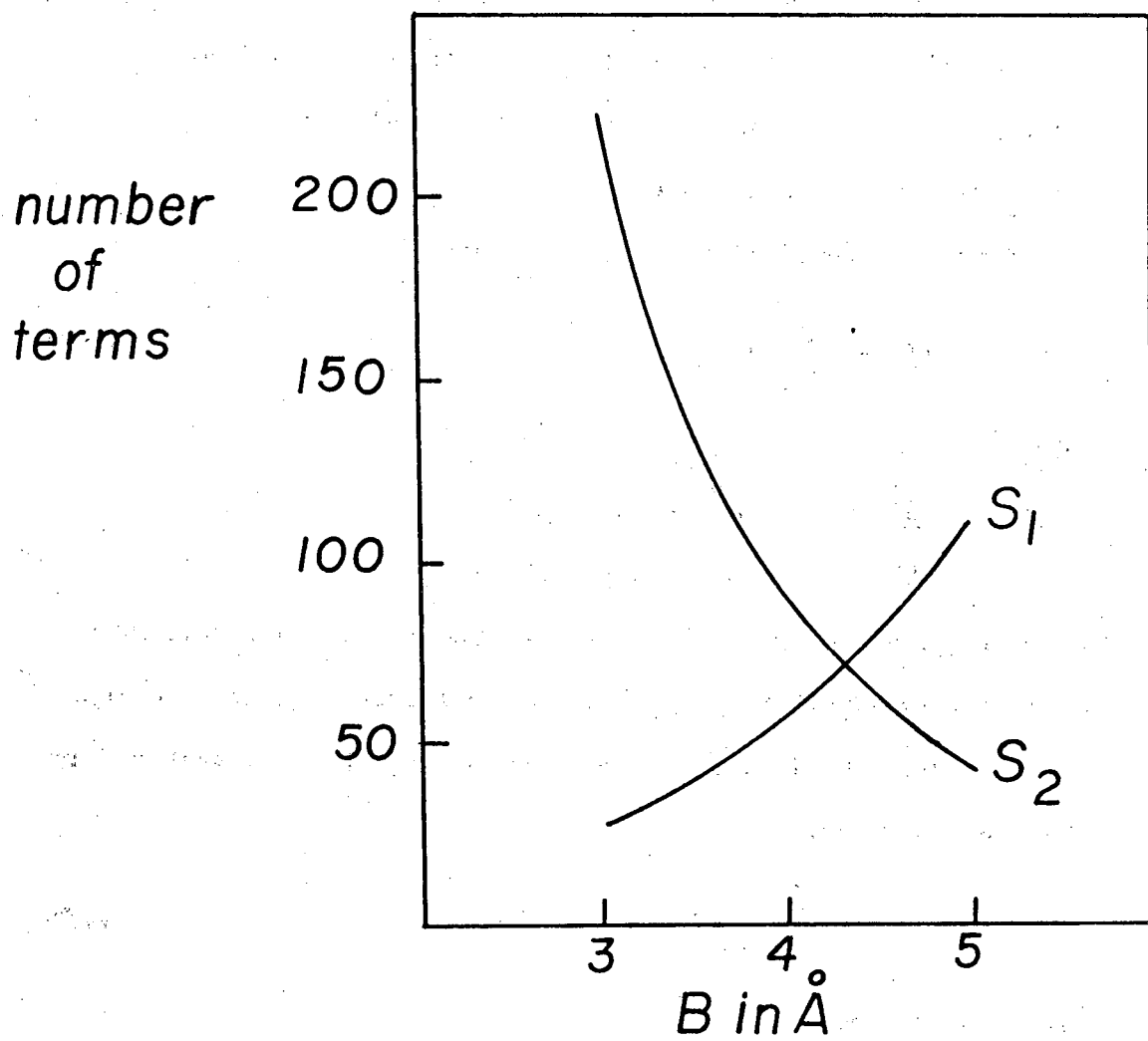
$$s_1(x_{ij}) = \sum_{\underline{\ell}}^3 \frac{3 \hat{x}_{ij\underline{\ell}} \hat{x}_{ij\underline{\ell}} - \underline{I}}{(x_{ij\underline{\ell}})^3} \phi(x_{ij\underline{\ell}}) \quad (\text{IV.16})$$

$$s_2(x_{ij}) = -\frac{4\pi}{3v_c} \sum'_{\underline{k}} (3 \hat{k} \hat{k} - \underline{I}) e^{-\frac{k^2 B^2}{4\pi}} e^{-i \underline{k} \cdot \underline{x}_{ij}} \quad (\text{IV.17})$$

where the prime on the summation symbol means exclude  $\underline{k} = 0$ . To apply this result to  $\underline{A}^{ii}$  exclude the  $\underline{\ell} = 0$  term from  $s_1$ .

To apply these formulae a choice must be made for  $B$ . For small  $B$ ,  $s_1$  converges rapidly and  $s_2$  converges slowly; for large  $B$ ,  $s_2$  converges rapidly and  $s_1$  slowly. The best value of  $B$  is a compromise.

Figure (IV.1) shows the result of a test calculation in which  $B$  was varied. The structure had a cubic lattice with a 5 Å cell. The number of terms for convergence to ten decimal places was plotted for  $s_1$  and  $s_2$  as a function of  $B$ . The best value of  $B$  ( $\approx 4.3$  Å) is somewhat less than the lattice constant. For extensive calculations,  $B$  should be determined by similar techniques for each crystal.



XBL 773-8166

Figure (IV.1). Number of terms for convergence to ten decimal places plotted for  $S_1$  and  $S_2$  as a function of  $B$ .  $S_1$  is direct space sum;  $S_2$  is Fourier space sum.

## V. The Matrix Elements of the Lattice Sums

In this section a cartesian coordinate system will be defined, and explicit expressions will be derived for the components of  $S_1$  and  $S_2$  relative to this system.

First a useful identity will be proven:

$$\underline{I} = \sum_{i=1}^3 \underline{a}^i \cdot \underline{b}^i \quad (\text{V.1})$$

where

$$\begin{aligned} \underline{a}^1 &= \underline{a}, & \underline{a}^2 &= \underline{b}, & \underline{a}^3 &= \underline{c} \\ \underline{b}^1 &= \underline{a}^*, & \underline{b}^2 &= \underline{b}^*, & \underline{b}^3 &= \underline{c}^* \end{aligned}$$

where  $\underline{a}$ ,  $\underline{b}$ , and  $\underline{c}$  are the lattice vectors of a general triclinic structure, and  $\underline{a}^*$ ,  $\underline{b}^*$ , and  $\underline{c}^*$  are the reciprocal lattice vectors.

To prove the identity, first express an arbitrary vector  $\underline{v}$  in the direct system:

$$\underline{v} = \sum_{i=1}^3 f_i \underline{a}^i \quad (\text{V.2})$$

Now dot both sides with  $\underline{b}^j$ :

$$\underline{b}^j \cdot \underline{v} = \sum_{i=1}^3 f_i (\underline{b}^j \cdot \underline{a}^i)$$

The reciprocal lattice is defined so that

$$\underline{b}^j \cdot \underline{a}^i = \delta_{ij}.$$

Therefore,

$$\underline{b}^j \cdot \underline{v} = \sum_{i=1}^3 f_i \delta_{ij} = f_j$$

Inserting this result into (V.2) gives

$$\underline{v} = \sum_{i=1}^3 \underline{a}^i (\underline{b}^i \cdot \underline{v})$$

Introducing dyadic notation this becomes

$$\underline{v} = \sum_{i=1}^3 (\underline{a}^i \underline{b}^i) \underline{v}$$

$$= \left( \sum_{i=1}^3 \underline{a}^i \underline{b}^i \right) \underline{v}.$$

Therefore,

$$\underline{I} = \sum_{i=1}^3 \underline{a}^i \underline{b}^i.$$

Because the reciprocal lattice of the reciprocal lattice is the direct lattice, it is also true that

$$\underline{I} = \sum_{i=1}^3 \underline{b}^i \underline{a}^i. \quad (V.3)$$

For the special case of a cartesian system of unit vectors this becomes

$$\underline{I} = \sum_{i=1}^3 \hat{\underline{x}}^i \hat{\underline{x}}^i \quad (V.4)$$

because the reciprocal lattice of an orthonormal system is the direct lattice.

The cartesian system used for the calculation of the susceptibility and in particular the lattice sums is

$$\hat{\underline{z}} = \hat{\underline{c}} \quad (= \hat{\underline{x}}^3)$$

$$\hat{\underline{y}} = \hat{\underline{b}}^* \quad (= \hat{\underline{x}}^2)$$

$$\hat{\underline{x}} = \hat{\underline{y}} \times \hat{\underline{z}} \quad (= \hat{\underline{x}}^1)$$

To continue, the  $\underline{a}^i$  must be expanded in terms of the  $\hat{\underline{x}}^i$  and vice versa. Using identities (V.4) and (V.1),  $\underline{a}^i$  and  $\hat{\underline{x}}^i$  can be written

$$\begin{aligned}\underline{a}^i &= \left( \sum_{j=1}^3 \hat{\underline{x}}^j \hat{\underline{x}}^j \right) \underline{a}^i & \hat{\underline{x}}^i &= \left( \sum_{j=1}^3 \underline{a}^j \underline{b}^j \right) \hat{\underline{x}}^i \\ &= \sum_{j=1}^3 (\underline{a}^i \cdot \hat{\underline{x}}^j) \hat{\underline{x}}^j & &= \sum_{j=1}^3 (\hat{\underline{x}}^i \cdot \underline{b}^j) \underline{a}^j \\ &= \sum_{j=1}^3 Q_{ij} \hat{\underline{x}}^j & &= \sum_{j=1}^3 Q_{ij}^{-1} \underline{a}^j\end{aligned}$$

where  $Q_{ij} = \underline{a}^i \cdot \hat{\underline{x}}^j$  and  $Q_{ij}^{-1} = \hat{\underline{x}}^i \cdot \underline{b}^j$ .

$$\underline{Q} = \begin{pmatrix} a \sin\beta & 0 & a \cos\beta \\ -b \sin\alpha \cos\gamma^* & 1/b^* & b \cos\alpha \\ 0 & 0 & c \end{pmatrix} \quad (V.5)$$

$$\underline{Q}^{-1} = \begin{pmatrix} a^* \sin\gamma^* & 0 & -c^* \sin\alpha^* \cos\beta \\ a^* \cos\gamma^* & b^* & c^* \cos\alpha^* \\ 0 & 0 & 1/c \end{pmatrix} \quad (V.6)$$

The unstarred and starred varieties of  $a$ ,  $b$ ,  $c$ ,  $\alpha$ ,  $\beta$ ,  $\gamma$  are respectively the direct and reciprocal lattice constants.

To illustrate the method,  $Q_{11}^{-1}$  will be calculated. Similar manipulations will produce the remaining matrix elements.

$$\begin{aligned}Q_{11}^{-1} &= \underline{b}^1 \cdot \hat{\underline{x}}^1 \\ &= \underline{a}^* \cdot \hat{\underline{x}} \\ &= \underline{a}^* \cdot (\hat{\underline{y}} \times \hat{\underline{z}})\end{aligned}$$

$$\begin{aligned}
 &= \underline{a}^* \cdot (\hat{\underline{b}}^* \times \hat{\underline{c}}) \\
 &= \frac{1}{b^*} \hat{\underline{c}} \cdot (\underline{a}^* \times \underline{b}^*) \\
 &= \frac{1}{b^*} \hat{\underline{c}} \cdot \left( \frac{\underline{a}^* \times \underline{b}^*}{|\underline{a}^* \times \underline{b}^*|} \right) |\underline{a}^* \times \underline{b}^*| \\
 &= \frac{1}{b^*} (\hat{\underline{c}} \cdot \hat{\underline{c}}) |\underline{a}^* \times \underline{b}^*| \\
 &= \frac{1}{b^*} (1) a^* b^* \sin \gamma^* \\
 &= a^* \sin \gamma^*
 \end{aligned}$$

$s_1$  and  $s_2$  can now be evaluated. First  $s_1$ :

$$\begin{aligned}
 (s_1)_{st} &= \hat{\underline{x}}^s \cdot s_1 \hat{\underline{x}}^t \\
 &= \hat{\underline{x}}^s \cdot \left( \sum_{\ell} \phi(x_{ij\ell}) \frac{3 \underline{x}_{ij\ell} \underline{x}_{ij\ell} - \underline{x}_{ij\ell}^2 \underline{I}}{x_{ij\ell}^5} \right) \hat{\underline{x}}^t \\
 &= \sum_{\ell} \frac{3(\hat{\underline{x}}^s \cdot \underline{x}_{ij\ell})(\hat{\underline{x}}^t \cdot \underline{x}_{ij\ell}) - \underline{x}_{ij\ell}^2 \delta_{st}}{x_{ij\ell}^5} \phi(x_{ij\ell})
 \end{aligned}$$

Because  $\hat{\underline{x}}^s$  is an orthonormal system

$$x_{ij\ell} = \left[ \sum_{s=1}^3 (\hat{\underline{x}}^s \cdot \underline{x}_{ij\ell})^2 \right]^{\frac{1}{2}}$$

Therefore, determining the  $\hat{\underline{x}}^s \cdot \underline{x}_{ij\ell}$  will evaluate  $s_1$ . Now

$$\begin{aligned}
 x_{ij\ell} &= x_i - x_j - \underline{\ell} \\
 &= \sum_{t=1}^3 (\Delta_t - \ell_t) a^t
 \end{aligned} \tag{V.7}$$

where

$$\Delta_1 = x_i - x_j$$

$$\Delta_2 = y_i - y_j$$

$$\Delta_3 = z_i - z_j$$

where  $x_i, y_i, z_i$  are the crystal coordinates of atom i, and  $x_j, y_j, z_j$  are the crystal coordinates of atom j. These coordinates are the fractional coordinates ( $0 \leq x, y, z < 1$ ) that are known from an x-ray structure analysis. The  $\ell_t$  are the integers which label the lattice points.

Dotting (V.7) with  $\hat{x}^s$  gives

$$\begin{aligned}\hat{x}^s \cdot \underline{x}_{ij\ell} &= \sum_{t=1}^3 (\Delta_t - \ell_t) (\hat{x}^s \cdot \underline{a}^t) \\ &= \sum_{t=1}^3 (\Delta_t - \ell_t) Q_{ts}.\end{aligned}$$

The evaluation of  $S_2$  is similar

$$\begin{aligned}(S_2)_{st} &= \hat{x}^s \cdot S_2 \hat{x}^t \\ &= \hat{x}^s \left( -\frac{4\pi}{3V_c} \sum_{\underline{k}} e^{-\frac{\underline{k}^2 B^2}{4\pi}} (3 \underline{k} \cdot \underline{k} - \underline{I}) e^{i\underline{k} \cdot \underline{x}_{ij}} \right) \hat{x}^t \\ &= -\frac{4\pi}{3V_c} \sum_{\underline{k}} e^{-\frac{\underline{k}^2 B^2}{4\pi}} \left( \frac{3(\underline{k} \cdot \hat{x}^s)(\underline{k} \cdot \hat{x}^t) - k^2 \delta_{st}}{k^2} \right) e^{i\underline{k} \cdot \underline{x}_{ij}}\end{aligned}$$

Three expressions must be evaluated:

$$1) \quad \underline{k} \cdot \underline{x}_{ij}$$

$$2) \quad \underline{k} \cdot \hat{x}^s$$

$$3) \quad k^2$$

Because  $\hat{\underline{x}}^s$  is an orthonormal system

$$\underline{k}^2 = \sum_{s=1}^3 (\underline{k} \cdot \hat{\underline{x}}^s)^2$$

so 2) determines 3).

To determine  $\underline{k} \cdot \underline{x}_{ij}$  note that

$$\underline{k} = 2\pi \sum_{s=1}^3 h_s \underline{b}^s \quad (V.8)$$

$$\underline{x}_{ij} = \sum_{s=1}^3 \Delta_t \underline{a}^t$$

where  $h_s$  are the integers that label the reciprocal lattice points,  
and the  $\Delta_t$  are defined in (V.7). Therefore

$$\underline{k} \cdot \underline{x}_{ij} = 2\pi \sum_{s=1}^3 h_s \Delta_s$$

using the fact that  $\underline{a}^t \cdot \underline{b}^s = \delta_{ts}$ .

Dotting (V.8) with  $\hat{\underline{x}}^s$  gives

$$\begin{aligned} \underline{k} \cdot \hat{\underline{x}}^s &= \hat{\underline{x}}^s \cdot 2\pi \sum_{t=1}^3 h_t \underline{b}^t \\ &= 2\pi \sum_{t=1}^3 h_t \hat{\underline{x}}^s \cdot \underline{b}^t \\ &= 2\pi \sum_{t=1}^3 h_t Q_{st}^{-1}. \end{aligned}$$

## VI. Discussion of Calculation Procedure

Before discussing the results of the calculations with the point-dipole model, a few words will be said about the calculation procedure. A FORTRAN program was developed which calculated the lattice sums from the lattice constants and atomic coordinates by the methods of the previous two sections. A second program, whose input was the lattice sums and the empirical scalar polarizabilities, computed  $\underline{X}$  by calculating and inverting  $\underline{M}$ . A third program computed the optical parameters by diagonalizing  $\underline{\epsilon} = \underline{I} + 4\pi \underline{X}$ . The latter two programs were mostly compilations of subroutines specific to the University of California CDC 6400 system. However, the lattice sum routine required a substantial amount of programming and has, therefore, been included as an appendix to this chapter.

To test the programs several trial calculations were run. The most rigorous test was a series of calculations of the optical parameters of a structure which was described in two equivalent ways:

- 1) As a triclinic structure with two atoms in the primitive unit cell.
- 2) As a face-centered orthorhombic structure with eight atoms in the non-primitive unit cell.

The optical parameters for these two calculations were equal to ten decimal places which was the accuracy of the lattice sum calculation. The successful result of this test eliminates a large class of possible sources of error.

For a structure with  $N$  atoms in a unit cell there are

$$5 \left( \frac{N^2 - N}{2} + 1 \right)$$

lattice sums. The factor in parentheses is the number of distinct pairs of atoms. The factor 5 is the number of distinct components of each lattice sum matrix ( $A_{ij}$  are symmetric with zero trace, that is,  $A_{st}^{ij} = A_{ts}^{ij}$  and  $\sum_{t=1}^3 A_{tt}^{ij} = 0$ ). For enstatite ( $N=80$ ), this formula gives over 15,000 sums! However, the number of independent sums is considerably smaller; the space group symmetry can be used to find relationships between the lattice sum matrices. In this work only a center of symmetry when present was exploited in this manner. A systematic treatment of the effect of space group symmetry on the lattice sum matrices was not attempted, for the savings in computing time on a restricted series of calculations would not have made the additional programming and debugging effort worthwhile.

Each lattice sum required approximately 0.5 to 1.0 second of computing time on a CDC 6400 computer for convergence to ten decimal places. The longer computing time was associated with structures that had markedly dissimilar unit cell edges. This is due to the isotropic nature of the cutoff function  $\phi$ . A compromise Bertaut parameter  $B$  based on an average lattice constant had to be used for these structures.

The actual calculations consisted of finding scalar polarizabilities which when entered into these programs would reproduce the experimental optical parameters. The method of finding the polarizabilities was

trial and error aided by a linear extrapolation procedure. After a calculation with an initial estimate of the polarizabilities, the calculation was repeated after changing the polarizabilities by small amounts. By varying one polarizability at a time, it was possible to obtain partial derivatives of the form

$$\partial(\text{optical parameter})/\partial(i^{\text{th}} \text{ polarizability}).$$

Assuming a linear dependence of the optical parameters on the polarizabilities, the partial derivatives and the experimental optical parameters could be used to obtain a second estimate of the polarizabilities. This method was usually successful. That is, by repeating the procedure several times, it was usually possible to obtain a set of polarizabilities that would allow the optical parameters to be calculated to within experimental error. However, there were exceptions which will be discussed in later sections. Table (VI.1) is a summary of the successful extrapolation procedure for low quartz. The procedure converged after three cycles.

Table (VI.1) Summary of the extrapolation procedure for low quartz.  
The first cycle was the initial guess.

	1 <sup>st</sup> cycle	2 <sup>nd</sup> cycle	3 <sup>rd</sup> cycle
$\alpha_{Si}$	2.6	4.5	4.546
$\alpha_0$	15.25	13.5	13.456
$n_o$	1.5450	1.5442	1.5542
$n_e$	1.5500	1.5532	1.5533

## VII. Enstatite Revisited with the Point-Dipole Model

The enstatite-clinoenstatite system was not the first or the simplest system on which calculations with the point-dipole model were attempted. However, because it was the source of the motivation for these calculations, this system will be discussed first. The optical behavior of this system would be said to have been understood in the context of the point-dipole model if the polarizabilities of Mg, O, and Si in clinoenstatite were nearly equal to the analogous polarizabilities of enstatite. Unfortunately, the point-dipole model appears to be inadequate for such understanding.

The lattice constants of enstatite are<sup>9</sup>

$$a_e = 18.22 \text{ \AA}$$

$$b_e = 8.81 \text{ \AA}$$

$$c_e = 5.21 \text{ \AA}.$$

Those for clinoenstatite are<sup>10</sup>

$$a_c = 9.620 \text{ \AA}$$

$$b_c = 8.825 \text{ \AA}$$

$$c_c = 5.188 \text{ \AA}$$

$$\beta = 108.33^\circ.$$

If as implied by Figure (I.1a) the unit cell of enstatite were formed from two undistorted unit cells of clinoenstatite then from simple geometry

$$\left. \begin{aligned} a_e &= 2a_c \sin\beta (=18.264 \text{ \AA}) \\ b_e &= b_c \\ c_e &= c_c \end{aligned} \right\} \quad (\text{VII.1})$$

These relationships hold among the data to one-half of one percent or better. Figure (I.1a) is slightly misleading. The origins of each cell do not coincide; the origin of the enstatite cell is located at

$$x_c = -\frac{1}{2}$$

$$y_c = 0$$

$$z_c = -\frac{1}{2} + \frac{a_e}{2c \tan\beta}$$

where  $x_c$ ,  $y_c$ , and  $z_c$  are fractional coordinates. With this information and Figure (I.1a) a transformation between the atomic coordinates in the monoclinic unit cell and those in the enstatite cell can be derived<sup>1</sup> under the assumption that no changes of the atomic positions occur when the monoclinic cells twin to form enstatite:

$$\left. \begin{aligned} x_c &= 2x_e - \frac{1}{2} \\ y_c &= y_e \\ z_c &= z_e - \frac{1}{2} - (x_e - \frac{1}{2}) \frac{a_e}{c \tan\beta} \end{aligned} \right\} \quad (\text{VII.2})$$

Table (VII.1) is a list of the atomic coordinates for enstatite and clinoenstatite that were used in the calculations. Also included is a list of ideal coordinates for clinoenstatite computed from the enstatite coordinates with (VII.2). The good agreement between the ideal and experimental coordinates of clinoenstatite shows that the model of enstatite as polysynthetically twinned clinoenstatite is a good description of the system.

The calculation for enstatite will now be discussed. From Table (I.1) the optical parameters of this phase are

Table (VII.1). Atomic coordinates of enstatite<sup>15</sup> and clinoenstatite<sup>16</sup> used in this work.  
 Also included is a list of ideal clinoenstatite coordinates computed from  
 the enstatite coordinates with equations (VII.2).

	Enstatite			Clinoenstatite			Ideal Clinoenstatite		
	x	y	z	x	y	z	x	y	z
Mg(1)	.375	.667	.875	.253	.653	.220	.250	.667	.229
Mg(2)	.375	.464	.375	.258	.486	.693	.250	.464	.729
Si(1)	.278	.328	.028	.043	.342	.294	.056	.328	.268
Si(2)	.472	.336	.767	.447	.339	.264	.444	.336	.234
O(1)	.311	.653	.528	.138	.656	.820	.122	.653	.807
O(2)	.303	.506	.050	.123	.502	.298	.106	.506	.320
O(3)	.306	.236	.792	.105	.225	.101	.112	.236	.065
O(4)	.561	.353	.781	.624	.341	.388	.622	.353	.403
O(5)	.439	.497	.700	.363	.482	.103	.378	.497	.129
O(6)	.442	.267	.500	.395	.187	.051	.384	.267	.932

$$\left. \begin{array}{l} n_{\alpha} = 1.650(1) \\ n_{\beta} = 1.652(1) \\ n_{\gamma} = 1.658(1) \end{array} \right\} \quad (\text{VII.3})$$

with  $n_{\alpha}$ ,  $n_{\beta}$ ,  $n_{\gamma}$  along the crystal axes b, a, c, respectively. The extrapolation procedure yielded

$$\begin{aligned} n_{\alpha} &= 1.6503 \\ n_{\beta} &= 1.6522 \\ n_{\gamma} &= 1.6583 \end{aligned}$$

along the b, a, c axes respectively for\*

$$\left. \begin{array}{l} \alpha_{\text{Mg}} = 1.952 \text{ } \text{\AA}^3 \\ \alpha_{\text{Si}} = .4317 \text{ } \text{\AA}^3 \\ \alpha_0 = 18.00 \text{ } \text{\AA}^3 \end{array} \right\} \quad (\text{VII.4})$$

Notice that the oxygen dominates the polarization response of the crystal.

From Table (I.1) the optical parameters of clinoenstatite are

$$\left. \begin{array}{l} n_{\alpha} = 1.651(1) \\ n_{\beta} = 1.654(1) \\ n_{\gamma} = 1.660(1) \end{array} \right\} \quad (\text{VII.5})$$

with  $n_{\alpha}$  along the b axis. The  $n_{\gamma}$  axis is  $22^\circ$  from c in the direction of a. When the empirical polarizabilities of enstatite (VII.4) were used to calculate the optical parameters of clinoenstatite the following results were obtained

\*Divide by 4π to obtain C.G.S. values.

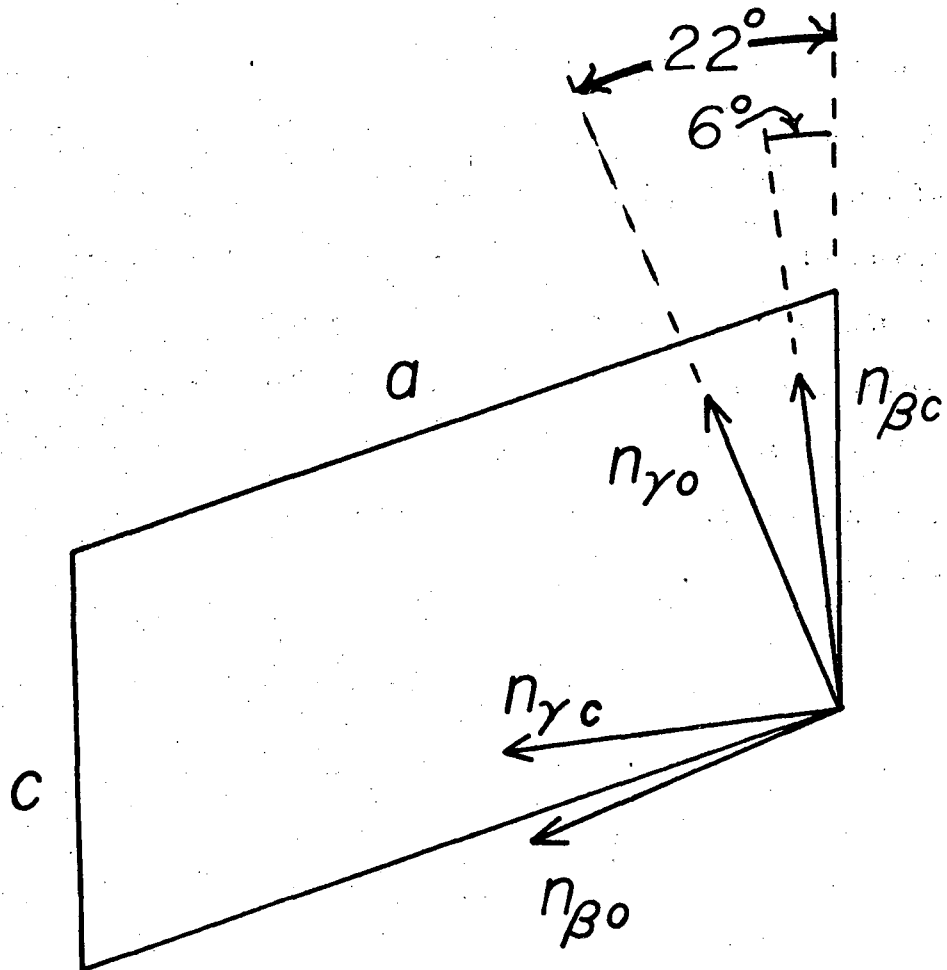
$$\left. \begin{array}{l} n_{\alpha} = 1.6386 \\ n_{\beta} = 1.6498 \\ n_{\gamma} = 1.6539 \end{array} \right\} \quad (\text{VII.6})$$

with  $n_{\alpha}$  along the  $b$  axis. The  $n_{\beta}$  axis is  $6^\circ$  from  $c$  in the direction of  $a$ . The calculated indices for clinoenstatite (VII.6) are roughly equal to the experimental indices of this phase (VII.5). This is expected for assigning enstatite polarizabilities to clinoenstatite gives both structures the same average polarizability per atom per unit volume. However, the calculated indicatrix is rotated  $72^\circ$  from the experimentally measured indicatrix [see Figure (VII.1)]. Although the smallest calculated index is in the  $b$  direction which agrees with experiment, the calculated  $n_{\beta}$  and  $n_{\gamma}$  axes have nearly been interchanged when compared to the experimental results.

It was hoped that when the extrapolation procedure was applied using (VII.4) as a first guess, the polarizabilities would converge to values not far from (VII.4). However, the procedure led to negative values for  $\alpha_{Si}$  regardless of the initial values of the polarizabilities. A negative polarizability is unphysical, for it implies that electric charges move in the opposite direction from the electric force. More importantly for the calculation is that the program for inverting  $\underline{M}$  was designed for positive definite matrices because of memory restrictions and, therefore, could not be used with negative polarizabilities. The extrapolation procedure could not be followed into the region  $\alpha_{Si} < 0$ .

0 0 0 0 4 7 1 0 9 1 8

107



XBL 773-8163

Figure (VII.1). The calculated and observed principal directions for clinoenstatite. The  $n_{\alpha 0}$  and  $n_{\beta c}$  axes are parallel to  $b_c$ .

These calculations have shown that the version of the point-dipole model in which each atomic species is assigned a scalar polarizability does not adequately describe the optical properties of the enstatite-clinoenstatite system. The model did describe one aspect of the data: the same set of polarizabilities correctly predicted that the smallest refractive index is along the same physical direction in both structures. However, this was the model's only success. This is not surprising when one notes that the indicatrices of these phases depart from a sphere by less than one percent.

### VIII. Solid Solutions and the Point-Dipole Model

This section describes calculations with the point-dipole model for two solid solution series. The calculation began with the determination of empirical polarizabilities for each end member. The polarization response of a general member of a series was modeled by assigning site polarizations of the form

$$\alpha_{\text{site}} = f_1 \alpha_1 + f_2 \alpha_2 \quad (\text{VIII.1})$$

where  $\alpha_i$  are the empirical polarizabilities of the end members. The  $f_i$  are the mole percentages of the end members in the mixed crystal. This way of modeling the polarization is similar to the method of assigning x-ray scattering-factors to a site in mixed crystals. However, equation (VIII.1) has much less theoretical justification. Each site has either one type of atom or another; there are no fractional atoms. Although the properties of the Fourier transform allows a derivation of a formula similar to (VIII.1) for an effective scattering-factor of a substitution site, the point-dipole theory will not allow such a simplification to be made rigorously.

Equation (VIII.1) implies a mean-field approximation to the point-dipole model. Consider an atom at a substitution site in the mixed crystal. The cell containing this atom (type i) is surrounded by cells which contain an atom of type 1 or type 2 at the analogous site. The bulk of the crystal is assumed to form a framework which is common to both pure end members. Equation (VIII.1) implies that the local field at the atom under consideration is not due to the actual distribution of atoms in the surrounding cells, but is due to

a hypothetical mean distribution in which each surrounding cell contains at the analogous site a dipole of the form

$$\underline{P}_{\text{effective}} = \alpha_{\text{site}} \underline{e}_{\text{mean}} \quad (\text{VIII.2})$$

where  $\alpha_{\text{site}}$  is given by (VIII.1) and  $\underline{e}_{\text{mean}}$  is self-consistently the local field at the site under consideration due to the hypothetical mean distribution of charge. This mean field will induce a dipole at the site under consideration

$$\underline{P}_i = \alpha_i \underline{e}_{\text{mean}}$$

Averaging this dipole over a region that contains many cells gives

$$\underline{P}_{\text{average}} = (f_1 \alpha_1 + f_2 \alpha_2) \underline{e}_{\text{mean}}$$

which by (VIII.1) and (VIII.2) identifies the effective dipole of the hypothetical charge distribution with the average dipole.

A theoretical justification of the mean-field model of the polarization response will not be attempted. It is clear that it could be a good approximation whenever the substitution site is dilute and contains atoms with relatively small polarizabilities. Both of these conditions are satisfied in silicate minerals in which most of the volume and polarization is due to the oxygen ions.

The first solid solution to be discussed is the enstatite ( $\text{MgSiO}_3$ ) - ferrosilite ( $\text{FeSiO}_3$ ) system. The empirical polarizabilities of the magnesium end member were discussed in the previous section:

$$\left. \begin{aligned} \alpha_{\text{Mg}} &= 1.952 \text{ } \text{\AA}^3 \\ \alpha_{\text{Si}} &= .4317 \text{ } \text{\AA}^3 \\ \alpha_0 &= 18.00 \text{ } \text{\AA}^3 \end{aligned} \right\} \quad (\text{VIII.3})$$

Because the lattice constants and atomic coordinates of the iron end member differed from those of enstatite by a few percent, the lattice sums of enstatite were used to obtain the empirical polarizabilities of ferrosilite. That is, first (VIII.3) was obtained from the enstatite structural parameters and measured indices, then empirical polarizabilities

$$\left. \begin{array}{l} \alpha_{\text{Fe}} = .7744 \text{ \AA}^3 \\ \alpha_{\text{Si}} = .4221 \text{ \AA}^3 \\ \alpha_0 = 20.89 \text{ \AA}^3 \end{array} \right\} \quad (\text{VIII.4})$$

were obtained for ferrosilite from the enstatite structural parameters and the experimental indices<sup>11</sup> of ferrosilite:

$$n_\alpha = 1.768 \text{ along } \underline{b}$$

$$n_\beta = 1.772 \text{ along } \underline{a}$$

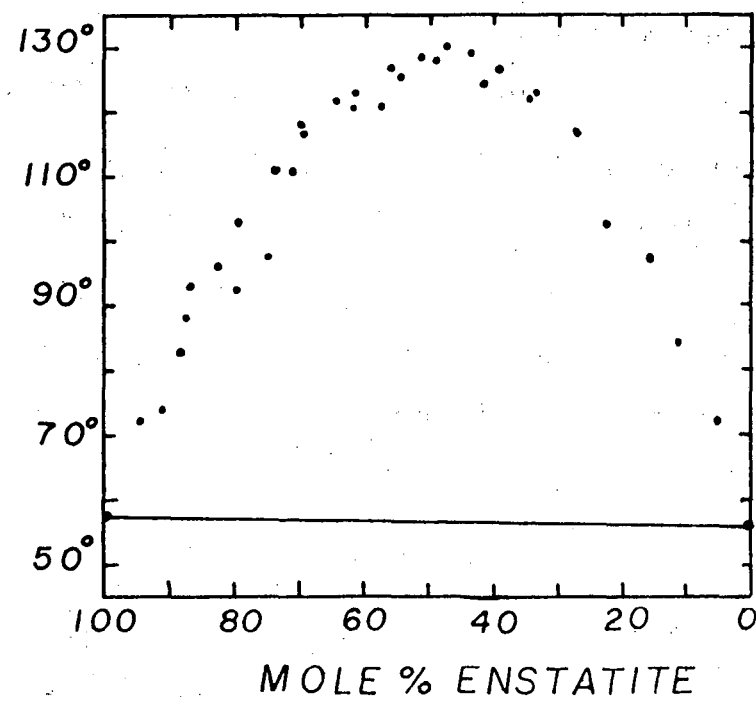
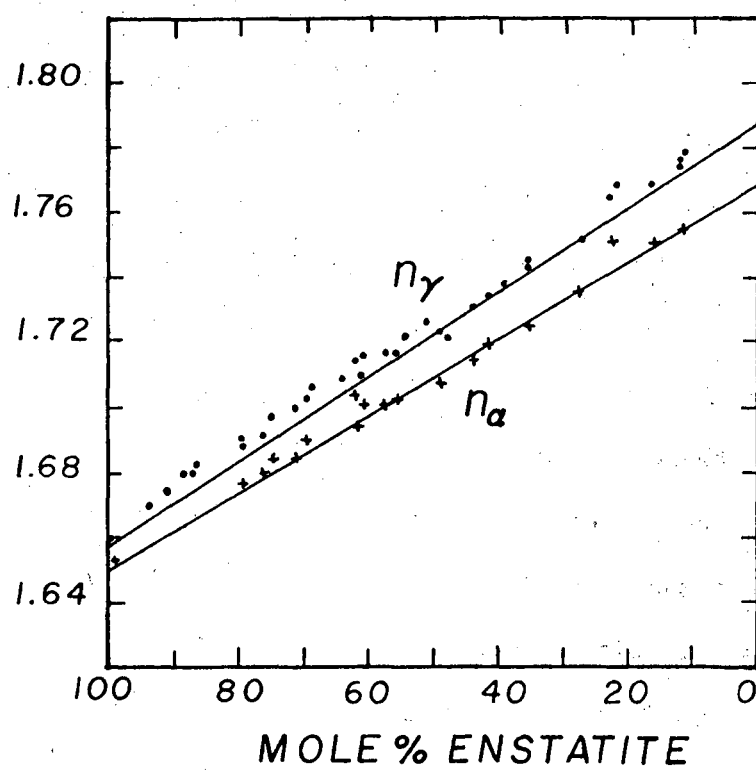
$$n_\gamma = 1.788 \text{ along } \underline{c}$$

This procedure for determining the polarizabilities of the end members is equivalent to assuming that the structural parameters of enstatite do not change when Fe replaces Mg. The optical parameters of an arbitrary member of the solution series were also calculated from the structural parameters of enstatite. This is equivalent to assuming that the enstatite structure is not disturbed by the substitution of any amount of iron.

One of the goals of the application of the point-dipole model to silicate minerals was to determine if it were possible to assign a polarizability to each common ion which could be used to predict the optical properties of most silicates. The numbers of (VIII.3) and

(VIII.4) indicate that this is not possible. The oxygen ion in ferrosilite is 16% more polarizable than in enstatite. This change is too big to be an artifact of the model. This conclusion is supported by direct inspection of the measured indices of these two phases, for it is difficult to believe that the large change in the indices ( $n_\beta$ : 1.652 → 1.772) could be due only to the substitution of one mildly polarizable ion for another. Apparently, the oxygen ion is able to draw more electron density from  $\text{Fe}^{+2}$  than  $\text{Mg}^{+2}$ . This extra electron density would account for the larger polarizability of the oxygen. Notice that the Si polarizability is nearly the same in the two end members. This is understandable when one notes that this ion is shielded from the substituted ions by the oxygen; silicon has the same nearest neighbors in both phases.

The interpolation scheme was carried out by assigning effective polarizabilities to all three ions with formula (VIII.1). The results are in Figure (VIII.1). Experimentally and according to the model there is a linear relationship between the mole percentage of iron and the indices  $n_\alpha$  and  $n_\gamma$ . Although this is a successful prediction of the model, many other possible interpolation schemes can be devised which will predict straight lines. The volume averaged dielectric tensor predicts the same straight lines on the scale of Figure (VIII.1). Unfortunately, the point-dipole model (and the volume averaged dielectric tensor) predicts a straight lines for the axial angle 2V. Experimentally, the axial angle deviates considerably from the straight line prediction. This



XBL 773-8157

Figure (VIII.1). Calculated (lines) and observed<sup>12</sup> optical parameters of the enstatite - ferrosilite solid solution series. Top:  $n_\alpha$  and  $n_\gamma$ . Bottom: 2V.

deviation represents a relative distortion of the indicatrix of only 0.2% from the shape implied by the straight line. Perhaps it was asking too much from the model with all its approximations to predict refractive indices to 0.2%. However, the object of the research was to see if the model could give a quantitative understanding of the optics of these systems in spite of the approximations.

That the largest discrepancy occurs for an equal mixture of the end members can be understood, perhaps, as a breakdown of the mean field approximation, for in this region neither Fe or Mg can be considered as dilute. Another explanation is that lattice distortion is a maximum in this region due to the mismatch of the unit cells. The resulting atomic displacements could invalidate the approximation of using enstatite structural parameters to predict the optics.

In an attempt to remove this discrepancy a second model was assumed for the polarization response of this system. There is evidence<sup>13</sup> that iron has a tendency to replace magnesium in the MII site [see Table (VII.1)] before replacing the magnesium in the MI site. Therefore, a calculation was done in which the mole percentage of iron increased to 50% by replacing first the magnesium in the MII site. The polarizabilities were

$$\alpha_{MI} = \alpha_{Mg}$$

$$\alpha_{MII} = f_1 \alpha_{Mg} + f_2 \alpha_{Fe}$$

where  $f_1$  and  $f_2$  were chosen to reproduce the mole fraction of each ion. After the MII site was filled, the iron was allowed to enter

the MI site. The polarizabilities were

$$\alpha_{MI} = f_1 \alpha_{Mg} + f_2 \alpha_{Fe}$$

$$\alpha_{MII} = \alpha_{Fe}$$

where  $f_1$  and  $f_2$  were chosen as above. The calculation did not remove the discrepancy. The ordered iron model gave the same results as the original model on the scale of Figure (VIII.1). The reason is that in both models the oxygen polarizability was assigned in the same manner. The oxygen dominates the polarization response of this system.

The second solid solution is the high albite-high anorthite system discussed in Chapter I in the context of the volume averaged dielectric tensor. In this series CaSi replaces NaAl. Table (VIII.2) lists the structural parameters of triclinic high albite.

This system is more complicated than the enstatite series for several reasons. Because of the charge difference between  $\text{Ca}^{+2}$  and  $\text{Na}^{+1}$ , the Al/Si ratio must change correspondingly throughout the series. Also, there is complete Al/Si disorder in the tetrahedral sites. Therefore, even to describe the end members with the point-dipole model, the mean field approximation must be used to assign polarizabilities to the tetrahedral sites.

The chemical formula for a general member of the series can be written  $(\text{Na}, \text{Ca}) \text{T}_4 \text{O}_8$  where T represents a tetrahedral site. In particular, high albite has the formula  $\text{NaT}_4 \text{O}_8$ . Assigning the sodium and oxygen atomic polarizations, and the T site a site polarization gives three parameters which can be used to calculate the optical

Table (VIII.2). Atomic coordinates of high albite<sup>17</sup> used in this work. The T stands for the tetrahedral sites. These coordinates are relative to space group Cl. These coordinates were transformed to a primitive cell for the calculations. The C-centered cell has dimensions

$$a = 8.16 \text{ \AA} \quad b = 12.87 \text{ \AA} \quad c = 7.11 \text{ \AA}$$

$$\alpha = 93.5^\circ \quad \beta = 116.4^\circ \quad \gamma = 90.3^\circ.$$

	x	y	z
Na	.2727	.0070	.1339
T <sub>1</sub> (0)	.0091	.1650	.2146
T <sub>1</sub> (M)	.0049	.8149	.2294
T <sub>2</sub> (0)	.6904	.1080	.3200
T <sub>2</sub> (M)	.6846	.8770	.3539
O <sub>A</sub> (1)	.0054	.1345	.9835
O <sub>A</sub> (2)	.5918	.9908	.2782
O <sub>B</sub> (0)	.8195	.1091	.1962
O <sub>B</sub> (M)	.8179	.8474	.2449
O <sub>C</sub> (0)	.0159	.2908	.2772
O <sub>C</sub> (M)	.0211	.6875	.2187
O <sub>D</sub> (0)	.1963	.1119	.3862
O <sub>D</sub> (M)	.1878	.8674	.4272

properties. However, triclinic albite has six optical parameters, so the problem is underdetermined. The best that can be done is to vary the three polarizabilities until three calculated optical parameters match experiment and hope that the model works well enough so the remaining three calculated parameters also match the experiment. Unfortunately this program failed.

The measured indices are found in Table (VII.1) in Chapter I:

$$n_{\alpha} = 1.5284$$

$$n_{\beta} = 1.5349$$

$$n_{\gamma} = 1.5363$$

The three polarizabilities were varied with the help of the extrapolation procedure until the calculated values were

$$n_{\alpha} = 1.5272$$

$$n_{\beta} = 1.5337$$

$$n_{\gamma} = 1.5361$$

The polarizabilities were

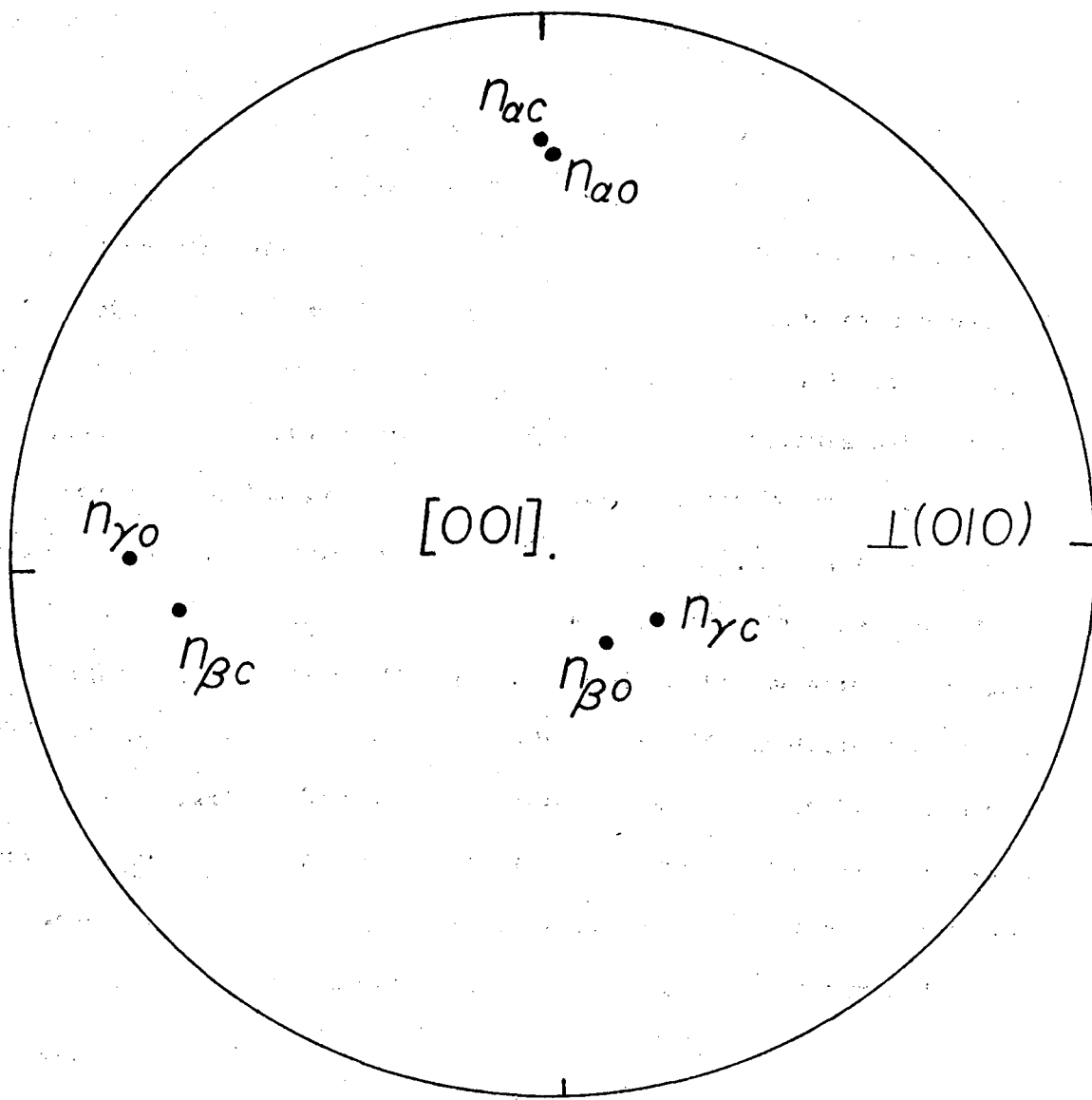
$$\left. \begin{array}{l} \alpha_{Na} = 5.599 \\ \alpha_T = .728 \\ \alpha_0 = 17.67 \end{array} \right\} \quad (VIII.5)$$

No effort was made to calculate indices which were closer to the experiment results, for it was clear that the three orientation angles were not behaving properly. Although the calculated  $n_{\alpha}$  axis was only a few degrees from the experimental result, the calculated  $n_{\beta}$  and  $n_{\gamma}$  axes were interchanged relative to the experimental result

[see Figure (VIII.2)]. Being unable to correctly describe the optical properties of one end member the calculations for this solid solution series were terminated.

0.0.0 0.4 7.1 0.9 2.4

119



XBL 773-8162

Figure (VIII.2). Stereogram showing the calculated and observed principal axes for high albite. Observed axes are from Table (VII.1), Chapter 1.

## IX. Quartz and Corundum

Calculations with the point-dipole model on the uniaxial phases low quartz ( $\text{SiO}_2$ ) and corundum ( $\text{Al}_2\text{O}_3$ ) were completed as part of the program to determine how the empirical polarizabilities vary from structure to structure. The optical and structural parameters of low quartz are listed in Table (IX.1). The oxygen and silicon ions form tetrahedra similar to those in the other structures of this chapter. The parameters of corundum are found in Table (IX.2). The oxygen ions form a hexagonal close-packed structure with the aluminum in two-thirds of the octahedrally coordinated interstices. It was hoped that any large variation in the oxygen polarizability could be correlated with the chemical environment, that is, the oxygen which form the silicate tetrahedra would have one polarizability, and oxygen in other chemical environments such as that of corundum would have a different polarizability. However, this was not the case.

The empirical polarizabilities for quartz are

$$\left. \begin{array}{l} \alpha_{\text{Si}} = 4.546 \text{ } \text{\AA}^3 \\ \alpha_0 = 13.456 \text{ } \text{\AA}^3 \end{array} \right\} \quad (\text{IX.1})$$

and those for corundum are

$$\left. \begin{array}{l} \alpha_{\text{Al}} = 2.222 \\ \alpha_0 = 15.973 \end{array} \right\} \quad (\text{IX.2})$$

It should be noted that these phases each have only one crystallographically distinct oxygen ion and metal ion. In enstatite, for example, the single oxygen polarizability is assigned to six crystallographically distinct ions.

Table (IX.1). Structural<sup>18</sup> and optical<sup>19</sup> parameters of low quartz used in this study. The space group is P3<sub>2</sub>1.

Lattice constants

$a = 4.9128 \text{ \AA}$	$\alpha = 90^\circ$
$b = 4.9128 \text{ \AA}$	$\beta = 90^\circ$
$c = 5.4042 \text{ \AA}$	$\gamma = 120^\circ$

3 Si atoms in

$$(u, 0, 0), (\bar{u}, \bar{u}, 1/3), (0, u, 2/3)$$

6 O atoms in

$$(x, y, z), (y-x, \bar{x}, z+1/3), (\bar{y}, x-y, z-1/3)$$

$$(x-y, \bar{y}, \bar{z}), (\bar{x}, y-x, 1/3-z), (y, x, 2/3-z)$$

$$u = .4697$$

$$x = .4125$$

$$y = .2662$$

$$z = .1188$$

Low quartz is optically uniaxial with

$$n_o = 1.5442$$

$$n_e = 1.5533$$

Table (IX.2). Structural<sup>20</sup> and optical<sup>21</sup> parameters of corundum used in this study. The space group is R̄3c. All structural parameters are relative to hexagonal axes.

Lattice constants:

$$a = 4.7589 \text{ \AA}$$

$$\alpha = 90^\circ$$

$$b = 4.7589 \text{ \AA}$$

$$\beta = 90^\circ$$

$$c = 12.991$$

$$\gamma = 120^\circ$$

12 Al atoms in c,  $z = .352$

18 O atoms in e,  $x = .306$

Corundum is optically uniaxial with

$$n_o = 1.768$$

$$n_e = 1.760.$$

To close the chapter, the polarizabilities that were determined for more than one structure are discussed;

$$\text{Quartz} \quad \alpha_0 = 13.456 \text{ \AA}^3$$

$$\text{Corundum} \quad \alpha_0 = 15.973 \text{ \AA}^3$$

$$\text{High albite} \quad \alpha_0 = 17.67 \text{ \AA}^3$$

$$\text{Enstatite} \quad \alpha_0 = 18.00 \text{ \AA}^3$$

$$\text{Ferrosilite} \quad \alpha_0 = 20.89 \text{ \AA}^3$$

$$\text{Quartz} \quad \alpha_{\text{Si}} = 4.546 \text{ \AA}^3$$

$$\text{Enstatite} \quad \alpha_{\text{Si}} = .4317 \text{ \AA}^3$$

$$\text{Ferrosilite} \quad \alpha_{\text{Si}} = .4221 \text{ \AA}^3$$

It is clear that these numbers preclude the possibility of using the polarizabilities derived from a subset of silicate minerals to predict successfully the optical properties of other silicates. Much of the variation of the polarizabilities is probably due to an artifact of the model rather than reflecting a change in the actual polarization response. To see this note that when the difference between the local field  $e_{\text{loc}}$  and the macroscopic field  $E$  is ignored the index of refraction has a simple form

$$n^2 = 1 + 4\pi \frac{1}{V_c} \sum_{i=1}^N \alpha_i$$

where  $n$  is the isotropic refractive index in this approximation.

Using the relation

$$n \approx \langle n \rangle = \frac{1}{3} (n_\alpha + n_\beta + n_\gamma)$$

gives

$$\sum_{i=1}^N \alpha_i \approx V_c \frac{\langle n \rangle^2 - 1}{4\pi} = \text{constant.}$$

Therefore, as the polarizabilities are varied to give a non-spherical indicatrix, it must be approximately true that

$$\sum_{i=1}^N \alpha_i \approx \text{constant.} \quad (\text{IX.3})$$

This behavior was noted in the actual calculations. It means that some polarizabilities grow at the expense of others in the attempt to reproduce the experimental indicatrix. Therefore, if the model fails to describe accurately the optics of these systems, one would expect large oxygen polarizabilities to be associated with small silicon polarizabilities and vice versa. Experimentally, this is the case. For quartz  $\alpha_0 = 13.456 \text{ \AA}^3$ ,  $\alpha_{Si} = 4.546 \text{ \AA}^3$  while for ferrosilite  $\alpha_0 = 20.89 \text{ \AA}^3$ ,  $\alpha_{Si} = .4221 \text{ \AA}^3$ .

## X. Conclusions

It has been demonstrated that the version of the point-dipole model in which each atomic species is assigned a scalar polarizability does not adequately describe the geometric optical behavior of complex silicate minerals. The model did describe some aspects of the optical behavior of these systems. For example, the empirical polarizabilities of enstatite when applied to clinoenstatite correctly predicted that the smallest refractive index was along the b axis. Also, only three empirical polarizabilities were necessary to predict five optical parameters of high albite. However, the model was not accurate enough to describe more subtle features. The indicatrices of these systems are spherical to within one percent. The striking difference between optically isotropic and anisotropic materials in the polarizing microscope is the result of small differences of relatively large numbers (e.g. enstatite:  $\delta = 1.658 - 1.650$ ). Such effects are notoriously difficult to describe quantitatively. Perhaps it was asking too much of the model with all its approximations to predict the refractive indices to within one percent. However, it was the point of the research to determine if the model could describe the optical behavior of silicate minerals in spite of the approximations.

There are two distinct types of approximation. First, is the application of the point-dipole model instead of a more sophisticated one. Secondly, only an approximate version of the point-dipole model was actually used.

Although quantum mechanics allows a rigorous definition of the polarizability of free ions, it is not possible according to quantum mechanics to assign polarizabilities to atoms in a crystal. The electronic wavefunctions in a crystal are not localized; they extend in a continuous manner throughout the crystal. However in dielectric crystals as opposed to metals and semiconductors, the electrons are sufficiently localized as to raise the question whether it is possible to consider the polarization response of the crystal as located at the atomic sites. If so a polarized ion would to first order have a dipole electric field which would in turn polarize the other ions; the point-dipole model would be valid. Other workers<sup>14</sup> have shown that the point-dipole model works well enough for ionic crystals with cubic symmetry to make lists of atomic polarizabilities analogous to a list of ionic radii. However, these polarizabilities are sensitive to the chemical environment of the atom. Work by Reijnhart<sup>4</sup> indicates that the point-dipole model can be used to describe the optical properties of more complicated structures. He used the point-dipole model to calculate the refractive indices and optical rotation of several uniaxial crystals. His work was successful in the sense that for several systems he was able to calculate accurately three optical parameters (two refractive indices and the optical rotation) from only two polarizabilities. The key to his success was, perhaps, that he worked with systems that were simple enough to allow each crystallographically distinct ion to be assigned a different polarizability. He also found that the atomic polarizabilities were sensitive to the chemical and structural environment.

Therefore, in the light of Reijnhart's work it appears that the failure of the model to describe the optics of silicate minerals is due to the approximation of assigning the same polarizability to crystallographically distinct atoms, rather than the failure of the point-dipole model itself. The polarizabilities appear to be too sensitive to the atomic environment.

Another possible source of error is the scalar approximation to the tensor polarizabilities. In the light of Reijnhart's successful work using scalar polarizabilities this source of error is felt to be not as important as assigning the same polarizability to distinct ions.

There are additional sources of error in the solid solution calculations. The mean field approximation to the local field is not rigorously valid. This approximation in itself is enough to explain the discrepancy between the calculated and observed parameters in the enstatite-ferrosilite system. Also, in this system errors were introduced when the differences between the structural parameters of the end members were ignored. Calculations on low quartz has shown that changing the structural parameters by 1% will change the calculated indices by about 0.1%. Although these figures indicate that the source of the discrepancy could be due to errors in the structural parameters, this source of error is probably not the cause of the poor results for the enstatite-clino-enstatite system. That the extrapolation procedure lead to negative polarizabilities for clinoenstatite indicates a larger source of

error: ten crystallographically distinct ions were assigned only a total of three polarizabilities.

## XI. Appendix

This section is a listing and description of a FORTRAN program which calculates the dipole lattice sums. The program consists of two subroutines SUM and TERM. The input of SUM is

A = a	ASTAR = a*
B = b	BSTAR = b*
C = c	CSTAR = c*
SA = sin $\alpha$	SASTAR = sin $\alpha$ *
SB = sin $\beta$	SBSTAR = sin $\beta$ *
SG = sin $\gamma$	SGSTAR = sin $\gamma$ *
CA = cos $\alpha$	CASTAR = cos $\alpha$ *
CB = cos $\beta$	CBSTAR = cos $\beta$ *
CG = cos $\gamma$	CGSTAR = cos $\gamma$ *

$$V = abc(1 - \cos^2\alpha - \cos^2\beta - \cos^2\gamma + 2\cos\alpha\cos\beta\cos\gamma)^{1/2}$$

DEL(I) = three components of the interatomic vector defined after equation (V.7). The notation in the text is

$$\text{DEL}(I) = \Delta_I.$$

The output of SUM is

VS(I,J) = the (I,J) components of the lattice sum defined in equations (IV.15) - (IV.17). The notation in the text is

$$VS(I,J) = (\underline{\underline{A}}^{\ell m})_{IJ}.$$

The superscripts  $\ell, m$  refer to the end points of the interatomic vector.

SUM is concerned with generating the integers which label the unit cells in both spaces and with testing if the lattice sums have converged to within the limits specified by ERROR.

The input to TERM in addition to the lattice parameters is L1, L2, L3 which are the labels of the cells in both spaces.

The same set of integers label the cells in both spaces.

The output of term is

$T(I,J) =$  the term of  $VS(I,J)$  which is the contribution from the direct space cell specified by  $L1_a + L2_b + L3_c$ , and the contribution in reciprocal space from the reciprocal lattice vector with Miller indices L1, L2, L3.

TERM is concerned with computing each term of  $VS(I,J)$ .

BERT is the Bertaut parameter denoted by B in the text.

D1, D2, D3 are defined in equation (V.7). The notation in the text is  $D1 = \Delta_1 - \ell_1$ , etc.

The first set Q1, Q2, Q3 are defined in section V as

$$QS = \underline{\hat{x}}^s \cdot \underline{x}_{ij\ell}$$

The second set Q1, Q2, Q3 are defined in section V as

$$QS = k \cdot \underline{\hat{x}}^s$$

PHI is the cutoff function defined by equation (IV.12).

To evaluate this function a subroutine for the complimentary error function is required.

```

SUBROUTINE SUM(DEL,VS)
COMMON/DATA2/A,B,C,SA,SB,SG,CA,CR,CG,ASTAR,BSTAR,CSTAR,SASTAR,SBS
IAR,SGSTAR,CASTAR,CSTAR,CGSTAR,V
DIMENSION DEL(3),VS(3,3),T(3,3),TEST1(3,3),TEST2(3,3)
ERROR=.0000000001
DO 10 I1=1,3
DO 10 I2=1,3
10 VS(I1,I2)=0.
L1MAX=1
L2MAX=1
L3MAX=1
LL1=2*L1MAX+1
LL2=2*L2MAX+1
LL3=2*L3MAX+1
DO 9 LLL1=1,LL1
DO 9 LLL2=1,LL2
DO 9 LLL3=1,LL3
L1=LLL1-1-L1MAX
L2=LLL2-1-L2MAX
L3=LLL3-1-L3MAX
CALC_TERM(L1,L2,L3,DEL,T)
VS(1,1)=VS(1,1)+T(1,1)
VS(1,2)=VS(1,2)+T(1,2)
VS(1,3)=VS(1,3)+T(1,3)
VS(2,2)=VS(2,2)+T(2,2)
9 VS(2,3)=VS(2,3)+T(2,3)
DO 13 I1=1,3
DO 13 I2=1,3
13 TEST2(I1,I2)=VS(I1,I2)
DO 11 I1=1,3
DO 11 I2=1,3
11 TEST1(I1,I2)=0.
NCYCLE=1
L1MAX=L1MAX+1
L2MAX=L2MAX+1
L3MAX=L3MAX+1
8 NCYCLE=NCYCLE+1
LL1=2*L1MAX+1
LL2=2*L2MAX+1
LL3=2*L3MAX+1
DO 5 LLL3=1,LL3
L3=LLL3-1-L3MAX
L3MIN=-L3MAX
IF(L3.EQ.0.L3MAX.O.R.L3.EQ.L3MIN) GO TO 1
DO 3 LLL2=1,LL2
L2=LLL2-1-L2MAX
L2MIN=-L2MAX
IF(L2.EQ.0.L2MAX.O.R.L2.EQ.L2MIN) GO TO 4
L1=L1MAX
CALC_TERM(L1,L2,L3,DEL,T)
VS(1,1)=VS(1,1)+T(1,1)
VS(1,2)=VS(1,2)+T(1,2)
VS(1,3)=VS(1,3)+T(1,3)
VS(2,2)=VS(2,2)+T(2,2)

```

```

VS(2,3)=VS(2,3)+T(2,3)
L1=L1MAX
CALL TERM(L1,L2,L3,DEL,T)
VS(1,1)=VS(1,1)+T(1,1)
VS(1,2)=VS(1,2)+T(1,2)
VS(1,3)=VS(1,3)+T(1,3)
VS(2,2)=VS(2,2)+T(2,2)
VS(2,3)=VS(2,3)+T(2,3)
GO TO 3
4 DO 5 LLL1=1,LLL1
L1=LLL1-1-L1MAX
CALL TERM(L1,L2,L3,DEL,T)
VS(1,1)=VS(1,1)+T(1,1)
VS(1,2)=VS(1,2)+T(1,2)
VS(1,3)=VS(1,3)+T(1,3)
VS(2,2)=VS(2,2)+T(2,2)
5 VS(2,3)=VS(2,3)+T(2,3)
3 CONTINUE
GO TO 6
1 DO 2 LLL2=1,LLL2
DO 2 LLL1=1,LLL1
L2=L2-1-L2MAX
L1=LLL1-1-L1MAX
CALL TERM(L1,L2,L3,DEL,T)
VS(1,1)=VS(1,1)+T(1,1)
VS(1,2)=VS(1,2)+T(1,2)
VS(1,3)=VS(1,3)+T(1,3)
VS(2,2)=VS(2,2)+T(2,2)
2 VS(2,3)=VS(2,3)+T(2,3)
6 CONTINUE
DO 12 I1=1,3
DO 12 I2=1,3
TEST1(I1,I2)=TEST2(I1,I2)
12 TEST2(I1,I2)=VS(I1,I2)
DO 14 I1=1,3
DO 14 I2=1,3
14 IF(ABS(TEST2(I1,I2)-TEST1(I1,I2)).GT.ERROR) GO TO 7
GO TO 15
7 L1MAX=L1MAX+1
L2MAX=L2MAX+1
L3MAX=L3MAX+1
GO TO 8
15 VS(2,1)=VS(1,2)
VS(3,1)=VS(1,3)
VS(3,2)=VS(2,3)
VS(3,3)=-VS(1,1)-VS(2,2)
RETURN
END

```

```

SUBROUTINE TERM(L1,L2,L3,DEL,T)
COMMON/DATA2/A,B,C,SA,SB,SG,CA,CH,CG,ASTAR,BSTAR,CSTAR,SASTAR,SBST
1AR,SGSTAR,CASTAR,CHSTAR,CGSTAR,V
DIMENSION DEL(3),T(3,3)
BERT=.88*(A+B+C)/3.
S=3.141592653589793
Z1=L1
Z2=L2
Z3=L3
DO 1 I1=1,3
DO 1 I2=1,3
1 T(I1,I2)=0.
D1=DEL(1)-Z1
D2=DEL(2)-Z2
D3=DEL(3)-Z3
IF(D1.EQ.0.0 AND D2.EQ.0.0 AND D3.EQ.0.0) GO TO 2
Q1=D1*A*SB-D2*B*SA*CGSTAR
Q2=D2/HSTAR
Q3=D1*A*CB+D2*B*CA+D3*C
Q=SQRT(Q1*Q1+Q2*Q2+Q3*Q3)
TE=Q/BERT
YY=SORT(S)*TE
CALL MERFC(YY,ERFC)
PHI=EFFC*EXP(-S*TE*TE)*(S*TE**3.0+3.0*TE/2.0)*4.0/3.0
Q5=V*PHI/0**5.
T(1,1)=T(1,1)+(2.0*Q1*Q1-Q2*Q2-Q3*Q3)*Q5
T(1,2)=T(1,2)+3.0*Q1*Q2*Q5
T(1,3)=T(1,3)+3.0*Q1*Q3*Q5
T(2,2)=T(2,2)+(2.0*Q2*Q2-Q1*Q1-Q3*Q3)*Q5
T(2,3)=T(2,3)+3.0*Q2*Q3*Q5
2 IF(Z1.EQ.0.0 AND Z2.EQ.0.0 AND Z3.EQ.0.0) GO TO 3
Q1=Z1*ASTAR*SGSTAR-Z3*CSTAR*SASTAR*CH
Q2=Z1*ASTAR*CGSTAR+Z2*BSTAR+Z3*CSTAR*CASTAR
Q3=Z3/C
Q=SORT(Q1*Q1+Q2*Q2+Q3*Q3)
TE=Q*EEFT
Q5=(-1.0*4.0*S/3.0)*EXP(-S*TE*TE)*COS(2.0*S*(DEL(1)*Z1+DEL(2)*Z2
1+DEL(3)*Z3))/Q**2.0
T(1,1)=T(1,1)+(2.0*Q1*Q1-Q2*Q2-Q3*Q3)*Q5
T(1,2)=T(1,2)+3.0*Q1*Q2*Q5
T(1,3)=T(1,3)+3.0*Q1*Q3*Q5
T(2,2)=T(2,2)+(2.0*Q2*Q2-Q1*Q1-Q3*Q3)*Q5
T(2,3)=T(2,3)+3.0*Q2*Q3*Q5
3 CONTINUE
RETURN
END

```

## XII. References

1. J. V. Smith (1969). In "Pyroxenes and Amphiboles: Crystal Chemistry and Phase Petrology", J. J. Papike edit., p. 13. Mineralogical Society of America, Special Paper Number Two.
2. P. P. Ewald (1916). Ann. der Physik, 49, 117.
3. P. P. Ewald (1921). Ann. der Physik, 64, 253.
4. R. Reijnhart (1970). Ph.D. Thesis. Technische Hogeschool Delft, Holland.
5. Reference 3.
6. D. E. Williams (1971). Acta Cryst., A27, 452.
7. B. R. A. Nijboer and F. W. DeWette (1957). Physica, 23, 309-321.
8. C. Kittel (1970). "Introduction to Solid State Physics". Wiley and Sons, New York.
9. Reference 1, p. 17.
10. Reference 1, p. 17.
11. W. E. Tröger (1959). "Optische Bestimmung der gesteinsbildenden Minerale", p. 53. E. Schweizerbart'sche Verlagsbuchhandlung, Stuttgart.
12. W. A. Deer, R. A. Howie and J. Zussman (1965). "Rock-Forming Minerals", Vol. 2, p. 28. Longmans, Green and Co. Ltd., London.
13. D. Virgo and S. S. Hafner (1969). In "Pyroxenes and Amphiboles: Crystal Chemistry and Phase Petrology", J. J. Papike edit., p. 75. Mineralogical Society of America, Special Paper Number Two.
14. J. Tessman, A. Kahn and W. Shockley (1953). Phys. Rev., 92, 890.

0 0 0 0 4 7 1 0 9 3 2

135

15. As abstracted in "Structure Reports", A. J. C. Wilson edit., Vol. 9, p. 255. International Union of Crystallography.
16. N. Morimoto, D. E. Appleman and H. T. Evans, Jr. (1960). Z. Krist., 114, 120.
17. J. V. Smith (1974). "Feldspar Minerals", p. 86. Springer, Berlin, Heidelberg, New York.
18. W. H. Zachariasen and H. A. Plettner (1965). Acta Cryst., A18, 710.
19. Reference 12, Vol. 5, p. 11.
20. H. Saalfeld (1964). Z. Krist., 120, 342.
21. Reference 12, Vol. 4, p. 179.

CHAPTER 3: THE CRYSTAL STRUCTURES OF  $\text{Na}_3(\text{UO}_2)_7 \cdot n\text{H}_2\text{O}$  FOR  $n = 2, 6$ 

## I. Introduction

A study of the uranyl nitrate-sodium fluoride system has shown the existence of two new double fluorides:  $\text{Na}_3(\text{UO}_2)_2 \cdot n\text{H}_2\text{O}$  with  $n = 2$  and  $6$ . They are additons to the series of double salts of the form  $M_x(\text{UO}_2)_y F_z \cdot n\text{H}_2\text{O}$  where  $M$  is an alkali metal and  $n$  may be zero. In all such salts whose structures had been determined previously, the uranium has seven-fold coordination. In almost all such salts two uranyl oxygen atoms form the axis and five fluorine atoms form the equator of a pentagonal bipyramid centered at the uranium. Both of the new double fluorides have this structural feature.

## II. Experimental Section

An aqueous solution of uranyl nitrate and sodium fluoride with  $[Na]:[UO_2] \approx 3:1$  was allowed to evaporate slowly at room temperature ( $\sim 24^\circ C$ ). The bulk of the residue was sodium nitrate and an opaque yellow polycrystalline mass of unknown composition. There were also a few transparent yellow monoclinic crystals of  $Na_3(UO_2)_2F_7 \cdot 2H_2O$ . This experiment was repeated several times with the same result. One time, however, the residue consisted primarily of sodium nitrate and yellow transparent triclinic crystals of  $Na_3(UO_2)_2F_7 \cdot 6H_2O$ . Although the experiment was repeated several times, the triclinic phase appeared only once in the residue of the uranyl nitrate-sodium fluoride solution. The experiment was repeated several times at a lower temperature ( $\sim 5^\circ C$ ) and at higher temperatures ( $30^\circ$ - $50^\circ$ ) combined with varying the  $[Na]:[UO_2]$  ratio from 1/10 to 10. These experiments were repeated with the addition of small amounts of HF to the solution. However, the triclinic phase failed to appear again in the uranyl nitrate-sodium fluoride system.

Another series of experiments produced the two salts. Uranyl fluoride was first made by evaporating to dryness the solution obtained by dissolving in HF the precipitate formed by mixing NaOH and uranyl nitrate solutions. An x-ray powder photograph confirmed the existence of uranyl fluoride. The triclinic phase was obtained when an aqueous solution of uranyl fluoride and sodium fluoride with  $[Na]:[UO_2] \approx 1:1$  evaporated to dryness at room temperature ( $\sim 24^\circ C$ ). Repeating this experiment at  $50^\circ C$  produced the lower hydrate.

X-ray photographs obtained with the Weissenberg technique and copper radiation established the diffraction symmetry of each phase. A triclinic crystal  $.1 \times .03 \times .1$  mm and a monoclinic crystal  $.1 \times .1 \times .16$  mm were selected for collecting intensity data. Accurate unit cell dimensions were determined from measurements of high angle reflections using a Picker automatic diffractometer equipped with a full-circle goniostat, graphite monochromator, pulse-height analyzer, and PDP-8I computer. Intensity data were collected with the same instrument using Mo radiation. The integrated intensity of each reflection was measured using a  $\theta$ - $2\theta$  scan technique with a scanning rate of one degree per minute from  $.75^\circ$  below the  $2\theta$  angle at which  $K\alpha_1$  was diffracted to  $.75^\circ$  above the angle at which  $K\alpha_2$  was diffracted. Two 10 second background counts were taken with the apparatus stationary  $.2^\circ$  below and  $.2^\circ$  above the  $2\theta$  angle at which the scanning was begun and ended. Three strong reflections were remeasured every 100 reflections to check for crystal decomposition and/or instrument malfunction. From these three standard reflections it was determined that there was negligible decay in the intensities during the experiments. Intensities of equivalent reflections and those measured more than once were averaged after they were corrected for Lorentz, polarization, and absorption effects. The absorption correction was calculated by an analytical method based on crystal dimensions and absorption parameters verified by measurements of several reflections at various azimuthal angles, as described by Volz, Zalkin and Templeton.<sup>1</sup> Absorption correction factors ranged from 2.55 to 9.98 for the triclinic

phase and from 6.25 to 24.52 for the monoclinic phase. Actual counts were converted into structure factors and standard deviations  $\sigma(F)$  using the formulae given by St. Clair, Zalkin, and Templeton<sup>2</sup> except that the additional term in  $\sigma^2(I)$  was  $(0.04 I)^2$  for the triclinic phase and  $(0.02 I)^2$  for the monoclinic phase.

For the triclinic phase 6866 reflections were measured in the full sphere of reciprocal space out to  $2\theta = 70^\circ$  except for those reflections omitted to avoid instrument collision. This gave 3380 unique reflections of which 3169 were greater than  $\sigma(I)$ . 2846 reflections greater than  $3\sigma(I)$  were used in the final least-squares refinement of 109 parameters. For the monoclinic phase 7324 reflections not excluded by the space group were measured in the half-sphere with  $k > 0$  out to  $2\theta = 80^\circ$ . This gave 3661 unique reflections of which 3085 were greater than  $\sigma(I)$ . 2534 reflections greater than  $3\sigma(I)$  were used in the final least-squares refinement of 99 parameters.

Calculations were made with a CDC 7600 computer using a full-matrix least-squares program. The function that was minimized was

$$R_2 = (\sum w(|F_o| - |F_c|)^2 / \sum w F_o^2)^{1/2} \text{ with } w = 1/\sigma^2(F).$$

Atomic scattering factors were taken from Doyle and Turner<sup>3</sup> for Na<sup>+</sup>, F<sup>-</sup>, and neutral U, O, and H. The values of the real and imaginary dispersion corrections are those of Cromer and Liberman.<sup>4</sup>

A listing of the observed and calculated structure factors is found in the appendix to this chapter.

### III. Unit Cells and Space Group

The higher hydrate has a triclinic cell containing one formula unit with cell dimensions (at 23°C)

$$\begin{aligned}
 a &= 7.177 \pm .002 \text{ \AA} \\
 b &= 8.633 \pm .003 \text{ \AA} \\
 c &= 7.000 \pm .002 \text{ \AA} \\
 \alpha &= 113.28 \pm .03^\circ \\
 \beta &= 104.92 \pm .03^\circ \\
 \gamma &= 77.88 \pm .03^\circ.
 \end{aligned}$$

From the x-ray data the density is calculated as  $3.69 \text{ g/cm}^3$ . A careful search for symmetry in reciprocal space using the Weissenberg camera and G.E. manual diffractometer found only the usual center. Successful solution of the structure has shown the space group to be  $P\bar{1}$ .

The lower hydrate has a monoclinic cell containing four formula units with cell dimensions (at 23°C)

$$\begin{aligned}
 a &= 15.127 \pm .005 \text{ \AA} \\
 b &= 6.926 \pm .002 \text{ \AA} \\
 c &= 11.235 \pm .004 \text{ \AA} \\
 \beta &= 94.77 \pm .03^\circ.
 \end{aligned}$$

The calculated density is  $4.41 \text{ g/cm}^3$ . This larger density is consistent with the lower water content. Reflections are absent unless  $h + k = 2 \times (\text{integer})$  showing that the monoclinic cell is C-centered. All reflections in the  $h0l$  layer have  $l = 2 \times (\text{integer})$  implying a c-glide plane. Only space groups Cc and C2/c are consistent with these facts. The successful structure determination has shown the centric group C2/c to be the correct choice.

0 0 0 0 4 7 1 0 9 3 5

141

The cell dimensions for both phases are based on  $\lambda = .70926 \text{ \AA}$   
for  $\text{MoK}\alpha_1$ .

#### IV. Determination of the Structures

A three-dimensional Patterson function was calculated for each hydrate from the observed intensities after correction for Lorentz, polarization, and absorption effects. The uranium atom in each hydrate was easily located in a general position. The uranium position and isotropic temperature parameter were refined with four least-squares cycles using 2593 (2942) reflections with  $I > 3\sigma(I)$  for the monoclinic (triclinic) phase.  $R_1 = \Sigma(|F_o| - |F_c|)/\Sigma|F_o|$  at this point was .133 (.136). With phases determined by the uranium parameters, an electron density Fourier synthesis showed the location of all nine (eleven) remaining nonhydrogen atoms in the asymmetric unit. With ten (twelve) atoms and isotropic temperature factors, four cycles of refinement using 2593 (2942) reflections reduced  $R_1$  to .066 (.081). At this point a small extinction correction was made in the form  $F'_o = F_o(1 + \epsilon I)$ . The ten (twelve) atoms were given anisotropic temperature factors. As a result of four more cycles using 2593 (2942) reflections,  $R_1$  dropped to .024 (.026).

A difference Fourier synthesis at this point showed both independent hydrogen atoms in the monoclinic phase. These were included with isotropic temperature factors in the final refinement. Although a similar synthesis showed evidence for two or perhaps three of the six independent hydrogen atoms of the triclinic phase, they were not included in the final refinement.

All data with  $\sin\theta/\lambda$  less than .232 (.250) were excluded from the final refinement. This was because of the poor agreement in

this region probably due to small errors in the description of the crystal shape in the absorption correction.

After four cycles of the final refinement  $R_1$  was .022 (.024) for 2534 (2846) reflections with  $I > 3\sigma(I)$  and  $\sin\theta/\lambda$  greater than .232 (.250);  $R_2$  was .021 (.029). For all 3661 (3380) unique reflections  $R_1$  was .044 (.033). In the last cycle, no parameter changed more than  $.02\sigma$  (.01 $\sigma$ ).

Coordinates of the atoms are listed in Tables (IV.1) and (IV.3), and thermal parameters are given in Tables (IV.2) and (IV.4).

Table (IV.1).  $\text{Na}_3(\text{UO}_2)_2\text{F}_7 \cdot 6\text{H}_2\text{O}$ , triclinic phase. Atomic coordinates ( $\text{\AA}$ ) with estimated standard deviations in parentheses.

ATOM	X	Y	Z
U	.01023(2)	.76652(2)	.00059(2)
O1	.0409(6)	.8525(6)	.2808(6)
O2	.9736(6)	.6830(5)	.7176(6)
NA1	.500	0	0
NA2	.4780(3)	.4771(3)	.2153(4)
F1	0	.500	0
F2	.3043(4)	.2521(4)	.0181(5)
F3	.3165(4)	.6472(4)	.0230(5)
F4	.1818(4)	.9759(4)	.0134(6)
O3	.6710(7)	.7189(8)	.3682(8)
O4	.3038(8)	.5931(8)	.4997(9)
O5	.599(1)	.0836(9)	.373(1)

Table (IV.2)).  $\text{Na}_3(\text{UO}_2)_2\text{F}_7 \cdot 6\text{H}_2\text{O}$ , triclinic phase. Thermal parameters ( $\text{\AA}^2$ ) with estimated standard deviations in parentheses. Temperature factor has the form  $\exp(-\sum_{I J} B_{IJ} b_I b_J h_I h_J)$  where  $h_I$  is the Miller index and  $b_I$  is the reciprocal cell length.

ATOM	B11	B22	B33	B12	B13	B23
U	.832(5)	.736(5)	1.517(6)	-.038(3)	.287(3)	.518(3)
O1	2.8(2)	2.5(1)	1.9(1)	-.2(1)	.5(1)	.5(1)
O2	2.2(1)	2.7(1)	1.8(1)	-.3(1)	.3(1)	.8(1)
NA1	1.35(9)	1.9(1)	2.9(1)	-.30(8)	.54(8)	.68(9)
NA2	2.17(8)	2.50(8)	2.35(8)	-.47(7)	.41(6)	.93(7)
F1	2.2(2)	1.4(1)	5.5(3)	-.3(1)	1.5(2)	1.9(2)
F2	1.26(9)	1.6(1)	3.5(1)	-.11(8)	.67(8)	.95(9)
F3	1.24(9)	2.3(1)	3.1(1)	-.41(8)	.59(8)	1.4(1)
F4	1.13(9)	1.42(9)	4.8(2)	-.07(7)	.58(9)	1.7(1)
O3	2.9(2)	4.7(2)	2.7(2)	-.7(2)	.2(1)	1.4(2)
O4	3.7(2)	4.8(3)	3.8(2)	-.5(2)	1.1(2)	2.3(2)
O5	5.3(3)	4.5(3)	3.6(2)	-.6(2)	.2(2)	.8(2)

Table (IV.3).  $\text{Na}_3(\text{UO}_2)_2\text{F}_7 \cdot 2\text{H}_2\text{O}$ , monoclinic phase. Atomic coordinates ( $\text{\AA}$ ) with estimated standard deviations in parentheses.

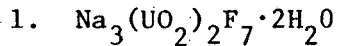
ATOM	X	Y	Z
U	.17985(1)	.02612(2)	.05824(1)
O1	.2507(2)	.03121(5)	.1931(3)
O2	.3884(2)	.4717(5)	.0790(3)
NA2	.1109(1)	.4903(2)	.1900(2)
F1	.250	.250	.500
F2	.1946(2)	.3698(3)	.0383(2)
F3	.4022(2)	.2935(4)	.3701(3)
F4	.0750(2)	.1772(4)	.1522(2)
O3	.0518(2)	.4667(7)	.3785(3)
NA1	.500	.4495(4)	.250
H1	.034(6)	.36(1)	.389(7)
H2	.421(5)	.021(9)	.064(7)

Table (IV.4).  $\text{Na}_3(\text{UO}_2)_2\text{F}_7 \cdot 2\text{H}_2\text{O}$ , monoclinic phase. Thermal parameters

( $\text{\AA}^2$ ) with estimated standard deviations in parentheses. The temperature factor has the form given in Table (IV.2) except for the isotropic temperature of the hydrogen atoms which has the form  $\exp[-B(\sin\theta/\lambda)^2]$ . B is listed in the B11 column for the hydrogen atoms.

ATOM	B11	B22	B33	B12	B13	B23
U	.927(3)	.786(3)	1.224(4)	.019(4)	.340(2)	.010(4)
O1	1.9(1)	2.9(1)	1.8(1)	-.0(1)	-.03(8)	.24(9)
O2	2.0(1)	3.3(1)	1.8(1)	-.0(1)	-.31(8)	-.1(1)
NA2	2.23(6)	1.55(6)	2.21(6)	-.00(5)	.59(5)	-.06(5)
F1	2.8(2)	1.4(1)	4.0(2)	-.7(1)	1.4(1)	.1(1)
F2	1.77(8)	1.05(7)	2.39(9)	.02(6)	1.12(7)	-.00(6)
F3	2.3(1)	1.26(8)	3.5(1)	-.09(7)	1.32(9)	-.23(7)
F4	1.88(9)	1.66(9)	2.9(1)	-.04(7)	1.35(8)	-.05(7)
O3	2.4(1)	3.5(2)	2.3(1)	-.7(1)	.0(1)	-.2(1)
NA1	1.61(7)	2.2(1)	1.91(8)	0	.64(6)	0
H1	4.3(18)					
H2	2.1(11)					

## V. Description of the Structures



The structure of the monoclinic phase consists of identical layers parallel to the (101) plane.\* Adjacent layers are related by the c-glide plane. Figure (V.1) is a projection of one of these layers in the (101) plane. It consists of infinite  $[(\text{UO}_2)_2\text{F}_7]_n^{-3n}$  chains held together by sodium atoms [Na(1), Na(2)]. The chains are formed from  $\text{UO}_2\text{F}_5$  pentagonal bipyramids similar to that first described by Zachariasen<sup>5</sup> for  $\text{K}_3\text{UO}_2\text{F}_5$ . In the potassium salt and both salts of this study, the uranyl group is the axis and the fluorines form the equator of a pentagonal bipyramid centered at the uranium. In the monoclinic phase the pentagons share an edge [F(2) and F(2)'] and a vertex F(1). Therefore, the pentagons are much more distorted than in  $\text{K}_5\text{UO}_2\text{F}_5$  where they are found in isolated  $\text{UO}_2\text{F}_5^{-3}$  groups. The edges (F-F distances) of the pentagon in the monoclinic phase range from 2.56 Å to 2.81 Å, the smaller value being that for the shared edge.

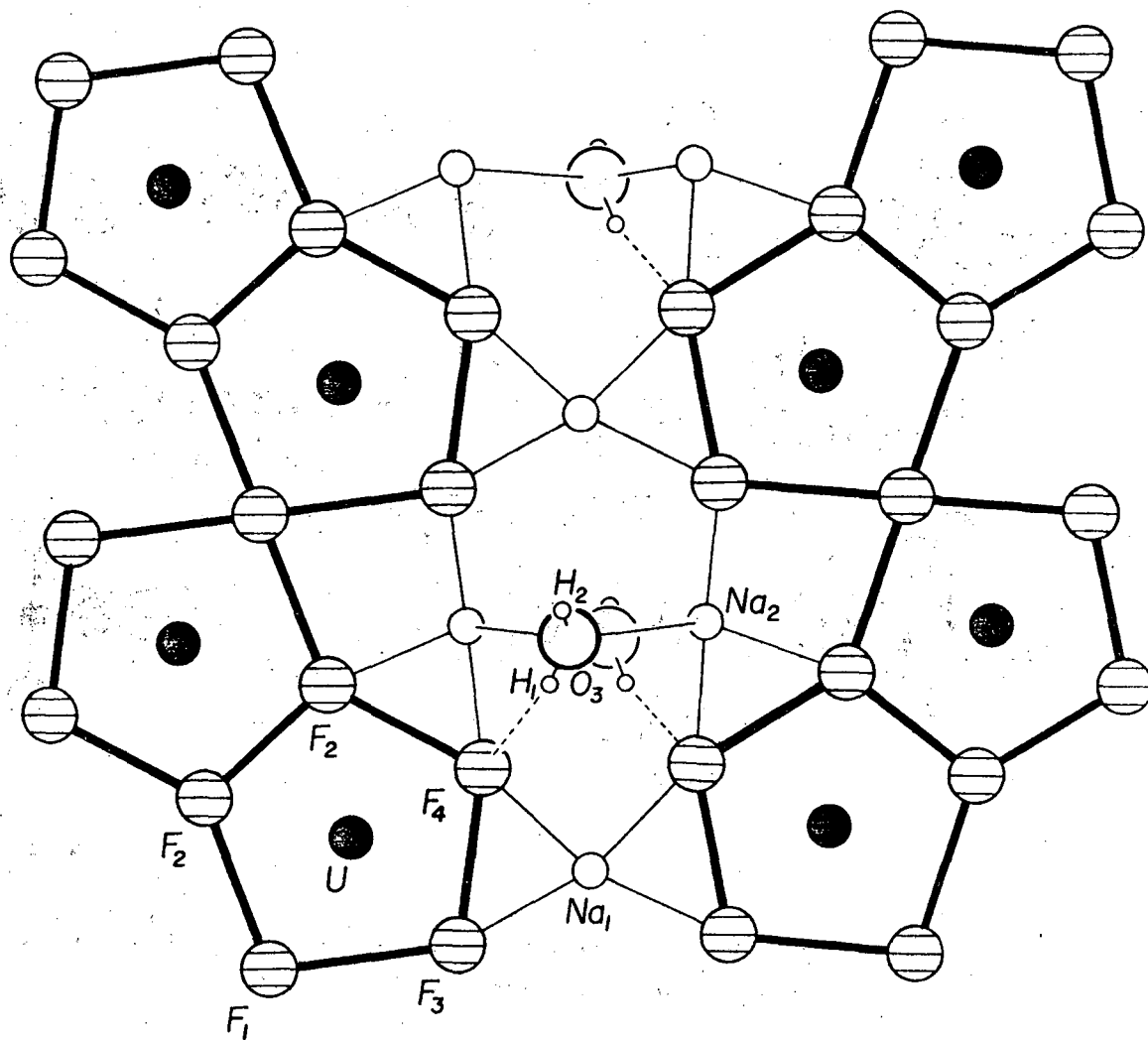
There are centers of symmetry at the shared vertex and the middle of the shared edge. This fact constrains the chains to be nearly planar: no fluorine or uranium atom deviates from the plane

---

\*The crystals have a perfect (101) cleavage.

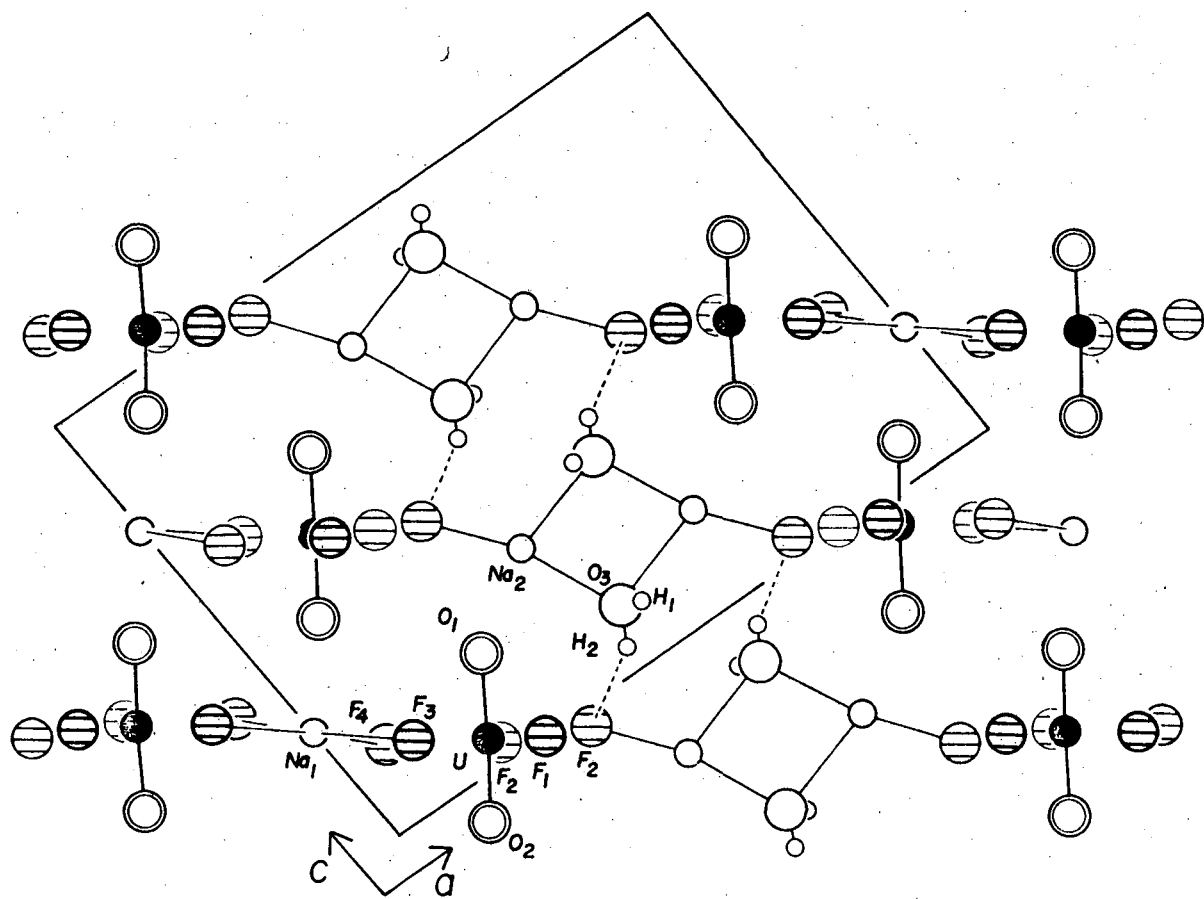
0 0 0 0 4 7 1 0 9 3 8

147



XBL 774-8324

Figure (V.1).  $\text{Na}_3(\text{UO}_2)_2\text{F}_7 \cdot 2\text{H}_2\text{O}$ , monoclinic phase. Projection of the structure in the (101) plane. For clarity, only one water molecule is shown in the top half of the figure; both are shown in the bottom half.



XBL 774-8323

Figure (V.2).  $\text{Na}_3(\text{UO}_2)_2\text{F}_7 \cdot 2\text{H}_2\text{O}$ , monoclinic phase. Projection of the structure looking along the  $b$ -axis.

Table (V.1). Interatomic distances ( $\text{\AA}$ ) for  $\text{Na}_3(\text{UO}_2)_2\text{F}_7 \cdot 2\text{H}_2\text{O}$   
(monoclinic phase).

U	-O(1)	1.782(3)	Na(2)-F(2)	2.360(3)
U	-O(2)	1.783(3)	Na(2)-F(3)	2.210(3)
U	-F(1)	2.308(1)	Na(2)-F(4)	2.267(3)
U	-F(2)	2.403(3)	Na(2)-O(3)	2.372(4)
U	-F(2)'	2.376(2)	Na(2)-O(3)	2.521(4)
U	-F(3)	2.225(3)	Na(2)-O(1)	2.394(4)
U	-F(4)	2.236(2)	F(4)-F(3)	2.694(4)
Na(1)-F(3)		2.347(3)	F(3)-F(1)	2.843(3)
Na(1)-F(4)		2.278(3)	F(1)-F(2)	2.807(3)
Na(1)-O(2)		2.455(3)	F(2)-F(2)'	2.557(4)
			F(2)-F(4)	2.660(3)

#### Distances Involved in Hydrogen Bonds

O(3)-H(1)	0.8(1)
H(1)-F(4)	2.1(1)
O(3)-F(4)	2.776(5)
O(3)-H(2)	0.8(1)
H(2)-F(2)	2.2(1)
O(3)-F(2)	2.921(5)
H(1)-H(2)	1.4(1)

Table (V.2). Bond angles ( $^{\circ}$ ) for  $\text{Na}_3(\text{UO}_2)_2\text{F}_7 \cdot 2\text{H}_2\text{O}$ , monoclinic phase.

$\text{O}(1)-\text{U}-\text{O}(2)$	177.7(2)
$\text{F}(2)-\text{U}-\text{F}(4)$	69.9(1)
$\text{F}(4)-\text{U}-\text{F}(3)$	74.3(1)
$\text{F}(3)-\text{U}-\text{F}(1)$	77.7(1)
$\text{F}(1)-\text{U}-\text{F}(2)$	73.6(1)
$\text{F}(2)-\text{U}-\text{F}(2)$	64.7(1)
$\text{O}(1)-\text{U}-\text{F}(1)$	90.0(1)
$\text{O}(1)-\text{U}-\text{F}(2)$	90.3(1)
$\text{O}(1)-\text{U}-\text{F}(2)$	86.3(1)
$\text{O}(1)-\text{U}-\text{F}(3)$	91.2(1)
$\text{O}(1)-\text{U}-\text{F}(4)$	89.4(1)
$\text{O}(2)-\text{U}-\text{F}(1)$	90.5(1)
$\text{O}(2)-\text{U}-\text{F}(2)$	87.9(1)
$\text{O}(2)-\text{U}-\text{F}(2)$	91.7(1)
$\text{O}(2)-\text{U}-\text{F}(3)$	91.1(1)
$\text{O}(2)-\text{U}-\text{F}(4)$	91.3(1)

Angles involved in hydrogen bonds.

$\text{O}(3)-\text{H}(1) \dots \text{F}(4)$	143(8)
$\text{O}(3)-\text{H}(2) \dots \text{F}(2)$	155(6)
$\text{H}(1)-\text{O}(3) - \text{H}(2)$	117(7)

containing these centers by more than 0.2 Å. Both kinds of sodium atoms [Na(1) and Na(2)] are within 0.4 Å of this plane.

The uranyl oxygen atoms [O(1) and O(2)] and the water O(3) are the only atoms which are not near the plane. They bind the layers together: the uranyl oxygen atoms are coordinated to sodium atoms in adjacent layers, and the water forms weak hydrogen bonds to F(4) in the layer closest to the water oxygen O(3) and to F(2) in an adjacent layer. The relationship of adjacent layers is illustrated in Figure (V.2).

Tables (V.1) and (V.2) are respectively lists of selected interatomic distances and bond angles.

## 2. $\text{Na}_3(\text{UO}_2)_2\text{F}_7 \cdot 6\text{H}_2\text{O}$

The structure of the triclinic phase also consists of layers of infinite  $[(\text{UO}_2)_2\text{F}_7]_n^{-3n}$  chains. The layers are parallel to the (001) plane and are related by the c-translation. Between these layers are sodium atoms and water which bind the layers together.

Figure (V.3) is a z = 0 section of the structure which passes through a layer.

The fluorouranylate chains are similar geometrically to those in the monoclinic phase. That is, analogous bond lengths and angles are similar. However, they differ topologically. In both hydrates the pentagons share one edge and one vertex; in both hydrates the shared edge and shared vertex are located at centers of symmetry.

However, the shared edge is opposite the shared vertex in the triclinic phase and adjacent to the shared vertex in the monoclinic phase.

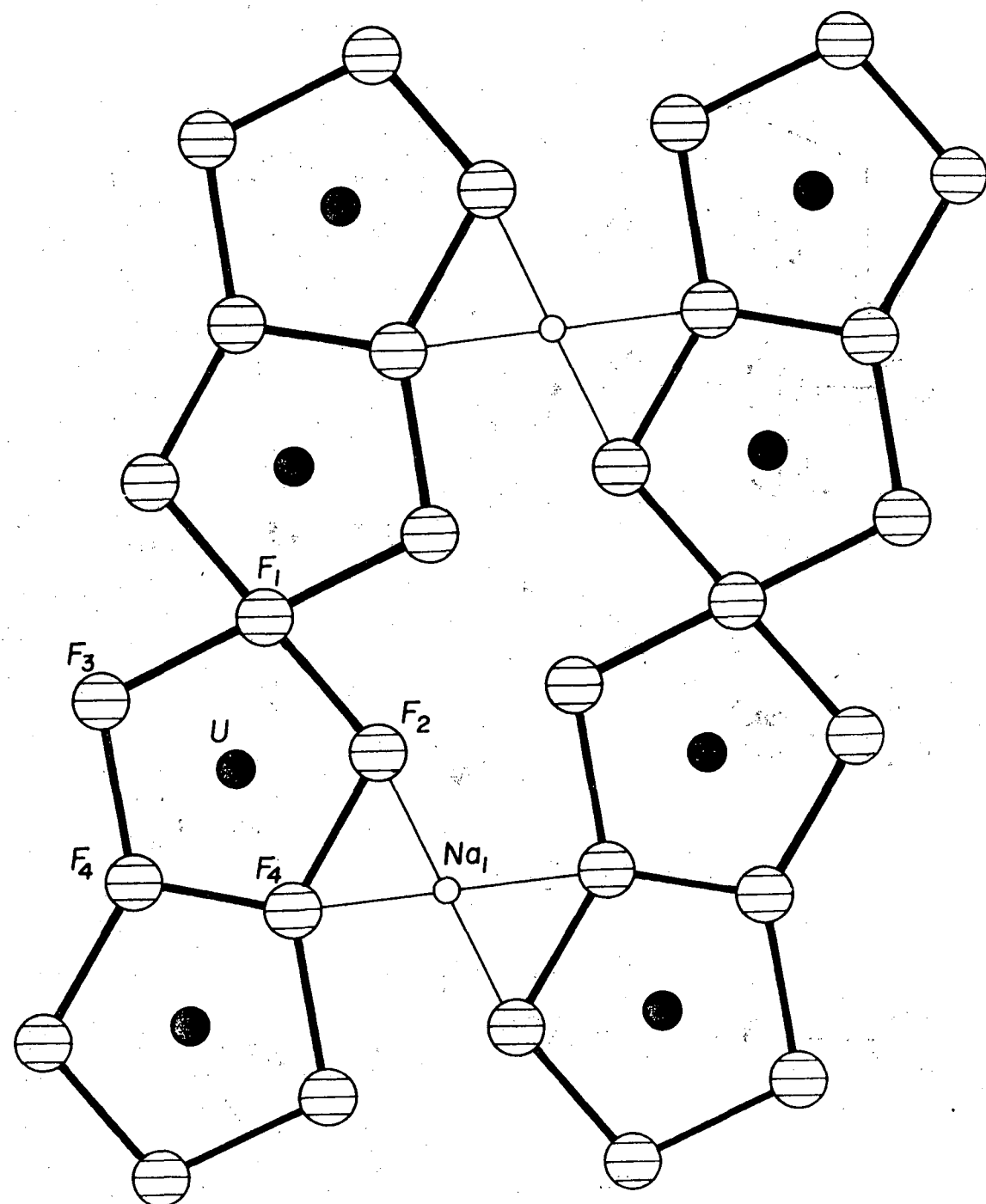
Another difference is that in the triclinic phase there is only one kind of sodium atom [Na(1)] in the layer binding the chains together. The other type of sodium Na(2) and the three kinds of water [O(3), O(4), and O(5)] are between the layers. This is illustrated in Figure (V.4) which is a projection of the structure looking down the a-axis.

The hydrogen atom positions in Figure (V.4) were not included in the least-squares refinement. Some of the hydrogen positions in this figure correspond to peaks in a final difference Fourier synthesis. The other positions were assigned on the basis of bond geometry to obtain the most reasonable hydrogen bonding scheme.

Tables (V.3) and (V.4) are respectively lists of selected interatomic distances and bond angles.

0 0 0 0 4 7 1 0 9 4 1

153



XBL 774-8325

Figure (V.3).  $\text{Na}_3(\text{UO}_2)_2\text{F}_7 \cdot 6\text{H}_2\text{O}$ , triclinic phase. A  $z = 0$  section of the structure.

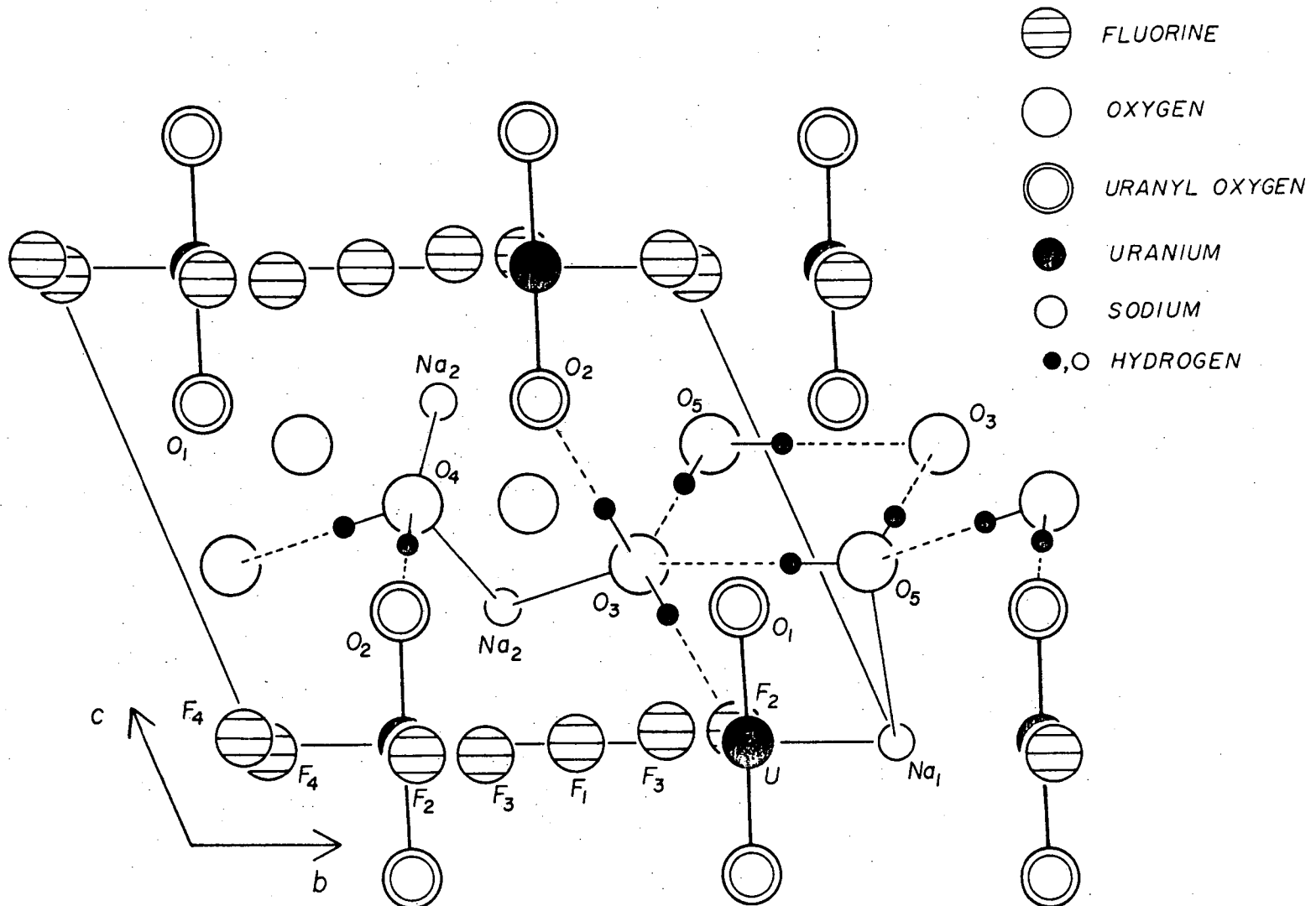


Figure (V.4).  $\text{Na}_3(\text{UO}_2)_2\text{F}_7 \cdot 6\text{H}_2\text{O}$ , triclinic phase projection of the structure looking along the negative  $a$ -axis.

XBL 774-8322

Table (V.3). Interatomic distances ( $\text{\AA}$ ) for  $\text{Na}_3(\text{UO}_2)_2\text{F}_7 \cdot 6\text{H}_2\text{O}$   
(triclinic phase).

U	-O(1)	1.773(4)	Na(2)-F(2)	2.290(4)
U	-O(2)	1.787(4)	Na(2)-F(3)	2.315(4)
U	-F(1)	2.316(1)	Na(2)-F(3)	2.302(4)
U	-F(2)	2.264(3)	Na(2)-O(3)	2.471(6)
U	-F(3)	2.218(3)	Na(2)-O(4)	2.389(6)
U	-F(4)	2.354(3)	Na(2)-O(4)	2.397(6)
U	-F(4)	2.381(3)	F(1) -F(2)	2.734(3)
Na(1)-F(2)		2.305(3)	F(2) -F(4)	2.696(4)
Na(1)-F(4)		2.365(3)	F(4) -F(4)	2.524(6)
Na(1)-O(5)		2.368(6)	F(4)'-F(3)	2.820(4)
			F(3) -F(1)	2.768(3)

Distances involved in the suggested hydrogen bonding scheme of Figure (V.4).

O(3)-F(2)	2.865(6)
O(3)-O(2)	2.894(6)
O(4)-O(5)	2.757(10)
O(4)-O(2)	2.949(7)
O(5)-O(3)	2.816(8)
O(5)-O(3)	3.070(10)

Table (V.4). Bond angles ( $^{\circ}$ ) for  $\text{Na}_3(\text{UO}_2)_2\text{F}_7 \cdot 6\text{H}_2\text{O}$  (triclinic phase).

O(1) -U-O(2)	178.6(2)
F(1) -U-F(2)	73.3(1)
F(2) -U-F(4)	70.9(1)
F(4) -U-F(4)'	64.4(1)
F(4)' -U-F(3)	76.1(1)
F(3) -U-F(1)	75.2(1)
O(1) -U-F(1)	90.4(2)
O(1) -U-F(2)	88.9(2)
O(1) -U-F(3)	90.7(2)
O(1) -U-F(4)'	89.9(2)
O(1) -U-F(4)	89.3(2)
O(2) -U-F(1)	90.2(2)
O(2) -U-F(2)	90.1(2)
O(2) -U-F(3)	90.7(2)
O(2) -U-F(4)'	90.2(2)
O(2) -U-F(4)	89.4(2)

Bond angles involved in the suggested hydrogen bonding scheme of Figure (V.4).

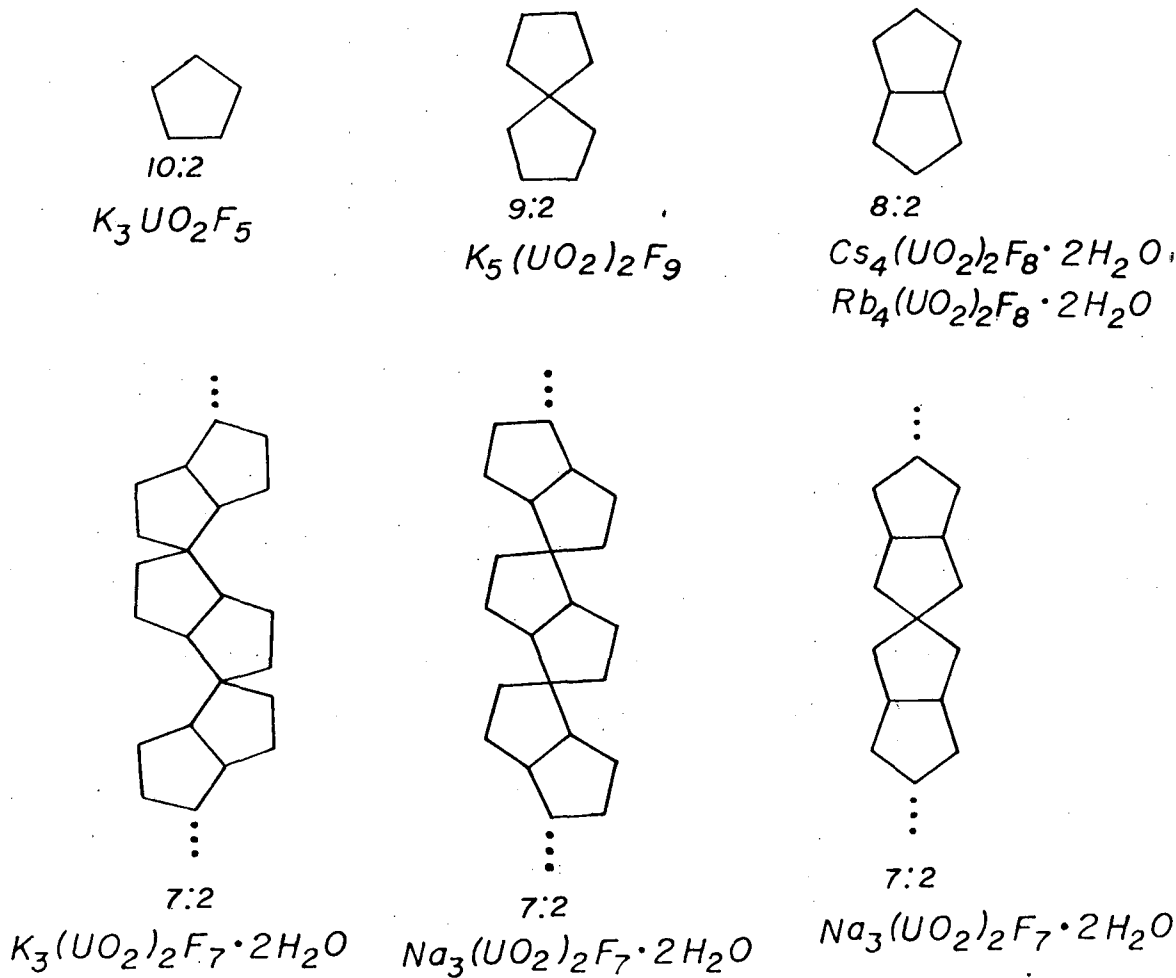
F(2)-O(3)-O(2)	130.4(2)
O(5)-O(4)-O(2)	97.7(3)
O(3)-O(5)-O(3)	109.9(3)

## VI. Other Alkali Metal-Uranyl Fluorides

It is interesting to examine the fluorouranylate ions in the series of double salts (alkali metal)<sub>x</sub>(UO<sub>2</sub>)<sub>y</sub>F<sub>z</sub>·nH<sub>2</sub>O as the UO<sub>2</sub>:F ratio increases. In all such salts whose structures have been determined, the uranium has seven-fold coordination with the two uranyl oxygen atoms forming the axis of a pentagonal bipyramid. In one structure the equator of the bipyramid is formed by one water molecule and four fluorine atoms; in the majority of the structures the pentagonal equator is formed by five fluorine atoms. The fluorouranylate ions can, therefore, be visualized as pentagons which may share edges and vertices [see Figure (VI.1)].

When UO<sub>2</sub>:F = 2:10 there are isolated fluorine pentagons. With UO<sub>2</sub>:F = 2:9 there are isolated pairs of fluorine pentagons with a common vertex. For UO<sub>2</sub>:F = 2:8 the isolated pairs of fluorine pentagons share an edge. For UO<sub>2</sub>:F = 2:7 there are three different infinite chain structures in which the fluorine pentagons each share an edge and a vertex.

From the increasing number of shared edges and vertices of each fluorine pentagon as the UO<sub>2</sub>:F ratio increases one might expect that Cs<sub>2</sub>(UO<sub>2</sub>)<sub>2</sub>F<sub>6</sub>·2H<sub>2</sub>O with UO<sub>2</sub>:F = 2:6 would be an infinite chain structure in which each fluorine pentagon shares two edges. However, this is not the case. This structure consists of isolated pairs of fluorine-water pentagons each formed by one water molecule and four fluorine atoms; the shared edge is formed by two fluorine atoms.<sup>11</sup>



XBL 774-8341

Figure (VI.1). The fluorine pentagon in the series  $(\text{alkali metal})_x(\text{UO}_2)_y\text{F}_z \cdot n\text{H}_2\text{O}$ . The two Na salts are discussed in  $x$  this work. The other are discussed as follows:

$K_3UO_2F_5$	reference 5
$K_5(UO_2)_2F_9$	reference 7
$Cs_4(UO_2)_2F_8 \cdot 2H_2O$	reference 8
$Rb_4(UO_2)_2F_8 \cdot 2H_2O$	reference 9
$K_3(UO_2)_2F_7 \cdot 2H_2O$	reference 10

Except for the last structure discussed, the progression of structures as  $\text{UO}_2:\text{F}$  increases in similar to the series of borate structures as the ratio B:O increases.<sup>6</sup> In this series the  $\text{BO}_3$  triangle is the structural unit.  $(\text{BO}_3)^{-3}$  is an isolated triangle.  $(\text{B}_2\text{O}_5)^{-4}$  is a pair of triangles with a common vertex.  $(\text{B}_2\text{O}_4)^{-2}$  is a pair of triangles with a shared edge. There is also an infinite chain  $(\text{BO}_2)_n^{-n}$  in which each triangle shares two vertices with adjacent triangles.

## VII. Appendix

The following is a listing of observed structure factors, standard deviations, and differences for  $\text{Na}_3(\text{UO}_2)_2\text{F}_7 \cdot 2\text{H}_2\text{O}$  and  $\text{Na}_3(\text{UO}_2)_2\text{F}_7 \cdot 6\text{H}_2\text{O}$ .

0 0 0 0 4 7 1 0 9 4 5

161

OBSERVED STRUCTURE FACTORS, STANDARD DEVIATIONS, AND DIFFERENCES (ALL X 4.0)  
 NA3(U02)2F7.2H2O  
 $F(0,0,0) = 2523$

FOB AND FCA ARE THE OBSERVED AND CALCULATED STRUCTURE FACTORS.

SG = ESTIMATED STANDARD DEVIATION OF FOB. DEL = |FOB| - |FCA|.

\* INDICATES ZERO WEIGHTED DATA.

L	FOB	SG	DEL	L	FOB	SG	DEL	L	FOB	SG	DEL	L	FOB	SG	DEL	
H,K= 0, 0	19	84	12	14	1	88	14	-1	-14	219	4	-5	0	260	4	-2
2 855	14	-1*	H,K= 0, 6	2	64	27	-20*	-13	100	5	2	1	457	5	-4	
4 29	4	10*	0 477	6	-6	3 217	5	1	-12	360	5	-2	2 140	3	-2	
6 447	6	11	1 153	3	4	4 2 39	-5*	-11	90	4	-2	3 363	5	-1		
8 610	178	-130*	178	2 223	3	2	5 228	6	5	-10	389	5	-2	4 472	8	-10
10 537	6	11	3 475	5	-5	H,K= 1, 1	-9	244	4	0	5	46	10	-5*		
12 174	3	4	4 37	24	19*	-20	186	6	2	-8	122	4	4	6 415	7	2
14 146	4	6	5 512	8	-1	-19	0 51	-16*	-7	367	5	2	7 273	4	5	
16 303	6	-6	6 151	3	4	-18	161	6	7	-6	271	10	9	8 231	5	4
18 196	10	-2	7 319	4	-2	-17	65	12	23*	-5	127	2	1	9 386	5	1
20 93	12	-0	8 321	4	0	-16	36	47	30*	-4	944	11	-19	10 43	48	2*
H,K= 0, 2	9	60	9	-2	-15	39	54	3*	-3	46	7	13	11 221	3	-3	
01068	11	-221*	10 201	3	-3	-14	246	4	-4	-2	782	40	-45	12 201	4	-2
1 69	2	5*	11 236	4	-8	-13	9 47	-14*	-1	476	5	4*	13 113	6	4	
2 575	18	-1*	12 58	24	-12*	-12	440	5	5	0 210	2	11*	14 223	7	-6	
3 199	2	12*	13 262	6	-8	-11	9 62	-19*	1 636	7	-5*	15 77	19	4*		
4 144	2	2*	14 55	15	-6*	-10	543	6	6	2 87	2	8	16 127	8	4	
5 163	2	6	15 152	9	1	-9	143	5	-5	3 446	15	-7	17 131	11	-6	
6 554	7	6	16 118	14	-2	-8	126	3	5	4 565	9	-11	18 41	56	18*	
7 167	3	5	17 26	45	3*	-7	257	4	6	5 58	4	-2	H,K= 1,	7		
8 779	9	4	H,K= 0,	8	-6	244	3	8	6 843	12	-3	-16	40 46	32*		
9 77	7	1	0 149	4	-6	-5	48	6	2	7 164	3	-2	-15	216	5	-0
10 424	5	3	1 177	3	0	-4	899	22	5*	8 378	5	6	-14	66 39	9*	
11 150	7	1	2 123	4	-6	-3	23	4	9*	9 276	3	9	-13	135	5	-4
12 137	7	-0	3 420	4	-8	-21059	34	1*	10 34	24	21*	-12	135	5	4	
13 142	5	0	4 57	14	4*	-1	155	2	16*	11 169	5	5	-11	59 11	-5	
14 118	5	0	5 396	5	-4	0 469	10	-21*	12 304	4	2	-10	135	4	-1	
15 54	13	-7*	6 36	23	-11*	1 234	3	1*	13 102	9	2	-9	305	5	-9	
16 287	7	1	7 232	5	9	2 329	11	1*	14 326	6	4	-8	59	8	4	
17 22	40	14*	8 139	8	5	3 150	2	4*	15 54	15	4*	-7	448	5	-9	
18 181	6	-5	9 51	24	5*	4 702	13	-7*	16 190	11	2	-6	72	13	3	
19 67	15	25*	10 51	20	-4*	5 37	9	12*	17 97	16	2	-5	235	3	-2	
20 69	71	-14*	11 228	5	-4	6 869	11	6	18 47	42	19*	-4	216	3	-2	
H,K= 0,	4	12	42	24	7*	7	61	3	7	19 88	11	1	-3	44	18	30*
0 845	12	-59	13 259	4	-0	8 388	5	6	H,K= 1,	5	-2	205	3	1		
1 121	2	4	14 26	46	13*	9 155	3	3	-18	105	20	16*	-1	374	4	-3
2 407	5	2	15 134	14	-10	10 39	17	1*	-17	155	8	1	0	36	10	2*
3 466	6	1	H,K= 0,	10	11	101	4	7	-16	43	23	29*	1 562	6	-7	
4 56	5	25	0 41	25	21*	12 406	5	4	-15	216	5	1	2	30	17	14*
5 439	6	3	1 106	11	-2	13 30	35	-6*	-14	142	5	7	3 385	4	-5	
6 308	5	2	2 32	33	-4*	14 392	5	-9	-13	131	7	-2	4 189	3	3	
7 251	3	1	3 296	4	-6	15 42	21	28*	-12	270	4	-3	5 57	8	-11	
8 498	6	1	4 52	12	23*	16 215	6	1	-11	90	7	7	6 196	9	5	
9 73	5	3	5 330	5	-2	17	0 44	-22*	-10	267	3	-7	7 217	4	2	
10 290	3	1	6 32	40	6*	18 35	60	11*	-9	287	4	-7	8 98	7	-4	
11 185	4	-0	7 152	6	-7	19 40	48	10*	-8	27	29	5*	9 352	4	-8	
12 97	8	1	8 24	41	12*	20 100	14	3	-7	494	6	-7	10 0	41	-17*	
13 246	4	-4	9 37	65	-15*	H,K= 1,	3	-6	185	3	3	11 253	5	-2		
14 115	7	3	10 29	56	10*-19	37 50	4*	-5	285	4	-0	12 99	30	-9*		
15 133	6	-3	11 179	12	-6	-18 131	16	4	-4	425	6	-9	13 105	7	4	
16 221	5	-5	12 22	63	19*-17	113 14	1	-3	46	6	-4	14 102	8	-5		
17 42	52	31*	H,K= 0,	12	-16	18 41	1*	-2	555	7	-5	15 76	16	-3*		
18 146	16	-1	0 107	12	-8	-15 159	4	1	-1	385	5	3	16 64	16	6*	

STRUCTURE FACTORS CONTINUED FOR  
NA3(UO2)2F7.2H2O

PAGE 2

L	F08	SG	DEL	L	F08	SG	DEL	L	F08	SG	DEL	L	F08	SG	DEL				
H,K=	1,	9	-8	810	10	3	-19	97	16	-7	0	203	3	1	-6	45	48	31*	
-14	52	20	44*	-6	866	10	9	-18	74	13	13	1	229	3	-0	-5	115	7	4
-13	92	18	-8*	-4	326	3	21*	-17	118	8	-4	2	393	5	-4	-4	33	34	-3*
-12	51	25	14*	-2	68	1	-6*-16	201	6	1	3	79	4	3	-3	343	5	1	
-11	79	16	-6*	0	678	7	-51*-15	0	48	-14*	4	231	4	-3	-2	62	10	24	
-10	45	20	31*	21131	13-399*	-14	295	6	-5	5	437	5	-3	-1	340	5	-9		
-9	270	5	-10	4	816	9	-22*-13	138	5	-1	6	69	11	-6	0	32	43	1*	
-8	38	43	34*	6	365	6	2	-12	176	6	-1	7	454	6	4	1	146	4	-7
-7	374	6	-6	8	338	5	5	-11	303	4	-4	8	121	5	7	2	30	48	16*
-6	50	16	38*	10	487	6	2	-10	33	17	6*	9	276	4	0	3	47	17	-13*
-5	234	3	-9	12	441	5	-3	-9	256	4	-3	10	224	5	-2	4	11	44	-26*
-4	31	31	-3*	14	190	4	-3	-8	372	5	-3	11	22	37	8*	5	260	6	-6
-3	41	16	36*	16	75	16	11*	-7	135	4	5	12	176	4	4	6	18	36	-5*
-2	37	22	-8*	18	184	5	4	-6	529	6	-6	13	176	7	-3	7	309	4	5
-1	306	4	-5	20	171	11	5	-5	129	2	2	14	91	20	5*	8	23	44	10*
0	24	30	10*	H,K=	2,	2	-4	300	3	4	15	214	5	-1	9	170	11	4	
1	453	5	-15	-20	41	45	-11*	-3	450	7	-2	16	32	42	0*	10	30	42	18*
2	39	14	14*-19	53	22	-16*	-2	60	11	-1*	17	116	12	-5	11	35	54	29*	
3	325	5	-5	-18	85	31	3*	-1	666	9	-10	H,K=	2,	8	12	24	49	3*	
4	61	12	7*-17	75	13	-3	0	409	5	13	-15	0	40	-15*	H,K=	2,	12		
5	70	8	0	-16	255	5	-4	1	198	3	6	-14	70	24	8*	-5	78	13	-13
6	37	28	12*-15	21	35	18*	2	644	9	-8	-13	143	8	-1	-4	87	17	5*	
7	196	6	-2	-14	375	6	-3	3	72	4	12	-12	13	41	-8*	-3	228	6	-1
8	31	41	25*-13	54	13	2*	4	408	6	2	-11	293	6	-14	-2	19	57	15*	
9	306	5	-1	-12	176	4	-5	5	438	8	-7	-10	15	37	-13*	-1	240	4	3
10	36	41	35*-11	153	3	0	6	193	3	1	-9	306	4	-7	0	69	14	-1*	
11	230	7	-3	-10	57	7	3	7	394	5	3	-8	40	44	-20*	1	122	10	-2
12	38	49	24*	-9	211	4	3	8	243	5	7	-7	117	8	7	2	99	10	-6
13	108	8	4	-8	591	8	-2	9	214	3	6	-6	155	5	6	3	52	58	3*
14	57	58	36*	-7	146	3	2	10	362	5	7	-5	157	4	-2	4	98	12	5
H,K=	1,	11	-6	884	11	-4	11	5	40	4*	-4	68	7	4	5	184	6	-5	
-9	193	6	3	-5	76	3	5	12	262	4	-2	-3	402	5	-6	H,K=	3,	1	
-8	61	18	32*	-4	592	7	8	13	137	5	-4	-2	43	27	30*-20	109	22	-2*	
-7	266	9	-6	-3	165	2	13*	14	121	9	-2	-1	493	6	-10	-19	0	43	-15*
-6	38	42	17*	-2	65	2	11*	15	182	11	-10	0	143	8	7	-18	258	7	0
-5	171	5	-5	-1	365	8	9*	16	72	12	17	1	249	3	3	-17	0	49	-21*
-4	47	40	-12*	0	576	13	-26*	17	111	10	5	2	142	3	1	-16	257	4	0
-3	32	42	3*	1	103	3	10*	18	135	9	-0	3	97	4	-3	-15	59	17	-2*
-2	68	12	13	2	711	27	-30*	19	48	55	26*	4	112	4	-1	-14	71	8	-9
-1	221	5	-4	3	64	3	-1*	H,K=	2,	6	5	391	5	-1	-13	53	13	25*	
0	37	40	5*	4	534	19	-2	-17	130	17	-4	6	70	10	-7	-12	222	3	-4
1	315	8	-2	5	257	4	7	-16	107	18	-13	7	381	16	8	-11	43	9	19*
2	53	13	23*	6	394	6	4	-15	2	42	-6*	8	18	42	-13*	-10	647	7	-1
3	232	5	-4	7	164	5	5	-14	151	6	-4	9	219	6	6	-9	0	23	-8*
4	33	38	-6*	8	379	6	8	-13	152	5	-4	10	94	19	-4*	-8	717	8	4
5	82	9	7	9	119	6	5	-12	88	7	-4	11	20	39	9*	-7	165	3	3
6	68	11	2	10	522	6	4	-11	313	4	-5	12	59	17	11*	-6	181	3	4
7	136	8	1	11	19	35	5*	-10	29	34	-7*	13	170	12	1	-5	338	4	5
8	43	51	17*	12	385	4	6	-9	329	4	-6	14	53	60	14*	-4	95	2	24*
9	230	9	4	13	113	7	5	-8	250	4	-4	15	194	7	-10	-3	152	2	7*
H,K=	2,	0	14	173	8	9	-7	142	5	-3	H,K=	2,	10	-21060	14	-29*			
-20	25	47	-29*	15	119	11	4	-6	370	5	-1	-12	22	44	13*	-1	20	22	13*
-18	99	9	1	16	45	23	-10*	-5	237	3	4	-11	228	5	-6	0	917	35	-97*
-16	282	6	3	17	59	27	7*	-4	162	4	1	-10	53	16	49*	1	111	5	8*
-14	411	5	2	18	164	6	-4	-3	550	6	-0	-9	230	6	-10	2	619	8	-45*
-12	223	5	-0	19	13	43	0*	-2	81	4	-7	-8	67	15	47*	3	126	3	4*
-10	75	4	4	H,K=	2,	4	-1	619	7	-12	-7	114	6	8	4	170	3	8*	

0 0 0 0 4 7 1 0 9 4 6

**STRUCTURE FACTORS CONTINUED FOR  
NA<sub>3</sub>(UO<sub>2</sub>)<sub>2</sub>F<sub>7</sub>.2H<sub>2</sub>O**

PAGE 3

L	FOB	SG	DEL	L	FOB	SG	DEL	L	FOB	SG	DEL	L	FOB	SG	DEL	
5	155	3	3	-17	28	59	-18*	4	49	8	34	5	237	6	-4	
6	797	12	-15	-16	131	20	-5	5	414	6	-3	6	57	14	21*	
7	53	11	-1*	-15	189	8	-5	6	170	10	3	7	111	13	6	
8	599	9	0	-14	36	45	9*	7	143	7	7	8	57	23	-3*	
9	34	35	25*	-13	241	5	-2	8	146	8	-2	9	108	9	25	
10	302	5	4	-12	108	7	-15	9	116	6	-3	H,K=	4,	0	14	
11	102	5	4	-11	196	4	-3	10	102	11	-3	-20	166	7	-2	
12	74	7	-0	-10	373	4	-6	11	276	7	-4	-18	119	9	2	
13	95	7	9	-9	32	37	-2*	12	40	31	34*	-16	98	7	4	
14	248	5	-6	-8	354	4	-0	13	246	4	-0	-14	321	6	-1	
15	37	30	6*	-7	271	4	-2	14	97	10	23	-12	496	6	2	
16	247	5	-4	-6	80	4	4	15	101	13	-0	-10	355	4	4	
17	36	39	28*	-5	509	6	-5	16	84	17	7*	-8	93	5	6	
18	186	7	4	-4	144	3	4	H,K=	3,	9	-6	701	9	2	-17	
19	28	42	11*	-3	408	6	-11	-14	26	47	21*	-41004	10	-9*	-16	
	H,K=	3,	3	-2	487	8	2	-13	217	11	-8	-2	867	10	8*	-15
-19	25	50	-4*	-1	111	3	2	-12	37	37	31*	0	303	3	5*	-14
-18	214	5	7	0	523	7	-1	-11	148	6	-6	2	509	5	-18*	-13
-17	42	52	4*	1	322	5	5	-10	41	55	-9*	41143	13-176*	-12	361	
-16	202	8	-4	2	354	4	1	-9	43	18	-9*	6	750	13	-32	-11
-15	151	8	4	3	345	6	2	-8	26	35	16*	8	324	5	-2	-10
-14	59	9	11	4	60	14	8*	-7	299	19	12	10	167	5	1	-9
-13	176	4	1	5	395	6	-2	-6	32	37	14*	12	371	6	-12	-8
-12	219	7	-3	6	440	5	-3	-5	404	6	-2	14	364	4	-8	-7
-11	157	3	2	7	132	4	-4	-4	27	34	12*	16	143	6	-18	-6
-10	530	6	-4	8	322	5	3	-3	316	4	-2	18	36	40	8*	-5
-9	67	5	6	9	145	4	10	-2	50	14	14*	H,K=	4,	2	-4	547
-8	496	6	-2	10	204	6	4	-1	77	15	7*	-20	162	7	0	-3
-7	242	3	-2	11	293	4	-6	0	29	49	-5*	-19	61	56	17*	-2
-6	201	3	3	12	77	12	21	1	250	4	-2	-18	114	12	2	-1
-5	381	5	4	13	227	4	-7	2	19	37	13*	-17	113	9	11	0
-4	134	3	11	14	126	8	-6	3	396	4	-6	-16	73	19	3*	1
-3	253	3	9	15	101	16	2	4	19	32	-2*	-15	103	6	-8	2
-21038	56	-99	16	143	6	-8	5	336	5	-10	-14	288	6	-7	3	
-1	81	10	17	17	65	63	29*	6	46	35	3*	-13	34	27	5*	4
0	797	22	-64	18	99	10	-5	7	133	9	7	-12	463	5	2	5
1	372	5	7	H,K=	3,	7	8	41	63	21*	-11	36	10	1*	6	
2	355	5	4	-16	95	14	17	9	118	8	0	-10	281	4	4	7
3	420	6	-1	-15	208	9	3	10	25	46	8*	-9	209	3	3	8
4	37	7	14	-14	21	42	9*	11	247	7	8	-8	62	8	-1	9
5	440	7	-7	-13	247	6	-4	12	49	59	48*	-7	237	4	2	10
6	572	9	-7	-12	46	18	-2*	13	209	9	-3	-6	460	6	4	11
7	134	5	0	-11	203	4	-2	H,K=	3,	11	-5	186	2	5	12	
8	581	8	5	-10	165	4	1	-9	41	44	26*	-4	962	11	-5	13
9	74	10	8	-9	6	29	-4*	-8	43	60	-12*	-3	126	3	11*	14
10	309	5	1	-8	154	5	-1	-7	180	13	-7	-21023	11	-40*	15	
11	209	4	0	-7	298	4	-4	-6	45	25	15*	-1	160	2	14*	16
12	41	17	-14*	-6	114	7	7	-5	290	7	-0	0	199	2	1*	17
13	177	8	1	-5	491	18	9	-4	25	43	15*	1	168	3	6*	18
14	196	5	-2	-4	48	12	8*	-3	219	5	-7	2	514	6	-13*	H,K=
15	68	15	-14*	-3	327	4	-3	-2	61	13	7*	3	142	4	-5	-17
16	198	8	-7	-2	245	3	4	-1	35	36	14*	4	748	11	-42	-16
17	49	21	25*	-1	78	5	6	0	62	12	-2*	5	33	26	26*	-15
18	154	7	-2	0	196	3	-1	1	186	5	-4	6	541	9	-2	-14
19	62	25	-2*	1	299	4	-4	2	31	51	-1*	7	198	5	-1	-13
	H,K=	3,	5	2	81	6	9	3	268	9	-15	8	330	4	-4	-12
-18	130	11	-13	3	465	5	-0	4	49	53	29*	9	131	7	4	-11

**STRUCTURE FACTORS CONTINUED FOR  
NA<sub>3</sub>(UO<sub>2</sub>)<sub>2</sub>F<sub>7</sub>.2H<sub>2</sub>O**

PAGE 4

L	F08	SG	DEL	L	F08	SG	DEL	L	F08	SG	DEL	L	F08	SG	DEL	L	F08	SG	DEL
-10	135	4	-0	13	72	12	38	-3	413	5	7*	14	73	10	10	-3	520	7	1
-9	407	6	-3	14	28	48	-18*	-2	226	2	16*	15	122	16	6	-2	34	27	11*
-8	24	27	2*	15	88	11	-13	-1	219	2	4*	16	111	7	1	-1	381	5	-0
-7	385	4	-4	H,K=	4,	10	0	785	14	-31*	17	88	10	15	0	208	4	4	
-6	250	3	2	-12	0	57	-14*	1	78	2	4*	18	141	8	-5	1	154	4	2
-5	224	6	2	-11	98	22	-11*	2	540	6	-14*	19	51	34	46*	2	177	5	4
-4	402	6	-1	-10	32	49	21*	3	90	3	3	H,K=	5,	5	3	233	4	-4	
-3	220	4	3	-9	274	7	2	4	712	10	-44	-18	80	26	-5*	4	113	9	-3
-2	249	4	9	-8	11	52	10*	-5	155	3	0	-17	98	15	1	5	442	6	0
-1	537	7	-1	-7	281	6	7	6	30	14	9*-16	181	5	-5	6	29	35	10*	
0	155	5	-0	-6	13	40	8*	7	109	7	-4	-15	45	36	30*	7	365	8	5
1	525	7	-2	-5	152	6	-5	8	404	6	-10	-14	160	5	-3	8	126	6	10
2	171	4	3	-4	0	47	-18*	9	42	9	9*-13	199	5	-6	9	127	8	-9	
3	304	5	-5	-3	53	16	-21*	10	483	7	-13	-12	72	7	-6	10	119	6	3
4	339	6	-0	-2	46	21	-4*	11	0	30	-5*-11	327	5	-6	11	53	16	-15*	
5	17	40	3*	-1	320	6	-3	12	357	4	-9	-10	116	4	-1	12	103	11	-3
6	254	4	2	0	37	49	0*	13	68	24	10*	-9	277	3	-3	13	196	5	-3
7	330	4	-2	1	323	5	-7	14	76	9	2	-8	404	5	-2	14	35	41	18*
8	111	6	6	2	41	21	20*	15	40	24	-12*	-7	18	31	14*	15	180	8	1
9	344	5	6	3	188	8	-6	16	152	6	12	-6	390	5	-0	16	63	30	21*
10	88	10	18	4	16	46	-10*	17	28	44	-0*	-5	228	5	4	H,K=	5,	9	
11	260	5	2	5	36	37	22*	18	181	5	0	-4	205	4	4	-13	172	6	-5
12	160	6	-5	6	44	47	17*	19	27	45	25*	-3	546	8	-8	-12	54	28	36*
13	65	11	28	7	216	7	8	H,K=	5,	3	-2	159	6	6	-11	281	5	-4	
14	139	6	-7	8	0	51	-13*-19	87	21	-6*	-1	469	7	1	-10	17	48	14*	
15	96	9	-7	9	249	5	2	-18	138	10	14	0	395	5	-3	-9	213	9	-4
16	86	21	10*	10	16	44	13*-17	47	43	-10*	1	209	3	0	-8	49	19	-9*	
17	131	11	-9	11	173	9	6	-16	269	5	-3	2	405	6	10	-7	49	29	39*
	H,K=	4,	8	H,K=	4,	12	-15	9	33	-9*	3	273	4	6	-6	5	44	-4*	
-15	165	6	-12	-5	98	9	4	-14	233	5	-6	4	411	5	1	-5	273	5	4
-14	56	15	-3*	-4	89	15	-7	-13	160	4	1	5	385	5	-6	-4	31	40	4*
-13	56	25	-8*	-3	59	15	-7*-12	130	7	-2	6	53	14	26*	-3	426	6	-2	
-12	82	8	2	-2	94	11	-5	-11	257	4	0	7	324	5	-2	-2	41	17	24*
-11	119	6	-12	-1	210	8	-6	-10	235	3	-1	8	273	4	-1	-1	359	5	-2
-10	36	43	-1*	0	0	53	-16*	-9	235	3	3	9	124	9	2	0	50	58	23*
-9	371	8	-4	1	230	7	1	-8	581	7	2	10	264	6	3	1	138	8	-0
-8	34	45	25*	2	53	23	5*	-7	51	5	7	11	82	11	5	2	25	33	-3*
-7	377	17	10	3	148	9	-3	-6	512	7	2	12	213	5	3	3	195	6	4
-6	64	13	-2*	4	103	11	3	-5	217	3	2	13	211	5	3	4	54	15	36*
-5	174	5	1	H,K=	5,	1	-4	420	6	8	14	57	26	4*	5	358	7	-6	
-4	154	7	4	-20	0	44	-16*	-3	455	7	10	15	163	7	-1	6	24	38	11*
-3	133	7	-1	-19	50	25	17*	-2	142	3	12	16	67	15	-4*	7	305	6	-4
-2	101	5	12	-18	153	6	7	-1	299	4	2	17	103	9	10	8	30	53	-4*
-1	381	5	-5	-17	54	17	23*	0	836	11	-73	H,K=	5,	7	9	135	7	0	
0	55	12	23*-16	346	5	1	1	180	5	7	-16	97	10	-4	10	44	38	31*	
1	427	5	-10	-15	18	32	4*	2	615	9	-21	-15	36	39	6*	11	69	34	6*
2	128	5	0	-14	295	4	0	3	272	5	-5	-14	82	30	-18*	12	34	53	15*
3	297	4	-3	-13	89	5	11	4	488	8	-14	-13	221	5	-5	13	172	10	1
4	113	5	0	-12	188	3	1	5	417	7	-8	-12	56	11	14*	H,K=	5,	11	
5	35	36	15*-11	60	7	14	6	78	5	21	-11	325	5	-6	-9	155	7	1	
6	111	9	4	-10	216	3	1	7	328	5	-1	-10	26	42	-17*	-8	66	28	21*
7	316	6	10	-9	22	31	2*	8	309	5	1	-9	277	4	-3	-7	50	24	28*
8	89	17	8*	-8	668	9	-4	9	103	6	0	-8	169	4	0	-6	78	17	14*
9	299	8	-2	-7	11	20	9*	10	436	5	-4	-7	64	8	6	-5	165	7	-3
10	43	22	24*	-6	763	10	6	11	56	23	17*	-6	159	6	8	-4	16	46	-17*
11	209	5	-1	-5	144	2	3	12	334	4	0	-5	267	5	8	-3	296	8	-1
12	78	14	11	-4	482	6	16	13	143	5	-1	-4	172	7	10	-2	40	49	35*

0 0 0 0 4 7 - 0 9 4 7

**STRUCTURE FACTORS CONTINUED FOR  
Na<sub>3</sub>(UO<sub>2</sub>)<sub>2</sub>F<sub>7</sub>.2H<sub>2</sub>O**

PAGE 5

L	F08	SG	DEL	L	FOB	SG	DEL	L	FOB	SG	DEL	L	FOB	SG	DEL	L	FOB	SG	DEL
-1	262	4	4	6	569	9	-20	-14	17	35	13*	10	72	19	6*	-1	343	4	7
0	63	14	18*	7	28	16	11*-13	233	4	-5	11	255	5	-2	0	48	7	8	
1	88	11	17	8	422	6	-10	-12	172	4	4	12	0	41	-5*	1	172	2	1
2	67	14	6*	9	108	5	-1	-11	86	6	1	13	195	6	4	2	687	9	-16
3	154	11	7	10	286	5	-6	-10	219	5	-1	14	56	20	16*	3	89	3	2
4	10	38	-21*	11	130	4	3	-9	140	4	2	H,K=	6,	10	4	737	11	-21	
5	253	6	1	12	106	10	-1	-8	180	3	2	-11	115	10	9	5	44	13	9*
6	16	41	8*	13	102	8	-3	-7	364	4	-2	-10	30	45	1*	6	574	9	-13
7	228	8	9	14	207	4	-12	-6	71	8	0	-9	72	27	-14*	7	69	8	-5
8	43	44	19*	15	0	50	-16*	-5	438	6	-2	-8	11	44	2*	8	45	11	21*
	H,K=	6,	0	16	216	8	-3	-4	267	4	4	-7	270	6	8	9	104	6	2
-20	174	11	9	17	43	60	7*	-3	373	5	5	-6	22	40	20*	10	265	5	-9
-18	235	7	-3	18	139	10	4	-2	385	7	8	-5	301	5	-1	11	49	10	3*
-16	177	7	-4	19	77	13	20	-1	125	6	-3	-4	0	46	-5*	12	367	6	-8
-14	38	41	9*	H,K=	6,	4	0	256	4	6	-3	224	4	8	13	43	19	41*	
-12	392	4	5	-19	29	45	5*	1	435	5	0	-2	45	51	21*	14	257	5	-6
-10	676	8	-3	-18	180	11	-2	2	183	4	1	-1	0	37	-26*	15	50	16	18*
-8	482	6	7	-17	97	8	-3	3	533	7	2	0	50	32	11*	16	85	13	-3
-6	202	4	5	-16	129	9	-2	4	135	11	6	1	272	4	5	17	42	45	4*
-4	915	10	-10	-15	163	5	-2	5	326	5	1	2	39	40	16*	18	76	12	-2
-2	958	10	-10*	-14	34	35	25*	6	244	4	-5	3	325	8	3	19	34	51	12*
0	565	6	-2*-13	198	4	-1	7	62	12	11*	4	37	37	26*	H,K=	7,	3		
2	438	6	-6*-12	256	4	-3	8	226	4	4	5	217	4	4	-19	73	19	-8*	
4	332	6	-3	-11	124	4	2	9	193	4	-4	6	23	42	-7*-18	58	15	5*	
6	814	13	-41	-10	466	6	1	10	114	6	6	7	21	41	1*-17	124	7	-1	
8	570	8	-16	-9	92	8	-7	11	282	5	-1	8	0	52	-17*-16	109	6	-7	
10	302	4	-6	-8	369	4	2	12	35	52	-3*	9	137	16	-2	-15	73	15	3*
12	114	5	2	-7	395	5	1	13	220	5	-3	10	48	34	36*-14	311	4	2	
14	209	4	-3	-6	158	3	-0	14	97	11	-2	11	201	6	-3	-13	0	39	-4*
16	232	4	-7	-5	366	5	3	15	60	15	9*	H,K=	6,	12	-12	343	5	-1	
18	154	7	2	-4	373	6	7	16	117	10	13	-4	8	57	-64*-11	177	3	-3	
	H,K=	6,	2	-3	312	4	3	H,K=	6,	8	-3	133	10	-3	-10	244	3	5	
-19	46	52	26*	-2	489	6	-2	-15	198	12	-6	-2	80	12	-22	-9	278	3	2
-18	228	8	-4	-1	70	4	-4	-14	0	38	-2*	-1	19	40	-15*	-8	220	3	2
-17	70	10	20	0	405	6	-4	-13	221	4	-4	0	101	13	7	-7	306	4	3
-16	178	4	1	1	322	6	5	-12	82	8	7	1	187	11	5	-6	548	7	2
-15	110	9	-10	2	260	4	1	-11	127	12	8	2	37	41	5*	-5	42	8	11*
-14	35	18	27*	3	491	8	-11	-10	90	17	0*	3	213	7	-4	-4	625	10	8
-13	146	4	-1	4	254	6	-6	-9	109	8	6	H,K=	7,	1	1	-3	273	5	2
-12	345	4	3	5	279	4	1	-8	43	46	-16*-19	0	43	-22*	-2	552	8	-6	
-11	48	9	-4*	6	429	7	-11	-7	369	19	19	-18	60	14	-8*	-1	367	6	7
-10	621	7	1	7	45	11	-5*	-6	41	55	35*-17	42	50	1*	0	50	7	-4	
-9	33	22	17*	8	347	5	-3	-5	426	17	8	-16	130	8	1	1	231	5	3
-8	376	5	5	9	177	4	-3	-4	42	55	-26*-15	43	49	0*	2	685	10	-18	
-7	129	3	3	10	200	5	4	-3	276	6	2	-14	391	5	-1	3	195	3	-3
-6	131	4	4	11	248	5	-2	-2	125	7	-1	-13	25	29	23*	4	691	12	-26
-5	262	4	6	12	75	9	-6	-1	77	11	-0	-12	440	5	4	5	137	5	-0
-4	609	8	10	13	193	4	4	0	118	5	4	-11	113	4	6	6	439	6	-9
-3	325	5	9	14	168	7	4	1	314	4	-1	-10	321	5	2	7	224	4	-1
-2	849	11	-8	15	19	49	-14*	2	66	9	9	-9	54	5	5	8	36	50	-8*
-1	77	4	-1	16	170	6	6	3	415	7	-6	-8	183	10	14	9	272	5	-6
0	787	10	-34	17	71	34	21*	4	109	7	5	-7	29	11	11*	10	197	3	-2
1	128	3	4	18	108	17	5	5	309	4	-0	-6	571	7	3	11	128	5	-2
2	367	7	-9	H,K=	6,	6	6	78	10	-5	-5	26	11	9*	12	319	7	-2	
3	222	4	6	-17	91	10	-10	7	15	38	-16*	-4	916	11	-1	13	21	35	7*
4	391	6	-5	-16	86	15	8	8	75	39	-17*	-3	155	5	6	14	242	6	1
5	136	3	0	-15	215	6	-0	9	195	6	-1	-2	694	9	1	15	75	14	-11

STRUCTURE FACTORS CONTINUED FOR  
NA3(U02)2F7.2H2O

PAGE 6

L	FOB	SG	DEL	L	FOB	SG	DEL	L	FOB	SG	DEL	L	FOB	SG	DEL
16	54	29	-20*	0	15	47	12*	5	89	11	-5	14	36	30	11*
17	94	16	3	1	361	4	-2	6	45	29	18*	15	74	17	5*
18	35	65	-26*	2	161	4	1	7	189	11	-2	16	145	6	-1
	H,K=	7,	5	3	196	6	-0	H,K=	8,	0	17	28	41	2*	0
-18	47	54	9*	4	176	5	5	-18	214	6	1	18	105	6	5
-17	190	5	3	5	143	4	5	-16	268	5	-9	H,K=	8,	4	2
-16	57	15	-23*	6	128	9	2	-14	261	4	-0	-18	152	9	-4
-15	124	11	-7	7	293	4	-2	-12	30	38	20*	-17	55	18	2*
-14	212	5	1	8	30	38	11*	-10	405	5	1	-16	210	5	-7
-13	37	33	6*	9	328	14	6	-8	577	7	3	-15	82	8	-6
-12	218	5	-7	10	72	11	-0	-6	679	9	4	-14	184	5	-8
-11	221	4	2	11	152	7	-7	-4	457	6	6	-13	190	5	-1
-10	140	4	-3	12	105	8	12	-2	721	10	-5	-12	46	19	6*
-9	347	4	-4	13	36	39	8*	0	735	10	-23	-11	270	3	-5
-8	93	7	3	14	99	11	12	2	769	11	-29	-10	249	4	-2
-7	347	4	0	15	130	7	5	4	363	6	-2	-9	183	3	-3
-6	378	5	-2	H,K=	7,	9	6	120	6	2	-8	412	4	-2	13
-5	83	6	8	-13	13	43	11*	8	446	6	-10	-7	55	8	2
-4	460	6	-1	-12	0	38	-16*	10	537	6	-11	-6	492	6	1
-3	249	3	5	-11	192	11	7	12	290	4	-3	-5	457	6	3
-2	318	5	0	-10	45	47	12*	14	34	36	8*	-4	267	4	-3
-1	442	7	-5	-9	317	17	9	16	137	6	-11	-3	389	6	-5
0	98	7	14	-8	26	58	20*	18	196	5	-0	-2	280	4	1
1	404	5	3	-7	279	4	4	H,K=	8,	2	-1	277	3	3	-12
2	332	5	3	-6	60	15	0*-19	58	22	0*	0	370	7	-3	-11
3	253	4	7	-5	53	35	-1*	-18	208	7	6	1	25	31	12*
4	395	6	-2	-4	31	51	20*	-17	58	13	19*	2	490	6	-0
5	162	7	5	-3	255	6	3	-16	273	5	-2	3	253	3	1
6	351	4	-4	-2	50	21	11*	-15	38	42	8*	4	243	3	-7
7	238	4	-7	-1	381	5	-4	-14	259	5	-1	5	410	7	-3
8	48	12	3*	0	34	49	32*	-13	129	8	-10	6	122	5	-4
9	297	5	-3	1	351	4	-4	-12	44	10	4*	7	241	4	-0
10	173	4	2	2	12	54	-2*-11	219	4	-1	8	269	4	-2	-3
11	154	5	-1	3	190	4	10	-10	344	4	3	9	62	10	-3
12	209	5	4	4	35	50	16*	-9	89	5	3	10	338	6	-0
13	38	45	6*	5	103	10	-9	-8	535	6	-1	11	119	6	-11
14	165	7	4	6	22	39	-4*	-7	20	27	9*	12	185	5	-1
15	123	11	-4	7	258	6	-3	-6	538	7	4	13	150	8	-6
16	61	16	8*	8	0	51	-9*	-5	152	2	8	14	0	63	-23*
17	129	7	1	9	275	7	2	-4	296	4	5	15	134	6	5
	H,K=	7,	7	10	0	59	-17*	-3	241	3	10	16	102	12	-8
-16	65	13	25*	11	161	18	15	-2	458	6	0	17	50	26	3*
-15	152	8	6	12	20	42	7*	-1	259	4	2	H,K=	8,	6	7
-14	111	7	-5	H,K=	7,	11	0	610	9	-4	-17	71	19	10*	8
-13	51	14	41*	-8	67	16	53*	1	6	23	4*	-16	132	8	5
-12	129	7	-4	-7	196	6	4	2	841	12	-57	-15	74	10	-6
-11	250	5	0	-6	22	62	-22*	3	126	3	3	-14	123	9	3
-10	77	7	-4	-5	44	62	-18*	4	357	5	-3	-13	242	4	-7
-9	354	4	-3	-4	75	17	4*	5	199	4	3	-12	0	47	-25*
-8	10	42	-20*	-3	144	7	-0	6	184	4	2	-11	327	5	-4
-7	342	5	2	-2	44	53	12*	7	119	5	0	-10	172	4	-2
-6	160	5	7	-1	263	6	-3	8	349	6	-3	-9	144	8	-2
-5	138	5	1	0	20	39	1*	9	35	20	7*	-8	200	3	-2
-4	160	4	2	1	262	9	-1	10	434	5	-4	-7	114	6	3
-3	253	6	10	2	0	53	-40*	11	90	15	3	-6	242	4	6
-2	211	9	9	3	97	19	-12*	12	264	4	-3	-5	397	5	-0
-1	456	17	7	4	64	32	-1*	13	77	8	-4	-4	126	4	5

STRUCTURE FACTORS CONTINUED FOR  
NA3(U02)2F7.2H20

PAGE 7

L	FOB	SG	DEL	L	FOB	SG	DEL	L	FOB	SG	DEL	L	FOB	SG	DEL
-4	52	24	47*	H,K=	9,	3		1	407	6	3	-5	340	17	8 -15
-3	309	5	0 -19	44	47	38*		2	47	27	9*	-4	42	53	-0*-14
-2	37	52	29*-18	174	5	-4		3	451	6	1	-3	111	7	-0 -13
-1	237	5	3 -17	72	34	-11*		4	211	4	0	-2	20	53	4*-12
0	31	42	6**-16	86	11	-11		5	213	3	-3	-1	174	5	1 -11
1	32	62	7**-15	153	6	5		6	285	4	-4	0	56	15	14*-10
2	35	49	0**-14	113	6	2		7	93	13	5	1	342	5	-2 -9
3	204	5	-6 -13	106	9	-9		8	303	7	1	2	0	47	-2*-8
4	38	45	26**-12	351	5	-3		9	197	5	-5	3	361	6	-3 -7
5	278	6	-7 -11	20	29	4*		10	83	16	7*	4	44	21	39*-6
6	0	58	-7*-10	402	4	3		11	244	5	4	5	182	5	-1 -5
7	191	10	-11	-9	169	3	1	12	96	10	5	6	17	57	-8*-4
8	32	41	8*	-8	363	5	6	13	111	10	-10	7	61	19	10*-3
9	45	29	1*	-7	263	3	3	14	142	6	7	8	0	53	-21*-2
10	60	65	48*	-6	198	3	4	15	0	49	-8*	9	189	7	-6 -1
	H,K=	8,	12	-5	391	5	7	16	115	8	-9	10	0	51	-5*
-1	172	9	13	-4	589	8	2	H,K=	9,	7	11	227	5	4	1 254
0	93	10	-3	-3	109	4	6	-16	51	22	3*	H,K=	9,	11	2 544
	H,K=	9,	1	-2	549	7	-4	-15	203	9	-11	-7	239	9	2 32
-19	58	18	47*	-1	137	4	4	-14	52	16	16*	-6	0	43	-4*
-18	218	8	-4	0	484	8	-2	-13	215	11	-2	-5	241	7	12
-17	32	37	12*	1	351	6	-1	-12	130	8	7	-4	32	63	-18*
-16	124	5	4	2	84	4	0	-11	68	11	16	-3	108	9	11 7 136
-15	53	22	11*	3	325	4	2	-10	163	4	3	-2	77	11	12 8 89
-14	113	5	1	4	410	6	1	-9	228	8	-2	-1	103	12	7 9 132
-13	64	13	-7*	5	160	4	-3	-8	125	6	7	0	49	25	19*
-12	450	5	-2	6	474	6	-5	-7	355	5	1	1	225	10	-7 11 25
-11	24	29	11*	7	76	6	3	-6	30	36	4*	2	0	43	-24*
-10	504	6	-2	8	411	5	-7	-5	401	5	-2	3	263	9	1 13 42
-9	118	4	-4	9	169	4	-1	-4	128	5	-1	4	36	41	3*
-8	467	6	4	10	93	8	-2	-3	207	4	9	5	125	14	2 15 69
-7	60	4	7	11	201	5	-4	-2	141	6	-3	6	51	33	4* 16 24 39
-6	139	4	3	12	107	6	-1	-1	129	9	0	H,K=	10,	0	17 59 16
-5	21	22	-2*	13	111	6	15	0	204	5	6	-18	0	53	-8*
-4	629	8	7	14	203	5	2	1	413	5	6	-16	204	4	2 H,K=
-3	43	5	11	15	15	60	3*	2	43	14	28*-14	337	4	1 -18	23 66
-2	764	10	-6	16	190	6	7	3	404	5	-1	-12	408	5	-1 -17
-1	58	4	3	17	74	12	14	4	108	6	9	-10	44	16	-12*-16
0	557	8	-9	H,K=	9,	5	5	187	5	-3	-8	380	4	4 -15	86
1	270	5	-2	-17	115	19	-9	6	147	5	1	-6	697	9	9 -14
2	64	8	12	-16	66	12	-4*	7	81	8	11	-4	748	10	4 -13
3	199	4	1	-15	221	4	-4	8	123	7	5	-2	433	6	14 -12
4	415	8	6	-14	73	11	-4	9	227	5	3	0	375	5	-3 -11
5	65	9	-4	-13	206	4	-0	10	28	57	1*	2	698	10	-7 -10
6	464	7	0	-12	236	4	-0	11	259	5	-0	4	736	12	-16 -9
7	22	26	2**-11	68	7	-1	12	0	41	-39*	6	299	4	0 -8	
8	515	6	-10	-10	262	4	-2	13	132	7	1	8	47	10	-1* -7
9	54	21	-5*	-9	186	6	-1	14	56	18	-8*	10	341	5	-7 -6
10	106	9	0	-8	208	3	0	H,K=	9,	9	12	347	5	0 -5	
11	80	12	4	-7	334	4	2	-13	170	13	5	14	193	6	-4 -4
12	144	5	-7	-6	80	6	7	-12	40	41	27*	16	38	50	12* -3
13	32	46	-1*	-5	421	5	-3	-11	33	39	2*	18	94	9	11 -2
14	229	6	-9	-4	353	6	-6	-10	19	66	2*	H,K=	10,	2 -1	
15	0	39	-8*	-3	141	7	4	-9	172	7	8	-19	89	23	9* 0 156
16	210	5	3	-2	431	5	-2	-8	57	15	16**-18	50	19	42*	1 316
17	23	54	2*	-1	122	4	7	-7	311	5	4	-17	67	12	-8 2 356
18	79	33	-8*	0	333	4	1	-6	54	20	49**-16	190	7	-2	3 39 12 15*

STRUCTURE FACTORS CONTINUED FOR  
Na3(UO2)2F7·2H2O

PAGE 8

L	FOB	SG	DEL	L	FOB	SG	DEL	L	FOB	SG	DEL	L	FOB	SG	DEL				
4	457	5	-4	-5	49	17	42*	-3	48	14	25*	17	9	48	-10*	5	319	4	-3
5	135	10	3	-4	125	7	6	-2	305	5	10	H,K=	11,	5	6	45	17	-4*	
6	212	3	2	-3	296	6	6	-1	25	26	8*-17	38	57	29*	7	197	7	-3	
7	281	4	4	-2	42	24	18*	0	772	10	-27	-16	158	7	3	8	127	9	6
8	57	19	1*	-1	410	6	6	1	36	18	11*-15	115	7	-7	9	0	54	-12*	
9	239	4	4	0	43	28	5*	2	656	10	-18	-14	109	7	-5	10	97	16	-6
10	214	8	2	1	330	4	4	3	168	3	0	-13	273	6	2	11	159	7	8
11	92	7	5	2	88	11	10	4	92	5	3	-12	63	10	-7	12	45	49	11*
12	229	10	-2	3	55	29	20*	5	130	6	3	-11	257	4	1	13	182	6	2
13	46	20	-11*	4	112	13	-6	6	233	5	1	-10	218	4	6	14	29	41	12*
14	137	6	4	5	168	6	9	7	80	11	8	-9	142	5	6	H,K=	11,	9	
15	118	8	1	6	65	20	3*	8	417	5	-2	-8	294	5	1	-12	19	59	-1*
16	10	51	-6*	7	271	8	-3	9	0	38	-1*	-7	156	4	4	-11	205	9	-2
17	114	17	6	8	53	61	24*	10	399	4	-4	-6	267	3	7	-10	14	48	7*
	H,K=	10,	6	9	265	5	12	11	44	14	5*	-5	360	4	-3	-9	79	21	6*
-16	98	15	10	10	0	48	-37*	12	116	6	-1	-4	28	30	13*	-8	19	39	-3*
-15	76	13	-22	11	89	14	2	13	75	12	27	-3	400	5	-5	-7	138	9	2
-14	150	5	1	12	53	24	-8*	14	66	18	12*	-2	230	6	4	-6	29	53	-14*
-13	82	17	6*	13	66	20	1*	15	31	42	3*	-1	149	4	5	-5	313	6	3
-12	177	4	3	H,K=	10,	10	16	194	5	8	0	437	5	-1	-4	8	47	-4*	
-11	255	5	-1	-10	61	72	55*	17	29	51	21*	1	76	8	2	-3	336	6	-2
-10	53	19	-4*	-9	251	6	-0	H,K=	11,	3	2	366	5	3	-2	9	44	-22*	
-9	345	4	-0	-8	0	46	-12*-18	157	10	-5	3	303	4	4	-1	144	8	-1	
-8	165	7	7	-7	214	8	8	-17	45	21	37*	4	29	43	6*	0	13	55	-10*
-7	225	5	5	-6	61	72	15*-16	229	5	0	5	321	4	-0	1	110	10	3	
-6	216	4	4	-5	25	43	17*-15	89	7	8	6	113	10	-6	2	46	22	14*	
-5	56	11	-1*	-4	0	42	-6*-14	168	8	2	7	221	5	-0	3	276	7	2	
-4	266	4	-2	-3	219	8	6	-13	190	6	7	8	246	4	5	4	30	47	27*
-3	337	4	5	-2	0	40	-7*-12	113	11	7	9	44	17	22*	5	300	5	0	
-2	138	4	6	-1	284	7	-6	-11	144	6	2	10	243	5	6	6	37	42	28*
-1	420	5	7	0	31	38	23*-10	316	5	-3	11	132	11	-8	7	177	5	-7	
0	127	5	6	1	249	7	4	-9	54	19	-0*	12	81	9	1	8	23	45	3*
1	411	16	14	2	55	62	32*	-8	430	5	1	13	167	5	4	9	29	45	25*
2	276	8	9	3	71	16	17*	-7	160	3	4	14	0	41	-35*	10	9	43	-10*
3	38	26	5*	4	47	49	21*	-6	453	6	2	15	104	13	0	H,K=	11,	11	
4	283	4	4	5	137	15	2	-5	311	4	9	16	110	8	7	-6	60	28	10*
5	196	4	-5	6	0	44	-4*	-4	89	6	6	H,K=	11,	7	-5	237	9	0	
6	140	7	-1	7	223	8	-2	-3	360	5	-0	-15	131	11	7	-4	58	32	43*
7	326	7	-0	8	44	28	39*	-2	360	5	1	-14	54	17	-17*	-3	240	8	3
8	0	37	-21*	9	189	11	-0	-1	111	5	1	-13	250	5	1	-2	31	42	-9*
9	280	4	4	H,K=	11,	1	0	595	8	-7	-12	0	44	-25*	-1	107	9	-10	
10	117	9	2	-19	31	50	8*	1	94	4	4	-11	270	5	4	0	56	57	-4*
11	104	8	4	-18	209	5	-1	2	530	7	-8	-10	104	7	1	1	51	52	-2*
12	152	15	2	-17	44	36	31*	3	263	3	5	-9	116	9	-1	2	64	15	28*
13	64	16	-1*	-16	291	4	2	4	114	10	1	-8	189	8	6	3	188	7	2
14	84	13	3	-15	47	18	26*	5	221	6	-0	-7	208	4	7	4	25	50	1*
15	130	7	-6	-14	210	5	1	6	215	6	0	-6	154	4	7	H,K=	12,	0	
	H,K=	10,	8	-13	33	29	-13*	7	173	4	3	-5	378	5	0	-18	188	6	5
-14	60	16	11*	-12	95	11	-1	8	399	6	1	-4	0	48	-2*	-16	44	56	2*
-13	73	22	1*	-11	83	6	-3	9	0	32	-15*	-3	399	15	8	-14	228	4	-1
-12	31	46	-10*	-10	403	4	2	10	334	4	-2	-2	99	8	14	-12	357	4	-1
-11	235	4	-1	-9	51	10	4*	11	110	6	-0	-1	211	4	4	-10	440	5	-2
-10	44	49	32*	-8	539	6	2	12	104	13	2	0	156	7	7	-8	152	3	15
-9	313	5	6	-7	129	3	0	13	139	6	8	1	71	9	3	-6	300	4	4
-8	78	16	4*	-6	570	7	-4	14	51	16	13*	2	185	4	4	-4	627	9	10
-7	241	4	2	-5	107	5	6	15	61	15	-19*	3	319	4	5	-2	699	10	-4
-6	85	15	-7	-4	16	23	9*	16	159	9	6	4	51	13	21*	0	430	6	-9

0 0 0 0 4 7 1 0 9 4 9

169

STRUCTURE FACTORS CONTINUED FOR  
NA3(UO2)2F7.2H2O

PAGE 9

L	FOB	SG	DEL	L	FOB	SG	DEL	L	FOB	SG	DEL	L	FOB	SG	DEL	L	FOB	SG	DEL
2	219	4	-3	-6	144	4	2	-12	91	16	39	-5	106	4	4	H,K=	13,	5	
4	422	8	5	-5	264	3	3	-11	42	43	3*	-4	532	7	4	-16	124	8	-4
6	537	8	-0	-4	381	5	-4	-10	54	23	-1*	-3	87	14	-2	-15	0	39	-41*
8	329	4	6	-3	77	6	-0	-9	223	5	4	-2	47	8	1	-14	207	6	7
10	59	18	1*	-2	505	10	-9	-8	45	20	30*	-1	52	6	-2	-13	125	6	5
12	175	4	-7	-1	255	5	2	-7	350	5	4	0	247	3	2	-12	146	5	-4
14	263	5	4	0	278	5	5	-6	52	18	-6*	1	49	8	9	-11	275	5	-1
16	172	8	-1	1	369	6	-7	-5	271	5	3	2	620	8	-14	-10	33	42	4*
H,K=	12,	2	2	75	12	2	-4	82	23	-6*	3	23	30	20*	-9	284	6	-1	
-18	158	8	-4	3	302	6	-1	-3	46	24	-1*	4	462	6	-5	-8	205	6	4
-17	86	10	1	4	229	3	-0	-2	143	7	17	5	99	8	-1	-7	178	4	-0
-16	0	43	-40*	5	81	7	12	-1	215	4	9	6	184	9	1	-6	343	6	0
-15	101	9	2	6	352	5	3	0	34	38	7*	7	98	5	-2	-5	72	10	-8
-14	211	4	-1	7	99	7	4	1	392	5	12	8	145	4	0	-4	248	4	-4
-13	93	14	-1	8	215	4	-2	2	42	48	33*	9	51	12	-6*	-3	260	3	-3
-12	359	6	-3	9	234	4	-0	3	318	6	4	10	307	4	2	-2	23	29	-7*
-11	40	12	30*	10	34	34	14*	4	60	21	5*	11	11	38	2*	-1	413	5	-1
-10	442	5	-1	11	158	6	-1	5	80	9	3	12	261	5	3	0	165	4	2
-9	113	4	-1	12	120	6	-2	6	106	9	9	13	36	60	17*	1	204	5	-1
-8	196	4	2	13	88	9	17	7	102	11	-5	14	117	7	3	2	375	13	7
-7	272	3	1	14	176	5	2	8	37	51	-21*	15	51	19	13*	3	21	38	0*
-6	203	3	2	15	34	57	10*	9	224	6	-0	16	63	17	46*	4	297	4	8
-5	155	3	9	16	108	9	-7	10	0	48	-4*	H,K=	13,	3	5	207	8	-3	
-4	560	6	6	H,K=	12,	6	11	185	8	-1	-17	110	26	12*	6	77	7	1	
-3	60	8	15	-16	17	44	9*	12	43	60	18*-	16	171	8	1	7	275	4	2
-2	591	8	-12	-15	180	5	-4	H,K=	12,	10	-15	44	55	11*	8	60	40	-12*	
-1	53	6	4	-14	82	15	-8*	-9	178	6	-2	-14	287	6	-5	9	184	5	-1
0	297	4	2	-13	150	7	2	-8	0	49	-3*-	13	87	11	5	10	179	6	3
1	178	4	-1	-12	151	9	-7	-7	271	6	-2	-12	219	4	-2	11	26	54	6*
2	152	3	3	-11	37	46	-2*	-6	49	63	35*-	11	187	4	0	12	151	17	-4
3	217	4	1	-10	209	4	3	-5	234	5	3	-10	55	18	17*	13	90	14	11
4	325	4	4	-9	235	4	-1	-4	39	44	-6*	-9	156	4	-1	14	90	10	15
5	12	48	-22*	-8	91	9	-1	-3	53	56	16*	-8	312	5	-2	15	136	7	5
6	524	8	-1	-7	413	6	3	-2	0	44	-6*	-7	82	5	4	H,K=	13,	7	
7	34	20	-22*	-6	115	5	-5	-1	157	8	-1	-6	520	7	1	-14	87	10	-14
8	314	4	0	-5	257	4	-2	0	36	47	21*	-5	112	4	8	-13	118	7	-2
9	131	6	7	-4	193	7	-4	1	271	5	-2	-4	429	5	-2	-12	88	13	-3
10	38	18	9*	-3	37	41	27*	2	20	49	16*	-3	213	3	3	-11	248	4	1
11	95	6	13	-2	265	6	1	3	238	9	6	-2	33	34	11*	-10	0	40	-2*
12	151	5	-12	-1	248	4	9	4	40	41	25*	-1	363	5	-1	-9	296	5	1
13	62	11	25	0	140	9	4	5	78	22	-1*	0	287	4	-2	-8	92	18	5*
14	227	6	3	1	410	6	9	6	7	59	-9*	1	175	4	2	-7	172	4	4
15	51	60	33*	2	53	27	4*	7	85	31	1*	2	503	6	-8	-6	205	5	7
16	156	13	0	3	377	11	9	H,K=	13,	1	3	34	37	-0*	-5	136	9	5	
17	64	14	22*	4	188	4	6	-18	77	15	8*	4	392	5	4	-4	139	9	-7
H,K=	12,	4	5	84	8	-4	-17	53	32	20*	5	180	7	-0	-3	309	4	4	
-17	123	14	9	6	227	4	3	-16	224	5	-1	6	173	3	3	-2	13	58	-11*
-16	34	39	-2*	7	128	11	-4	-15	0	48	-15*	7	206	4	6	-1	400	5	6
-15	176	5	-5	8	137	7	1	-14	372	6	-3	8	123	12	2	0	40	26	-17*
-14	167	4	7	9	270	4	2	-13	42	21	14*	9	136	5	-3	1	249	6	9
-13	163	6	11	10	0	43	-17*	-12	278	4	1	10	290	6	9	2	138	9	3
-12	289	5	4	11	199	11	5	-11	35	16	-2*	11	28	43	11*	3	43	18	32*
-11	78	16	2*	12	91	9	21	-10	28	28	23*	12	223	5	2	4	138	5	-5
-10	326	4	-1	13	80	11	-5	-9	89	8	0	13	64	29	7*	5	229	4	5
-9	190	4	1	14	121	7	12	-8	389	5	1	14	90	9	-8	6	35	43	-10*
-8	143	4	1	H,K=	12,	8	-7	84	6	11	15	100	17	-2	7	280	8	2	
-7	312	4	4	-13	146	7	-3	-6	659	8	1	16	33	54	24*	8	38	33	13*

**STRUCTURE FACTORS CONTINUED FOR  
Na<sub>3</sub>(UO<sub>2</sub>)<sub>2</sub>F<sub>7</sub>.2H<sub>2</sub>O**

PAGE 10

L	F08	SG	DEL	L	F08	SG	DEL	L	F08	SG	DEL	L	F08	SG	DEL	L	F08	SG	DEL
9	177	6	-1	-12	161	7	-1	10	158	6	-1	8	84	15	13	-12	309	4	-1
10	83	11	-9	-11	98	10	-4	11	143	10	5	9	47	43	-3*	-11	55	18	11*
11	35	41	10*	-10	369	6	-2	12	42	46	1*	10	51	28	4*	-10	252	4	2
12	63	16	-8*	-9	46	12	4*	13	127	11	-3	H,K=	14,	10	-9	200	4	-4	
13	101	13	14	-8	536	6	3	14	89	9	13	-7	158	6	-0	-8	27	33	6*
	H,K=	13,	9	-7	84	6	-5	15	95	15	25	-6	16	41	9*	-7	203	7	1
-11	233	7	3	-6	230	3	5	H,K=	14,	6	-5	264	8	-0	-6	242	5	2	
-10	40	42	20*	-5	254	3	2	-15	157	9	-4	-4	46	26	30*	-5	91	5	0
-9	243	9	5	-4	73	6	14	-14	40	56	14*	-3	244	5	8	-4	435	5	-3
-8	32	41	27*	-3	161	7	8	-13	211	5	2	-2	57	29	22*	-3	76	6	7
-7	118	9	8	-2	444	5	1	-12	54	40	-16*	-1	67	36	-7*	-2	438	5	-8
-6	23	46	3*	-1	60	12	6*	-11	179	7	9	0	31	49	22*	-1	195	3	-2
-5	89	10	3	0	602	7	-15	-10	169	6	6	1	129	7	14	0	127	5	9
-4	53	22	18*	1	57	7	-3	-9	55	43	46*	2	31	45	14*	1	288	5	-1
-3	261	7	3	2	324	4	-2	-8	236	5	4	3	216	9	-1	2	178	9	0
-2	20	40	-0*	3	114	4	5	-7	205	5	-6	4	37	43	34*	3	150	7	1
-1	343	6	3	4	0	30	-5*	-6	116	6	1	5	201	6	3	4	383	6	4
0	0	40	-12*	5	139	5	-7	-5	395	5	-3	H,K=	15,	1	5	10	32	-15*	
1	189	9	6	6	282	12	3	-4	68	12	12	-17	29	40	-5*	6	329	4	-1
2	60	15	31*	7	64	10	7	-3	277	6	-4	-16	35	41	-7*	7	151	4	15
3	38	40	-7*	8	427	5	-1	-2	175	5	-1	-15	27	37	-17*	8	179	5	5
4	23	49	-5*	9	29	40	8*	-1	68	12	12	-14	243	6	1	9	150	8	1
5	196	5	-3	10	223	7	4	0	263	4	4	-13	23	40	7*	10	39	23	8*
6	0	45	-4*	11	79	9	6	1	200	6	4	-12	400	6	-3	11	92	13	-9
7	247	5	-3	12	33	55	-21*	2	146	6	6	-11	12	35	-13*	12	181	5	9
8	18	48	9*	13	74	14	4*	3	291	5	-0	-10	309	4	-2	13	35	39	11*
9	167	12	3	14	97	15	-5	4	10	36	3*	-9	24	30	-15*	14	194	10	12
	H,K=	13,	11	15	29	54	-9*	5	294	6	7	-8	80	8	7	15	59	18	24*
-2	77	40	57*	16	150	9	-2	6	135	6	-6	-7	98	5	2	H,K=	15,	5	
-1	245	6	8	H,K=	14,	4	7	128	12	4	-6	286	4	6	-15	186	7	13	
0	35	54	-1*-17	31	63	11*	8	188	6	9	-5	83	5	-2	-14	133	14	2	
	H,K=	14,	0	-16	191	5	2	9	57	16	1*	-4	536	6	1	-13	66	13	-9*
-18	199	6	-5	-15	125	14	-5	10	106	8	2	-3	66	6	-3	-12	229	4	10
-16	248	6	-5	-14	78	14	-3	11	164	10	-1	-2	538	6	-10	-11	51	22	-20*
-14	100	7	-1	-13	205	8	0	12	43	56	13*	-1	103	5	3	-10	181	5	9
-12	180	4	0	-12	113	6	-4	13	153	17	-2	0	169	6	-1	-9	297	5	8
-10	372	5	4	-11	181	6	0	H,K=	14,	8	1	66	9	6	-8	42	51	28*	
-8	543	6	1	-10	292	5	-2	-12	16	44	1*	2	138	3	-4	-7	323	5	-8
-6	176	3	5	-9	48	14	14*	-11	183	13	1	3	37	15	3*	-6	154	5	0
-4	143	4	4	-8	391	4	5	-10	85	10	28	4	443	5	-6	-5	193	4	-4
-2	494	7	-3	-7	188	7	6	-9	45	28	37*	5	42	24	24*	-4	307	4	-2
0	684	8	-17	-6	166	7	-0	-8	73	11	11	6	402	5	3	-3	28	39	-2*
2	427	5	-10	-5	294	4	3	-7	190	7	-5	7	64	13	-1*	-2	258	4	-4
4	52	11	32*	-4	49	10	8*	-6	19	39	-3*	8	199	4	4	-1	236	6	-3
6	358	4	7	-3	252	3	-3	-5	333	6	-1	9	68	14	-0*	0	87	7	-1
8	464	5	3	-2	311	9	2	-4	0	39	-30*	10	54	15	14*	1	345	6	1
10	221	5	-3	-1	113	4	-3	-3	277	6	3	11	16	56	-24*	2	96	7	0
12	83	26	13*	0	481	6	-9	-2	90	20	8*	12	185	5	-2	3	188	6	4
14	102	11	-9	1	201	5	0	-1	96	9	7	13	25	41	15*	4	270	5	2
16	175	5	4	2	268	4	-4	0	127	10	4	14	217	7	2	5	8	44	-30*
	H,K=	14,	2	3	262	4	-1	1	158	8	5	15	43	43	31*	6	245	5	5
-18	185	7	-11	4	29	35	13*	2	34	38	-2*	H,K=	15,	3	-5	8	108	9	5
-17	41	43	25*	5	231	4	1	3	288	4	1	-17	86	11	-5	8	200	9	0
-16	223	6	-1	6	196	5	-4	4	27	38	22*	-16	36	49	-0*	9	0	38	-21*
-15	114	14	10	7	89	12	-11	5	262	4	2	-15	124	9	-0	10	0	144	15
-14	96	7	6	8	292	4	0	6	74	14	30*	-14	188	6	9	11	144	15	7
-13	111	16	-5	9	0	42	-35*	7	116	8	7	-13	41	55	-16*	12	123	9	10

0 0 0 0 4 7 1 0 9 5 0

**STRUCTURE FACTORS CONTINUED FOR  
Na<sub>3</sub>(UO<sub>2</sub>)<sub>2</sub>F<sub>7</sub>.2H<sub>2</sub>O**

PAGE11

STRUCTURE FACTORS CONTINUED FOR  
NA3(U02)2F7.2H2O

PAGE12

L	FOB	SG	DEL	L	FOB	SG	DEL	L	FOB	SG	DEL	L	FOB	SG	DEL	
-7	221	4	-1	-9	139	5	2	-7	216	4	-2	5	59	15	2*	
-6	49	23	-0*	-8	43	18	-11*	-6	138	6	-3	6	37	21	16*	
-5	294	5	3	-7	125	8	0	-5	90	8	5	7	43	30	7*	
-4	46	27	11*	-6	307	5	2	-4	208	5	11	8	195	5	5	
-3	238	6	6	-5	83	7	9	-3	114	7	2	9	38	40	21*	
-2	159	11	2	-4	437	5	-9	-2	166	9	10	10	213	4	4	
-1	30	60	22*	-3	39	14	12*	-1	308	4	1	11	43	33	25*	
0	138	6	10	-2	318	5	-5	0	25	49	0*	12	162	6	5	
1	206	12	1	-1	170	6	-4	1	247	5	-1	13	22	57	-6*	
2	93	10	24	0	88	5	-3	2	120	8	5	H,K=	19,	3	-8	
3	272	6	7	1	116	6	-8	3	115	10	-9	-14	169	12	-4	
4	10	39	-9*	2	254	4	-1	4	159	11	1	-13	82	11	-12	
5	202	9	4	3	64	8	-3	5	27	59	-27*	-12	36	40	-4*	
6	93	9	9	4	370	4	2	6	121	14	-1	-11	157	13	6	
7	54	17	-6*	5	7	39	-7*	7	172	5	8	-10	142	13	3	
8	97	9	13	6	287	4	8	8	29	40	-18*	-9	109	17	4	
9	91	9	2	7	44	44	-21*	9	177	5	3	-8	309	5	-2	
10	44	49	-5*	8	92	7	18	10	37	41	-11*	-7	0	39	-5*	
	H,K=	17,	9	9	79	12	-2	H,K=	18,	8	-6	283	6	2	1	
-7	220	5	4	10	69	17	-21*	-9	251	5	-0	-5	153	8	-1	
-6	19	47	16*	11	58	23	10*	-8	28	56	18*	-4	161	4	4	
-5	253	7	-1	12	189	5	8	-7	237	5	2	-3	185	4	2	
-4	19	41	17*	13	20	59	19*	-6	67	13	11*	-2	143	4	1	
-3	168	6	3	H,K=	18,	4	-5	93	13	2	-1	126	6	-3	6	
-2	46	50	26*-14	203	5	7	-4	73	15	13*	0	311	5	-2	7	
-1	36	43	35*-13	37	40	16*	-3	111	8	5	1	26	40	14*	8	
0	20	46	4*-12	242	6	0	-2	27	40	-13*	2	299	5	-5	H,K=	
1	172	6	4	-11	101	8	6	-1	259	7	-0	3	88	11	1	-2
2	39	45	10*-10	167	5	0	0	10	51	6*	4	175	6	-8	-1	
3	242	8	5	-9	216	4	-3	1	236	11	3	5	174	4	-1	0
4	0	51	-3*	-8	29	47	10*	2	75	12	24	6	51	13	16*	H,K=
5	172	8	-2	-7	243	4	1	3	132	8	1	7	120	9	-1	-14
	H,K=	18,	0	-6	242	5	-1	4	73	14	1*	8	175	5	6	-12
-16	83	17	21*	-5	71	14	15*	5	36	49	-0*	9	17	49	-23*	-10
-14	253	6	5	-4	326	4	-6	6	50	28	8*	10	179	6	2	-8
-12	328	5	8	-3	117	12	1	7	164	8	7	11	56	17	12*	-6
-10	215	5	2	-2	227	5	-10	H,K=	19,	1	12	144	7	10	-4	290
-8	78	15	4*	-1	228	4	-8	-15	29	54	21*	H,K=	19,	5	-2	410
-6	315	4	2	0	80	15	13	-14	219	9	6	-13	156	13	1	0
-4	454	5	-5	1	184	4	-11	-13	50	19	21*	-12	69	26	22*	2
-2	308	4	-7	2	180	7	3	-12	52	17	-11*	-11	222	6	6	4
0	54	24	2*	3	139	5	4	-11	58	34	-4*	-10	97	16	-3	6
2	291	4	-5	4	276	4	-3	-10	184	6	1	-9	147	7	3	8
4	399	6	-4	5	46	16	-0*	-9	0	37	-11*	-8	223	8	-1	10
6	333	4	4	6	214	6	-2	-8	408	6	-2	-7	15	37	11*	12
8	97	9	12	7	143	8	-1	-7	49	16	18*	-6	194	5	-1	H,K=
10	118	14	9	8	78	13	11	-6	343	4	-4	-5	202	6	-5	-14
12	212	5	12	9	138	6	-5	-5	0	32	-32*	-4	99	11	-4	-13
14	171	6	15	10	67	13	-2*	-4	225	4	-2	-3	268	4	-8	-12
	H,K=	18,	2	11	96	10	12	-3	65	8	2	-2	97	10	10	-11
-16	49	65	-19*	12	142	7	10	-2	147	4	-1	-1	216	7	1	-10
-15	75	18	6*	H,K=	18,	6	-1	86	6	4	0	221	4	1	-9	77
-14	252	6	3	-12	154	9	10	0	366	5	-7	1	57	19	4*	-8
-13	34	42	13*-11	151	7	15	1	20	43	16*	2	193	6	-1	-7	113
-12	286	7	-0	-10	59	29	-13*	2	354	7	-9	3	106	7	-1	-6
-11	83	11	-8	-9	238	5	0	3	71	7	20	4	130	5	5	-5
-10	190	4	3	-8	24	48	2*	4	209	4	-5	5	221	5	2	-4

00004710951

173

STRUCTURE FACTORS CONTINUED FOR  
NA3(U02)2F7.2H2O

PAGE13

L	FOB	SG	DEL	L	FOB	SG	DEL	L	FOB	SG	DEL	L	FOB	SG	DEL	L	FOB	SG	DEL
-3	75	10	-5	3	242	8	12	-1	152	4	-2	6	121	6	13	-1	124	11	11
-2	390	5	-10	4	84	15	8	0	72	9	9	8	170	5	-3	0	113	10	-14
-1	43	22	33*	5	140	11	7	1	119	5	-4	10	200	10	10	1	0	57	-18*
0	273	4	-5	6	113	13	-3	2	213	4	-6	H,K=	22,	2	2	143	8	10	
1	112	7	4	7	21	39	2*	3	33	34	7*-13	83	16	2*	3	161	11	3	
2	101	10	-4	8	101	15	3	4	274	6	-2	-12	0	42	-4*	4	70	13	22*
3	119	5	1	H,K=	20,	8	5	64	10	6	-11	85	12	-7	5	174	8	-2	
4	170	4	-2	-6	48	51	34*	6	166	5	-3	-10	223	7	-2	H,K=	23,	1	
5	84	19	15*	-5	227	7	-3	7	104	7	2	-9	61	20	-3*-12	235	6	-0	
6	253	5	-2	-4	54	24	4*	8	0	37	-3*	-8	264	7	-6	-11	13	41	-2*
7	25	56	20*	-3	120	12	-2	9	88	9	-1	-7	48	30	-0*-10	261	7	-4	
8	216	4	5	-2	53	37	3*	10	109	8	-6	-6	245	5	-2	-9	30	44	13*
9	47	48	8*	-1	60	14	6*	H,K=	21,	5	-5	113	9	2	-8	147	13	-9	
10	82	10	-3	0	40	42	-4*-11	159	9	6	-4	53	21	-2*	-7	60	30	3*	
11	58	21	-5*	1	189	6	-0	-10	80	15	5*	-3	116	10	1	-6	58	13	-12*
12	70	23	17*	2	40	41	27*	-9	201	12	-7	-2	174	5	-3	-5	26	38	-2*
	H,K=	20,	4	3	215	7	6	-8	72	13	-1	-1	55	19	-13*	-4	289	9	-6
-13	114	19	-0	H,K=	21,	1	-7	152	6	-2	0	287	4	-4	-3	29	34	14*	
-12	179	7	-12	-14	232	11	-0	-6	188	6	-3	1	23	36	10*	-2	304	6	-7
-11	58	19	14*-13	56	42	44*	-5	54	15	12*	2	272	5	-2	-1	21	39	-1*	
-10	256	5	2	-12	260	6	2	-4	190	5	-8	3	69	9	-8	0	218	4	-0
-9	63	14	-20*-11	48	56	22*	-3	163	6	-1	4	118	6	7	1	0	38	-35*	
-8	201	5	-1	-10	132	15	12	-2	121	6	0	5	75	10	-10	2	40	23	20*
-7	183	6	5	-9	59	17	-2*	-1	227	4	3	6	95	7	5	3	65	10	10
-6	66	10	32	-8	120	9	-10	0	40	29	3*	7	46	24	-9*	4	170	5	-4
-5	221	6	-8	-7	23	37	7*	1	186	7	-5	8	163	10	3	5	40	23	24*
-4	212	6	1	-6	346	4	-3	2	157	6	1	9	27	37	20*	6	216	9	1
-3	78	8	-16	-5	0	36	-22*	3	67	11	6	10	183	5	12	7	28	41	12*
-2	284	6	-10	-4	344	5	-10	4	178	7	-1	H,K=	22,	4	8	163	5	8	
-1	72	17	11*	-3	61	9	29	5	65	27	-5*-11	114	9	-19	9	40	24	11*	
0	206	5	-6	-2	233	4	-2	6	128	6	13	-10	182	7	8	H,K=	23,	3	
1	159	4	-4	-1	60	9	12	7	135	6	1	-9	68	15	3*-11	20	46	12*	
2	76	8	-4	0	54	16	-0*	8	39	32	35*	-8	229	10	6	-10	228	7	8
3	182	8	-1	1	60	9	-6	H,K=	21,	7	-7	51	17	3*	-9	76	11	-3	
4	116	8	-2	2	248	5	-7	-7	183	5	15	-6	212	4	-2	-8	112	10	-2
5	130	6	-0	3	19	33	10*	-6	97	19	2*	-5	149	8	-12	-7	129	6	-2
6	194	4	0	4	331	5	0	-5	21	45	-6*	-4	37	47	-28*	-6	70	19	7*
7	6	37	-9*	5	61	11	27	-4	88	13	-13	-3	213	5	-5	-5	110	14	-5
8	161	9	-4	6	200	4	3	-3	153	13	4	-2	139	6	2	-4	224	4	-2
9	82	12	-4	7	56	65	20*	-2	84	9	9	-1	103	6	5	-3	42	20	1*
10	89	13	20	8	34	45	22*	-1	218	5	-4	0	215	4	-5	-2	246	6	-8
11	109	13	-1	9	24	44	-4*	0	57	15	52*	1	54	20	26*	-1	82	8	9
	H,K=	20,	6	10	121	9	-11	1	212	5	11	2	203	5	-4	0	168	8	-2
-11	74	27	11*	11	15	38	-3*	2	77	12	-3	3	127	6	-0	1	120	7	1
-10	155	7	6	H,K=	21,	3	3	39	69	-20*	4	94	14	11	2	15	36	-14*	
-9	119	9	-0	-13	33	45	10*	4	98	8	8	5	143	5	6	3	127	6	6
-8	99	9	2	-12	219	11	7	5	92	10	8	6	66	67	5*	4	158	5	9
-7	203	12	-4	-11	106	13	10	H,K=	22,	0	7	109	7	7	5	45	48	6*	
-6	29	39	27*-10	75	23	-10*	-12	46	47	40*	8	109	9	-12	6	187	7	4	
-5	213	9	0	-9	131	7	-11	-10	224	6	7	H,K=	22,	6	7	34	38	8*	
-4	128	6	4	-8	96	8	-8	-8	277	10	-14	-8	126	10	-7	8	136	9	1
-3	121	6	5	-7	106	7	-3	-6	275	4	-5	-7	93	12	16	H,K=	23,	5	
-2	169	5	2	-6	258	5	-7	-4	56	16	8*	-6	121	15	8	-8	98	12	4
-1	77	9	23	-5	0	37	-34*	-2	184	4	-6	-5	183	5	-11	-7	186	9	-7
0	137	6	-7	-4	285	4	-2	0	304	6	-5	-4	27	39	4*	-6	59	37	15*
1	221	5	6	-3	126	5	1	2	282	5	-8	-3	216	4	5	-5	167	10	2
2	33	50	-10*	-2	172	5	-4	4	109	6	3	-2	84	10	-2	-4	157	5	-3

**STRUCTURE FACTORS CONTINUED FOR  
Na<sub>3</sub>(UO<sub>2</sub>)<sub>2</sub>F<sub>7</sub>.2H<sub>2</sub>O**

PAGE 14

00304710952

175

OBSERVED STRUCTURE FACTORS, STANDARD DEVIATIONS, AND DIFFERENCES (ALL X 6.0)  
NA3(UO2)2F7.6H2O F(0,0,0) = 2060

FOR AND FCA ARE THE OBSERVED AND CALCULATED STRUCTURE FACTORS.  
SS = ESTIMATED STANDARD DEVIATION OF FOB AND FCA.

SG = ESTIMATED STANDARD DEVIATION OF FOB. DEL = |FOB| - |FCA|.

\* INDICATES ZERO WEIGHTED DATA.

L	FOB	SG	DEL	L	FOB	SG	DEL	L	FOB	SG	DEL	L	FOB	SG	DEL
H,K= 0, 0	H,K= 0, 3			1 298	7	19	-3 417	9	-0	2 194	7	-18	H,K= 0, 12		
1 969 23-174*-10	74 14	21*		2 347	7	6	-2 424	9	2	H,K= 0, 12			-8 79	19	-7*
2 965 22 -32*-9	82 12	11		3 249	6	7	-1 345	7	-4	-8 79	19	-5			
3 941 19 -39*-8	94 7	3		4 211	5	2	0 361	8	-6	-7 87	10	-5			
4 800 17 -3	-7 93	6	3	5 145	6	5	1 374	8	-3	-6 103	10	11			
5 587 12 2	-6 47	13	2*	6 140	9	5	2 261	7	-12	-5 108	10	8			
6 445 9 -5	-5 193	4	-8	7 100	9	-9	3 216	6	-1	-4 132	7	9			
7 333 7 -3	-4 211	5	-4	8 109	11	28	4 197	8	1	-3 126	7	2			
8 287 6 1	-3 35	7	1*	H,K= 0,	6		5 176	8	12	-2 105	8	-8			
9 201 6 7	-2 107	3	1*-10	170	8	1	H,K= 0,	9	-1	97 11	11	-3			
10 166 12 1	-1 87	3	8*-9	193	8	-3	-10 157	6	-2	0 88	15	-15			
H,K= 0, 1	0 146	4	19*-8	255	6	-1	-9 182	6	4	1 100	9	6			
-10 25 39 15*	1 198	4	11*-7	277	6	-2	-8 182	8	-4	H,K= 0,	13				
-9 34 31 30*	2 49	7	5	-6 377	8	-6	-7 267	7	1	-6 252	7	12			
-8 0 43 -29*	3 86	4	5	-5 398	9	-11	-6 309	7	1	-5 255	8	2			
-7 61 7 -6	4 99	5	1	-4 334	8	-5	-5 314	7	3	-4 254	6	-6			
-6 26 18 -6*	5 91	8	5	-3 393	8	1	-4 313	7	4	-3 240	6	-11			
-5 54 4 -5	6 94	7	-4	-2 566	13	-7	-3 362	8	9	-2 229	6	-12			
-4 17 21 -6*	7 45	26	-8*	-1 426	9	14	-2 386	8	6	-1 234	7	-11			
-3 189 4 -2*	8 34	52	-9*	0 387	8	7	-1 350	8	-3	H,K= 1,-13					
-2 174 4 1*	9 66	15	12*	1 339	7	9	0 308	7	-9	2 226	6	-6			
-1 124 3 -9*	H,K= 0,	4	2 379	8	10	1 296	7	-11	3 243	9	-9				
0 42 55 11*-10	167	7	3	3 327	7	13	2 245	6	-10	4 262	8	7			
1 147 3 3*	-9 247	6	2	4 253	6	13	3 231	6	-1	5 241	7	9			
2 124 3 9*	-8 312	7	0	5 211	9	1	4 204	7	-2	H,K= 1,-12					
3 230 5 -5	-7 315	7	-6	6 183	6	7	5 148	7	-10	-1 45	47	-25*			
4 35 7 8*	-6 366	8	-12	7 125	9	-4	H,K= 0,	10	0	0 79	10	-7			
5 44 7 1	-5 604	13	-11	H,K= 0,	7		-9 127	6	8	1 95	8	1			
6 61 6 -1	-4 641	14	-22	-10 132	7	4	-8 121	8	-5	2 89	9	-5			
7 70 7 2	-3 647	14	-28	-9 191	8	6	-7 182	7	7	3 95	8	5			
8 41 27 3*	-2 663	14	-22*	-8 197	5	-1	-6 203	6	7	4 102	18	11			
9 24 38 -1*	-1 812	17	-93*	-7 228	5	-2	-5 202	5	-2	5 94	12	-0			
H,K= 0, 2	0 785	17	-5	-6 267	6	-4	-4 203	6	9	6 105	20	7*			
-10 165 6 8	1 754	16	22	-5 342	7	2	-3 221	6	9	7 79	13	-6			
-9 180 9 -5	2 646	14	10	-4 358	8	-3	-2 212	5	-2	H,K= 1,-11					
-8 287 7 -2	3 533	11	15	-3 399	9	0	-1 208	8	-6	-2 203	7	-14			
-7 364 8 -4	4 405	9	6	-2 369	8	8	0 164	6	-17	-1 252	10	-9			
-6 350 7 -6	5 383	8	3	-1 346	8	7	1 156	7	-5	0 290	7	-11			
-5 475 10 -6	6 305	7	4	0 326	7	-2	2 127	12	-8	1 301	8	-14			
-4 530 11 -10	7 206	6	-0	1 355	8	2	3 116	14	-10	2 336	8	-1			
-3 615 13 -6*	8 153	13	-1	2 277	6	1	4 99	11	-9	3 342	8	4			
-2 746 15 -16*	H,K= 0,	5	3 203	6	3	H,K= 0,	11	0	4 328	8	7				
-1 753 18 -86*-10	118	10	16	4 187	6	1	-9 188	6	0	5 320	7	10			
0 793 41 37*	-9 122	5	-1	5 194	6	12	-8 232	8	4	6 293	7	-1			
1 647 18 17*	-8 155	5	-3	6 137	8	4	-7 264	8	2	7 275	7	10			
2 641 13 9*	-7 209	5	-2	H,K= 0,	8		-6 285	7	9	8 222	7	12			
3 763 16 2	-6 283	7	-3	-10 149	9	-0	-5 280	7	4	H,K= 1,-10					
4 443 10 1	-5 272	6	-1	-9 186	6	-4	-4 347	9	10	-3 119	7	-13			
5 339 7 3	-4 326	7	-15	-8 228	6	3	-3 330	7	-2	-2 161	6	5			
6 361 8 -5	-3 273	6	3	-7 260	6	-2	-2 290	7	-7	-1 183	5	-12			
7 291 7 -2	-2 505	11	-17	-6 284	7	-7	-1 270	6	-9	0 204	6	-4			
8 200 7 -3	-1 459	10	12	-5 360	8	1	0 266	6	-13	1 175	8	-8			
9 153 11 -5	0 271	6	9	-4 395	9	-4	1 239	6	-14	2 215	6	4			

STRUCTURE FACTORS CONTINUED FOR  
NA3(U02)2F7.6H20

PAGE 2

L	FOB	SG	DEL	L	FOB	SG	DEL	L	FOB	SG	DEL	L	FOB	SG	DEL
3	237	8	8	10	105	8	-6	8	282	6	-1	1	71	4	1*
4	218	8	1	H,K=	1,	-6		9	203	5	2	2	143	3	-1*
5	197	6	10	-7	143	17	-4	10	151	9	-4	3	27	9	5*
6	177	7	4	-6	209	8	2	H,K=	1,	-3	4	41	5	5	-3
7	159	8	3	-5	289	8	11	-9	68	27	31*	5	41	11	7*
8	157	6	10	-4	298	7	9	-8	68	15	-1*	6	0	30	-6*
9	128	7	8	-3	335	8	17	-7	77	11	-10	7	31	16	8*
	H,K=	1,	-9	-2	452	10	2	-6	121	5	9	8	0	33	-1*
-5	150	7	-4	-1	491	12	-3	-5	111	5	2	9	0	42	-11*
-4	167	6	-7	0	506	11	-1	-4	142	5	0	10	0	38	-0*
-3	169	6	-13	1	566	13	13	-3	288	6	5	H,K=	1,	0	4
-2	224	6	-2	2	501	11	-5	-2	411	9	13	-10	164	8	-1
-1	264	6	-7	3	509	11	-3	-1	190	4	20*	-9	183	9	-2
0	272	6	-6	4	497	11	-9	0	476	10	17*	-8	264	8	-6
1	229	8	-5	5	443	9	-8	1	373	8	5*	-7	407	9	-7
2	280	7	2	6	367	8	0	2	461	10	-5*	-6	383	8	-6
3	302	7	9	7	266	6	-6	3	348	8	-17	-5	455	10	-6
4	276	7	5	8	266	7	-0	4	216	5	-2	-4	670	14	1
5	240	6	1	9	245	6	14	5	167	4	-3	-3	719	15	-20*
6	229	6	-2	10	146	11	-6	6	185	5	-3	-2	842	29	-29*
7	192	6	-3	H,K=	1,	-5	7	103	6	-5	-1	868	35	-39*	
8	191	15	7	-8	69	70	-3*	8	107	9	1	0	902	23	90*
9	158	6	3	-7	91	17	7	9	47	20	5*	1	923	22	37*
	H,K=	1,	-8	-6	138	6	-5	10	51	17	15*	2	548	11	-12*
-5	160	10	-4	-5	179	6	4	H,K=	1,	-2	3	721	15	-2	-3
-4	186	6	-3	-4	166	5	5	-9	163	8	-7	4	533	12	-3
-3	231	6	-1	-3	227	7	7	-8	209	7	-0	5	296	7	-2
-2	256	6	-5	-2	232	6	17	-7	286	6	-2	6	353	8	-2
-1	264	6	-7	-1	318	8	11	-6	334	7	-4	7	329	7	-1
0	284	7	-4	0	335	8	6	-5	446	9	0	8	211	6	-3
1	328	7	2	1	265	6	13	-4	483	10	8	9	174	5	10
2	350	9	12	2	245	6	-1	-3	606	13	-0	H,K=	1,	1	
3	338	7	8	3	225	5	-3	-2	583	12	22*	-10	27	43	5*
4	227	5	0	4	214	5	-1	-1	570	24	20*	-9	36	21	4*
5	276	6	-3	5	249	6	-12	0	809	41	-92*	-8	42	42	11*
6	271	7	-1	6	112	5	-1	1	884	22	8*	-7	30	34	8*
7	210	5	-0	7	102	5	1	2	339	7	-10*	-6	32	14	5*
8	170	5	1	8	130	5	5	3	633	14	-18	-5	52	10	-1*
9	158	6	2	9	105	6	7	4	619	14	-6	-4	209	5	-5
10	119	18	-7	10	72	12	9	5	497	11	-6	-3	62	3	-5*
	H,K=	1,	-7	H,K=	1,	-4		6	360	8	-3	-2	51	7	4*
-6	124	15	-15	-8	168	8	5	7	314	7	-2	-1	101	3	6*
-5	179	7	4	-7	216	7	0	8	274	6	-4	0	203	5	3*
-4	221	6	7	-6	290	7	4	9	211	6	-4	1	160	4	12*
-3	269	6	0	-5	296	7	5	10	157	9	2	2	47	4	-6*
-2	308	7	-6	-4	361	8	8	H,K=	1,	-1	3	22	11	-4*	-3
-1	334	8	-7	-3	515	11	10	-10	0	52	-12*	4	141	3	-4
0	320	7	-1	-2	626	14	20	-9	34	38	17*	5	70	5	-3
1	419	9	3	-1	460	10	20	-8	0	33	-10*	6	61	7	-6
2	456	11	2	0	566	13	11	-7	0	40	-8*	7	34	19	-3*
3	363	8	0	1	667	15	-10	-6	34	12	29*	8	39	40	7*
4	282	7	2	2	670	15	-34	-5	60	10	6	9	57	33	19*
5	307	8	-9	3	476	11	-6	-4	44	9	6*	H,K=	1,	2	
6	277	6	-1	4	492	11	-12	-3	41	7	7	-10	179	6	0
7	219	5	2	5	426	9	-8	-2	88	3	11*	-9	232	6	-5
8	162	5	3	6	392	8	-3	-1	29	8	4*	-8	319	7	-9
9	145	5	6	7	313	7	-5	0	106	4	2*	-7	349	7	-2

0 0 0 0 4 7 1 0 9 5 3

177

STRUCTURE FACTORS CONTINUED FOR.  
NA3(UO2)2F7.6H2O

PAGE 3

L	F08	SG	DEL	L	F08	SG	DEL	L	F08	SG	DEL	L	F08	SG	DEL				
H,K=	1,	5	5	179	6	8	-4	323	8	3	7	165	7	-1	-2	399	9	3	
-11	66	43	-3*	6	142	8	10	-3	337	8	0	8	137	7	2	-1	399	9	-1
-10	82	15	-5	H,K=	1,	8	-2	311	7	-3	H,K=	2,	-9	0	347	8	2		
-9	150	5	-0	-10	159	6	11	-1	302	7	-13	-4	164	6	-5	1	501	11	7
-8	164	4	2	-9	167	6	2	0	288	7	-13	-3	185	6	-3	2	504	12	-1
-7	127	5	-3	-8	172	5	-5	1	236	6	-11	-2	212	8	-4	3	391	9	-7
-6	179	4	-5	-7	225	6	-4	2	204	7	-10	-1	228	6	-9	4	343	7	-4
-5	245	5	-5	-6	318	7	-0	H,K=	1,	12	0	234	6	-4	5	374	8	-3	
-4	251	6	-3	-5	259	7	-7	-8	77	11	9	1	264	6	-3	6	307	7	-7
-3	263	6	-9	-4	294	7	5	-7	93	9	3	2	296	7	3	7	278	6	-1
-2	199	4	12	-3	305	7	5	-6	107	13	4	3	281	8	8	8	222	6	5
-1	262	6	14	-2	344	8	0	-5	118	8	9	4	233	7	2	9	195	7	8
0	286	6	7	-1	316	7	-0	-4	110	13	9	5	233	8	-5	10	136	8	-5
1	277	6	20	0	261	6	-2	-3	92	11	-3	6	255	7	5	H,K=	2,	-5	
2	276	6	14	1	218	6	-11	-2	75	21	-19*	7	203	6	2	-8	78	13	8
3	173	5	1	2	222	6	1	-1	104	8	4	8	160	6	4	-7	91	23	-5*
4	167	7	11	3	164	9	-10	0	85	14	7	9	137	9	-6	-6	113	7	12
5	192	7	-0	4	172	6	6	1	62	13	2*	H,K=	2,	-8	-5	117	8	-2	
6	153	6	13	5	132	8	8	H,K=	1,	13	-5	172	6	1	-4	114	7	-0	
7	91	15	-4	H,K=	1,	9	-7	240	7	12	-4	194	6	1	-3	174	8	0	
H,K=	1,	6	-10	164	8	1	-6	233	11	2	-3	181	7	-7	-2	220	6	9	
-11	117	12	4	-9	224	6	15	-5	245	7	-1	-2	253	6	-2	-1	91	6	2
-10	160	7	5	-8	238	6	4	-4	262	7	-10	-1	293	8	-9	0	82	7	12
-9	235	7	7	-7	282	6	3	-3	253	7	-11	0	286	6	-1	1	207	5	3
-8	228	5	-5	-6	309	7	2	-2	238	8	-11	1	299	7	7	2	125	6	7
-7	266	6	-6	-5	313	7	1	-1	225	7	-11	2	316	7	6	3	136	4	-4
-6	282	6	-3	-4	363	8	1	H,K=	2,	-12	3	303	7	-3	4	71	5	1	
-5	363	8	-16	-3	428	10	10	0	108	20	-6*	4	329	7	6	5	98	5	3
-4	413	10	0	-2	329	7	-8	1	109	8	-8	5	275	8	-0	6	127	4	3
-3	376	8	-4	-1	317	7	-3	2	139	7	15	6	263	6	5	7	96	10	1
-2	407	9	11	0	321	7	-9	3	141	11	-4	7	217	6	5	8	72	11	-3
-1	403	10	10	1	311	7	-11	4	149	7	6	8	194	8	1	9	74	9	5
0	330	8	4	2	258	6	-2	5	149	10	18	9	184	8	7	10	53	26	11*
1	459	10	11	3	198	7	-8	6	135	7	15	H,K=	2,	-7	H,K=	2,	-4		
2	346	8	14	4	187	8	-3	H,K=	2,	-11	-6	122	9	2	-8	156	11	-6	
3	250	6	8	H,K=	1,	10	-2	187	11	-14	-5	157	10	1	-7	224	7	5	
4	249	6	6	-10	92	21	-6*	-1	225	6	-17	-4	165	6	9	-6	310	7	11
5	231	6	7	-9	124	8	0	0	249	7	-13	-3	168	7	1	-5	361	9	4
6	175	8	2	-8	147	10	5	1	251	6	-5	-2	226	6	-2	-4	414	9	11
7	123	11	-1	-7	166	5	9	2	260	8	-4	-1	243	6	-5	-3	491	11	19
H,K=	1,	7	-6	148	5	-5	3	304	7	5	0	277	7	1	-2	583	13	26	
-11	107	9	-5	-5	159	6	3	4	287	7	15	1	237	6	5	-1	585	13	16
-10	159	9	4	-4	188	5	3	5	250	8	7	2	264	6	3	0	684	16	-3
-9	180	7	3	-3	200	5	8	6	231	8	4	3	247	6	-1	1	716	16	-20
-8	194	5	-3	-2	141	6	-8	7	207	8	-1	4	248	5	-3	2	549	12	5
-7	237	6	-3	-1	127	5	-3	8	179	8	1	5	232	5	5	3	497	11	-15
-6	340	8	-12	0	144	5	0	H,K=	2,	-10	6	190	5	-3	4	599	13	-6	
-5	302	7	-2	1	138	6	2	-3	115	10	-15	7	136	5	5	5	491	11	-6
-4	292	6	2	2	108	7	-1	-2	140	8	-8	8	153	6	7	6	344	7	-5
-3	324	7	4	3	94	12	5	-1	140	8	-19	9	123	6	-3	7	292	6	-6
-2	441	10	12	4	75	12	-2	0	172	6	-8	10	95	8	6	8	277	6	1
-1	350	7	5	H,K=	1,	11	1	196	5	-3	H,K=	2,	-6	9	220	7	5		
0	302	7	1	-9	197	9	1	2	208	7	-3	-7	149	10	-7	10	152	8	-3
1	283	7	-1	-8	236	7	8	3	208	10	1	-6	211	7	11	H,K=	2,	-3	
2	287	6	3	-7	278	8	3	4	192	6	3	-5	243	7	9	-9	59	25	17*
3	245	6	8	-6	314	7	10	5	192	5	5	-4	268	6	4	-8	37	51	-0*
4	216	6	3	-5	329	7	14	6	216	6	14	-3	358	8	8	-7	56	18	-1*

STRUCTURE FACTORS CONTINUED FOR  
NA3(U02)2F7.6H20

PAGE 4

L	F08	SG	DEL	L	F08	SG	DEL	L	F08	SG	DEL	L	F08	SG	DEL
-6	74	7	7	8	9	34	0*	2	567	13	2	-5	387	8	-12
-5	110	5	-3	9	41	41	19*	3	562	12	-4	-4	274	6	4
-4	143	5	4	H,K=	2,	0	4	345	8	1	-3	400	9	-6	
-3	89	15	-1	-10	153	6	-3	5	290	6	-7	-2	546	12	-13
-2	117	5	10	-9	208	6	-2	6	292	6	3	-1	526	12	5
-1	212	5	5	-8	261	6	-0	7	236	6	-4	0	377	8	24
0	192	4	17	-7	323	7	-3	8	185	7	13	1	407	9	16
1	244	5	-13	-6	358	8	-1	9	125	16	-8	2	360	8	9
2	18	14	-0*	-5	451	10	-3	H,K=	2,	3	3	342	8	5	1
3	50	6	-6	-4	646	14	-5	-11	70	22	17*	4	243	8	7
4	142	4	-8	-3	675	14	-3	-10	62	11	-7*	5	200	6	5
5	79	4	3	-2	319	7	-2*	-9	99	6	-4	6	160	9	0
6	44	8	17	-1	902	25	-7*	-8	170	5	4	7	122	8	1
7	13	28	-12*	0	981	24	81*	-7	106	7	4	H,K=	2,	6	H,K=
8	15	31	-8*	1	674	16	11*	-6	167	4	-4	-11	126	7	1
9	48	21	10*	2	584	12	2*	-5	299	7	-7	-10	152	8	4
10	5	37	-10*	3	576	13	-8	-4	345	8	-8	-9	191	8	-5
	H,K=	2,	-2	4	535	12	-5	-3	348	7	-11*	-8	198	5	-2
-9	165	8	10	5	453	10	-8	-2	383	8	-19*	-7	237	6	-7
-8	198	7	-1	6	331	7	-1	-1	370	8	39*	-6	354	8	-5
-7	306	7	1	7	311	7	2	0	601	13	-17*	-5	337	8	-4
-6	351	8	4	8	219	6	5	1	355	8	8	-4	249	6	-1
-5	298	6	7	9	181	6	11	2	343	7	9	-3	392	10	-0
-4	510	11	15	H,K=	2,	1	3	263	6	3	-2	420	10	10	-1
-3	609	13	27	-10	29	45	-3*	4	191	5	8	-1	442	10	8
-2	673	22	15	-9	43	15	4*	5	204	5	3	0	328	8	8
-1	670	37	52*	-8	77	7	1	6	167	5	6	1	314	7	18
0	668	14	-22*	-7	95	7	-0	7	78	12	-8	2	337	8	4
1	786	17	10*	-6	153	4	-2	8	92	9	12	3	278	7	10
2	757	16	11*	-5	90	3	2	H,K=	2,	4	4	219	7	2	H,K=
3	581	13	-8	-4	116	3	6	-11	128	10	-5	5	200	7	3
4	638	14	-12	-3	252	5	-2*	-10	179	6	6	6	134	8	-2
5	399	9	1	-2	195	4	-11*	-9	256	7	-5	7	106	10	-8
6	369	8	-5	-1	272	6	18*	-8	324	7	-1	H,K=	2,	7	-7
7	363	8	-3	0	198	5	10*	-7	304	7	-3	-11	110	9	4
8	259	6	-5	1	28	7	-0*	-6	424	9	-5	-10	152	7	6
9	182	6	4	2	278	6	-0	-5	509	11	-11	-9	197	7	6
10	154	11	1	3	187	5	-3	-4	662	14	-35	-8	218	7	-1
	H,K=	2,	-1	4	97	6	5	-3	536	12	-9	-7	231	5	-1
-10	35	43	30*	5	83	5	1	-2	601	13	-46	-6	271	6	-7
-9	36	45	30*	6	62	11	-15	-1	669	15	2	-5	313	7	-4
-8	32	33	19*	7	86	10	2	0	613	13	10	-4	346	8	0
-7	36	15	11*	8	75	17	10*	1	553	13	6	-3	423	9	1
-6	29	17	-2*	9	29	62	-5*	2	551	13	6	-2	391	9	11
-5	41	8	9*	H,K=	2,	2	3	341	7	6	-1	327	7	3	H,K=
-4	29	13	25*-10	160	8	2	4	324	7	5	0	374	9	4	-9
-3	30	9	29*	-9	204	7	-0	5	304	7	5	1	380	8	-7
-2	136	3	9*	-8	278	6	-3	6	241	7	-0	2	326	7	13
-1	128	4	21*	-7	334	7	-8	7	160	6	-1	3	243	6	11
0	71	4	-6*	-6	365	8	-3	8	119	21	-7	4	224	8	8
1	137	3	-9*	-5	429	9	-6	H,K=	2,	5	5	5	202	8	2
2	55	3	-5*	-4	448	10	-6	-11	89	10	-7	6	143	8	-4
3	32	6	-2	-3	471	10	-16*-10	124	6	7	H,K=	2,	8	-2	
4	38	14	5*	-2	528	11	-26*	-9	157	5	4	-11	102	8	4
5	81	4	-4	-1	689	39	-50*	-8	173	5	-0	-10	120	8	-1
6	28	15	18*	0	511	17	5*	-7	237	5	-4	-9	173	5	6
7	11	34	7*	1	364	8	-2*	-6	301	7	-2	-8	192	6	-1
												2	204	6	-15

STRUCTURE FACTORS CONTINUED FOR  
NA3(U02)2F7.6H20

PAGE 5

L	FOB	SG	DEL	L	FOB	SG	DEL	L	FOB	SG	DEL	L	FOB	SG	DEL
H,K=	2,	12	3 253	6	8	H,K=	3,	-5	H,K=	3,	-2	5 332	8	-4	
-9	45	71	-11*	4 225	6	2	-7	54	20	7*	-9	182	12	0	
-8	60	16	-14*	5 219	6	6	-6	76	11	2	-8	238	6	2	
-7	72	14	-3*	6 186	5	2	-5	58	13	-11*	-7	295	7	-3	
-6	70	13	-1	7 165	6	4	-4	94	11	5	-6	391	8	4	
-5	80	22	6*	8 128	11	-8	-3	53	23	1*	-5	465	10	9	
-4	102	7	17	H,K=	3,	-8	-2	67	12	3	-4	596	13	6	
-3	91	15	-2	-5 154	7	-9	-1	104	7	4	-3	745	16	8	
-2	73	9	1	-4 192	6	-3	0	115	9	7	-2	639	15	24	
-1	53	14	-7*	-3 238	6	2	1	98	4	-1	-1	753	29	-16	
0	47	49	-11*	-2 268	7	-7	2	105	5	1	01010	22	-68	-6	
1	53	16	0*	-1 297	7	-2	3	51	8	6	1	786	17	1	
H,K=	2,	13	0 310	7	1	4	172	5	-5	2	642	14	-16	-4	
-7	271	8	9	1 342	9	0	5	129	5	-1	3	634	14	1	
-6	288	9	9	2 415	9	8	6	74	10	-7	4	582	13	-8	
-5	310	7	4	3 348	8	5	7	80	10	6	5	483	10	-10	
-4	313	9	-4	4 307	7	1	8	86	12	8	6	339	7	-4	
-3	273	7	-17	5 325	7	7	9	79	12	12	7	292	6	-1	
-2	273	7	-9	6 293	6	2	H,K=	3,	-4	8	258	6	10	2	
-1	267	7	-14	7 243	6	4	-8	158	21	-6	9	172	6	1	
H,K=	3,	-12	8 208	6	10	-7	245	6	10	H,K=	3,	-1	4		
1	148	8	4	9 155	8	-7	-6	301	7	10	-10	34	47	23*	
2	146	7	-4	H,K=	3,	-7	-5	296	7	4	-9	20	38	15*	
3	155	13	7	-6 89	32	-19*	-4	360	8	14	-8	45	15	15*	
4	139	8	-5	-5 137	8	7	-3	537	12	23	-7	60	13	6*	
5	139	14	1	-4 155	10	-2	-2	521	12	15	-6	79	18	3*	
H,K=	3,	-11	-3 193	5	1	-1	502	11	1	-5	59	14	-3*		
-1	190	7	-14	-2 242	6	-4	0	498	11	19	-4	87	4	3	
0	214	7	-5	-1 231	6	-2	1	610	14	-10	-3	209	6	13	
1	225	8	-4	0 216	6	-2	2	556	12	-6	-2	318	7	6	
2	242	7	-0	1 313	7	12	3	492	11	0	-1	248	5	24*	
3	241	7	6	2 313	7	3	4	426	10	-12	0	236	5	-2*	
4	236	7	16	3 258	6	8	5	407	9	-1	1	179	5	-5	
5	200	8	-2	4 221	6	3	6	306	7	-2	2	264	6	-11	
6	211	6	5	5 202	8	-6	7	301	7	-4	3	212	5	-5	
7	191	8	10	6 203	5	2	8	255	6	10	4	106	3	-1	
H,K=	3,	-10	7 166	5	8	9	173	6	-0	5	57	6	0		
-3	147	9	-1	8 118	10	1	H,K=	3,	-3	6	74	6	-3		
-2	167	9	-9	9 98	12	-5	-9	38	43	17*	7	58	10	-3	
-1	224	6	1	H,K=	3,	-6	-8	48	23	19*	8	34	50	-8*	
0	213	7	-10	-7 148	11	-5	-7	53	28	0*	9	0	37	-23*	
1	220	7	-4	-6 229	10	10	-6	54	13	-1*	H,K=	3,	0		
2	229	7	-6	-5 273	7	4	-5	12	38	-16*	-10	152	7	-4	
3	258	7	11	-4 302	7	13	-4	43	13	9*	-9	170	9	-2	
4	243	6	8	-3 336	8	6	-3	144	6	5	-8	275	6	-3	
5	222	6	6	-2 410	9	0	-2	103	5	15	-7	345	7	1	
6	186	8	-1	-1 431	10	-3	-1	107	4	4	-6	378	8	-9	
7	173	6	-0	0 485	11	5	0	25	27	-3*	-5	437	10	-0	
8	144	10	-2	1 482	11	6	1	85	5	1	-4	556	12	-6	
H,K=	3,	-9	2 465	10	2	2	135	4	-9	-3	653	14	2		
-4	123	10	-19	3 414	9	0	3	109	4	5	-2	789	16	-1*	
-3	154	6	2	4 432	10	-3	4	36	8	4*	-1	685	14	-44*	
-2	184	9	-0	5 409	9	'1	5	36	19	-17*	0	967	20	47*	
-1	217	7	-11	6 311	7	1	6	26	27	-0*	1	589	13	10*	
0	209	6	-11	7 243	6	-2	7	70	7	9	2	659	15	-16	
1	218	6	0	8 253	6	9	8	40	16	9*	3	707	16	-8	
2	233	7	4	9 189	6	-5	9	20	41	11*	4	465	10	-11	
												-2	608	13	-34

STRUCTURE FACTORS CONTINUED FOR  
NA3(UO2)2F7.6H2O

PAGE 6

L	FOB	SG	DEL	L	FOB	SG	DEL	L	FOB	SG	DEL	L	FOB	SG	DEL	
-1	560	12	7*	-5	391	9	-5	-3	413	9	6	0	184	8	-12	5 165 6 2
0	345	7	18	-4	428	10	-14	-2	350	8	-7	1	190	10	3	6 99 7 -1
1	358	8	-1	-3	441	10	-8	-1	316	7	-5	2	200	8	-2	7 71 10 -15
2	343	8	0	-2	528	12	13	0	317	7	-7	3	229	9	16	8 62 13 -22*
3	309	7	6	-1	342	8	9	1	313	8	-10	4	204	12	3	H,K= 4, -6
4	230	6	-1	0	437	11	9	2	259	6	5	5	194	6	10	-6 216 9 6
5	137	8	-2	1	432	10	11	3	205	8	-4	H,K=	4,-10	-5	245 8 12	
6	149	5	3	2	331	7	12	4	192	6	0	-2	157	6	-3	-4 268 9 6
7	123	7	9	3	243	7	4	H,K=	3,	10	-1	167	6	-4	-3 331 7 -4	
8	81	12	-2	4	216	8	7	-10	69	12	1	0	176	7	-5	-2 391 8 -3
	H,K=	3,	4	5	189	6	1	-9	76	10	-10	1	180	7	-4	-1 354 8 1
-11	145	7	7	6	156	8	7	-8	109	6	1	2	196	9	-5	0 373 8 11
-10	169	6	6	H,K=	3,	7	-7	128	6	0	3	206	9	17	1 433 9 7	
-9	209	5	3	-11	136	6	-1	-6	109	13	-2	4	165	9	4	2 433 9 -3
-8	260	6	1	-10	200	7	9	-5	135	6	4	5	169	7	3	3 359 8 -3
-7	281	6	-4	-9	225	6	-0	-4	163	11	4	6	169	6	3	4 338 8 -1
-6	374	8	-12	-8	235	6	5	-3	185	6	3	7	132	11	-7	5 311 8 -5
-5	455	10	-10	-7	348	7	0	-2	148	5	-0	H,K=	4,	-9	6 285 6 -1	
-4	315	7	-5	-6	408	9	-10	-1	132	5	2	-4	146	8	3	7 235 6 0
-3	429	10	-14	-5	462	10	-6	0	127	8	-10	-3	155	11	-8	8 204 6 -3
-2	579	13	-9	-4	419	9	-1	1	126	11	-6	-2	189	9	-5	9 159 7 -1
-1	549	12	3	-3	507	11	-5	2	94	11	-11	-1	200	6	-5	H,K= 4, -5
0	430	9	16	-2	567	13	4	3	89	11	5	0	201	7	-5	-7 74 14 5*
1	360	8	9	-1	511	11	-4	H,K=	3,	11	1	221	10	-4	-6 99 16 8	
2	428	10	0	0	427	10	-4	-9	229	6	10	2	267	6	14	-5 104 8 13
3	385	8	4	1	431	9	18	-8	271	8	14	3	227	6	7	-4 107 8 5
4	262	6	5	2	337	8	10	-7	303	7	5	4	197	6	5	-3 197 5 10
5	247	7	7	3	306	7	13	-6	350	8	16	5	189	7	1	-2 196 5 -3
6	197	6	0	4	260	7	12	-5	344	8	5	6	190	6	5	-1 169 5 5
7	151	6	5	5	191	8	0	-4	377	8	8	7	151	8	3	0 202 5 6
	H,K=	3,	5	6	135	14	-4	-3	343	8	-3	H,K=	4,	-8	1 205 5 1	
-11	81	10	-9	H,K=	3,	8	-2	326	8	-8	-5	197	6	-4	2 238 6 -1	
-10	141	8	4	-11	111	13	10	-1	325	7	-13	-4	212	10	-7	3 196 5 -2
-9	195	5	3	-10	145	9	9	0	299	7	-13	-3	239	8	-10	4 119 4 -7
-8	232	6	3	-9	148	6	-0	1	241	6	-10	-2	298	7	-8	5 131 4 -3
-7	222	5	-2	-8	149	5	-4	2	206	9	-13	-1	345	8	-4	6 105 5 1
-6	281	6	-4	-7	225	5	2	H,K=	3,	12	0	355	8	-3	7 87 7 3	
-5	329	7	-2	-6	261	7	0	-9	25	42	-8*	1	380	9	9	8 78 10 5
-4	401	9	-15	-5	279	6	1	-8	33	40	-4*	2	360	8	4	9 56 13 18*
-3	365	8	9	-4	246	6	3	-7	53	22	11*	3	362	8	1	H,K= 4, -6
-2	405	9	19	-3	279	7	11	-6	72	24	14*	4	328	8	4	-8 166 10 -7
-1	312	7	5	-2	297	7	1	-5	61	21	-1*	5	307	7	-4	-7 223 7 2
0	335	8	14	-1	275	6	-2	-4	27	40	-29*	6	263	8	8	-6 290 9 -1
1	359	8	12	0	220	6	-7	-3	53	23	14*	7	206	11	3	-5 355 8 13
2	307	7	6	1	205	7	-2	-2	57	13	4*	8	177	6	-7	-4 407 9 13
3	183	5	1	2	162	7	3	-1	44	20	-7*	H,K=	4,	-7	-3 491 11 18	
4	194	7	3	3	158	6	5	0	31	41	-14*	-6	94	24	-6*	-2 515 12 9
5	190	6	5	4	154	7	17	1	52	22	22*	-5	121	11	-1	-1 509 11 8
6	144	6	-1	5	94	13	-1	H,K=	3,	13	-4	113	9	-12	0 658 15 -14	
7	118	11	17	H,K=	3,	9	-7	272	8	5	-3	141	10	-4	1 624 14 3	
	H,K=	3,	6	-10	184	6	-3	-6	270	7	7	-2	155	7	-1	2 495 11 -5
-11	105	16	-6	-9	224	7	3	-5	281	10	1	-1	198	6	-0	3 483 11 -6
-10	172	9	7	-8	257	6	1	-4	285	7	-7	0	188	5	3	4 497 11 -9
-9	207	5	3	-7	320	7	1	-3	272	7	-10	1	188	6	7	5 419 9 -5
-8	267	6	-2	-6	320	7	5	-2	244	6	-16	2	175	5	5	6 324 7 -0
-7	264	6	2	-5	321	7	5	-1	230	7	-15	3	151	5	-2	7 258 7 -2
-6	312	7	-12	-4	409	9	11	H,K=	4,-11	4	152	5	2	8	243	6 3

STRUCTURE FACTORS CONTINUED FOR  
NA3(U02)2F7.6H20

PAGE 7

L	F08	SG	DEL	L	F08	SG	DEL	L	F08	SG	DEL	L	F08	SG	DEL
9	178	9	-1	7	39	16	18*	3	453	10	-2	-1	353	8	23
H,K=	4,	-3		8	41	45	21*	4	319	7	-4	0	272	6	10
-8	44	29	29*	9	46	37	18*	5	243	7	-2	1	252	6	4
-7	33	39	28*	H,K=	4,	0		6	241	6	-2	2	284	8	7
-6	24	59	5*-10	174	10	9		7	182	6	-0	3	246	6	7
-5	42	16	2*-9	212	7	1		8	132	8	-3	4	207	6	-1
-4	59	10	-2	-8	291	7	1	H,K=	4,	3	5	174	7	-0	
-3	12	35	-8*	-7	343	8	-1	-11	56	17	-12*	6	140	12	-6
-2	40	42	4*	-6	360	8	-2	-10	61	15	-17*	H,K=	4,	6	
-1	46	11	18*	-5	495	10	-9	-9	149	9	2	-11	105	15	-5
0	151	5	-7	-4	704	15	2	-8	154	5	1	-10	152	7	1
1	70	5	1	-3	595	13	2	-7	150	4	-4	-9	185	6	5
2	23	31	2*	-2	606	13	11	-6	163	4	-7	-8	164	5	-5
3	37	21	19*	-1	756	17	-1	-5	255	5	-8	-7	238	6	-8
4	63	5	-2	0	798	17	14	-4	290	6	-2	-6	316	7	-5
5	37	11	-7*	1	668	15	3	-3	320	7	-15	-5	297	7	-7
6	0	29	-24*	2	519	12	-7	-2	199	5	21	-4	284	7	-3
7	21	45	12*	3	481	11	-11	-1	373	8	16	-3	305	7	6
8	55	22	40*	4	442	10	-6	0	276	7	6	-2	384	9	7
9	24	56	16*	5	328	7	-5	1	312	8	8	-1	379	9	7
H,K=	4,	-2	6	303	7	-1	2	284	7	7	0	263	6	11	
-9	160	8	4	7	233	6	-2	3	180	6	-1	1	268	6	1
-8	216	6	2	8	164	7	4	4	162	4	3	2	245	6	7
-7	315	8	1	H,K=	4,	1	5	193	6	2	3	188	7	-4	
-6	310	7	-2	-10	40	27	-12*	6	134	6	1	4	195	6	10
-5	363	8	5	-9	75	8	14	7	100	14	-1	5	143	13	5
-4	423	9	11	-8	71	8	-6	H,K=	4,	4	6	90	11	-9	
-3	546	12	21	-7	131	5	5	-11	119	10	1	H,K=	4,	7	
-2	573	13	38	-6	152	7	1	-10	161	6	3	-11	138	7	4
-1	511	11	19	-5	105	4	3	-9	233	6	-4	-10	183	6	-0
0	495	11	-0	-4	181	4	0	-8	261	6	-5	-9	233	6	-1
1	545	12	4	-3	124	3	-3	-7	302	7	-6	-8	267	6	-4
2	378	8	-5	-2	250	5	3	-6	303	6	-8	-7	307	7	1
3	502	11	-16	-1	328	8	4	-5	459	10	-25	-6	368	8	-2
4	390	9	-3	0	121	4	2	-4	493	11	-15	-5	341	7	-1
5	276	6	-5	1	159	4	-0	-3	478	11	-17	-4	433	9	-7
6	279	6	-3	2	261	6	-3	-2	559	13	14	-3	478	10	8
7	262	6	-4	3	199	5	1	-1	544	13	20	-2	412	9	2
8	195	6	-1	4	184	5	1	0	444	10	12	-1	350	8	6
9	148	7	2	5	108	5	3	1	546	12	1	0	363	9	4
H,K=	4,	-1	6	103	6	-3	2	408	9	11	1	367	8	8	
-9	52	41	22*	7	111	15	3	3	306	7	2	2	296	8	2
-8	34	50	-1*	8	44	48	-26*	4	258	6	-0	3	204	7	-5
-7	18	35	-13*	H,K=	4,	2	5	248	7	7	4	201	8	-1	
-6	40	13	4*-10	176	9	6	6	200	8	4	5	173	7	-0	
-5	73	10	1	-9	203	7	-3	7	135	12	5	H,K=	4,	8	
-4	142	4	1	-8	295	6	3	H,K=	4,	5	-11	81	10	-2	
-3	26	18	-6*	-7	335	8	-6	-11	113	10	3	-10	105	9	-10
-2	70	9	9	-6	416	9	-5	-10	152	6	6	-9	138	6	0
-1	65	5	13	-5	487	10	-13	-9	170	5	-6	-8	170	5	-2
0	139	4	-2	-4	544	11	-4	-8	180	5	-2	-7	178	5	-4
1	100	3	-1	-3	494	11	-6	-7	217	5	-0	-6	201	5	1
2	30	15	4*	-2	711	15	-42	-6	310	7	-12	-5	174	5	3
3	29	11	11*	-1	677	15	-36	-5	281	6	-8	-4	252	6	6
4	76	6	4	0	555	13	-8	-4	232	6	2	-3	255	7	10
5	44	17	-3*	1	428	9	4	-3	259	7	2	-2	202	6	-1
6	39	13	-6*	2	528	12	2	-2	401	9	25	-1	156	6	2
													-3	45	57
													-2*		

STRUCTURE FACTORS CONTINUED FOR  
NA3(UO2)2F7.6H2O

PAGE 8

L	FOB	SG	DEL	L	FOB	SG	DEL	L	FOB	SG	DEL	L	FOB	SG	DEL
-2	39	61	10*	6	117	7	10	-5	0	47	-16*	-6	310	7	-2
-1	12	39	-9*	7	83	13	6	-4	31	45	12*	-5	364	8	-2
0	26	41	12*	H,K=	5,	-6	-3	59	11	11	-4	399	8	-3	
	H,K=	4,	13	-6	204	10	0	-2	76	9	5	-3	472	10	6
-7	216	7	-11	-5	252	8	6	-1	42	12	14*	-2	477	10	27
-6	257	7	11	-4	253	6	-8	0	26	27	7*	-1	596	13	-12
-5	250	7	-13	-3	298	7	-4	1	25	16	24*	0	466	11	2
-4	253	6	-8	-2	324	7	-6	2	17	37	-3*	1	388	9	-9
-3	232	6	-4	-1	346	8	-5	3	18	31	7*	2	446	10	-9
-2	218	8	-15	0	381	9	16	4	5	32	-9*	3	463	10	-7
	H,K=	5,-11	1	401	8	6	5	50	9	11	4	321	7	-8	
2	207	7	8	2	334	7	2	6	31	34	15*	5	270	6	1
3	200	7	2	3	313	7	-5	7	20	43	17*	6	231	7	-9
	H,K=	5,-10	4	326	7	-3	8	43	20	34*	7	224	7	5	
-1	171	7	-6	5	310	7	-0	H,K=	5,	-2	8	154	6	2	
0	175	8	-7	6	229	8	-5	-9	161	13	-2	H,K=	5,	1	
1	190	9	8	7	204	6	1	-8	213	6	9	-10	70	19	14*
2	199	7	9	8	183	6	-0	-7	263	6	6	-9	78	13	-7
3	197	6	1	H,K=	5,	-5	-6	294	7	4	-8	125	5	-1	
4	204	6	11	-7	60	20	17*	-5	326	8	5	-7	89	7	2
5	179	7	2	-6	57	20	9*	-4	479	10	16	-6	134	6	3
	H,K=	5,	-9	-5	73	17	-0*	-3	463	10	27	-5	180	4	2
-3	111	13	-10	-4	54	34	-17*	-2	393	9	19	-4	233	5	-0
-2	137	8	-9	-3	69	9	6	-1	495	11	4	-3	224	5	-4
-1	166	11	-1	-2	59	12	-2*	0	569	13	5	-2	160	4	-11
0	169	6	-0	-1	81	7	9	1	478	11	-13	-1	200	5	8
1	164	7	1	0	86	7	9	2	421	9	-7	0	331	8	-1
2	186	6	16	1	106	6	9	3	378	8	-10	1	196	5	0
3	167	11	1	2	23	27	6*	4	418	9	-10	2	218	6	-8
4	168	6	11	3	49	13	12*	5	331	7	-1	3	159	4	0
5	159	7	9	4	51	16	-4*	6	267	6	-2	4	128	4	-4
6	134	6	2	5	41	14	-7*	7	242	6	-1	5	155	5	1
	H,K=	5,	-8	6	36	24	10*	8	182	7	2	6	116	7	-3
-4	173	8	-13	7	25	34	9*	H,K=	5,	-1	7	75	25	0*	5
-3	214	7	-3	8	50	32	30*	-9	62	51	30*	8	77	28	11*
-2	255	7	-1	H,K=	5,	-4	-8	48	17	10*	H,K=	5,	2	H,K=	5,
-1	259	6	-1	-8	173	12	13	-7	78	10	9	-10	137	7	-14
0	250	6	-1	-7	237	7	7	-6	80	7	0	-9	215	8	-7
1	295	8	6	-6	279	8	8	-5	42	14	-18*	-8	270	6	-4
2	314	7	10	-5	290	8	14	-4	41	18	-7*	-7	269	6	-3
3	263	7	-1	-4	368	8	15	-3	130	5	3	-6	300	6	-8
4	246	6	3	-3	447	10	15	-2	110	6	18	-5	396	8	-6
5	232	10	-1	-2	489	10	-2	-1	160	4	0	-4	475	10	-18
6	218	7	2	-1	471	10	17	0	45	9	1*	-3	380	8	-7
7	188	6	5	0	475	11	-3	1	58	7	-3	-2	407	9	14
	H,K=	5,	-7	1	512	11	-13	2	122	4	-3	-1	465	11	13
-5	82	12	-7	2	471	10	-10	3	128	4	-0	0	412	10	9
-4	114	15	20	3	418	10	-14	4	68	6	-0	1	390	9	-3
-3	120	7	-3	4	409	9	-12	5	66	7	-1	2	380	8	-5
-2	149	6	-0	5	304	7	-10	6	59	13	6*	3	287	8	1
-1	112	6	-0	6	274	7	-3	7	70	12	2	4	244	6	-9
0	120	7	-1	7	253	6	-2	8	57	19	9*	5	242	6	-2
1	147	6	7	8	203	6	3	H,K=	5,	0	6	205	6	-6	
2	150	6	-1	H,K=	5,	-3	-10	136	7	-3	7	147	7	-2	
3	123	5	-4	-8	0	51	-15*	-9	173	6	-1	H,K=	5,	3	
4	111	9	10	-7	41	61	9*	-8	231	6	2	-10	121	10	10
5	104	7	3	-6	42	62	11*	-7	296	7	-3	-9	129	6	-7

STRUCTURE FACTORS CONTINUED FOR  
NA3(UO2)2F7.6H2O

PAGE 9

L	FOB	SG	DEL	L	FOB	SG	DEL	L	FOB	SG	DEL	L	FOB	SG	DEL
-9	176	7	-3	-3	364	8	-1	0	123	10	-2	5	0	40	-24*
-8	195	6	0	-2	331	7	-2	1	147	15	3	6	32	34	8*
-7	213	6	-4	-1	275	6	-8	2	157	13	8	7	46	35	13*
-6	235	6	-4	0	308	7	-0	3	135	8	-0	H,K=	6,	-4	-3
-5	269	6	-3	1	282	7	-1	4	118	7	5	-7	216	9	-4
-4	272	6	-1	2	238	7	8	5	112	14	-1	-6	279	7	18
-3	381	8	7	3	193	7	-11	H,K=	6,	-8	-5	313	8	14	0
-2	281	8	10	H,K=	5,	10	-3	207	6	-5	-4	376	9	17	1
-1	252	6	10	-10	76	10	31	-2	238	6	-11	-3	432	9	5
0	269	6	10	-9	47	19	-2*	-1	268	8	-4	-2	386	8	-3
1	271	7	3	-8	77	14	-0	0	291	7	3	-1	457	11	8
2	222	7	4	-7	64	12	-3*	1	298	7	7	0	497	10	-4
3	157	7	-1	-6	62	21	-6*	2	300	7	6	1	474	10	0
4	136	7	3	-5	44	49	-3*	3	266	6	-3	2	387	8	-8
5	147	7	11	-4	82	18	4*	4	269	6	1	3	372	9	-1
H,K=	5,	7	-3	82	15	-3	5	263	6	9	4	355	8	-7	H,K=
-11	154	9	7	-2	58	12	-4*	6	218	6	7	5	319	7	-3
-10	206	6	6	-1	38	59	-5*	H,K=	6,	-7	6	234	7	1	-7
-9	214	5	3	0	73	9	20	-5	0	45	-66*	7	213	9	3
-8	246	6	3	1	38	52	-11*	-4	77	11	3	H,K=	6,	-3	-5
-7	292	6	-4	2	61	22	13*	-3	54	16	-18*	-8	0	57	-19*
-6	382	8	-7	H,K=	5,	11	-2	99	11	9	-7	0	45	-29*	-3
-5	388	8	1	-9	233	8	-5	-1	105	9	3	-6	73	14	27*
-4	358	8	-3	-8	278	7	8	0	110	16	2	-5	46	45	8*
-3	429	11	13	-7	314	8	-0	1	121	10	3	-4	55	15	4*
-2	442	10	1	-6	336	8	10	2	111	10	6	-3	89	9	10
-1	389	10	-1	-5	381	9	16	3	84	10	-6	-2	135	9	4
0	402	9	10	-4	354	8	-12	4	122	7	8	-1	100	9	5
1	331	10	7	-3	337	8	-6	5	102	11	3	0	96	6	5
2	278	7	1	-2	308	7	-15	6	82	9	6	1	83	9	12
3	255	7	2	-1	320	7	-7	H,K=	6,	-6	2	111	6	-4	6
4	230	6	11	0	279	7	-12	-6	194	10	8	3	92	5	-3
5	165	13	-6	1	223	8	-15	-5	193	7	-4	4	53	10	-6*
H,K=	5,	8	H,K=	5,	12	-4	224	6	1	5	35	40	4*-10	85	13
-10	100	7	9	-8	0	45	-7*	-3	278	7	-1	6	47	15	2*
-9	92	16	-2	-7	32	41	21*	-2	307	7	-2	7	69	9	36
-8	92	9	3	-6	40	48	33*	-1	297	8	2	H,K=	6,	-2	-7
-7	110	10	-5	-5	35	39	33*	0	310	7	9	-8	202	6	3
-6	154	7	0	-4	39	55	18*	1	341	8	3	-7	261	8	9
-5	150	5	5	-3	38	49	15*	2	342	8	2	-6	293	8	6
-4	118	6	-1	-2	19	38	-3*	3	302	7	1	-5	308	7	7
-3	128	6	-6	-1	0	38	-12*	4	290	7	2	-4	378	8	15
-2	142	5	-2	0	54	19	46*	5	260	7	-4	-3	459	10	31
-1	150	5	-1	H,K=	5,	13	6	224	6	1	-2	450	10	12	0
0	135	8	-6	-7	241	7	9	7	203	7	2	-1	437	9	-6
1	120	6	10	-6	225	8	-7	H,K=	6,	-5	0	482	11	-8	2
2	97	13	5	-5	239	7	-7	-6	26	48	-9*	1	380	8	-4
3	107	11	11	-4	256	7	4	-5	42	53	25*	2	399	9	-17
4	47	61	-39*	-3	227	6	-18	-4	35	41	8*	3	412	9	-11
H,K=	5,	9	-2	227	8	-9	-3	55	13	12*	4	331	7	-4	6
-10	199	7	7	H,K=	6,	-10	-2	56	21	7*	5	260	6	-1	7
-9	207	6	2	1	199	7	-5	-1	28	35	-4*	6	239	6	2
-8	270	6	4	2	229	7	10	0	36	20	18*	7	209	6	-1
-7	295	7	-4	3	214	9	6	1	28	39	-3*	H,K=	6,	-1	-9
-6	300	7	9	H,K=	6,	-9	2	68	8	7	-9	61	18	21*	-8
-5	296	7	1	-2	121	17	-10	3	34	37	2*	-8	73	25	15*
-4	360	8	9	-1	126	8	-7	4	42	20	5*	-7	39	23	-12*

STRUCTURE FACTORS CONTINUED FOR  
NA3(U02)2F7.6H2O

PAGE10

L	F08	SG	DEL	L	F08	SG	DEL	L	F08	SG	DEL	L	F08	SG	DEL	
-5	328	7	-13	-3	432	9	10	H,K=	6,	9	-1	243	8	3	6 207 7 2	
-4	255	6	-4	-2	520	12	12	-10	214	6	6	0 242	7	4	H,K= 7, -3	
-3	313	7	-12	-1	466	10	17	-9	230	8	7	1 264	7	3	-7 29 44 10*	
-2	396	11	24	0	399	9	8	-8	251	7	-1	2 262	7	2	-6 19 42 5*	
-1	441	9	5	1	355	8	0	-7	300	7	-7	3 242	7	4	-5 46 59 12*	
0	318	7	0	2	305	8	2	-6	350	8	5	4 222	6	9	-4 43 50 7*	
1	293	6	6	3	268	7	7	-5	355	8	5	H,K=	7,	-7	-3 20 52 3*	
2	329	7	-7	4	219	7	-6	-4	400	9	14	-4 63	34	-10*	-2 28 44 13*	
3	319	7	-4	5	183	10	8	-3	360	8	-3	-3 90	19	-14*	-1 0 33 -13*	
4	219	6	-5	H,K=	6,	6	-2	345	8	-8	-2 121	7	9	0 26 42 10*		
5	207	8	-1	-10	135	11	5	-1	352	8	-7	-1 116	14	5	1 12 32 -11*	
6	178	5	5	-9	121	6	-7	0	326	8	-5	0 101	16	-6	2 24 33 3*	
7	129	12	-6	-8	139	5	-3	1	269	7	-5	1 118	15	-1	3 1 30 -15*	
H,K=	6,	3	-7	163	5	-3	2	233	7	4	2 131	7	7	4 38 16 25*		
-10	115	13	-0	-6	222	5	-4	3	210	9	5	3 110	7	5	5 23 39 4*	
-9	158	5	2	-5	214	6	-3	H,K=	6,	10	4	85	11	5	6 0 39 -17*	
-8	195	5	-2	-4	187	6	5	-9	37	38	6*	5 84	9	4	H,K= 7, -2	
-7	189	5	-5	-3	187	8	10	-8	36	44	9*	H,K=	7,	-6	-8 191 7 -6	
-6	221	5	-5	-2	254	6	6	-7	17	38	-17*	-5 221	8	1	-7 248 9 7	
-5	265	6	-11	-1	210	7	14	-6	22	43	-20*	-4 246	7	-5	-6 252 7 4	
-4	331	7	-12	0	193	6	4	-5	74	11	19	-3 290	8	-0	-5 326 8 4	
-3	288	6	-0	1	166	7	1	-4	44	22	6*	-2 308	7	-7	-4 405 9 18	
-2	360	8	34	2	133	15	-3	-3	21	37	-6*	-1 327	8	4	-3 419 10 27	
-1	278	7	10	3	127	9	-7	-2	40	48	2*	0 375	8	8	-2 379 9 12	
0	274	6	0	4	130	8	7	-1	62	14	18*	1 356	8	-7	-1 417 9 -2	
1	300	6	3	5	90	10	-0	0	26	38	-18*	2 338	8	7	0 431 10 -14	
2	256	6	1	H,K=	6,	7	1	0	42	-28*	3 302	7	-3	1 411 9 -11		
3	174	7	1	-10	184	8	1	2	0	53	-20*	4 305	7	1	2 316 7 -15	
4	165	5	-4	-9	231	6	4	H,K=	6,	11	5 273	6	3	3 330 7 -11		
5	156	7	2	-8	246	6	-7	-9	218	6	1	6 218	7	0	4 296 8 -3	
6	128	7	-6	-7	330	7	-3	-8	276	7	6	H,K=	7,	-5	5 235 6 -9	
H,K=	6,	4	-6	309	7	-10	-7	309	7	15	-6	71	20	57*	6 215 7 1	
-10	131	6	-7	-5	349	7	-1	-6	308	8	17	-5	53	54	34*	H,K= 7, -1
-9	194	6	8	-4	404	9	8	-5	301	8	3	-4	29	52	6*	-8 89 10 19
-8	234	6	-5	-3	448	11	9	-4	327	7	-2	-3	19	43	1*	-7 100 19 -2*
-7	227	6	-4	-2	386	9	-2	-3	304	7	-11	-2	0	41	-10*	-6 131 6 8
-6	269	6	-13	-1	344	8	7	-2	280	7	-8	-1	16	47	5*	-5 126 10 8
-5	348	8	-9	0	334	7	7	-1	262	6	-5	0	47	15	6*	-4 168 5 11
-4	360	8	-6	1	356	8	11	0	230	6	-13	1	23	34	-1*	-3 156 8 13
-3	412	9	-1	2	264	8	5	H,K=	6,	12	2	0	37	-9*	-2 224 6 7	
-2	445	10	19	3	218	6	4	-8	24	48	20*	3	25	46	19*	-1 201 5 -7
-1	340	7	12	4	203	6	13	-7	30	45	26*	4	0	35	-19*	0 153 5 -8
0	376	8	2	H,K=	6,	8	-6	29	44	17*	5	12	49	-12*	1 149 5 -2	
1	362	8	0	-10	90	22	12*	-5	44	45	23*	6	24	37	15*	2 170 4 -1
2	305	7	1	-9	104	7	1	-4	38	61	33*	H,K=	7,	-4	3 140 5 -7	
3	231	6	0	-8	131	6	5	-3	16	49	12*	-6	236	12	11	4 138 5 7
4	179	5	-2	-7	155	5	-6	-2	0	39	-5*	-5	252	7	10	5 75 9 -4
5	182	6	3	-6	139	7	-2	-1	4	52	-6*	-4	280	7	3	6 84 13 4
6	139	12	-3	-5	175	6	6	H,K=	6,	13	-3	337	8	3	H,K= 7, 0	
H,K=	6,	5	-4	200	6	9	-6	245	9	0	-2	352	8	-1	-9 162 11 0	
-10	187	7	8	-3	235	6	4	-5	263	7	-5	-1	333	7	2	-8 223 9 1
-9	199	5	-6	-2	185	5	0	-4	245	7	-15	0	357	8	-3	-7 257 9 -6
-8	226	7	-2	-1	162	6	6	H,K=	7,	-9	1	346	9	-2	-6 299 7 -5	
-7	287	6	-8	0	153	8	-1	1	98	11	7	2	309	7	-7	-5 350 7 -4
-6	376	8	-12	1	156	7	1	2	94	11	3	3	318	7	-7	-4 395 9 5
-5	407	9	-8	2	129	7	13	H,K=	7,	-8	4	286	8	2	-3 400 9 24	
-4	384	9	-5	3	84	30	-6*	-2	230	6	-7	5	221	6	-6	-2 438 9 -16

0 0 0 0 4 7 1 0 9 5 7

**STRUCTURE FACTORS CONTINUED FOR  
Na<sub>3</sub>(UO<sub>2</sub>)<sub>2</sub>F<sub>7.6</sub>H<sub>2</sub>O**

PAGE11

L	FOB	SG	DEL	L	FOB	SG	DEL	L	FOB	SG	DEL	L	FOB	SG	DEL
-1	448	10	-12	4	180	5	1	-6	355	8	-0	-2	245	8	-4
0	381	8	-16	5	160	7	6	-5	328	8	-7	-1	242	7	-8
1	312	7	-11	H,K=	7,	4	-4	349	8	6	H,K=	7,	12	1	39
2	341	7	-4	-10	122	7	-8	-3	360	9	4	-7	0	53	-12*
3	315	7	-9	-9	166	6	3	-2	337	9	5	-6	24	56	17*
4	243	6	-6	-8	149	6	-10	-1	347	8	13	-5	0	53	-9*
5	179	7	-9	-7	219	5	-7	0	321	8	8	-4	12	60	3*
6	177	6	-3	-6	264	6	-4	1	257	6	-3	-3	11	43	-1*
H,K=	7,	1	-5	300	6	-13	2	222	7	-2	-2	32	40	16*	-7
-9	101	12	-1	-4	272	6	0	3	202	7	5	H,K=	8,	-7	-6
-8	127	8	7	-3	302	9	12	H,K=	7,	8	-2	38	54	-14*	-5
-7	123	7	-2	-2	369	8	17	-10	82	15	-4	-1	64	41	15*
-6	125	5	-10	-1	365	9	14	-9	82	9	-4	0	57	30	-2*
-5	170	5	-2	0	252	6	6	-8	105	8	16	1	45	27	-12*
-4	229	6	3	1	262	6	-1	-7	117	6	6	2	11	63	-29*
-3	202	5	-1	2	223	6	6	-6	154	6	9	3	28	51	-8*
-2	171	4	-1	3	193	6	4	-5	144	7	6	H,K=	8,	-6	1
-1	216	6	-2	4	166	6	1	-4	155	13	15	-4	198	8	-9
0	192	6	-2	5	118	8	-10	-3	112	7	-3	-3	237	8	-11
1	204	5	-6	H,K=	7,	5	-2	134	10	9	-2	272	8	4	
2	190	5	-5	-10	148	6	-5	-1	124	8	2	-1	263	10	2
3	127	5	-7	-9	199	6	5	0	121	7	14	0	271	7	8
4	134	6	2	-8	215	8	-8	1	61	17	-16*	1	285	7	-4
5	134	8	3	-7	234	5	-10	2	72	55	14*	2	259	7	1
6	99	8	-6	-6	286	6	-2	3	50	57	-6*	3	238	6	-4
H,K=	7,	2	-5	262	6	-8	H,K=	7,	9	4	220	8	-5	-5	
-9	184	6	2	-4	329	7	-3	-9	222	7	2	H,K=	8,	-5	-4
-8	227	6	-6	-3	364	9	21	-8	267	6	3	-5	48	26	39*
-7	239	6	-3	-2	351	9	27	-7	304	7	-6	-4	24	48	21*
-6	256	6	-12	-1	275	7	9	-6	298	8	-3	-3	37	49	23*
-5	352	8	-6	0	274	6	2	-5	326	8	13	-2	45	50	32*
-4	391	8	-12	1	283	7	-2	-4	348	8	5	-1	39	42	38*
-3	367	8	-7	2	243	7	-2	-3	361	9	-7	0	46	18	28*
-2	428	10	5	3	174	6	-2	-2	300	7	-8	1	9	35	3*
-1	389	8	5	4	170	7	1	-1	282	8	-8	2	37	40	26*
0	375	8	-0	5	157	10	8	0	276	8	-0	3	20	43	17*
1	373	8	-6	H,K=	7,	6	1	244	7	2	4	46	16	32*	H,K=
2	325	8	-2	-10	95	12	-2	2	204	7	-2	'5	36	42	19*
3	250	6	-8	-9	113	10	-8	H,K=	7,	10	H,K=	8,	-4	-7	215
4	206	5	-6	-8	132	7	-6	-9	45	50	13*	-6	205	8	1
5	192	7	1	-7	150	7	-6	-8	0	51	-33*	-5	226	8	-2
6	162	6	-5	-6	163	5	1	-7	64	25	14*	-4	286	10	-1
H,K=	7,	3	-5	146	8	-2	-6	24	48	-3*	-3	295	9	-2	
-10	107	13	-8	-4	198	7	-0	-5	0	54	-21*	-2	298	7	1
-9	161	10	10	-3	235	6	26	-4	53	22	19*	-1	315	8	-0
-8	149	5	-2	-2	196	7	10	-3	48	52	5*	0	350	8	2
-7	190	6	-7	-1	148	6	0	-2	0	40	-25*	1	323	7	-9
-6	239	5	-11	0	165	7	11	-1	26	39	7*	2	284	7	-5
-5	266	6	-10	1	172	6	-1	0	24	45	12*	3	260	7	-5
-4	220	6	-11	2	154	8	11	1	38	42	17*	4	276	7	7
-3	277	8	6	3	97	26	-1*	H,K=	7,	11	5	206	6	-12	
-2	327	8	16	4	102	20	8*	-8	239	7	1	H,K=	8,	-3	H,K=
-1	347	9	8	H,K=	7,	7	-7	255	8	7	-6	26	44	-6*	-9
0	251	7	0	-10	190	7	-9	-6	274	7	5	-5	22	52	-1*
1	243	6	-1	-9	223	6	1	-5	294	7	7	-4	45	58	24*
2	245	6	1	-8	234	6	-3	-4	283	8	-6	-3	0	42	-34*
3	217	5	0	-7	281	9	-9	-3	255	7	-6	-2	51	33	13*

STRUCTURE FACTORS CONTINUED FOR  
NA3(UO2)2F7.6H2O

PAGE12

L	FOB	SG	DEL	L	FOB	SG	DEL	L	FOB	SG	DEL	L	FOB	SG	DEL				
-4	185	5	1	H,K=	8,	5	-8	241	6	3	3	68	12	-3	-6	173	8	-7	
-3	208	6	16	-9	162	6	-15	-7	265	7	-1	4	77	15	12*	-5	227	6	-1
-2	236	5	-7	-8	188	5	5	-6	283	10	0	H,K=	9,	-2	-4	212	6	-12	
-1	223	5	-6	-7	216	6	-10	-5	326	8	21	-6	204	8	1	-3	264	7	6
0	217	6	4	-6	272	6	-8	-4	315	10	6	-5	251	11	9	-2	245	6	-0
1	153	5	-8	-5	295	7	-3	-3	277	7	-11	-4	317	9	24	-1	236	7	1
2	186	5	-6	-4	263	6	5	-2	267	8	-7	-3	301	9	6	0	224	9	-6
3	172	6	-3	-3	330	9	20	-1	271	9	-1	-2	289	7	-1	1	226	6	-3
4	137	6	-0	-2	332	9	21	0	255	7	-2	-1	298	7	-11	2	205	6	-3
5	122	7	5	-1	318	7	14	1	212	14	2	0	327	7	-5	3	169	10	-1
H,K=	8,	2	0	296	8	10	H,K=	8,	10	1	286	6	-2	4	128	8	-3		
-9	156	8	5	1	254	7	-2	-8	51	20	42*	2	263	6	-7	H,K=	9,	3	
-8	169	6	-1	2	222	9	1	-7	61	22	37*	3	241	7	-4	-8	172	10	-6
-7	186	6	-4	3	203	8	-0	-6	44	38	35*	4	211	8	1	-7	198	8	-11
-6	244	6	-8	4	167	12	-9	-5	54	21	41*	H,K=	9,	-1	-6	266	6	-4	
-5	245	6	-9	H,K=	8,	6	-4	26	59	4*	-7	98	18	-1*	-5	280	8	-10	
-4	242	6	-14	-9	100	10	4	-3	51	59	22*	-6	119	9	4	-4	285	7	-2
-3	260	7	22	-8	68	19	-14*	-2	12	41	-15*	-5	160	11	17	-3	307	8	18
-2	296	7	-0	-7	109	9	-2	-1	0	56	-15*	-4	143	12	5	-2	355	8	14
-1	303	7	-3	-6	135	5	-4	0	42	54	36*	-3	164	7	6	-1	307	10	-0
0	231	7	-3	-5	150	6	4	H,K=	8,	11	-2	184	8	-5	0	276	7	-2	
1	206	5	-1	-4	115	8	3	-7	249	8	4	-1	190	6	-1	1	251	6	3
2	231	5	-1	-3	153	8	15	-6	244	11	9	0	165	5	-5	2	221	6	-1
3	185	5	-2	-2	141	13	10	-5	254	15	2	1	158	5	1	3	188	8	-2
4	159	6	-2	-1	136	11	-8	-4	257	7	0	2	140	5	-9	H,K=	9,	4	
5	138	10	4	0	125	7	-2	-3	245	11	-8	3	150	6	-4	-9	111	12	9
H,K=	8,	3	1	120	11	13	-2	229	6	-7	4	115	7	-1	-8	107	9	-5	
-9	146	6	-2	2	99	18	11	H,K=	9,	-6	H,K=	9,	0	0	-7	113	9	-6	
-8	181	6	6	3	81	12	-5	-1	227	7	3	-7	173	8	5	-6	155	5	-5
-7	184	5	-1	H,K=	8,	7	0	248	7	9	-6	196	8	-3	-5	160	6	-2	
-6	203	7	-14	-9	173	6	-8	1	236	8	-3	-5	229	7	-1	-4	129	12	-6
-5	251	6	-7	-8	232	9	-0	H,K=	9,	-5	-4	242	7	13	-3	146	9	9	
-4	269	6	-6	-7	252	7	-6	-3	0	61	-40*	-3	249	7	9	-2	183	10	9
-3	352	8	37	-6	261	7	-9	-2	42	54	-9*	-2	257	8	-12	-1	148	7	1
-2	315	7	12	-5	270	6	5	-1	39	47	-10*	-1	285	6	-8	0	156	5	13
-1	281	7	5	-4	318	9	13	0	57	25	16*	0	248	6	-10	1	124	11	0
0	278	6	0	-3	332	8	-0	1	29	48	-8*	1	215	5	-7	2	118	6	6
1	283	6	-2	-2	315	7	9	2	36	39	-7*	2	228	6	-10	3	111	13	7
2	246	6	-2	-1	261	7	7	3	37	38	-5*	3	221	6	-3	H,K=	9,	5	
3	192	6	-1	0	280	9	3	H,K=	9,	-4	4	164	7	-10	-9	176	10	3	
4	170	6	9	1	261	7	7	-4	208	9	-13	H,K=	9,	1	-8	192	7	-7	
5	153	14	0	2	215	8	3	-3	264	12	8	-8	125	7	5	-7	233	6	-6
H,K=	8,	4	H,K=	8,	8	-2	264	8	9	-7	122	7	-5	-6	243	7	-3		
-9	151	9	0	-9	59	14	5*	-1	269	9	1	-6	133	7	4	-5	259	7	-2
-8	171	9	-3	-8	40	27	-33*	0	275	6	3	-5	177	6	8	-4	300	7	15
-7	173	5	-9	-7	77	10	1	1	252	6	-0	-4	185	5	5	-3	332	10	22
-6	211	6	-10	-6	76	11	0	2	238	7	-5	-3	175	7	-5	-2	310	8	14
-5	216	5	-5	-5	43	52	-14*	3	231	6	-8	-2	176	5	-7	-1	249	10	-1
-4	247	7	-3	-4	91	19	9*	H,K=	9,	-3	-1	170	5	-4	0	252	7	4	
-3	292	8	18	-3	97	16	2	-5	49	57	-5*	0	167	5	-4	1	256	7	1
-2	261	6	20	-2	69	16	-1*	-4	70	47	0*	1	187	6	-2	2	204	8	-1
-1	211	7	3	-1	57	17	6*	-3	70	25	1*	2	154	5	-7	3	181	6	11
0	208	6	5	0	64	23	9*	-2	89	10	20	3	124	6	-13	H,K=	9,	6	
1	208	7	6	1	53	66	-0*	-1	82	24	12*	4	122	10	4	-9	69	36	-11*
2	192	5	6	2	49	30	0*	0	105	7	6	H,K=	9,	2	-8	106	7	2	
3	124	7	1	H,K=	8,	9	1	75	23	-12*	-8	148	13	-9	-7	116	6	2	
4	108	8	-1	-9	212	8	6	2	85	7	5	-7	155	6	-6	-6	120	7	4

STRUCTURE FACTORS CONTINUED FOR  
NA3(UO2)2F7.6H2O

PAGE 13

L	F08	SG	DEL	L	F08	SG	DEL	L	F08	SG	DEL	L	F08	SG	DEL
-5	118	12	1	1	70	14	-14*	-4	236	6	11	-5	258	8	15
-4	146	9	11	2	68	18	-13*	-3	251	8	9	-4	247	7	4
-3	161	7	6	H,K=	10,	-2	-2	232	9	3	-3	235	7	6	
-2	148	7	7	-5	208	10	9	-1	205	6	-4	H,K=	11,	-1	
-1	115	9	10	-4	211	7	-1	0	188	15	-5	-3	108	13	-6
0	106	11	-6	-3	226	9	10	1	210	6	7	-2	120	12	-3
1	119	7	6	-2	225	6	-3	2	172	11	-5	-1	140	6	12
2	80	24	-10*	-1	242	7	2	H,K=	10,	4	H,K=	11,	0		
	H,K=	9,	7	0	217	6	-3	-7	120	9	-8	-4	175	9	6
-9	204	11	4	1	189	11	-7	-6	128	11	-0	-3	156	9	-11
-8	213	6	-4	2	178	8	-11	-5	143	8	1	-2	170	6	-12
-7	277	8	2	H,K=	10,	-1	-4	169	9	14	-1	185	6	-8	
-6	297	7	-1	-5	130	9	11	-3	181	7	8	0	152	21	-8
-5	330	8	8	-4	153	9	5	-2	172	9	8	H,K=	11,	1	
-4	351	8	18	-3	143	9	7	-1	140	9	-4	-5	164	11	9
-3	337	9	6	-2	141	6	2	0	115	13	-16	-4	196	11	25
-2	331	8	13	-1	139	6	0	1	155	6	8	-3	173	13	-6
-1	327	7	12	0	126	7	-9	2	122	13	2	-2	189	8	8
0	292	8	4	1	131	6	-2	H,K=	10,	5	-1	161	7	-6	
1	255	7	5	2	113	11	-10	-8	164	6	-13	0	171	7	4
	H,K=	9,	8	H,K=	10,	0	-7	189	9	-16	H,K=	11,	2		
-8	30	48	1*	-6	193	7	3	-6	250	7	-1	-5	131	8	-7
-7	29	40	-12*	-5	235	9	3	-5	231	6	-7	-4	172	9	19
-6	43	26	1*	-4	274	8	13	-4	270	9	21	-3	138	9	-13
-5	55	19	-4*	-3	252	7	-1	-3	267	7	20	-2	148	7	0
-4	49	41	11*	-2	256	6	-14	-2	255	7	8	-1	129	7	-3
-3	21	46	-16*	-1	246	7	-12	-1	243	6	4	0	115	14	-6
-2	60	15	25*	0	246	11	-6	0	233	6	7	H,K=	11,	3	
-1	61	31	20*	1	226	7	-9	1	189	7	-8	-6	184	6	-6
0	33	50	-8*	2	212	6	-4	H,K=	10,	6	-5	200	7	-4	
	H,K=	9,	9	3	176	6	-4	-7	63	52	-10*	-4	205	21	15
-8	220	7	-1	H,K=	10,	1	-6	87	10	-7	-3	220	6	11	
-7	235	7	-9	-7	135	8	1	-5	99	10	9	-2	210	6	-1
-6	239	7	-3	-6	163	6	1	-4	99	16	8	-1	210	7	3
-5	248	8	9	-5	197	6	16	-3	67	76	-10*	0	199	8	6
-4	273	7	0	-4	193	7	16	-2	92	20	6*	H,K=	11,	4	
-3	264	8	-1	-3	184	5	-2	-1	81	12	-2	-6	128	7	8
-2	246	7	0	-2	207	5	-1	0	86	13	9	-5	131	11	9
-1	229	11	1	-1	219	6	-2	H,K=	10,	7	-4	112	19	-2	
	H,K=	9,	10	0	179	6	-5	-7	244	7	-10	-3	124	10	6
-7	33	59	30*	1	167	6	-9	-6	256	9	-3	-2	125	9	7
-6	30	52	17*	2	171	8	1	-5	259	10	3	-1	128	7	10
-5	24	63	7*	H,K=	10,	2	-4	286	8	5	0	110	9	7	
-4	35	49	27*	-7	147	12	0	-3	303	8	8	H,K=	11,	5	
-3	31	41	29*	-6	165	6	-11	-2	271	7	15	-6	182	8	-8
-2	25	66	19*	-5	198	7	-5	-1	235	9	-1	-5	187	8	-6
	H,K=	10,	-4	-4	185	5	-4	0	233	7	11	-4	220	8	14
-2	240	8	8	-3	191	6	4	H,K=	10,	8	-3	-2	252	15	18
-1	245	8	2	-2	226	6	2	-7	31	48	-15*	-2	219	10	5
0	259	8	-2	-1	214	7	-1	-6	41	56	5*	-1	195	11	3
1	244	6	-3	0	176	6	-3	-5	62	24	38*	H,K=	11,	6	
	H,K=	10,	-3	1	169	7	-2	-4	65	22	26*	-5	41	56	-8*
-4	83	15	3	2	144	8	-8	-3	34	57	-7*	-4	51	27	-3*
-3	93	11	8	H,K=	10,	3	-2	34	49	-1*	-3	85	12	15	
-2	103	10	2	-7	175	8	-3	-1	20	59	-3*	-2	48	24	-4*
-1	92	21	-11*	-6	189	7	-6	H,K=	10,	9	H,K=	11,	7		
0	93	8	7	-5	207	8	0	-6	240	10	15	-4	229	7	3

## VIII. References

1. K. Volz, A. Zalkin and D. H. Templeton (1976). Inorg. Chem., 15, 1827.
2. D. St. Clair, A. Zalkin and D. H. Templeton (1971). Inorg. Chem., 10, 2587.
3. P. A. Doyle and P. S. Turner (1968). Acta Cryst., A24, 390.
4. D. T. Cromer and D. Liberman (1970). J. Chem. Phys., 53, 1891.
5. W. H. Zachariasen (1954). Acta Cryst., 7, 783.
6. L. Bragg and G. F. Claringbull (1965). "Crystal Structures of Minerals", p. 150-158. Cornell University Press, Ithaca, New York.
7. Yu. N. Mikhailov, A. A. Udovenko, V. G. Kuznetsov and R. L. Davidovich (1972). J. Struct. Chem. (USSR), 13, 694.
8. Yu. N. Mikhailov, A. A. Udovenko, V. G. Kuznetsov and R. N. Shchelokov (1972). J. Struct. Chem. (USSR), 13, 695.
9. H. Brusset, Nguyen Quy Dao and A. Rubinstein-Auban (1972). Acta Cryst., B28, 2617.
10. Yu. N. Mikhailov, A. A. Udovenko, V. G. Kuznetsov and R. L. Davidovich (1972). J. Struct. Chem. (USSR), 13, 879.
11. Yu. N. Mikhailov, S. B. Ivanov, A. A. Udovenko, R. L. Davidovich, V. G. Kuznetsov and V. V. Peshkov (1974). J. Struct. Chem. (USSR), 15, 838.

This work was done with support from the U.S.  
Energy Research And Development Administration.

0 0 - 3 4 / 1 0 ) 3 9

This report was done with support from the United States Energy Research and Development Administration. Any conclusions or opinions expressed in this report represent solely those of the author(s) and not necessarily those of The Regents of the University of California, the Lawrence Berkeley Laboratory or the United States Energy Research and Development Administration.

TECHNICAL INFORMATION DIVISION  
LAWRENCE BERKELEY LABORATORY  
UNIVERSITY OF CALIFORNIA  
BERKELEY, CALIFORNIA 94720